MAGNETIC NAVIGATION IN PERCUTANEOUS CORONARY AND NON-CORONARY INTERVENTIONS

STEVE RAMCHARITAR

ISBN: 978-90-8559-451-2

Magnetic Navigation in Percutaneous Coronary and Non-Coronary Interventions

Magnetische navigatie in percutane coronaire en niet-coronaire interventies

Thesis

to obtain the degree of Doctor from the
Erasmus University Rotterdam
by command of the
rector magnificus

Prof.dr. S.W.J. Lamberts

and in accordance with the decision of the Doctorate Board

The public defence shall be held on

Wednesday October 29,
2008 at 11:45 hrs

by
Steve Ramcharitar

born in Trinidad

Doctoral Committee

Promotor(s):	Prof.dr. P.W. Serruys
Other members:	Prof.dr. L. Jordaens
	Prof.dr. P. de Feyter
	Prof.dr. W.J. van der Giessen
Copromotor(s):	Dr. R.J. van Geuns

Financial support by the Netherlands Heart Foundation (NHF) for the publication of this thesis is gratefully acknowledged.

Table of Contents

INTRODUCTION AND OVERVIEW OF THIS THESIS

Magnetic Navigation in Percutaneous Coronary and Non-Coronary Interventions

There is no question that Percutaneous Coronary Intervention has revolutionized the way we manage coronary artery disease. Over the past two decades we have witnessed maturity in several techniques and equipment enabling the interventional cardiologist to manage lesions that have previously been entirely in the domain of the cardiac surgeon[1]. Despite these remarkable achievements there still remain lesions that are complex enough to create a challenge in the most experienced hands[2,3]. The inherent tortuosity in complex vascular anatomies, branching segments and chronically occluded vessel have been all associated with lower procedural success and higher complication rates when compared to the "straight forward vessels"[4]. The Magnetic Navigation System (MNS) is a novel and versatile technology that allows the re-orientation of a wire within the patient's body. This unique ability means that the "trial and error" method of externally re-shaping the tip of the wire and re-engaging the vessel can be effectively eliminated. As such previously "unreachable areas" in the heart or within the vasculature can now be potentially reached[5].

The MNS is an established technique for cardiac electrophysiology procedures but as yet has not been proven in the field of percutaneous coronary interventions[6]. This aim of this Thesis is to critically evaluate the extension of the MNS in unselected patients and to identify the strengths and weaknesses of the current software and hardware. Chapter 1 introduces the reader to a general introduction to the MNS. It pays tribute to the early pioneers and gives an up-to-date analysis of what is currently possible with this technology and an insight into what the future holds, particularly with respect to chronic occluded arteries[7] and cell transplantation[8]. Chapter 2 attempts to evaluate the performance of the MNS hardware and software in an experimental setting. Phantom models were chosen so as to provide a precisely control environment for testing and validation. Direct comparisons were made with the magnetic wire and standard conventional wires in a 2-dimensional branching tortuous phantom simulating angulated coronary vessels. Also since the MNS uses 3-dimensional reconstruction software to create a precise roadmap for the magnetic wire to follow, the precision and accuracy of this software was assessed with an alternative system using stenotic phantoms in porcine models.

Having evaluated both the software and hardware, the evaluation of the MNS in a clinical setting was undertaken[9]. Attempts were made in Chapter 3 to identify the patient population that would be best suited to have a magnetically assisted procedure. Assumptions were made based on the length of time needed in crossing using conventional standard wire techniques. A scoring system was developed based on both vessel and lesion characteristics. This was then evaluated in patients admitted for treatment with the MNS to determine if the system had a role to play in vessels having anatomical complexities. Two complex lesions where the MNS was postulated to have an advantage were examined in the second part of this Thesis. In

Chapter 4, the ability of the system to reorient the wire's tip to cross bifurcating vessels and the struts of stent covering the ostium following treatment were evaluated. In managing another complex lesion subset, the chronically total occluded (CTO) vessel, an alternative method for deriving a pathway based on Multislice Computer Tomography (MSCT) was examined. Chapter 5 firstly assesses how the Navigant® software can facilitate magnetically assisted percutaneous interventions directly by co-integrating the MSCT scan. Then evaluates the possibility that in the future an entire intervention with stent positioning and deployment may be possible based entirely on the integration of 3D information without needing contrast agents. The technical aspects of the magnetic wire and the development of a dedicated wire for the CTO are discussed in Chapter 6. This chapter also examines the Thoraxcenter's experience in using the various generations of magnetically enabled wires from the initially installation of the system to the present time. It critically assesses the key elements that are important to address if the MNS is to compete with the sophistication of the modern conventional CTO wires.

The final part of this Thesis, Chapter 7 examines the application of the MNS to two important non-coronary intervention areas. Its use in guiding left ventricular lead implantation base on virtual 3D reconstructed image of the coronary sinus and the possibility to use a magnetically enabled injection needle to facilitate precise stem cell implantation within the myocardium. Finally Chapter 8 describes a couple of cases to demonstrate the wider spectrum in the clinical application of the MNS.

References

1. Serruys PW. Fourth annual American College of Cardiology international lecture: a journey in the interventional field. *J Am Coll Cardiol* 2006;47:1754-68.
2. Tsuchida K, Colombo A, Lefevre T, Oldroyd KG, Guetta V, Guagliumi G, von Scheidt W, Ruzyllo W, Hamm CW, Bressers M, Stoll HP, Wittebols K, Donohoe DJ, Serruys PW. The clinical outcome of percutaneous treatment of bifurcation lesions in multivessel coronary artery disease with the sirolimus-eluting stent: insights from the Arterial Revascularization Therapies Study part II (ARTS II). *Eur Heart J* 2007;28:433-42.
3. Hoye A, van Domburg RT, Sonnenschein K, Serruys PW. Percutaneous coronary intervention for chronic total occlusions: the Thoraxcenter experience 1992-2002. *Eur Heart J* 2005;26:2630-6.
4. Valgimigli M, Serruys PW, Tsuchida K, Vaina S, Morel MA, van den Brand MJ, Colombo A, Morice MC, Dawkins K, de Bruyne B, Kornowski R, de Servi S, Guagliumi G, Jukema JW, Mohr FW, Kappetein AP, Wittebols K, Stoll HP, Boersma E, Parrinello G. Cyphering the complexity of coronary artery disease using the syntax score to predict clinical outcome in patients with three-vessel lumen obstruction undergoing percutaneous coronary intervention. *Am J Cardiol* 2007;99:1072-81.
5. Raizner AE. Magnetic navigation: a pivotal technology. *Catheter Cardiovasc Interv* 2007;69:856.
6. Pappone C, Vicedomini G, Manguso F, Gugliotta F, Mazzone P, Gulletta S, Sora N, Sala S, Marzi A, Augello G, Livolsi L, Santagostino A, Santinelli V. Robotic magnetic navigation for atrial fibrillation ablation. *J Am Coll Cardiol* 2006;47:1390-400.
7. García-García HM, Kukreja N, Daemen J, Tanimoto S, van Mieghem C, Gonzalo N, van Weenen S, van der Ent M, Sianos G, de Feyter P, Serruys P.W. Contemporary treatment of patients with chronic total occlusion: critical appraisal of different state-of-the-art techniques and devices. *EuroIntervention* 2007;3:188-196.
8. Perin E, Silva G, Fernandes M, Munger T, Pandey A, Sehra R, Talcott M, Bichard C, Creed J, J W, Oliveira E, Zheng J, Canales J, Cardoso C, Patterson M, Serruys P.W. First experience with remote left ventricular mapping and transendocardial cell injection with a novel integrated magnetic navigation-guided electromechanical mapping system *Eurointervention* 2007;3:142-148.
9. Atmakuri SR, Lev EI, Alviar C, Ibarra E, Raizner AE, Solomon SL, Kleiman NS. Initial experience with a magnetic navigation system for percutaneous coronary intervention in complex coronary artery lesions. *J Am Coll Cardiol* 2006;47:515-21.

Chapter 1

INTRODUCTION AND OVERVIEW OF THIS THESIS

Magnetic Navigation in Coronary Intervention

Nature Clinical Practice Cardiovascular Medicine 2008 Mar; 5 (3): 148-56

Ramcharitar S, Patterson M, van Geuns RJ, van Meighem CAG, Serruys PW

Summary

Magnetic navigation is rapidly emerging as a useful technology in the field of interventional cardiology. Precise control of the direction of a guide wire or a device in three-dimensional space offers a means to access vessels and areas of the heart that are often challenging to access with conventional methods. In this comprehensive Review, we detail the development of magnetic navigation technology and how this tool has been adapted for use during percutaneous coronary intervention. We aim to provide an up-to-date analysis of what is currently possible with this technology and an insight into what the future holds, particularly with respect to chronic occluded arteries and cell transplantation.

Introduction

The growth of interventional cardiology has led to numerous technological developments:[1] the development of metallic and biodegradable stents that elute novel bioactive molecules;[2] specialized guidewires with subtle differences for accessing different types of lesion;[3] and various new pharmacological agents.[4] One area that has not seen substantial progress thus far is the technology used to precisely guide a wire across a lesion. In most instances, crossing a lesion still relies heavily on both the skills of the interventional cardiologist performing the procedure and the mechanical properties of the guidewire. The Niobe® Magnetic Navigation System (MNS; Stereotaxis Inc., St Louis, MO) is a novel technology that can precisely control the tip of a magnetically enabled wire or device *in vivo*.[5] Preliminary data suggest that the MNS could be useful in tortuous vessels or in complex lesions such as bifurcations, in which the initial bend placed on the wire might not be ideal for crossing tandem lesions.[6] Magnetic navigation also means the wire is less likely to deviate into side branches, therefore, reducing radiation exposure and the amount of contrast required.[7] The combination of dedicated magnetically enabled devices with three-dimensional (3D) imaging methodologies such as multislice CT (MSCT) and the NOGA® mapping system (Cordis Corporation, Miami Lakes, FL), can increase the accuracy in targeting chronic total occlusions (CTOs) and stem-cell implantation.

To date, the transition of this technology into interventional cardiology has been slow. In many centers the MNS was first used in cardiac electrophysiological procedures, for which the benefits are well established; only now are centers extending the use of this technology to the interventional setting, despite the obvious advantages that the MNS offers. This somewhat cautionary approach stems from the fact that no randomized clinical trials have currently compared the MNS with older, more-established techniques. This issue clearly needs addressing, with future developments in both the software and hardware designs being investigated in timely clinical trials. At present, the expenses incurred in setting up an MNS will also influence its popularity. This Review discusses some of the major technological developments in the context of interventional cardiology and provides an insight into what is currently possible and what might be possible with this novel technology in the future.

Early developments

Vascular studies using magnetic navigation first began over 50 years ago when Llander,[8] and later Tillander,[9] used magnetic fields to guide an articulated steel-tip catheter in rabbit aorta. After these initial investigations, small external permanent magnets were used to stereotactically direct iron particles for thrombosis of intracranial aneurysms,[10, 11, 12] later, rotating electromagnets were used, enabling better control.[13] In 1991, Ram and Meyer performed the first magnetically guided angiography in a human. They successfully used a magnetized catheter controlled with external permanent magnets in a neonate with anatomically complex congenital heart disease.[14] Despite initial success, further development was hampered by low

field strengths, the need for large magnets and the lack of precise 3D control.[15, 16] In order for stereotactic localization and computer-controlled vector guidance to be possible, considerable advances in both medical physics and magnet design were required.[17] Further advancements in these areas and the use of MRI coregistered with real-time fluoroscopy enabled the navigation of both a small object in a canine brain[18] and magnetically enabled catheters in pig brains.[19] These experiments led to the MNS first being used in interventional radiology and cardiac electrophysiology, and now in interventional cardiology.[20, 21, 22] Across these disciplines there are now more than 100 systems installed worldwide. It should be noted, however, that applying this technology in interventional cardiology presents a greater challenge than in more established indications such as neurosurgery. Unlike the brain, the heart is a dynamic structure, and the patient's chest moves with respiration.

The Niobe® magnetic navigation system

Navigation hardware

The Niobe® MNS (Figure 1a) has four key components: two permanent adjustable magnets mounted on mechanical frames situated at either side of the fluoroscopy table; navigation software (Navigant®, Stereotaxis, St Louis, MO) to control the magnets by creating a virtual roadmap and magnetic vectors after imaging data are gathered; a real-time fluoroscopy system to display a virtual map of the live image; and finally, a sterile touch-screen monitor for controlling the system, ideally placed at the operating table. In the second-generation system, Niobe® II, the mechanical frames enabling the magnets to be positioned were adapted to allow the magnets to translate or tilt about their axes. This tilting action enabled more angiographic projections—the previous version of Niobe® had limited right anterior oblique and left anterior oblique views because of the bulkiness of the magnets.

The majority of systems are integrated with a modified C-arm flat-panel detector fluoroscopic imaging suite (AXIOM Artis *d*FC; Siemens AG, Malvern, PA), but there are systems that can also incorporate biplane fluoroscopic imaging and rotational angiography. Biplane fluoroscopy has the advantage of reducing the amount of contrast used during image acquisition, but once the images are transferred into the Navigant® software the lateral C-arm must be stored in order for the magnets to be positioned. Rotational angiography, on the other hand, enables a 3D image to be generated directly from a single acquisition.When the patient is correctly positioned and isocentered, the magnets interact to produce a spherical magnetic field 15 cm in diameter and uniformly of 0.08 Tesla—the 'magnetic volume'. Within this volume any applied magnetic vector can precisely direct a 2–3 mm magnet mounted on the tip of a wire (Figure 1b) or steerable device so that a full 360° rotation can be achieved. Clinically approved devices include guidewire and electrophysiological ablation catheters; other devices currently in development include coronary and peripheral ablative radiofrequency

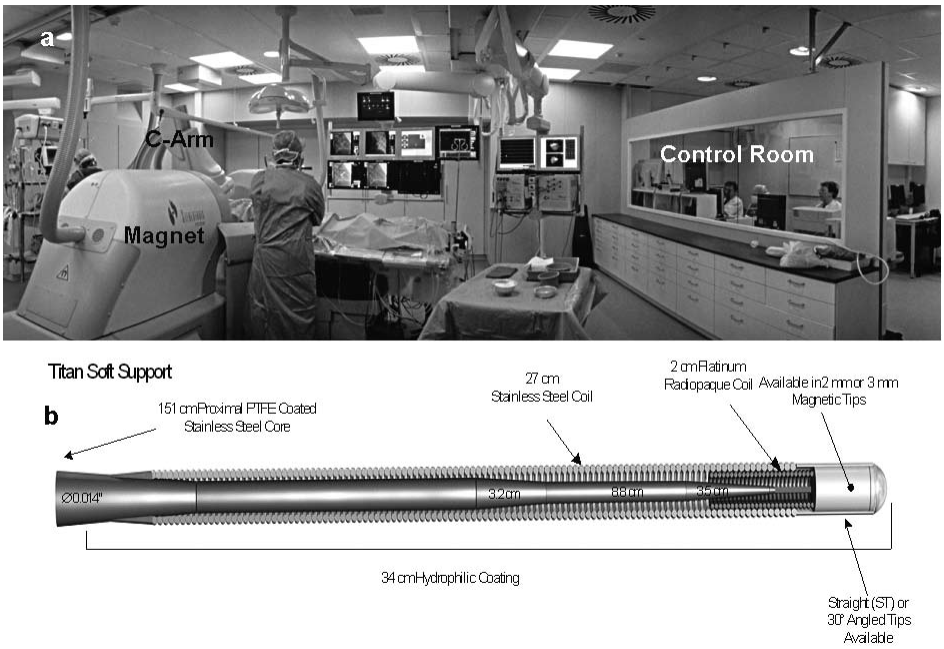

Figure 1 *The Niobe® Magnetic Navigation System.*
*(**a**) A typical magnetic navigation system set-up showing the magnets, C-arm and the control room.*
*(**b**) The Titan® magnetic navigation wire showing the 2 or 3 mm magnet located at its tip.*

wires, multidirectional probing catheters, and catheters fitted with needles that are designed for cell implantation.

Navigation software

Free-mode navigation

Magnetic navigation is performed by presetting a magnetic vector using the touch-screen monitor. Following programming, the vector is displayed as a dotted line on the live fluoroscopy image, and the permanent magnets—illustrated by a solid vector line—move to align a magnetic field to this vector. Wire advancement is controlled manually to follow a desired incremental distance and is guided by either two-dimensional (2D) or 3D software features in Navigant®. The 2D navigational modes include the use of preset navigational vectors that are adapted to a particular coronary anatomy. This software also allows the user to create new presets if necessary, for example in patients who have vascular anomalies or to target coronary artery bypass grafts. Other approaches include the 'bulls eye view', which allows navigation around a central axis, and is, hence, a particularly useful technique for CTOs. The 3D Navisphere® program (Stereotaxis, Inc., St Louis, MO) is a spherical navigation object that contains regularly spaced polar lines (e.g. latitude and longitude lines). The aim of this program is to improve

Figure 2 *The clockface navigational mode*
By touching the perimeter the vector moves in that direction; controls for anterior and posterior movements are at the edges.

recognition of the 3D structure of the coronary artery tree. Navigation is also feasible through the 'clock face' mode, which mimics the dial of a clock (Figure 2). This technique permits fast navigation relative to other techniques, but does require some understanding of the spatial coronary anatomy. Direct anatomical navigation is possible by directly introducing a fluoroscopic image in Navigant®; however, 2D image representation of a 3D structure has obvious limitations.

True-vessel navigation

True-vessel navigation uses an accurate 3D representation of the coronary artery. Navigant® software can create such a virtual map from two X-ray images provided that they are 30° apart. This program uses a feature called constellations to map identical points on both images, thus, generating a 3D navigational path or 'centerline' through the vessel lumen (Figure 3a). Alignment of the centerline with the live fluoroscopy image is required for navigation. A 3D representation of the coronary anatomy and centerline can also be created from two fluoroscopic images using the CardiOp®-B software (Paieon Inc., New York, NY; Figures 3 and 4). The advantage of using this program is that it can limit vascular foreshortening[23] and improve the accuracy of quantitative coronary angiography measurements.[24, 25] Using this software, navigational vectors can be

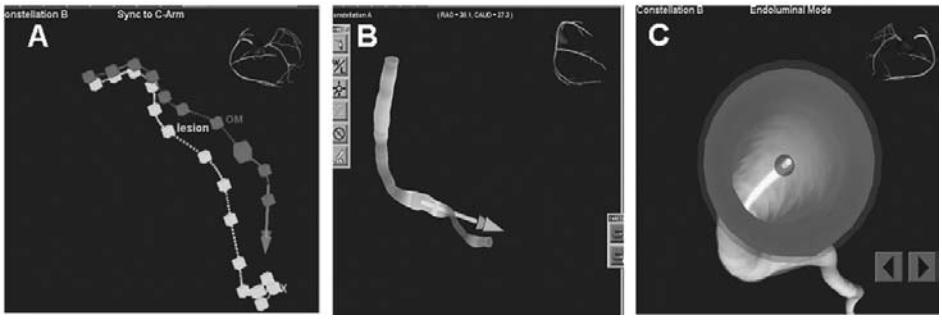

Figure 3. *True-vessel navigation using an accurate three-dimensional representation of the coronary artery* (**A**) A constellation road map created from two-dimensional X-ray images; chosen points are depicted by squares along the navigational path. (**B**) Navigation using a three-dimensional reconstruction created with the CardiOp®-B software. (**C**) Navigation by means of the endoluminal view. Abbreviation: OM, obtuse marginal branch.

directed through a virtual representation of the vessel lumen, so subtle changes in the vessel morphology can be accentuated (Figure 3c).[26]

A 3D road map can also be created from an MSCT dataset. The importance of MSCT in interventional cardiology stems from its ability to detect early-stage coronary artery disease,[27, 28] identify vascular anomalies and provide information on coronary plaques composition.[29] Using Navigant®, the vessels can be isolated from the dataset and a 3D volume-rendered reconstructed MSCT image can be incorporated into the virtual roadmap for magnetic navigation (Figure 4b). The mapping of points along the vessel is used to create a virtual lumen and a centerline (Figure 4d), which is coregistered and aligned to the fluoroscopic image for navigation. The ability of MSCT to 'fill in' the occluded vessel segments that are not seen angiographically means that it is a useful tool for navigating through CTOs (Figure 5a), with newer versions of Navigant® able to show both the endoluminal view and the multiplaner reconstructed cross-sections (Figure 5b).

The MNS and intervention: what is currently possible?

Patent coronary arteries

Tortuous and severely angulated coronary arteries are associated with reduced procedural success rates and a raised incidence of CABG surgery.[30] A guidewire must be maneuvered without causing complications such as dissection or perforation. Several phantom studies in hepatic celiac arteries and the cerebral arteries have demonstrated higher procedural success using the MNS than with manual manipulation, and shown that the MNS is easier, more accurate and faster even when used by inexperienced operators.[31, 32, 33] Studies in a coronary phantom, however, reported longer crossing times with the MNS than with a standard wire, although fluoroscopic times were significantly reduced.[34] The longer crossing times could have been

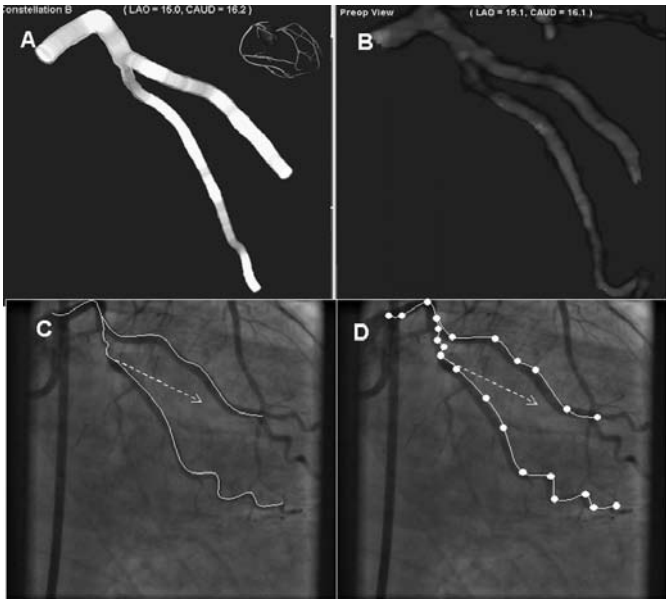

Figure 4 *Three-dimensional representation of the coronary artery.*
*(**A**) A three-dimensional reconstruction of the artery using the CardiOp®-B software. (**B**) The same arteries extracted from a multislice CT data set (**C** and **D**), displayed as navigational centerlines with a directional vector on the live fluoroscopic images.*

related to the use of first generation Cronus® (Stereotaxis Inc., St Louis, MO) magnetic wires—subsequent generations have been easier to track. Indeed, a recent 2D phantom study using five increasingly tortuous vessel models found that as vessel complexity increased the newer generation wires—Titan® and Pegasus® (Stereotaxis Inc., St Louis, MO) —were significantly better in reducing both the crossing and fluoroscopy times than were conventional wires.[35] Moreover, in some of the phantom models, prior experience of magnetic navigation was not a prerequisite for successful crossing. Overall wire usage was significantly reduced with the MNS.

A seminal paper by Atmakuri *et al*. showed the effectiveness of magnetic navigation during percutaneous coronary intervention (PCI) in native coronary arteries that would have been difficult to cross with conventional methods because of severe tortuousity.[36] In this study of 68 lesions in 59 patients, successful MNS crossings were achieved in 85% of cases. More importantly perhaps, magnetically guided intervention was successful in 9 (63%) of the 13 patients in whom PCI with a conventional wire had previously failed. The procedural success rates for magnetically guided intervention as the primary intervention and following failed conventional PCI ('secondary' intervention) were 84% and 62%, respectively, with longer median fluoroscopy and crossing times observed in secondary procedures. Similar success was reported in a study of 21 consecutive diseased coronary arteries, although guidewire navigation with the MNS was

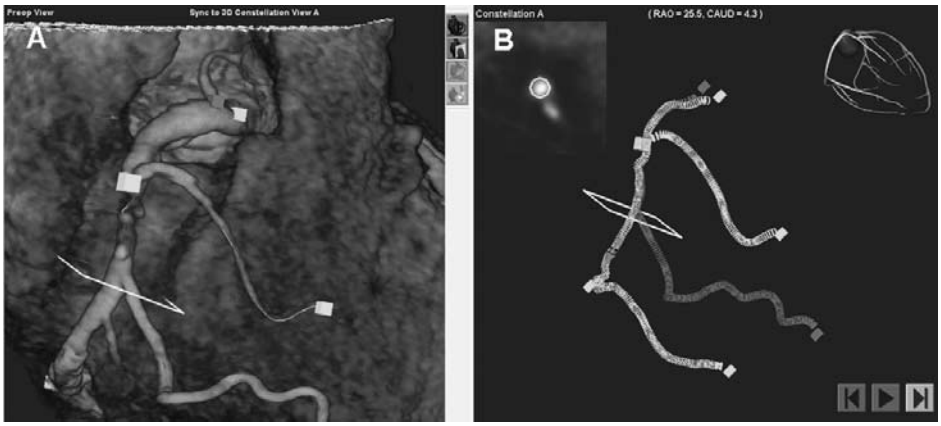

Figure 5 *Using the Navigant® system the multislice CT data set can be used to create: (A) a road map of a chronic total occlusion not seen angiographically and (B) cross-sections along the map.*

found to be slower than manual navigation.[37] The patients enrolled in this study did, however, have simple, straightforward lesions indicating that the MNS could be more suitable for use in complex coronary lesions and as a secondary procedure following failed conventional wire placement. This theory is exemplified further by the successful results seen when the MNS was used following an unsuccessful alcohol septal ablation that failed because of severe angulation (130°),[38] and when used to cross a crushed stent of a bifurcation that was complicated by dissection.[39] At present it is not clear how wide the applicability of magnetic-assisted navigation is likely to be in patent vessels. In order to evaluate this issue, our group has been assessing prolonged conventional crossing times to characterize the lesions and vessels that might be appropriate for magnetic navigation.

Occluded coronary arteries

CTOs have been described as one of the last frontiers in interventional cardiology.[40] Despite advances in technology and the development of specialized devices and dedicated wires, the rate of successful crossings is still unsatisfactory.[41] An attractive strategy for treatment of CTOs was postulated by Serruys in 2006.[1] The first stage of this strategy involves magnetic navigation to steer a guidewire through the occlusion. Second, optical coherence tomography, intravascular ultrasonography or MSCT cross sections are employed to 'look forward' within the vessel to ensure that the wire is ideally positioned in the true lumen. Finally, ablative power at the tip of the wire is used to recanalize the CTO.[42] The first successful study to demonstrate the feasibility of MSCT angiography and magnetic-enabled PCI used a system that 'looked forward' at the occlusion—the bull's eye view—making the search pattern for microchannels through the occlusion more uniform by avoiding repetitions.[43] Although mapping the occluded segments was easily accomplished, the bulky 2–3 mm magnetic tips used were a notable limitation. Furthermore, the fact that navigation was performed using a fixed roadmap (centerline)

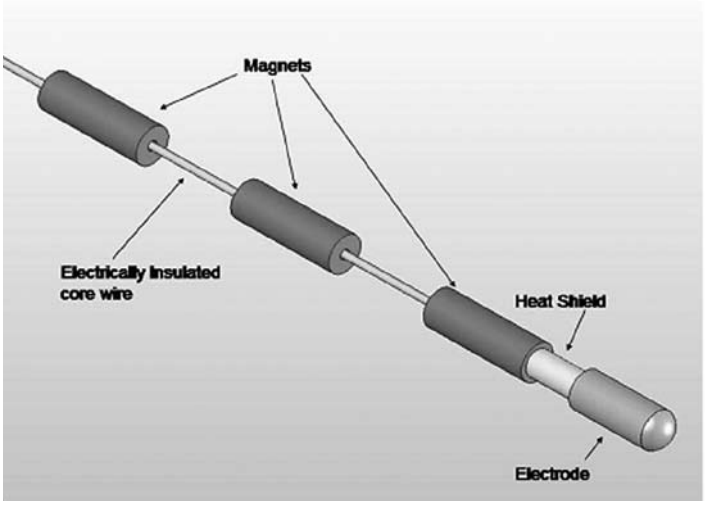

Figure 6 *A diagrammatic representation of the magnetically enabled radiofrequency ablating wire for chronic total occlusions.*

rather than a dynamic one gated to the electrocardiogram meant that there was discordance between the live fluoroscopy image and the centerline—another limitation. Ordinarily, when navigating through a patent vessel this discordance is not a problem as the wire is contained within the vessel's lumen, so that when the heart moves with each beat the wire can still follow the trajectory of the predetermined vectors. In CTOs, however, the lack of a patent lumen means that as the heart moves, the tip of the wire can be perpendicular to the vascular wall and when pushed can protrude. Hence, it is of paramount importance to develop technologies that allow dynamic road mapping (centerline) to be superimposed on the live fluoroscopy image, especially when considering magnetic-enabled radiofrequency ablation. Paieon Inc. is developing a dynamic road-mapping system based on their software that can recognize systolic and diastolic phases on fluoroscopic images. This system might have a role in patent vessels or those with subtotal occlusion, but not necessarily in CTOs because contrast media is needed to demarcate the vessel contours.

Much more appealing are methods aimed at electrocardiographic phase gating of the MSCT-derived centerline to the live fluoroscopic image following alignment to recognizable landmarks such as spinous processes and the catheter tip. This technique ensures that at a designated point in the cardiac cycle both the centerline and the live fluoroscopic image of the vessel are superimposed, enabling safe advancement of the ablating wire. Development of the magnetic-enabled wire with radiofrequency ablation functionality is nearing completion (Figure 6). This device is composed of a 0.014 inch wire with a small radiofrequency electrode

Figure 7 *A diagrammatic representation of magnetically enabled cell injection catheter following an automatic map in the myocardium.*

at its tip and three small magnets embedded proximally. An external generator supplies the radiofrequency energy needed for ablation. A safety and feasibility pilot study of this wire in 'within-stent' CTOs is planned for early 2008 at the Thoraxcenter, Rotterdam, The Netherlands.

Stem-cell injection

Intramyocardial injection of bone-marrow-derived stem cells is a novel technology that has the potential to induce myocardial regeneration and improvement in left ventricular function.[44] Currently, electromechanically guided injection is the preferred mode of delivery in patients with chronic myocardial ischemia.[45] Indeed, clinical studies have shown that transendocardial injections of stem cells using the NOGA® mapping system are feasible and safe[46] In this system, once the mapping electrode makes a good contact with the myocardium and the operator recognizes the appropriate electrical signal strengths, stem cells are injected through a needle linked to the device. One major drawback with this system is the difficulty of reaching remote areas of the left ventricle with manual manipulation of the catheter. This drawback can be addressed by using the magnetically enabled MNS-guided NOGA® electromechanical mapping catheter (Stereotaxis Inc.; Figure 7).

The guiding can be performed remotely to reduce operator radiation exposure. Moreover, the magnetic momentum at the catheter tip precludes the need for shaft support, allowing the

use of a softer catheter that is less likely to penetrate the myocardium and cause a perforation. By using MSCT or MRI to identify the infarcted area, relevant data can be integrated into Navigant® to further augment the accuracy of target localization. A recent animal study showed the preclinical feasibility of Stereotaxis-compatible NOGASTAR mapping and MYOSTAR® injection catheters (Cordis Corporation, Miami Lakes, FL) both equipped with a small permanent magnet at the tip.[47] Remote NOGA® mapping was possible with a computer-controlled catheter advancement system (Cardiodrive unit; Stereotaxis Inc., St Louis, MO). The introduction of the NOGA® map into Navigant® provided 3D vectors for the navigation of a magnetically enabled MYOSTAR® catheter. The combination of these technologies resulted in a 95.8% success rate of magnetic-guided injection of mesenchymal precursor cells into the myocardium. When labeled, cells were detected in all but one segment on histology.

What does the future hold?

Magnetic navigation is still in the developmental phase and as such will not revolutionize the way we currently perform PCI. By considering magnetic navigation as an adjunct technique to current practices, however, this technique could be used to beneficial effect in clinical situations that are technically difficult or associated with low procedural success. The development of both software and hardware is, therefore, in the context of adjunct therapy. More powerful magnetic fields (i.e. 0.1–0.12 Tesla, increased from the current 0.08) and software upgrades to further improve the precision of wire control are in development. In terms of CTOs, future developments include dynamic road mapping and appropriate gating of the MSCT images with real-time fluoroscopic images. In addition, alignment between angiographically determined 3D reconstructed nonoccluded segments and the occluded sections obtained through MSCT will be more accurate. Moreover, as MSCT cross-section analysis provides important information on plaque composition and can accurately identify the vessel's border—a 'true' centerline can be reconstructed by 'stacking' the gated cross sections if the center of each cross section (Figure 5b) is determined precisely. Incorporation of this idea in future versions of the Navigant® software is being contemplated, so that a gated wire can be advanced in a frame-like fashion to ensure central wire transit. The unwarranted complexity of several MNS workstations, which can slow processing speed, will be reduced in the future by a new single-screen user interface (Odyssey™ Network Solutions, Stereotaxis, St Louis, MO) that links diagnostic information from several sources. To further improve the speed of navigation without compromising safety there will, however, need to be improvements in alignment of the centerline to the real-time fluoroscopy image, possibly through dynamic electrocardiographic gating. This improvement would allow the operator to drag the vector with confidence, instead of using 1–5 mm jumps along the centerline. With this development, the MNS could then compete with conventional wires in all lesions, not just complex cases.

New advances in material science have permitted the development of several guidewires with variable degrees of support and flexibility, tailored to individual coronary lesions. The newest generation in wire design—the Pegasus®—is made from a nitinol–stainless steel composite for improved flexibility with minimal deformity. Future wire-related developments will include magnets that can change the stiffness of the wire to improve the delivery of a device, multi-magnet configurations to enable smoother transition across the tip, and wires with the ability to feedback their position in space. The ability to accurately identify a wire's position can be useful when combined with a robotic wire advancement system. To date, such systems have been successfully employed in electrophysiological procedures[48, 49] but have not yet been extended to MNS-guided PCI. A stand-alone remote navigation system (CorPath®, Corindus Ltd, Haifa, Israel) for wire advancement and stent deployment using a joystick to control the wire's axial (i.e. advance, retract) and rotational movements has been shown to be feasible,[50] which opens the possibility of linking such a device to the MNS to achieve full automation.

Limitations

Even though the concept of directional wire guidance has been effectively realized, the areas in which the system offers a clear advantage over current approaches still need to be identified, which explains the slow market penetration in interventional cardiology. In addition, apart from a few institutional registries, there are limited data on this new technology. The lack of randomized, controlled trials makes comparisons with existing technologies purely speculative. Furthermore, new operators experience a learning phase before achieving an adequate level of competence, irrespective of whether they are a physician or technical staff. Similarly, as the software develops, there is a need for continuing educational updates or seminars to ensure that operators are kept abreast of new developments.

At present, the main limitation with the software remains the alignment of the virtual image to the real-time image. There is also a need for dynamic road mapping of the vessel; at present operators navigate through a static image. The 3D-reconstruction packages used still have limitations with respect to accuracies in tracing the vascular contours from which the central path for navigation is ultimately derived. The physical limitations of magnets attached to the wire tip could hinder advancement in extremely tortuous vessels, highlighting the importance of the multimagnet design that offers a smoother transition. Ultimately, the success of 3D magnetic-enabled procedures still depends heavily on the time it takes to prepare the road map. The time taken can vary enormously depending on the vessel characteristics and must, therefore, be taken into account during procedural planning. The 2D navigation approach is quicker; however, the level of accuracy is compromised.

Conclusions

Magnetic navigation in coronary intervention is rapidly evolving. State-of-the-art magnetic devices are now competing with conventional nonmagnetically enabled wires and devices. These technological advances are creating new roles for stereotactic magnetic navigation, which in the future will include a wider range of invasive cardiac procedures.

References

1. Serruys PW. Fourth annual American College of Cardiology international lecture: a journey in the interventional field. J Am Coll Cardiol 2006;47(9):1754-68.
2. Ramcharitar S, Vaina S, Serruys PW. The next generation of drug-eluting stents: what's on the horizon? Am J Cardiovasc Drugs 2007;7(2):81-93.
3. Segev A, Strauss BH. Novel approaches for the treatment of chronic total coronary occlusions. J Interv Cardiol 2004;17(6):411-6.
4. Fox KA, Steg PG, Eagle KA, Goodman SG, Anderson FA, Jr., Granger CB, Flather MD, Budaj A, Quill A, Gore JM. Decline in rates of death and heart failure in acute coronary syndromes, 1999-2006. Jama 2007;297(17):1892-900.
5. Patterson MS, Schotten J, van Mieghem C, Kiemeneij F, Serruys PW. Magnetic navigation in percutaneous coronary intervention. J Interv Cardiol 2006;19(6):558-65.
6. Ellis SG, Vandormael MG, Cowley MJ, DiSciascio G, Deligonul U, Topol EJ, Bulle TM. Coronary morphologic and clinical determinants of procedural outcome with angioplasty for multivessel coronary disease. Implications for patient selection. Multivessel Angioplasty Prognosis Study Group. Circulation 1990;82(4):1193-202.
7. Bernardi G, Padovani R, Morocutti G, Vano E, Malisan MR, Rinuncini M, Spedicato L, Fioretti PM. Clinical and technical determinants of the complexity of percutaneous transluminal coronary angioplasty procedures: analysis in relation to radiation exposure parameters. Catheter Cardiovasc Interv 2000;51(1):1-9; discussion 10.
8. Llander H. Magnetic guidance of a catheter with articulated steel tip. Acta radiol 1951;35(1):62-4.
9. Tillander H. Selective angiography of the abdominal aorta with a guided catheter. Acta radiol 1956;45(1):21-6.
10. Alksne JF, Fingerhut AG, Rand R. Stereotactic magnetically controlled thrombosis of intracranial aneurysms. Paper presented at the 34th annual meeting of the Harvey Cushing Society. St. Louis, Missouri, April 18, 1966.
11. Fingerhut AG, Alksne JF. Thrombosis of intracranial aneurysms. Radiology 1966;86 342-343.
12. Meyers PM, Cronic F., Nice CM. Experimental approach in the use and magnetic control of metallic iron particles in the lymphatic and vascular systems of dogs as a contrast and isotopic agent. Am. J. Roentg 1963; 90 (1068-1077).
13. Yodh SB, Pierce NT, Weggel RJ, Montgomery DB. A new magnet system for 'intravascular navigation'. Med Biol Eng 1968;6(2):143-7.
14. Ram W, Meyer H. Heart catheterization in a neonate by interacting magnetic fields: a new and simple method of catheter guidance. Cathet Cardiovasc Diagn 1991;22(4):317-9.
15. Alksne JF. Stereotactic thrombosis of intracranial aneurysms. N Engl J Med 1971;284(4):171-4.
16. Hilal SK, Michelsen WJ, Driller J, Leonard E. Magnetically guided devices for vascular exploration and treatment. Radiology 1974;113(3):529-40.
17. Gillies G.T, Ritter RC, Broaddus WC, Grady MS, Howard MA. Magnetic Manipulation Instrumentation for Medical Physics Research. Rev.Sci.Instrum 1994;65(3):533-562.
18. Grady MS, Howard MA, 3rd, Molloy JA, Ritter RC, Quate EG, Gillies GT. Nonlinear magnetic stereotaxis: three-dimensional, in vivo remote magnetic manipulation of a small object in canine brain. Med Phys 1990;17(3):405-15.
19. Grady MS, Howard MA, 3rd, Dacey RG, Jr., Blume W, Lawson M, Werp P, Ritter RC. Experimental study of the magnetic stereotaxis system for catheter manipulation within the brain. J Neurosurg 2000;93(2):282-8.
20. Chu JC, Hsi WC, Hubbard L, Zhang Y, Bernard D, Reeder P, Lopes D. Performance of magnetic field-guided navigation system for interventional neurosurgical and cardiac procedures. J Appl Clin Med Phys 2005;6(3):143-9.

21. Raizner AE. Magnetic navigation: a pivotal technology. Catheter Cardiovasc Interv 2007;69(6):856.
22. Hertting K, Ernst S, Stahl F, Mathew S, Meulenbrug H, Reimers J, Kuck K.-H, K K. Use of the novel magnetic navigation system Niobe™ in percutaneous coronary interventions; the Hamburg experience Eurointervention 2005;1(336-339).
23. Green NE, Chen SY, Hansgen AR, Messenger JC, Groves BM, Carroll JD. Angiographic views used for percutaneous coronary interventions: a three-dimensional analysis of physician-determined vs. computer-generated views. Catheter Cardiovasc Interv 2005;64(4):451-9.
24. Gollapudi RR, Valencia R, Lee SS, Wong GB, Teirstein PS, Price MJ. Utility of three-dimensional reconstruction of coronary angiography to guide percutaneous coronary intervention. Catheter Cardiovasc Interv 2007;69(4):479-82.
25. Tsuchida K, van der Giessen W, Patterson M, Tanimoto S, García-García H, Regar E, Ligthart J, Maugenest A, Maatrijk G, Wentzel J and others. In Vivo Validation of A Novel Three-Dimensional Quantitative Coronary Angiography System (CardiOp-B): Comparison with A Conventional Two-Dimensional System (CAAS II) and with Special Reference to Optical Coherence Tomography Eurointervention 2007;accepted for publication.
26. Patterson M, Tanimoto S, Tsuchida K, PW. S. Magnetic Navigation with the Endo-Luminal View and the X-ray overlay - Major advances in novel technology. Eurointervention 2007;in press.
27. Fishman EK, Horton KM. The increasing impact of multidetector row computed tomography in clinical practice. Eur J Radiol 2007;62 Suppl:1-13.
28. Hoffmann MH, Lessick J. Multidetector-row computed tomography for noninvasive coronary imaging. Expert Rev Cardiovasc Ther 2006;4(4):583-94.
29. Sanz J, Dellegrottaglie S, Fuster V, Rajagopalan S. Calcium scoring and contrast-enhanced CT angiography. Curr Mol Med 2006;6(5):525-39.
30. Seshadri N, Whitlow PL, Acharya N, Houghtaling P, Blackstone EH, Ellis SG. Emergency coronary artery bypass surgery in the contemporary percutaneous coronary intervention era. Circulation 2002;106(18):2346-50.
31. Schiemann M, Killmann R, Kleen M, Abolmaali N, Finney J, Vogl TJ. Vascular guide wire navigation with a magnetic guidance system: experimental results in a phantom. Radiology 2004;232(2):475-81.
32. Wood BJ, Zhang H, Durrani A, Glossop N, Ranjan S, Lindisch D, Levy E, Banovac F, Borgert J, Krueger S and others. Navigation with electromagnetic tracking for interventional radiology procedures: a feasibility study. J Vasc Interv Radiol 2005;16(4):493-505.
33. Krings T, Finney J, Niggemann P, Reinacher P, Luck N, Drexler A, Lovell J, Meyer A, Sehra R, Schauerte P and others. Magnetic versus manual guidewire manipulation in neuroradiology: in vitro results. Neuroradiology 2006;48(6):394-401.
34. García-García Héctor M., Tsuchida Keiichi, Meulenbrug Hans, Ong Andrew T.L., Van der Giessen Willem J. W, PW. S. Magnetic navigation in a coronary phantom: experimental results. EuroIntervention 2005;1(3):321-328.
35. Ramcharitar S, Patterson MS, van Geuns RJ, van der Ent M, Sianos G, Welten GM, van Domburg RT, Serruys PW. A randomised controlled study comparing conventional and magnetic guidewires in a two-dimensional branching tortuous phantom simulating angulated coronary vessels. Catheter Cardiovasc Interv 2007.
36. Atmakuri SR, Lev EI, Alviar C, Ibarra E, Raizner AE, Solomon SL, Kleiman NS. Initial experience with a magnetic navigation system for percutaneous coronary intervention in complex coronary artery lesions. J Am Coll Cardiol 2006;47(3):515-21.
37. Tsuchida K, Garcia-Garcia HM, van der Giessen WJ, McFadden EP, van der Ent M, Sianos G, Meulenbrug H, Ong AT, Serruys PW. Guidewire navigation in coronary artery stenoses using a novel magnetic navigation system: first clinical experience. Catheter Cardiovasc Interv 2006;67(3):356-63.
38. Bach RG, Leach C, Milov SA, Lindsay BD. Use of magnetic navigation to facilitate transcatheter alcohol septal ablation for hypertrophic obstructive cardiomyopathy. J Invasive Cardiol 2006;18(6):E176-8.

39. Ramcharitar S, Patterson MS, van Geuns RJ, Serruys PW. Magnetic navigation system used successfully to cross a crushed stent in a bifurcation that failed with conventional wires. Catheter Cardiovasc Interv 2007;69(6):852-5.
40. Frangos C, Noble S, Noble J, Bilodeau L. [Chronic total occlusion: the last frontier of the interventional cardiology?]. Rev Med Suisse 2007;3(113):1392-4, 1396-8.
41. Di Mario C, Werner GS, Sianos G, Galassi A, Büttner J et al for the EuroCTO Club JS. European perspective in the recanalisation of Chronic Total Occlusions (CTO): consensus document from the EuroCTO Club Eurointervention 2007;3(30-43).
42. Baim DS, Braden G, Heuser R, Popma JJ, Cutlip DE, Massaro JM, Marulkar S, Arvay LJ, Kuntz RE. Utility of the Safe-Cross-guided radiofrequency total occlusion crossing system in chronic coronary total occlusions (results from the Guided Radio Frequency Energy Ablation of Total Occlusions Registry Study). Am J Cardiol 2004;94(7):853-8.
43. Garcia-Garcia HM, Tsuchida K, van Mieghem C, Daemen J, van Weenen S, Patterson M, van der Ent M, van der Giessen WJ, Meulenbrug H, Sehra R and others. Multi-slice computed tomography and magnetic navigation-initial experience of cutting edge new technology in the treatment of chronic total occlusions. Eurointervention 2007.
44. Mouquet F, Pfister O, Jain M, Oikonomopoulos A, Ngoy S, Summer R, Fine A, Liao R. Restoration of cardiac progenitor cells after myocardial infarction by self-proliferation and selective homing of bone marrow-derived stem cells. Circ Res 2005;97(11):1090-2.
45. Perin EC, Dohmann HF, Borojevic R, Silva SA, Sousa AL, Mesquita CT, Rossi MI, Carvalho AC, Dutra HS, Dohmann HJ and others. Transendocardial, autologous bone marrow cell transplantation for severe, chronic ischemic heart failure. Circulation 2003;107(18):2294-302.
46. Fuchs S, Satler LF, Kornowski R, Okubagzi P, Weisz G, Baffour R, Waksman R, Weissman NJ, Cerqueira M, Leon MB and others. Catheter-based autologous bone marrow myocardial injection in no-option patients with advanced coronary artery disease: a feasibility study. J Am Coll Cardiol 2003;41(10):1721-4.
47. Perin E, Silva G, Fernandes M, Munger T, Pandey A, Sehra R, Talcott M, Bichard C, Creed J, J W and others. First experience with remote left ventricular mapping and transendocardial cell injection with a novel integrated magnetic navigation-guided electromechanical mapping system Eurointervention 2007.
48. Ernst S, Ouyang F, Linder C, Hertting K, Stahl F, Chun J, Hachiya H, Bansch D, Antz M, Kuck KH. Initial experience with remote catheter ablation using a novel magnetic navigation system: magnetic remote catheter ablation. Circulation 2004;109(12):1472-5.
49. Pappone C, Vicedomini G, Manguso F, Gugliotta F, Mazzone P, Gulletta S, Sora N, Sala S, Marzi A, Augello G and others. Robotic magnetic navigation for atrial fibrillation ablation. J Am Coll Cardiol 2006;47(7):1390-400.
50. Beyar R, Gruberg L, Deleanu D, Roguin A, Almagor Y, Cohen S, Kumar G, Wenderow T. Remote-control percutaneous coronary interventions: concept, validation, and first-in-humans pilot clinical trial. J Am Coll Cardiol 2006;47(2):296-300.

Chapter 2

EVALUATING THE ACCURACY AND PERFORMANCE IN PHANTOM MODELS

A Randomised controlled study comparing Conventional and Magnetic guidewires in a 2-Dimensional Branching Tortuous Phantom simulating angulated coronary vessels

Catheter Cardiovasc Interv 2007 Nov 1;70 (5):662-8.

Ramcharitar S, Patterson M, van Geuns RJ, van der Ent M, Welten G, van Domburg RT, Serruys PW

Abstract

Objectives:
To directly compare the magnetic navigation system (MNS) guidewires with conventional guidewires in branching tortuous phantoms with operators of varying MNS and percutaneous coronary intervention experience.

Background:
Vessel tortuosity, angulation, and side branches remain limiting factors in coronary interventions. The MNS addresses these limitations by precisely directing the tip of a magnetised guidewire in vivo aided by two permanent adjustable external magnets.

Methods:
Crossing and fluoroscopy times of six operators were evaluated in five tortuous Perspex® phantom vessels in three consecutive attempts. Standard guidewire (SG) usage was unrestricted. Two 2nd generation magnetic guidewires (MG) were used. Failure was noted if the cross was unsuccessful within 5 min.

Results:
The magnetic navigation was vastly superior to SG techniques with increasingly tortuous phantoms. It dramatically decreased both the crossing and fluoroscopy times with maximal reduction from 201.7 ± 111 to 36.4 ± 13 sec, $P < 0.001$ and 204.7 ± 24 to 47.2 ± 19 sec, $P < 0.001$, respectively. The MNS had a 98.8% procedural success rate compared to 68% with SG techniques. Moreover it considerably limited the amount of wire usage from 5.5 to 1.3. Operators with prior MG experience performed significantly better than those without, except in the simplest phantom where the difference was nonsignificant (33.8 ± 13 sec vs. 41.7 ± 17 sec, $P = 0.2$).

Conclusion:
MNS significantly reduces both the crossing and fluoroscopy times in tortuous coronary phantom models achieving excellent success rates with dramatic reductions in guidewire usage. Operators with prior MNS experience had an advantage over the inexperienced

Introduction

The tortuosity and side branches in a coronary tree can determine the procedural outcome of a percutaneous coronary intervention (PCI) [[1]]. An appropriate guidewire that manoeuvres easily through a tortuous segment or side branch can avoid complications such as a dissection or a perforation. The success in crossing a lesion depends both on the appropriate shape at the tip of the guidewire and the manual dexterity of the operator. As such the tip of a guidewire may require reshaping several times during an interventional procedure in a process of trial and error. Additionally, the frictional contact of a preshaped wire on the vascular wall can limit the amount of torque transmitted by the operator leading to wire prolapse. As complexity increases these standard coronary guidewire limitations can often lead to longer procedural and fluoroscopy times together with the use of higher contrast loads [[2]]. The magnetic navigation system (MNS) with its steerable wire can potentially address some of the above limitations [[3]]. In a random set of patients who underwent PCI, both the procedural and fluoroscopy times were significantly reduced [[4]] and confirmed results obtained in a nontortuous coronary vessel phantom [[5]]. To address tortuosity, more complex and tortuous anatomy phantom models of the hepatic, coeliac arteries [[6]], and the cerebral arteries [[7]] have been previously used to compare MNS with standard techniques but thus far no comparison has been made with tortuous coronary phantoms by practicing interventional cardiologist.

In this randomised study we assessed the efficacy of the MNS guidewires with conventional guidewires in phantom vessels with varying degrees of angulation and reduction in vessel's caliber so as to mimic a coronary trunk and its' side branch. Our aims were to determine: (a) the crossing time to reach to a fixed point on the phantom using magnetic navigation in comparison to manual manipulation of the wire in the hands of interventional cardiologists with varying MNS experience, (b) to determine if there is a reduction in fluoroscopy time, (c) and to assess the procedural success and wire usage between the two different approaches for each of the phantom vessels evaluated.

Material and Methods

The Stereotaxis Niobe® II MNS (Stereotaxis, St. Louis, MO) has two permanent adjustable magnets that can be rotated, translated, or tilted to produce a uniform magnetic field of 0.08 T. This field precisely directs a tiny magnet mounted on the tip of a guidewire by changing its' magnetic moment and allows fine control of the orientation of the tip of the guidewire in space. The system is integrated with a modified C-arm flat-panel detector fluoroscopic imaging suite (AXIOM Artis dFC, Siemens Medical Solutions, Forchheim, Germany) for angiographic imaging. A three-dimensional (3D) virtual vessel roadmap can be created from two angiographic images provided that they are 30° apart by using reconstruction software (CardiOp-B, Paieon Medical, Rosh Ha'ayin, Israel). As our phantom models were two-dimensional (2D) we chose the alternative 2D mode displayed as a "clock face" on a touch screen monitor (Fig. 1). In this 2D navigation mode touching the screen at a particular point results in the Navigant software calculating a

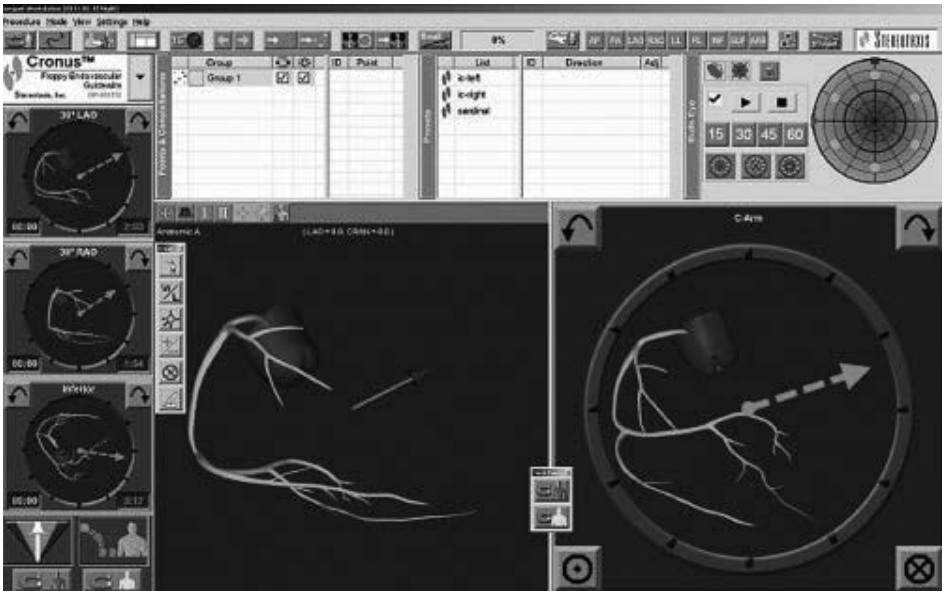

Figure 1 *The "clockface" navigation system*

vector that directs a magnetic field to align the wire tip in the desired direction. The advantage of this technology is that it allows a full 360° omni directional rotation of the tip of the wire at anytime during the procedure, in vivo, without the need for a preshaping wire's tip.

The Guidewires

The Titan™ Soft Support coronary guidewire (Stereotaxis, St. Louis, MO) is a 180 cm moderate support, hydrophilic coated wire with a diameter of 0.014 in./0.36 mm having a flexible 2-cm distal coiled tip that has a 2 or 3 mm gold cup neodynium magnet attached. The Pegasus™ guidewire is similar to the Titan Soft Support coronary guidewire apart from its more hydrophilic nitinol coating. The conventional wires used in the study were PT Graphix™ Intermediate, Choice™ PT Floppy (Boston Scientific, Miami, FL), Miracle bros™3G (Abbott Vascular Devices, Redwood, CA) and high torque BMW (Guidant, Santa Clara CA).

The Phantom

The phantom is a Perspex® model with 3 and 2 mm channels simulating five different tortuous vessels with varying degrees of difficulty graded 1-5 due to increasing angulations and side branches (Fig. 2). In the least tortuous phantom A both the magnetic (MG) and standard (SG) guidewires were required to traverse a 120° turn followed by a right angle bend in a simulated vessel of 3 mm calibre. This was in contrast to the most challenging and tortuous simulated vessel (phantom E) where upon a 3 mm vessel gave rise to a 2 mm side branch at a right angle and then made a sharp 120° turning. To simulate tissue lubricity the phantoms were wetted with a mixture of soap and diluted contrast.

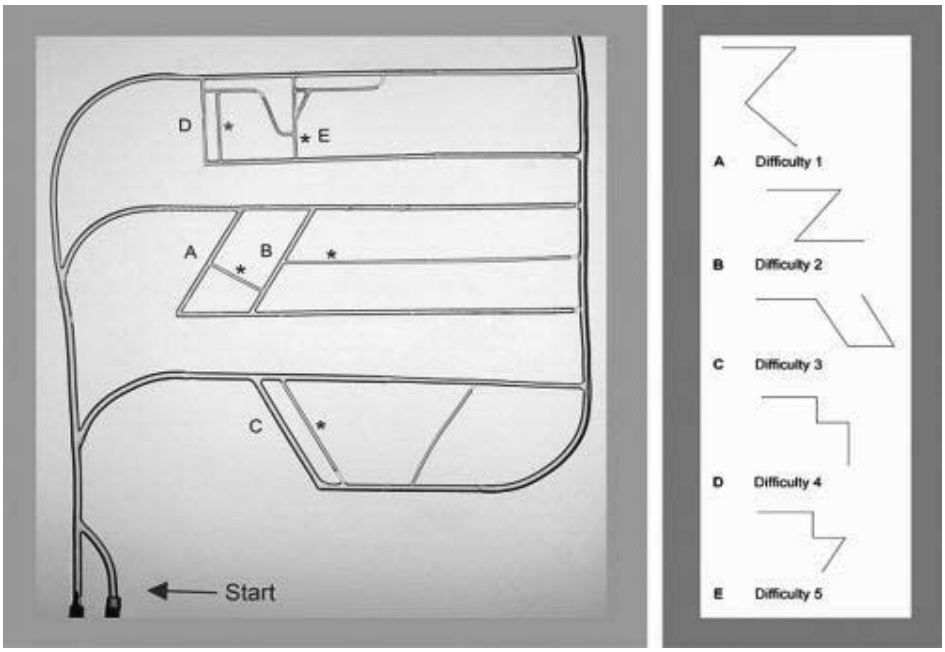

Figure 2 *The phantom A-E with diagramatic representation of the level of difficulty. The angles and "vessel" caliber are as follows: (A) 3 mm, 120° turn into a 3 mm, 90° turn; (B) 3 mm, 120° turn into a 3 mm, 90° turn; (C) 3 mm, 60° turn into a 3 mm, 120 turn and then into a 60° turn to a 2 mm vessel; (D) 3 mm, 90° into a 2 mm followed by a 90° turn; (E) 3 mm, 90° into a 2 mm followed by a 120° turn. The "arrow" indicates the starting point and the asterisk (*) show the end of each phantom run.*

The Procedure

The phantom model was fitted with a 6 French diagnostic catheter, filled with 20% contrast solution and placed in the magnetic field of the MNS. Six interventional cardiologists from our institution were divided into three groups depending on their level of experience with magnetic navigation and SG techniques. In the group 1, operators 1 and 2 had the most MNS experienced with each having performed more than 35 magnetic aided cases. Group 2 (operators 3 and 4) had moderate MNS experience with less than 35 cases and group 3 had MNS inexperienced operators (operators 5 and 6) and they were also the most junior of all the conventional interventionalists. The operators were randomly assigned to start with either a SG of their choice or one of the two 2nd-generation magnetically enabled wires. Operators had to manipulate their guidewire past a fixed point along the simulated phantom vessel (A-E). The crossing and fluoroscopy times were measured when the wire positioned at the tip of the catheter passed a predetermined fixed point on the phantom (Fig. 2). Recordings for both the MG and SG were triplicated for each simulated phantom vessel and an average crossing and fluoroscopy time was determined for each group of operators.

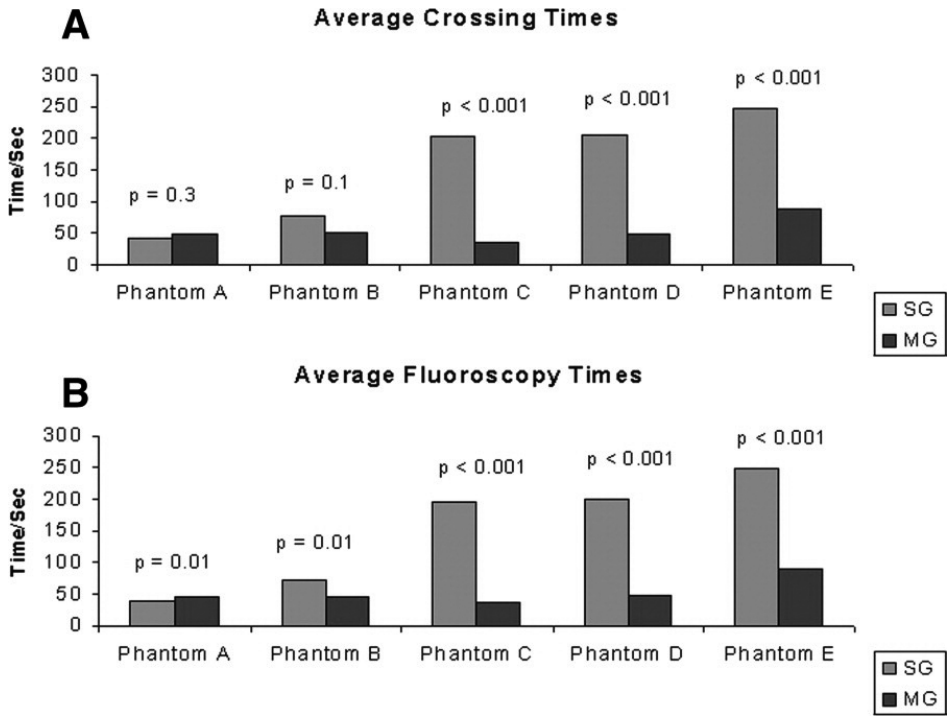

Figure 3 *(A) The average crossing times/sec obtained using SG and MG for all operators with phantoms A-E. (SG, standard guidewire; MG, magnetic guidewire). (B) The average fluoroscopy times/sec obtained using SG and MG for all operators with phantoms A-E. (SG, standard guidewire; MG, magnetic guidewire).*

To compensate for any deterioration in the guidewire's tip or wire performance during the procedure the operators were allowed to exchange a damaged wire for a new or different guidewire as many times as deemed necessary so as to achieve a successful cross within 5 min. If the vessel was not crossed during this 5-min period then the attempt was classed as unsuccessful due to a time failure. Each time failure was recorded as 300 sec for both the crossing and fluoroscopy times. However, it must be stressed, that this value was in fact an underestimation of the time it would have taken if the operator had eventually crossed the simulated vessel.

Statistics

As the crossing times and fluoroscopic exposure times were continuous variables they are presented as means and standard deviation. *T*-test and one-way ANOVA (Bonferoni) were used to determine if there were significant differences in the procedural time and fluoroscopic times. Analyses were performed using SPSS 11.5 for Windows (SPSS, Chicago, IL). *P* value <0.05 was considered statistically significant.

Results

Crossing and Fluoroscopy Times in Phantoms A-E

Overall, the MG was vastly superior to the SG in both the crossing and fluoroscopy times (Fig. 3). The SG was faster than the MG in phantom A (41.8 ± 26 sec vs. 47.9 ± 20 sec, $P = 0.3$) however the difference was not significant (Fig. 3A). In phantom B, the average MG crossing time was shorter than the SG (49.3 ± 23 sec vs. 76.5 ± 65 sec, $P = 0.1$) but was significantly less in the more tortuous phantoms C and D with dramatic reductions in crossing times from 201.7 ± 111 to 36.4 ± 13 sec, $P < 0.001$ and 204.7 ± 24 to 47.2 ± 19 sec, $P < 0.001$, respectively. Similar results were observed with the most angulated phantom E where it was greatly superior in manipulating through a 2 mm side branch (89.1 ± 65 sec vs. 247.3 ± 82 sec, $P < 0.001$).

In the majority of cases the trend of fluoroscopy times (Fig. 3B) closely mimicked that observed in the crossing times. As such, phantom A had longer fluoroscopy times with the MG (47.7 ± 23 sec vs. 72.0 ± 58 sec, $P = 0.1$) and phantom B had longer fluoroscopy times with the SG (47.7 ± 23 sec vs. 72 ± 58 sec, $P = 0.1$). With increasing complexity (phantoms C-E) there were both significant and dramatic reductions in fluoroscopy times similar to that reported with the crossing times.

Sub-Group Analysis of Crossing Times in Phantoms A-E

On the subgroup analysis of the operator performances (Fig. 4), in the simplest phantom A the most MNS experienced operators (group 1) were significantly faster (28.5 ± 9 sec vs. 60.7 ± 18 sec, $P < 0.007$) than those inexperienced (group 3). This was not surprising as the inexperienced group needed to get acquainted with the equipment. The overall decrease performance of the MG to the SG (41.8 ± 26 sec vs. 47.9 ± 20 sec, $P = 0.3$) was thus due to the longer times attained by groups 2 and 3 since group 1 was faster with the MG (28.5 sec vs. 32.8 sec). In phantom B, group 1 performances with the MG were also significantly faster than group 3 (26.2 ± 4 sec vs. 53.7 ± 13 sec, $P = 0.025$) but there was no significant difference observed between groups 2 and 3 (68.0 ± 24 sec vs. 53.7 ± 13 sec, $P = 0.4$). Of note in this phantom, both groups 1 and 3 times with the SG were more than twice that of MG (64.7 and 112.8 sec vs. 26.2 and 53.7 sec, respectively) with the intermediate experienced group 2 having no significant difference with either wire (MG, 68.0 sec and SG, 52.0 sec).

As the tortuosity and branching increased (phantoms C-E) there was a dramatic difference between the MG and SG performances amongst all the groups (Fig. 4). In phantoms C there was no significant difference between all the MG users regardless of previous MNS experience and in phantom D only group 1 remained significantly faster than group 3 (39.5 ± 12 sec vs. 62.7 ± 21 sec, $P = 0.008$). With the conventional wire technique a similar trend was observed with no significant differences between the senior (groups 1 and 2) and the junior (group 3) operators in both phantoms C (190.8 ± 113 sec vs. 223.7 ± 112 sec, $P = 0.6$) and phantom D (205.9 ± 106

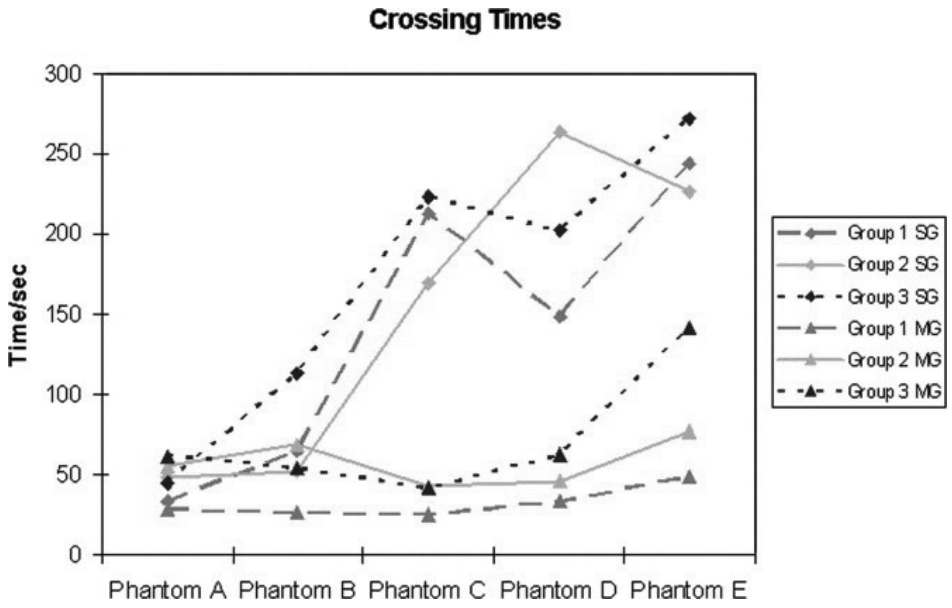

Figure 4 *The average crossing times/sec obtained using SG and MG for groups 1-3, operators with phantoms A-E. (SG. standard guidewire; MG, magnetic guidewire).*

sec vs. 202.3 ± 109 sec, $P = 0.9$). This trend continued in phantom E were groups 1 and 3 had non-significant time differences (244.2 ± 99 sec vs. 271.5 ± 70 sec, $P = 0.9$) with the SG and group 1 still being significantly faster with the MG than group 3 (48.8 ± 12 sec vs. 141.5 ± 85 sec, $P = 0.03$). Overall, the operators with previous MNS experienced (groups 1 and 2) performed better (62.8 ± 31 sec vs. 141.5 ± 85 sec, $P = 0.01$) in this phantom.

Procedural Success and Wire Usage in Phantom A-E

There were 100% successful crossings in phantoms A and B with both the MG and SG (Fig. 5A). In phantom C and D, the procedural success with the SG was (10/18) 56% and (9/18) 50%, respectively as compared to a 100% success with the MG. The success of the SG in the most tortuous phantom E was only (8/18) 33% and the MG (17/18) 94%. The one failure with the MG was observed in an operator with no prior MNS experience.

Up to eight SG were used by operator 1 with a 60% overall success rate (9/15 successful crossings), to manipulate through all the phantoms (Fig. 5B). In contrast, a maximum of two MG (operator 5) were used for the same task with a 93% success rate (14/15 successful crossings). The overall ratio of SG to MG usage was found to be 5.5 SG to 1.3 MG

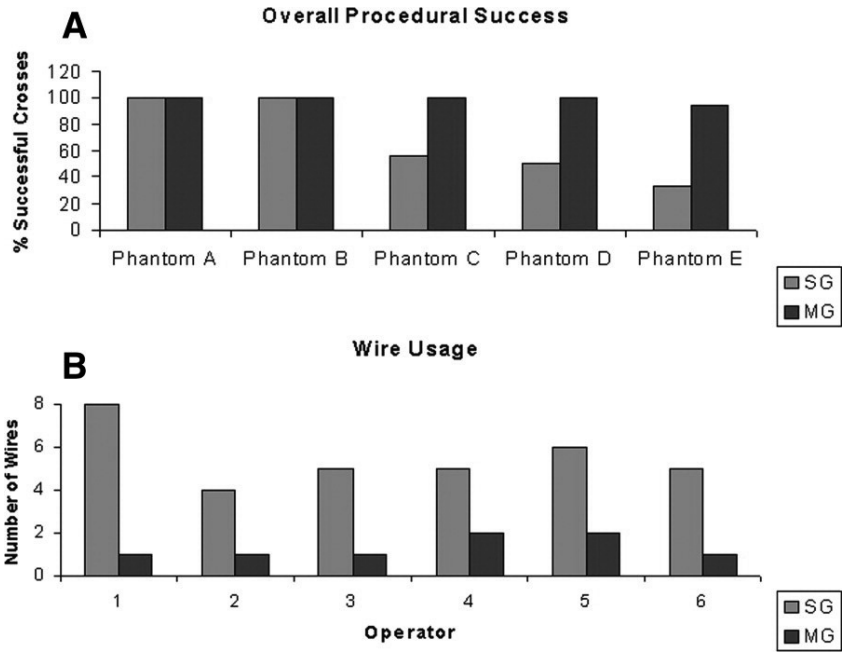

Figure 5 *(A) The overall procedural success using SG and MG for phantoms A-E. (SG, standard guidewire; MG, magnetic guidewire). (B) The SG and MG usage in operators 1-6 for phantoms A-E. (SG, standard guidewire; MG, magnetic guidewire).*

Limitations

Our study was limited by the fact that 2D phantoms were not representative of the 3D characteristics of ordinary coronary arteries. In addition, these 2D models were limited to "clockface" navigation rather than the more precise 3D reconstruction software. The phantoms also employed static road mapping for wire progression rather than the transient dynamic road mapping used in patients.

Conclusions

MNS is an emerging tool in interventional cardiology and has been successfully employed to cross lesions that failed with conventional techniques. In our phantom study we have unequivocally shown that a MG is vastly superior to a SG with dramatic reductions in crossing and fluoroscopy times in phantom models that mimic coronary arteries with increasing tortuosity and side branches. As the complexity of the phantoms increased operators with prior MNS experience performed better than those with no previous MNS exposure. There was an outstanding procedural success with the MNS (98.8% vs. 68%) together with a clear reduction guidewire usage (5.5 vs. 1.3).

Acknowledgements

We thank additional operators, Dr Sophia Vaina MD PhD and Mark van der Linden MD. Michael Dias, John Lovell, and Emanuel de Pins of Stereotaxis, Inc., St. Louis, Missouri for kindly supplying the phantom. Special thanks to Jan Tuin for image preparation.

References

1. Zaacks SM,Allen JE,Calvin JE,Schaer GL,Palvas BW,Parrillo JE,Klein LW. Value of the American College of Cardiology/American Heart Association stenosis morphology classification for coronary interventions in the late 1990s. *Am J Cardiol* 1998; **82**: 43-49.
2. Atmakuri SR,Lev EI,Alviar C,Ibarra E,Raizner AE,Solomon SL,Kleiman NS. Initial experience with a magnetic navigation system for percutaneous coronary intervention in complex coronary artery lesions. *J Am Coll Cardiol* 2006; **47**: 515-521
3. Tsuchida K,García-García Héctor M,Tanimoto Shuzou,Ong Andrew TL,Sehra Ruchir,van der Ent Martin,Sianos Georgios,van der Giessen Willem JWSP. Feasibility and safety of guidewire navigation using a magnetic navigation system in coronary artery stenoses. *EuroIntervention* 2005; **1**: 329-335.
4. Tsuchida K,Garcia-Garcia HM,van der Giessen WJ,McFadden EP,van der Ent M,Sianos G,Meulenbrug H,Ong AT,Serruys PW. Guidewire navigation in coronary artery stenoses using a novel magnetic navigation system: First clinical experience. *Catheter Cardiovasc Interv* 2006; **67**: 356-363.
5. García-García Héctor M,Tsuchida Keiichi,Meulenbrug Hans,Ong Andrew TL,Van der Giessen Willem JWSP. Magnetic navigation in a coronary phantom: Experimental results. *EuroIntervention* 2005; **1**: 321-328.
6. Schiemann M,Killmann R,Kleen M,Abolmaali N,Finney J,Vogl TJ. Vascular guide wire navigation with a magnetic guidance system: Experimental results in a phantom. *Radiology* 2004; **232**: 475-481.
7. Krings T,Finney J,Niggemann P,Reinacher P,Luck N,Drexler A,Lovell J,Meyer A,Sehra R,Schauerte P, et al. Magnetic versus manual guidewire manipulation in neuroradiology: In vitro results. *Neuroradiology* 2006; **48**: 394-401.
8. Faddis MN,Blume W,Finney J,Hall A,Rauch J,Sell J,Bae KT,Talcott M,Lindsay B. Novel, magnetically guided catheter for endocardial mapping and radiofrequency catheter ablation. *Circulation* 2002; **106**: 2980-2985
9. Ernst S,Ouyang F,Linder C,Hertting K,Stahl F,Chun J,Hachiya H,Bansch D,Antz M,Kuck KH. Initial experience with remote catheter ablation using a novel magnetic navigation system: Magnetic remote catheter ablation. *Circulation* 2004; **109**: 1472-1475.
10. Patterson M,Schotten J,van Mieghem C,Kiemeneij F,Serruys PW. Magnetic navigation in percutaneous coronary intervention. *J Interv Cardiol* 2006; **19**: 558-565.
11. Ramcharitar S,Patterson MS,van Geuns RJ,Serruys PW. Magnetic navigation system used successfully to cross a crushed stent in a bifurcation that failed with conventional wires. *Catheter Cardiovasc Interv* [Published online Dec 26, 2006].
12. Ellis SG,Vandormael MG,Cowley MJ,DiSciascio G,Deligonul U,Topol EJ,Bulle TM. Coronary morphologic and clinical determinants of procedural outcome with angioplasty for multivessel coronary disease. Implications for patient selection. Multivessel Angioplasty Prognosis Study Group. *Circulation* 1990; **82**: 1193-1202.
13. Seshadri N,Whitlow PL,Acharya N,Houghtaling P,Blackstone EH,Ellis SG. Emergency coronary artery bypass surgery in the contemporary percutaneous coronary intervention era. *Circulation* 2002; **106**: 2346-2350.
14. Bernardi G,Padovani R,Morocutti G,Vano E,Malisan MR,Rinuncini M,Spedicato L,Fioretti PM. Clinical and technical determinants of the complexity of percutaneous transluminal coronary angioplasty procedures: analysis in relation to radiation exposure parameters. *Catheter Cardiovasc Interv* 2000; **51**: 1-9; discussion 10.
15. Wilensky RL,Selzer F,Johnston J,Laskey WK,Klugherz BD,Block P,Cohen H,Detre K,Williams DO. Relation of percutaneous coronary intervention of complex lesions to clinical outcomes (from the NHLBI Dynamic Registry). *Am J Cardiol* 2002; **90**: 216-221
16. Dotter CT,Judkins MP. Transluminal treatment of arteriosclerotic obstruction. Description of a new technic and a preliminary report of its application. *Circulation* 1964; **30**: 654-670.

17. Dietrich T,Kleen M,Killmann R,Wiesinger B,Wiskirchen J,Tepe G,Claussen CD,Duda SH. Evaluation of magnetic navigation in an in vitro model of uterine artery embolization. *J Vasc Interv Radiol* 2004; **15**: 1457-1462.

EVALUATING THE ACCURACY AND PERFORMANCE IN PHANTOM MODELS

First direct in vivo comparison of two commercially available three-dimensional quantitative coronary angiography systems

Catheter Cardiovasc Interv 2008 Jan 1;71 (1):44-50

Ramcharitar S, Daemen J, Patterson M, van Geuns RJ, Boersma E, Serruys PW and van der Giessen WJ

Abstract

Objectives:

The in vivo comparison of the accuracy of two 3-dimensional quantitative coronary angiography (QCA) systems

Methods:

Precision-drilled plexiglass phantoms with five different luminal diameters (0.5-1.9 mm) were percutaneously inserted into the coronary arteries of four Yorkshire pigs. Twenty-one angiographic images of these stenotic phantoms were acquired for in vivo validation testing. Quantitative assessments of the minimum, maximum, and mean luminal diameters together with the minimum luminal area were determined using two 3D QCA systems, the CardiOp-B® and CAAS 5

Results:

The CardiOp-B system significantly underestimated the minimum luminal diameter MLD whilst both systems significantly overestimated the maximum luminal diameter at the minimal luminal area (MLA) over the phantom's true value. The CAAS 5 system had a greater degree of accuracy/mm (mean difference = 0.01 vs. 0.03) and precision/mm (SD = 0.09 vs. 0.23) than the CardiOp-B in assessing the minimal LD. An increased precision/mm (SD = 0.01 vs. 0.29) and accuracy/mm (mean difference = 0.03 vs. 0.11) in the mean LD was observed with the CAAS 5. In comparing the MLA/mm^2 the CAAS 5 was more precise/mm^2 (SD = 0.14 vs. 0.55) and accurate/mm^2 (mean difference = 0.12 vs. 0.02) to the true phantom MLA compared to the CardiOp-B system.

Conclusion:

In a 21 phantom study, the CAAS 5 3D QCA system had a greater degree of accuracy and precision in both the luminal and area measurements than the CardiOp-B 3D QCA system.

Introduction

In the percutaneous treatment of coronary artery disease the on-line two-dimensional quantitative angiography (QCA) is often the chosen method to determine both the vessel length and size to guide stent implantation [[1]]. There are, however, several limitations with this technique as depending on the angiographic views the vessels can appear foreshortened or overlapped resulting in inaccurate measurements [[2]]. Moreover, in tortuous vessels this can lead to an underestimation of the appropriate length of stent required to cover the lesion [[3]]. Recently, a novel method, the three-dimensional (3D) reconstruction of standard coronary angiography using an algorithm integrating single-plane images has been validated [[4]]. This technology is aimed at providing a solution to many of the limitations inherent with 2D-QCA. In addition, the enhanced accuracy in determining the lesion length and luminal diameter the 3D reconstructed image can be incorporated in a designated navigation software (Navigant® Stereotaxis, St Louis, MO) to enable magnetically aided guidewires to precisely transit through the vessel lumen [[5]]. The accuracy of the luminal diameter can be crucial for a successful wire transit to avoid vascular wall trauma or plaque disruption [[6]]. The potential benefits of this 3D-QCA technology has led two companies Paieon Medical, Rosh Ha'ayin, Israel and Pie Medical Imaging, Maastricht, the Netherlands to develop the CardiOp-B and CAAS 5 systems, respectively. Both systems are similar in using two angiographic images to reconstruct a 3D image but in the current version of the CardiOp-B the calibration standard is performed manually whilst in the CAAS 5 system it is automated. The aim of this study was to compare the accuracy of the detection of a luminal stenosis using two 3D QCA systems in vivo using radiolucent cylindrical plexiglass or polyamide stenotic phantoms with precision-drilled eccentric lumens implanted in porcine coronary arteries [[7]].

Material and Methods

The ethics committee on animal experimentation at the Erasmus Medical Center, Rotterdam, NL approved the study that was conducted in accordance to the guidelines of the American Heart Association on animal use in research.

Preparation and Insertion of the Stenotic Phantoms

The stenotic phantoms (Fig. 1) were precisely engineered by the Department of Bioengineering at the Erasmus Medical Center. Radiolucent plexiglass (acrylate) and polyacrylamide cylinders of diameters 3.0 or 3.5 mm and length of 8.28, 7.96, 7.85, 8.01, and 7.38 mm were precision-drilled to have circular lumens of 499 (aimed to be 0.5 mm), 707 (0.7 mm), 982 (1.0 mm), 1,367 (1.4 mm), and 1,921 (1.9 mm) μm in diameter, respectively. This accuracy calibrated optically at 40-fold magnification achieved a maximum tolerance of 0.003 mm. A second 1.3 mm diameter lumen was drilled parallel to the stenosis lumen to attach to the tip of 4-Fr Fogarty catheters (Vermed, Neuilly en Thelle, France) to facilitate the intracoronary insertion and positioning of the phantoms. Four Yorkshire pigs (average weight, 40-45 kg) were pretreated with intramuscular

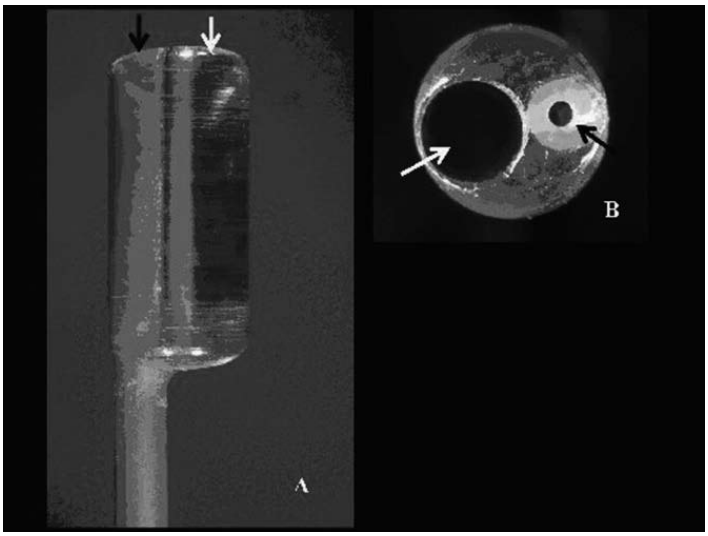

Figure 1. *The magnified tip of one of the Fogarty catheters view along its long (A) and short axis (B) with a transparent radiolucent cylinder (phantom) having a channel of 1.9 mm diameter (white arrow) and the catheter lumen used for insertion of removable metallic stylet (black arrow) to aid positioning.*

ketamine (20 mg/kg) and intravenous etomidate (5 mg/kg). The animals were then intubated and ventilated with a mixture of oxygen and isoflurane. Anesthesia was maintained with a continuous intravenous infusion of pentobarbital (5-20 mg/kg/hr). A 12-Fr introducer sheath was inserted into both carotid arteries to allow the sequential insertion of the guiding catheter and the phantoms. Jugular access was used for the administration of medication and fluids. An intravenous bolus (10,000 IU/l) followed by a continuous infusion of heparin was given. Following the experiments, the animals were humanely euthanized.

In Vivo Image Acquisition of Stenosis Phantoms by Fluoroscopy

Biplane cine angiographic system (Axiom Artis^{TM}, Siemens, Forchheim, Germany) was used to create digital angiograms of matrix size of 1024 × 1024 pixels. Identical radiographic imaging settings were employed (kVp, mA, ms) in the two projections used to image each phantom to maintain consistency. Following intubation of the left or right coronary artery with a 6-Fr guiding catheter (Mach 1^{TM}, Bos0ton Scientific, Natick, MA) intracoronary isosorbide-dinitrate (1 mg) was administered and an angiogram was made to aid orientation of the phantom in the vessel. The phantoms were wedged in the coronary arteries and positioned in the X-ray isocenter using the tip of a metal wire marker placed on the Fogarty catheter. Coronary angiography was performed by manual injection of contrast medium (Visipaque^{TM} 320 mg I/ml, Amersham Health B.V., Eindhoven, The Netherlands). The ventilator was disconnected transiently during contrast injection to minimize the effect of diaphragmatic movement on angiographic images.

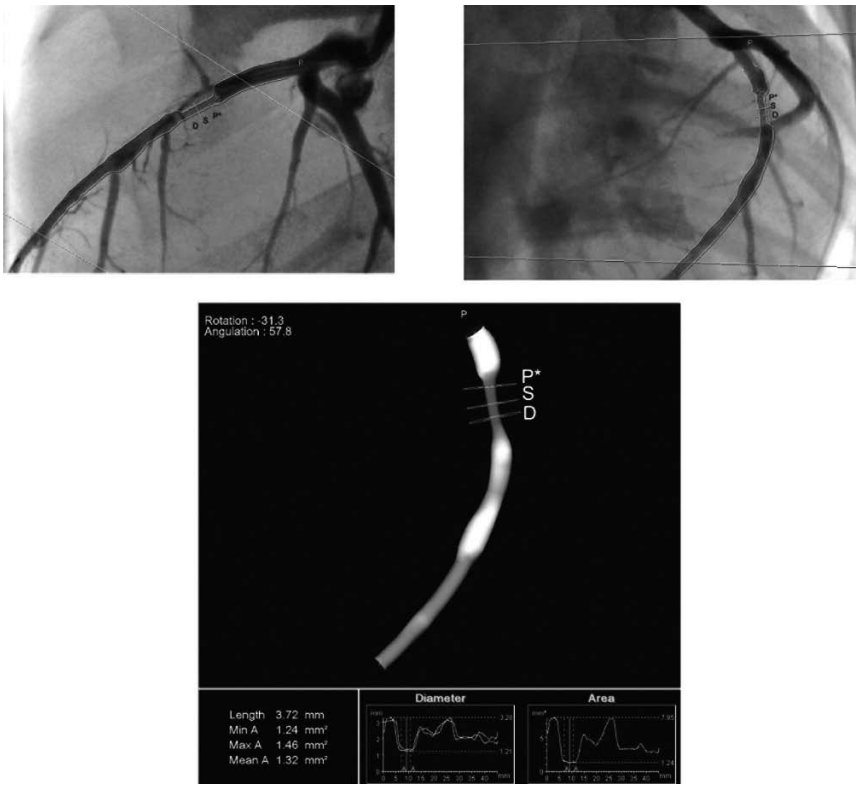

Figure 2. The 3D reconstruction of a phantom derived from two orthogonal views (frontal and lateral) using the CASS 5 system. The 3D color varies according to the severity of stenosis ranging from white (healthy vessel) to dark red (99% cross-sectional area stenosis). The yellow squares denote proximal reference point (P), most stenotic point (S), and distal reference point (D) of the target lesion, respectively. The region of interest (ROI) for calculation of mean luminal diameter can be manually defined by moving the proximal (P*) and distal (D) points (Definition of ROI for mean LD; Graph view).*

Three Dimensional QCA Analyses of In Vivo Phantom Images

In total, 21 readings were made in 21 different arteries; four arteries had phantoms of diameters 1.9 mm, six arteries had phantoms of 1.4 mm, six arteries had 1 mm diameter phantoms, four arteries had 0.7 mm phantoms, and one artery had a 0.5 mm phantom. The in vivo analysis of each phantom was performed in end-diastole on the same number of the frame count and was ECG gated so that all of the analyses using both QCA systems were performed on identical images. Calibration of the CardiOp-B system was done manually using the conventional catheter calibration of the nontapering part of the tip of each 6-Fr guiding catheter filled with contrast. The CAAS 5 system performs an automatic calibration based on the DICOM information in the image. Once calibrated, the two orthogonal views (at least 30° apart) that were simultaneously acquired in the biplane system were then used to reconstruct the 3D vessel image (Fig. 2). This was achieved by marking three points in the CardiOp-B system: proximally, distally, and at the

stenosis on the two angiographic images. In the CAAS 5, this was done by defining a common image point (a landmark common to both images), two points (distal and proximal) to the stenotic region [[8]]. The software then created automatic contour detection and if this was inaccurate then finer adjustments were made to the edge detection manually in the CardiOp-B system and the restriction option, an algorithm that excludes gross image artifacts such as the diagnostic catheter was applied in the CAAS 5 system. The restriction option is therefore not a manual edge correction but instead it offers users the possibility of excluding parts of the image of the detection by restricting the area of interest.

Following contour detection and corrections/restrictions if required, the 3D reconstruction of the artery was automatically created. The software determined the minimum luminal area (MLA) and the pixel size at each position in the 3D space. Based on the position of the MLA and the known pixel size, the minimum luminal diameter (MLD) for each of the angiographic images was automatically calculated. Assuming a noncircular shape at the MLA then there will be two MLD values (maximum and minimum LD) obtained, the smallest representing the absolute MLD. The mean luminal diameter was based on the values in between the borders of a predetermined segment in the phantom (Fig. 2). Along the centerline in between this segment, the diameter at each scanline was taken and divided by the total number of scanlines to automatically afford the mean LD. The following data was therefore compared, the minimum LD (MLD) and the maximum LD at the MLA, together with the minimum luminal area MLA and the mean LD over the region of interest (ROI) in each 3D QCA system to that of the phantom models. We purposely chose to perform only one measurement per phantom given the primary interest in the relative accuracy and precision of both techniques, instead of an assessment of the intra- and inter-observer variability of the QCA techniques. Expert users from both the Pie Medical and Paieon companies were used to perform the measurements.

Statistical Analysis

Continuous variables are presented as mean ± standard deviation and compared using the Wilcoxon signed-rank test. Categorical variables are expressed as counts and percentages. The mean of the differences between measurements and phantom dimensions of both systems was computed and considered to be an index of the accuracy of the measurements, while the standard deviation of the differences was defined as an index of precision. Bland-Altman plots [[9]] were used to assess the agreement between both 3D QCA systems and the phantom models. Pearson's correlation was used to determine the degree of correlation between the measurements. Statistical analyses were performed with SPSS 12.0.1 for Windows (SPSS, Chicago, IL). A P value < 0.05 was considered statistically significant.

Table 1 *Comparison of the two 3-D QCA systems (CardiOp-B® and CAAS 5) accuracy, precision and the correlation to the true luminal diameter of the 21 stenotic Phantoms. Accuracy = mean differences between recorded measurements and the phantom; Precision = standard deviation and p value is derived from the recorded measurements and the phantom*

	Accuracy	Precision	Correlation	Slope	Intercept	P value
CardiOp-B® vs. Phantoms						
min LD (MLD)	0.03	0.23	0.87	0.87	0.15	0.03
max LD	0.24	0.40	0.78	0.86	0.23	0.001
mean LD	0.11	0.29	0.84	1.02	0.08	0.31
MLA	0.12	0.55	0.87	1.09	0.01	0.74
CAAS 5 vs. Phantoms						
min LD (MLD)	0.01	0.09	0.99	0.92	0.06	0.26
max LD	0.06	0.11	0.97	1.12	0.10	0.015
mean LD	0.03	0.10	0.98	0.87	0.19	0.39
MLA	0.02	0.14	0.99	0.91	0.13	0.95

Results

Comparison of Minimum LD with Phantom "True" Values

In this study the CardiOp-B system had only one manual adjustment to correct the detected contour whilst six adjustments were used in the CAAS 5 system to restrict the contours to the region of interest. Overall, the comparison of both 3 D QCA systems with the true LD noted in the 21 phantom models revealed a closer association with the CAAS 5 system than in the CardiOp-B (Table I). The CardiOp-B system significantly underestimated the minimum LD (MLD) whilst both systems significantly overestimated the maximum LD at the MLA over the true value. In assessing the MLD, the CAAS 5 system had a greater degree of accuracy/mm (mean difference = 0.01 vs. 0.03) and precision/mm (SD = 0.09 vs. 0.23) compared with that observed with the CardiOp-B system. The Bland-Altman plots of the MLD (Fig. 3a and b) showed that both systems had one outlier reading beyond 2 SD. This value was, however, smaller in the CAAS 5 system resulting in a better overall correlation to that of the phantom's actual diameter ($r = 0.99$ vs. 0.87) and influencing the degree of precision. Notably, in the CardiOp-B system 11/21 (52%) of the measurements laid outside ± 10% of the true phantom LD compared with 3/21 (14%) of the measurements derived using the CAAS 5 system. Table I and Fig. 3a and b compares min LD (MLD) in both systems.

Comparison of Mean LD with Phantom ¨True" Values

There was no significant difference observed when the mean LD in either system was compared with the luminal diameter of the phantoms (Table I). The Bland-Altman plots revealed two observations outside ± 2 SD range in the CardiOp-B analysis compared with only one

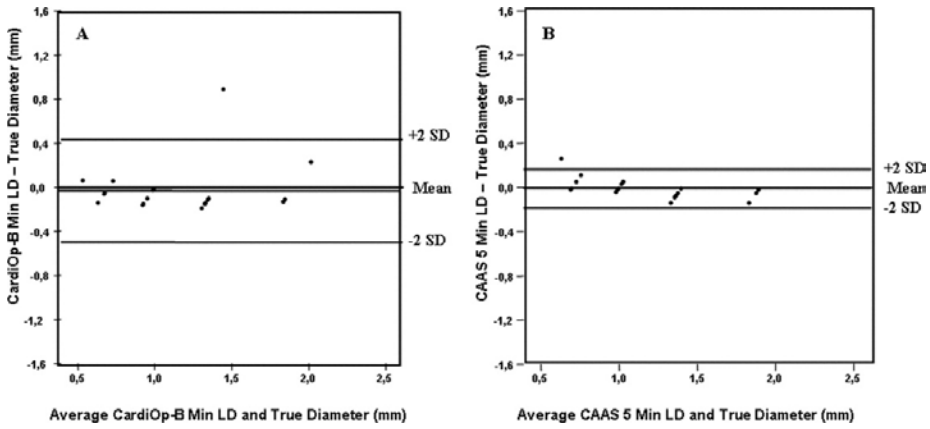

Figure 3. *Bland-Altman plots of the minimal LD (a) CardiOp-B® with the phantoms (b) CAAS 5 with the phantoms.*

observation noted in the CAAS 5 system (Fig. 4a and b). As observed with the minimum LD values there was an increased precision/mm (SD = 0.10 vs. 0.29) and accuracy/mm (mean difference = 0.03 vs. 0.11) with the CAAS 5 mean LD values with the latter having a closer correlation with the true value (r = 0.98 vs. 0.84). Figure 4a and b compares mean LD in both systems.

Comparison of Minimal Luminal Area with Phantom "True" Values

The Bland-Altman plots of the MLA further demonstrated higher precision/mm^2 (SD = 0.14 vs. 0.55) and accuracy/mm^2 (mean difference = 0.02 vs. 0.12) with the CAAS 5 (Fig. 5a and b). Moreover, in the CardiOp-B system 14/21 (67%) of the measurements laid outside ± 10% of the true phantom MLA compared with 7/21 (33%) of the measurements derived using the CAAS 5 system. Consequently, the Pearson coefficient demonstrated a closer correlation with the CAAS 5 than the CardiOp-B system (r = 0.99 vs. 0.87). Figure 5a and b compares mean LD in both systems.

Discussion

3D QCA has been shown in phantom models [[10]] as well as in stented vessel segments [[11]], and complex lesions like bifurcations [[12]] to have a closer correlation to the true vessel's dimensions than 2D QCA. Moreover in conventional angiography, overlapping vessel can impair the optimal visualization of a lesion and if the lesion is eccentric then it may be missed altogether [[13]]. In the formulation of a 3D QCA, the system uses a 3D computer-based modelling algorithm to integrate the 2D projections, identify key vessel features like bifurcations and the centreline, calculate and display the vessel's cross-sectional contours that are subsequently "filled in" to create the virtual vessel. Both the CardiOp-B system and CAAS 5 systems adopts

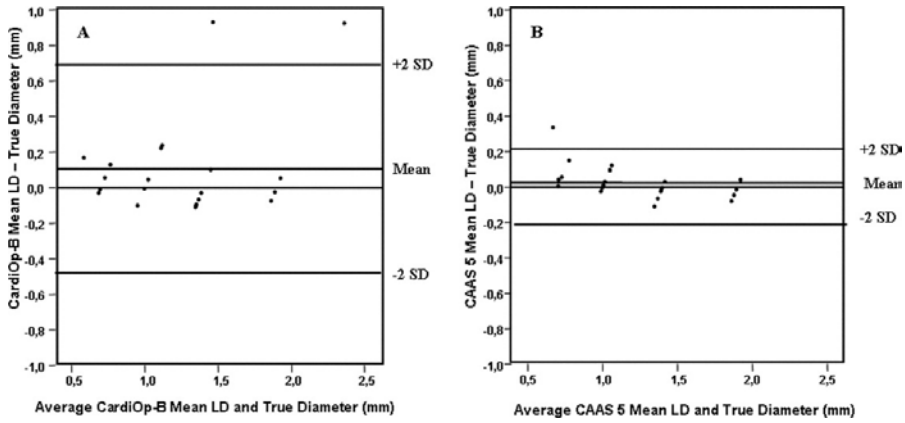

Figure 4. *Bland-Altman plots of the MLD (a) CardiOp-B® with the phantoms (b) CAAS 5 with the phantoms.*

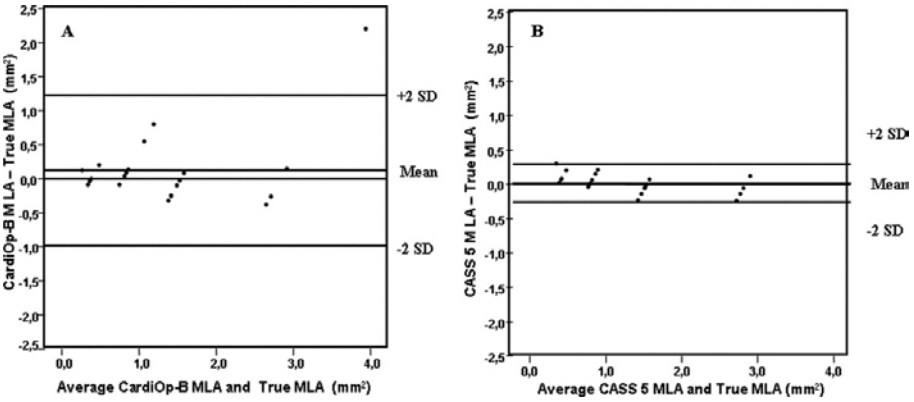

Figure 5. *Bland-Altman plots of the MLA (a) CardiOp-B® with the phantoms (b) CAAS 5 with the phantoms.*

this system when generating the reconstructed vessel but there are subtle differences between the two program that may influence the degree of accuracy. The CardiOp-B system utilizes a manual guide catheter mode calibration method in contrast to the CAAS 5 system that uses an automatic calibration at the region of interest (ROI). With the manual method, the catheter size in French or mm has to be inputted for system recognition and calibration. This is an established method that has been shown to have greater precision than the equivalent 2D measurements with respect to the minimal lesion diameter ($P < 0.005$), minimal lesion area ($P < 0.05$), and lesion length ($P < 0.01$) [[4]]. However, it has been reported that because the catheter may not be in the same plane as the ROI that this method of calibration can give rise to differences in magnification and measurements and influence the accuracy [[13]]. In addition, the way in which the contour is drawn on the 2D angiographic image also highlights an important difference that

may also influence the accuracy and precision between the two systems. Both the CardiOp-B and CAAS 5 systems have the ability to manually correct the generated contours if they are adjudged to be inaccurate. Although this is subjective, in this paired comparative study contour adjustment had to be performed on one of the 21 phantom models in the CardiOpB as the detected contour deviated significantly from the vessel's edge. In the rest of the models, edge detection was adjudged satisfactory. No edge corrections were needed in the CAAS 5 but the catheter had to be excluded from the ROI on six occasions. Because the edge detection is used to deduce the measurement, the less manual correction needed then greater is the accuracy of the automated system.

The aim of this study was to evaluate the accuracy and precision of both the CAAS 5 and CardiOp-B 3D QCA system with respect to precisely engineered stenotic phantoms in vivo. The rational was that in addition to evaluating precision in measurements, the importance of the study stems from the demand to accurately determine the luminal diameter so that a precise endoluminal road map of a vessel can be achieved for magnetic navigation when the 3D reconstructed image is incorporated in the Navigant software [[[14]]]. The lack of accuracy may result in the guidewire exiting from the vessel lumen to cause a perforation. The results demonstrated good overall correlation of the minimal LD and maximum LD at the MLA together with the mean LD and MLA in each system to the true values of the phantoms. However in the CardiOp-B system, the range of these correlations were slightly less (0.78-0.87) compared with the CAAS 5 system (0.97-0.99). In addition, systematic underestimation of luminal diameter measurements has been previously reported for the CardiOp-B system QCA system [[[11]]]. In assessing the minimum LD (MLD), greater precision and accuracy was observed with the CAAS 5 arguably because of two observations in the CardiOp-B system varying markedly from the true value (Δ min LD 47% and 25%) in comparison to one observation (Δ min LD 34%) in the CAAS 5 system. However, what is important to note is that in terms of the accuracy is that 11/21 (52%) of the measurements laid outside ± 10% of the true phantom LD using the CardiOp-B system compared with 3/21 (14%) of the measurements derived using the CAAS 5 system. This was also mirrored with the MLA measurements where two thirds of the values in the CardiOp-B system 14/21 laid outside ± 10% of the true phantom MLA compared with one third (7/21) with the CAAS 5 system. The result highlights the perceived superiority of automatic isocenter calibration together with improved edge detection [[[15]]].

Despite the variability in 3D QCA measurements in both systems, we should remain appreciative of the fact that this novel technology creates a 3-dimensional coronary map and as such have widespread application to both scientific research and clinical practice. By doing so, it solves many of the limitations currently observed with 2D QCA and unlike other imaging modalities like multislice computed tomography and magnetic resonance imaging it can provide absolute measurements of coronary luminal diameter and lengths in real time. It is therefore hopeful that the findings of our study will stimulate further research in this exciting new imaging field.

Limitations

This study is the first direct comparison of two commercially available 3D QCA systems. The study was, however, limited by the relatively small sample size of 21 phantom models. This was due to difficulties in obtaining more animal models. The concentric phantoms used in this study do not represent natural coronary lesions, as they do not allow the assessment of asymmetry. It is better to use eccentric phantoms but precise and validated eccentric phantoms were not available. The validation tests with these cylindrical concentric phantoms were, however, used by our group recently to test 2D and 3D QCA systems [[10]].

Conclusions

In a 21 phantom study, the CAAS 5 3-D QCA system had a greater degree of accuracy and precision in both the luminal and area measurements than the CardiOp-B 3D QCA system. Further development and validation studies are warranted in order for this novel technology to be increasingly adopted in routine clinical practice

Acknowledgements

The authors thank Avital Forsher and Vera Nyssen for performing the analyses.

References

1. Keane D,Haase J,Slager CJ,Montauban van Swijndregt E,Lehmann KG,Ozaki Y,di Mario C,Kirkeeide R,Serruys PW. Comparative validation of quantitative coronary angiography systems. Results and implications from a multicenter study using a standardized approach. *Circulation* 1995; **91**: 2174-2183.
2. Thomas AC,Davies MJ,Dilly S,Dilly N,Franc F. Potential errors in the estimation of coronary arterial stenosis from clinical arteriography with reference to the shape of the coronary arterial lumen. *Br Heart J* 1986; **55**: 129-139
3. Gollapudi RR,Valencia R,Lee SS,Wong GB,Teirstein PS,Price MJ. Utility of three-dimensional reconstruction of coronary angiography to guide percutaneous coronary intervention. *Catheter Cardiovasc Interv* 2007; **69**: 479-482.
4. Dvir D,Marom H,Guetta V,Kornowski R. Three-dimensional coronary reconstruction from routine single-plane coronary angiograms: In vivo quantitative validation. *Int J Cardiovasc Intervent* 2005; **7**: 141-145.
5. Tsuchida K,Garcia-Garcia HM,van der Giessen WJ,McFadden EP,van der Ent M,Sianos G,Meulenbrug H,Ong AT,Serruys PW. Guidewire navigation in coronary artery stenoses using a novel magnetic navigation system: First clinical experience. *Catheter Cardiovasc Interv* 2006; **67**: 356-363.
6. Ramcharitar S,Patterson MS,van Geuns RJ,Serruys PW. Magnetic navigation system used successfully to cross a crushed stent in a bifurcation that failed with conventional wires. *Catheter Cardiovasc Interv* 2007; **69**: 852-855.
7. Haase J,Di Mario C,Slager CJ,van der Giessen WJ,den Boer A,de Feyter PJ,Reiber JH,Verdouw PD,Serruys PW. In-vivo validation of on-line and off-line geometric coronary measurements using insertion of stenosis phantoms in porcine coronary arteries. *Catheter Cardiovasc Diagn* 1992; **27**: 16-27.
8. Green NE,Chen SY,Messenger JC,Groves BM,Carroll JD. Three-dimensional vascular angiography. *Curr Probl Cardiol* 2004; **29**: 104-142.
9. Bland JM,Altman DG. Statistical methods for assessing agreement between two methods of clinical measurement. *Lancet* 1986; **1**: 307-310.
10. Tsuchida K,van der Giessen W,Patterson M,Tanimoto S,García-García H,Regar E,Ligthart J,Maugenest A,Maatrijk G,Wentzel J, et al. In vivo validation of a novel three-dimensional quantitative coronary angiography system (CardiOp-B): Comparison with a conventional two-dimensional system (CAAS II) and with special reference to optical coherence tomography. *Eurointervention* 2007; **3**: 100-108.
11. Gradaus R,Mathies K,Breithardt G,Bocker D. Clinical assessment of a new real time 3D quantitative coronary angiography system: Evaluation in stented vessel segments. *Catheter Cardiovasc Interv* 2006; **68**: 44-49.
12. Dvir D,Marom H,Assali A,Kornowski K. Bifurcation lesions in the coronary arteries: Early experience with a novel 3-dimensional imaging and quantitative analysis before and after stenting. *Eurointervention* 2007; **3**: 95-99.
13. Fortin DF,Spero LA,Cusma JT,Santoro L,Burgess R,Bashore TM. Pitfalls in the determination of absolute dimensions using angiographic catheters as calibration devices in quantitative angiography. *Am J Cardiol* 1991; **68**: 1176-1182
14. Patterson MS,Schotten J,van Mieghem C,Kiemeneij F,Serruys PW. Magnetic navigation in percutaneous coronary intervention. *J Interv Cardiol* 2006; **19**: 558-565.
    Dmochowski J,Hoffmann KR,Singh V,Xu J,Nazareth DP. Effects of point configuration on the accuracy in 3D reconstruction from biplane images. *Med Phys* 2005; **32**: 2862-2869.

Chapter 3

ASSESSMENT OF SUCCESS IN NATIVE CORONARIES

Magnetic Catheter Navigation for Percutaneous Coronary Intervention

Cardiovascular Interventions in Clinical Practice

Ramcharitar S and Serruys PW

Editors Jürgen Haase, Hans-Joachim Schäfers, Horst Sievert and Ron Waksman

Wiley-Blackwell, 2008

Summary

Magnetic navigation is an emerging technology that has been effectively applied to neurological and cardiac electrophysiological procedures and now is being extended to percutaneous coronary interventions. A dedicate software package, Navigant® is able to accurately control a 0.08 Tesla magnetic field generated by two large permanent external magnets to change the magnetic moments of a tiny magnet located at the tip of a guidewire/device. The applied magnetic field can be changed at any time to precisely redirect the wire tip in order to improve navigation through complex and tortuous anatomy within the coronary tree. The incorporation of three-dimensional information in the Navigant® enhances the steering accuracy of the system. The combination of improved navigation together and newer generation of magnetic guidewires may potentially improve time, contrast and material usage in crossing difficult coronary lesions. Future potential development is aimed at addressing chronically occluded vessels and improving intramyocardial stem cell delivery.

Introduction

The fundamental technique that bridges all percutaneous intervention is the ability to precisely track a guidewire or a catheter at or through a lesion. In some cases this remains the Achilles' heel of the entire procedure as it determines success or failure. In order to increase success there is a repertoire of wires with varying weights, trackablity and torque that each cardiologist has in his or her 'tool-box'. But there is often a tradeoff since wires that excel in one feature as for example the support achieved with a stiffer wire may lose in its ability to maneuver though the subtle changes in a tortuous vascular anatomy. This provides the rationale for developing systems offering precise distal tip control so as to redirect a wire *in vivo* within the coronary tree without the need to removing it from the patient and reshaping the tip(1). The magnetic navigation system (MNS) uses a magnetically enabled wire tip to have full 360° omni-rotation(2). This is achieved by using large external permanent magnets to precisely control magnetic vectors created through a dedicated software called Navigant® (Figure 1). This novel technology is now firmly established in cardiac electrophysiology and in addition has been favorably accepted in neurosurgery following early animal and human studies(3,4). But its extension into the competitive world of interventional cardiology has had a cautionary start despite over 100 systems installed worldwide. This maybe because the technology still has to define areas where there are potential benefits over conventional percutaneous coronary interventions (PCI) in order to convince the skeptical interventional community(1). At present, the MNS is an expensive

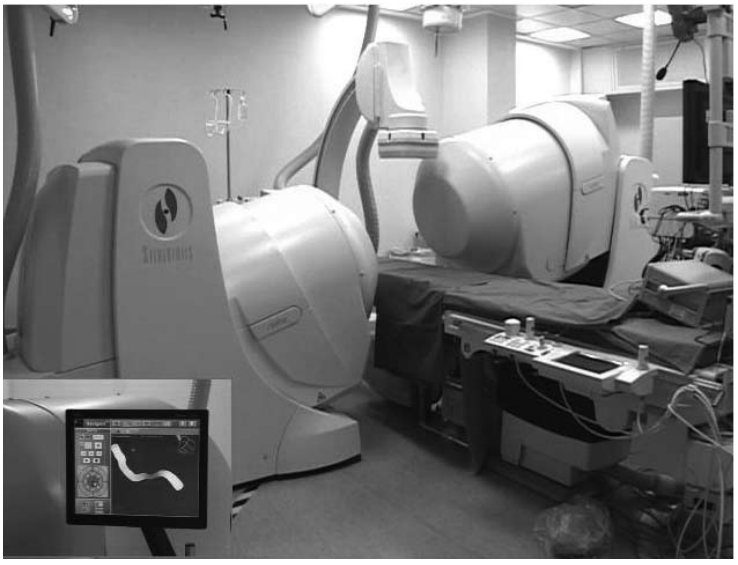

Figure 1. *Magnetic navigation system is shown with the magnets in the tilt position on either side of the patient. Inserted at the bottom left hand panel is the touch screen monitor used to direct the navigation along the chosen vessel*

technology that requires a learning phase for both the software and the hardware. Moreover unlike neurosurgery, targeting a moving structure- the beating heart presents a challenge for the navigational roadmaps created from static images. Nevertheless it is postulated that the system may provide new options to manage challenging and tortuous anatomy, chronic total occlusions (CTOs), reducing crossing/fluoroscopy time, contrast and materials, targeted stem cell therapies and ultimately in the realization of remote control PCI(5).

History

The use of magnets to control an intravascular catheter was first reported in 1951(6). Exactly 40years later Ram and Meyer described the first human magnetically guided heart catheterization in a neonate(7). Several key technological developments were needed in order to meet the level of sophistication achieved with the current magnetic navigation system (MNS)(8). Initially the early magnet designs used large and cumbersome electromagnets to redirect relatively large magnetized wires which meant that navigation was only permitted in relatively large vessels. It was only with the current smaller permanent magnets that the system allowed tiny magnets (≤ 0.014") to be deflected at the tip of the wires used for percutaneous coronary interventions. Following pre-clinical evaluation the Niobe® I system (Stereotaxis, St Louis, MO, USA) received regulatory approval for human clinical use in cardiac electrophysiology and interventional neuroradiology in 2000, and for interventional cardiology in 2003.

The Magnetic Guidewires

The magnetic guidewire used together with the MNS has a nominal diameter of 0.014inch /0.36mm and a nominal length of 185cm or 300cm. The wire is configured with a 2 or 3mm embedded gold encapsulate neodynium iron boron magnet at the distal tip (Figure 2). The Cronus™ was first generation hydrophilically coated magnetic guidewire available in both magnet tip dimensions. When subjected to a magnetic vector the tiny magnetic tip realigned in the direction of the applied field and steering of the tip is performed. Once achieved, the wire can

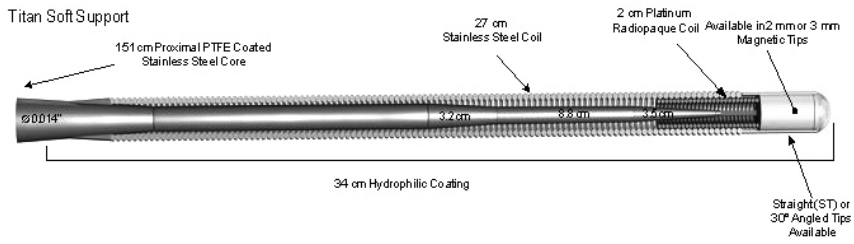

Figure 2. *The Magnetic Guidewire with the 2-3mm embedded gold encapsulate neodynium iron boron magnet at the distal tip*

***Table 1**: Characteristics of the Stereotaxis Guidewire Family*

Stereotaxis Guidewire Family Comparison				
Guidewire	Distal Core	Proximal Core	Magnet Tip Length	Hydrophilic distal coating
Cronus™	Nitinol	Nitinol	2 & 3 mm	25 cm
Titan™	Stainless Steel	Stainless Steel	2 & 3 mm	10-34 cm
Pegasus™	Nitinol	Stainless Steel	2 & 3 mm	40 cm

be manually advanced until another change of direction is required. This basic principle of wire orientation/guidance is conserved with the newer generation wires that include the Titan™ and the Pegasus™ range. Although the basic principle of steering is similar to the Cronus™ the newer wires are superior in their ability to deliver a device because of the different materials used in their shafts. Three point deflection testing performed by supporting the wires at two points and measuring the force required to deflect the mid-point to 4mm showed that they stiffen quicker in order to improve device delivery. The Titan™ soft support wire has a stiffness profile similar to a Balance Medium Weight (BMW, Abbott Vascular Devices, Redwood, CA, USA) moderate support wire with the even stiffer Titan™ Assert wire able to deliver a tip load of similar characteristics to a Miracle 3 gram (Asahi Intecc, Nagoya, Japan). The tip load measures the force needed to buckle the guidewire when applied 1 cm from the tip. In the newest wires, the Pegasus™ the distal shaft is made of nitinol to allow greater shape retention and the proximal shaft of stainless steel to maintain pushability. As with other magnetic wires they are hydrophilically coated to facilitate a smooth wire transit. The three-point deflection test pattern shows that the Pegasus™ Moderate and Assert have similar support profiles. However, the very distal 2cm of the Assert is stiffer to transmit more force when crossing tight or total occlusions.

The Mechanical forces exerted on the Magnetic Wire

Unlike standard non-magnetized guidewires used in conventional PCI procedures magnetic wires have different mechanical forces exerted at the tip of the wire(10). In standard guidewires there is only a push force that the operator uses to direct the wire transit across a lesion. In the magnetic guidewire however in addition to this push force there is also a deflection force. The deflection force is that applied through the permanent magnet to cause deflection of the magnetic guidewire in the direction of the magnetic field vector. The magnitude of this force can be calculated by combining the torque exerted at the tip of the wire to that acting in the opposite direction of the deflection. The torque (τ) exerted on the tip of the wire is equal to the product of the magnetization vector (**M**, measured in amperes per meter) of the magnet in the tip of the wire, cross-sectional area (*A*, measured in square meters) of the magnet in the tip of the wire, magnet length (*L*, measured in meters), external magnetic field vector (**B**, measured in teslas), and the sine of the angle between the field and magnetization vectors (θ): $\tau = \mathbf{M}AL\mathbf{B}$. $\sin(\theta)$ (1) The torque is also described by two identical forces (*F*, measured in grams) acting

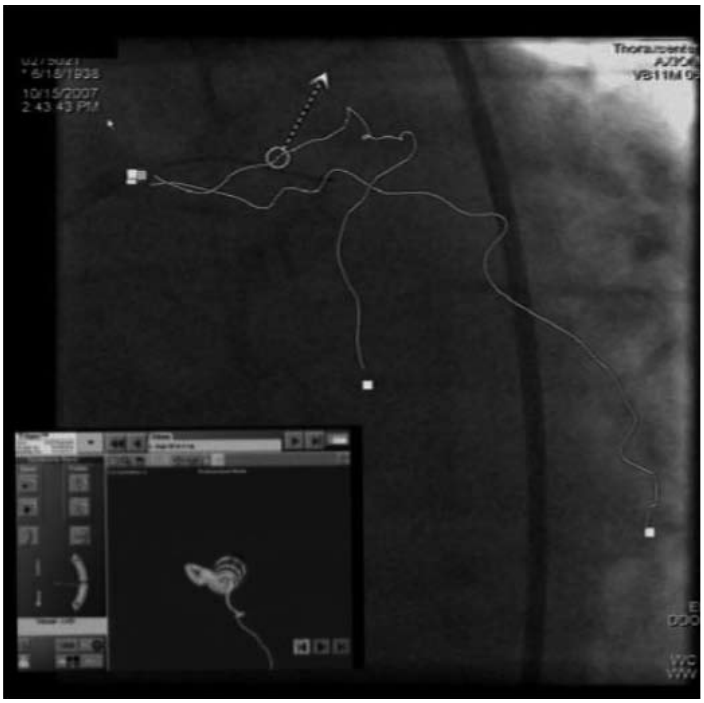

Figure 3. *The chosen vector is displayed as a dotted arrow on navigational path-line on the live fluoroscopy image. The bottom left panel shows what the operator sees on the touch screen monitor.*

in opposite directions on two poles of the permanent magnet through the moment arm: $\tau = 2(L/2)F$. (2) Combining the equations (1) and (2) yields a description of the force exerted by the magnetic field on the distal end of the guidewire: $F = \mathbf{M}A\mathbf{B}.\sin(\theta)$ (3). This force is maximal when the wire is perpendicular to the magnetic field (i.e., $\sin(\theta) = 1$) and zero when the wire is parallel to the magnetic field(11).

Navigation Software

The Navigant® software allows several possible modes to navigate through the coronary artery. Broadly speaking these can be divided into two main groups: the so called 'free mode' where navigational vectors are manually derived from the 2 dimensional X ray angiographic images and 'true vessel' navigation where vectors are derived automatically from a 3-dimensional image of the vessel (e.g. an Multislice Computer Tomography MSCT dataset) or through a dedicated 3D reconstruction software package (3RDC). Regardless of the chosen mode to create the vector in all cases the operator can manually change a vector though a sterile interactive touch screen monitor located at arms' length at the operation table. With this monitor the operator can also chose for the vector to be automatically updated at a desired incremental distance (1-9mm). The chosen vector is displayed as a dotted arrow on navigational pathline (centerline)

on the live fluoroscopy image (Figure 3). As the vector is updated the dotted arrow moves along the navigational pathline and the permanent magnets rotate about their axes to create a new magnetic field in line with the trajectory of the new coordinate (illustrated by solid arrow on the live fluoroscopy image). The operator manually pushes the wire forward to follow the preset incremental distance imposed by the desired vector.

a) Free Mode Navigation

The 'free mode' 2-D navigational modes include the use of 'preset navigational vectors' that are adapted to particular coronary anatomies e.g. left anterior descending and circumflex arteries. Other anatomical vasculature can be added if required such as coronary artery bypass grafts and peripheral arteries. The presets allow relative fast navigation but it lacks accuracy as it is based on the assumption of standardized vasculature. Similarly, the 'clock face' navigational mode where the vectors can move in a chosen direction by touching the periphery of a circle mimicking the dial of a clock is equally simple to use but also lacks accuracy(12). Its effectiveness depends on skill of the operator and his or her spatial understanding of coronary anatomy. In combination with a 'Bulls Eye View' where the tip of the wire can be made to move along the contours of a dartboard offers some degree of accuracy and this is particularly useful in locating microchannels within chronic total occlusions (CTO). Some spatial understanding of the coronary anatomy is required in the more complex 'spherical navigational approach' where the vessel or object is contained within the boundaries of a sphere having regularly spaced polar lines (e.g. latitude and longitude lines). In all the above navigational modes the vectors are generic, as they are not directly created from the anatomy of the vessel being treated. However, 'true' anatomical navigation is possible on the vessel being treated by directly introducing two orthogonal fluoroscopic images of the vessel in Navigant® but such a 2-D image representation of a 3-D structure has obvious limitations(13). Much more accurate is the creation of a virtual 3D reconstructed vessel (3DRC) or using MSCT to accurately derive the vector coordinates.

b) 'True' Vessel Navigation

'True' vessel navigation is an accurate representation of a 3D navigational roadmap of the coronary artery(14). Navigant® can create such a virtual map from two X-ray images provided that they are 30º apart. To do this identical points on both images in the same cardiac phase are simultaneously linked to generate the 3D navigational path or 'centerline' through the vessel lumen. This creates a static roadmap map that is co-registered with the live fluoroscopy image. It should be noted because the images are not gated it means that only in the phase where the images were taken will the navigational road map be perfectly aligned. But for the purposes of navigation the trajectory of the vector will be sufficiently good enough to permit the adequate wire transit. The 3-DRC centerline can also be created from two fluoroscopic images using dedicated software (CardiOpB®, Paieon Medical Inc., Rosh Ha'ayin, Israel) that has the added advantage to fine tune the direction of the vector by visualizing subtle changes in the vessel

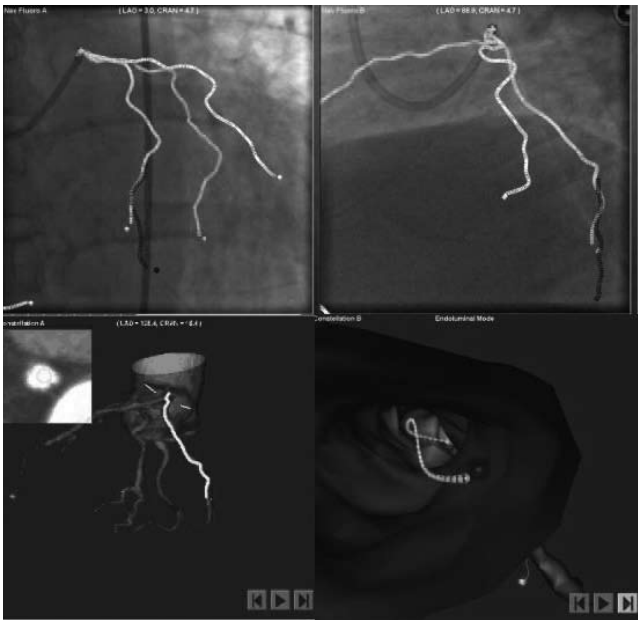

Figure 4. *Top panels showing the tip of the catheters in fluoroscopy image co-registered with the extracted coronaries derived from the MSCT dataset. These give the specific 3-D coordinates that allow integration of the 2 modalities. Bottom panels showing the extracted coronaries with the centerline together with multiplaner reconstructed cross-section displayed in the Navigant® and the endoluminal views for MSCT based navigation.*

through a virtual lumen - so called endoluminal view. A far more accurate 3D road map can be obtained by employing multislice computer tomography (MSCT) datasets (Figure 4). This imaging modality can also identifying vascular anomalies and provide information on coronary plaques composition(15,16). The vessels can be directly extracted from the MSCT dataset through post-processing software and be directly incorporated, co-registered and aligned to the fluoroscopic image in the Navigant®(17).

Current status

It is not the intention of the MNS to revolutionize current practices in PCI but rather to facilitate in areas where conventional techniques may be met with difficulty. Potential areas are in the challenging anatomies associated with tortuosity, chronic total occlusions where the path of the vessel is not visible so the required tip direction is unclear and in improving the efficacy of myocardial stem cell implantation.

i) Challenging anatomy

Challenging anatomy often is associated with lower crossing success and higher rates for surgical referral. In a study comparing magnetic and conventional wires in phantoms models

mimicking tortuous coronary arteries magnetic wires crossings were found to be superior in the more tortuous phantoms(18). More than 5 fold reduction in crossing times were recorded (201.7 ± 111sec to 36.4 ± 13sec, p<0.001) compared to standard guidewire techniques. Moreover the magnetic wires achieved a 98.8% crossing success compared to 68% with the standard guidewires with considerably fewer wires usage (1.3 vs. 5.5) as a result of wire tip damage. But much more interesting was the finding that in certain cases operators without prior MNS experience had equally good crossing successes with the magnetic wires as compared to senior operators. In the more difficult phantoms however, a learning curve was clearly demonstrable in those operators with limited MNS experience.

In addition to this phantom study the ability to negotiate challenging anatomy has also been shown in several clinical scenarios where the procedural success was inherently dependent on the MNS. In a case of hypertrophic obstructive cardiomyopathy (HOCM) the origin of the major septal artery had an unusually extreme angulation (approximately 130 degrees) on coronary angiography that was impossible to access with a conventional guidewire approach(19). However by employing MNS guidewire the balloon catheter cannulation of the septal artery was possible to facilitate a successful transcatheter alcohol septal ablation procedure. MNS guided septal ablation has now been evaluated in a randomized study comprising 44 consecutive patients(20). In all cases the procedures were successful and the only complication, a vessel dissection occurring in the conventional group. Interestingly as observed in the phantom studies, the time required for guidewire cannulation of the septal branch decreased progressively with increasing experience (third tertile vs. first tertile (3 [1.25-4.75 vs. 10.5 [6-17] minutes, P = 0.004) compared with the conventional group (6 [2-10.25] minutes, P = 0.075 vs. third tertile), suggesting a learning curve.

Early experience of the magnetic navigation in crossing coronary lesions showed relatively low success (88%) with the first generation Cronus™ wires. Although the majority of lesions were relatively straightforward four of the sixty-eight target lesions were complex and had previously failed with conventional wire techniques (21). When directly compared in crossing 21 consecutive simple and straightforward lesions the magnetic wires had significantly longer crossing times compared to standard guidewires (median, 120 vs. 40 sec, P=0.001; 105 vs. 38 sec, P=0.001, respectively)(22). In addition the contrast media usage and amount of radiation exposure were also higher with magnetic wires (median, 13 vs. 9 ml, P=0.018; 215 vs. 73 Gym2, P=0.002, respectively). Without a demonstrable advantage in simple lesions many groups have focused on vessels having various degrees of complexity or in cases that were previously met with failure using a conventional wire approach. One of the first study evaluated 59 patients grouped to attempt MNS guided PCI as a first option ("primary attempt"; n = 46) or following failure to pass a conventional guidewire ("secondary attempt"; n = 13)(23). It demonstrated that the target lesion was successfully crossed in 49 of 55 lesions (89%) and in 9 of 13 conventional

failed lesions (69%) the MNS was successful giving procedural successes of 84% and 62%, respectively. As expected the median crossing, fluoroscopy and contrast media usage was longer or higher among the secondary attempt group. Other reports where MNS was successful in cases that failed conventionally were in recrossing of a crush stent to facilitate kissing balloon post dilatation and in crossing a jump saphenous vein graft (SVG) having an acute angulation to a stenosis just before it anastomosed to an obtuse marginal branch (OM) and a right posterior descending coronary artery(24,25). To try to identify other cases that are more likely to be crossed with the magnetic system a novel complexity scoring system is being evaluated. It uses 3-D information of both the vessel and lesion characteristics in an attempt to address some of the notable limitations encountered with existing classification (26). Preliminary results have shown that there is a trend to support MNS in more complex vascular anatomies. In one of the largest prospective studies MNS was performed on 439 lesions in 350 consecutive PCI patients predominantly using the radial approach(27). Successful crossing was accomplished in 93% of the lesions with twenty-five of the 35 failures occurred in attempting chronic total occlusions. Lesion crossing time was 81 ± 168 sec (mean ± SD), and fluoroscopy time was 64 ± 123 sec. A clear learning curve was evident after the first 80 patients. In addition contrast agent usage was reduced when compared to a historical control group. Low success in crossing (sub) chronic total occlusions with magnetic wires was also reported in a study comparing guidewire steering by either 2D guidance or virtual 3DRC(28). In 30 patients with 36 coronary arteries lesions an overall crossing success of 86% (31/36 lesions) was recorded with the 5 failures occurring in patients having (sub) chronic total occlusions. The study did reveal that significantly less contrast medium was needed to position the magnetic guidewire by using the 3DRC (60 +/- 101 ml vs. 14 +/- 15 ml. $p < 0.05$).

ii) Chronic total occlusions

Chronic total occlusion (CTO) often presents a challenge and its variable success rate (65 to 80%) is dependent on both the skill of the operator, the materials and the technique used(29). As a result a number of strategies have been suggested to facilitate the treatment of CTOs e.g. intracoronary thrombolytic infusion(30), tapered-tip, laser (31) and radiofrequency guidewires(32). A novel approach to manage a CTO is to integrate the MNS ability to steer a guidewire through the occlusion with a forward-looking technology such as MSCT cross-sections to ensure ideal positioning of the wire in the true lumen (Figure 4). Once the ideal position is accepted then ablative radiofrequency power can be delivered to the tip of the wire to recanalize the CTO (33). Early evaluation of MNS-MSCT approach to CTO used magnetic wires without ablative power and navigation was aided by the bull's eye view to 'looked forward' at the occlusion –– to make the search pattern for micro-channels through the occlusion more uniform(34). Even though the success was limited by the bulkiness of the 2-3mm magnetic tips the feasibility of using a 3-D map generated from an MSCT dataset to navigate was demonstrated. This is important because the lack of a fluoroscopic lumenogram in a CTO does not allow navigation using 3DRC

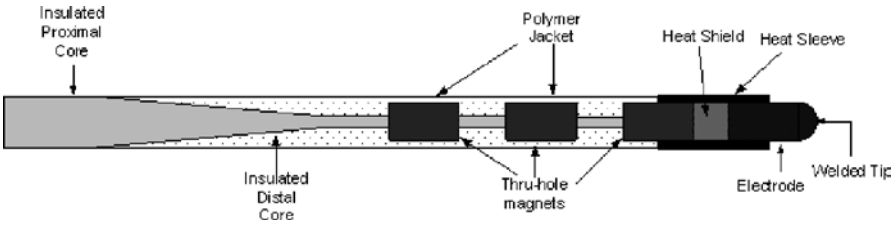

***Figure 5**: The magnetically enabled RF wire*

software. With MSCT both the distal vessel filled via collaterals and a tissue attenuation line (the scarred tissue of the original vessel lumen) can be identified. The navigational centerline is however fixed and as a result the mismatch with the moving artery in the live fluoroscopy image persists except in the phase in which the navigational path was constructed from the MSCT image. Ordinarily, when navigating through a patent vessel this is not a problem as the wire is contained within the vessel's lumen so that when the heart moves with each beat the wire can still follow the trajectory of the predetermined vectors. In a CTO however, the lack of a patent lumen means that as the heart moves along its axis, the tip of the wire can be perpendicular to the vascular wall and when pushed can protrude. With magnetically enabled RF powered wires it is therefore crucial to have a dynamic road map (centerline) to superimpose on the live fluoroscopy image or to ECG phase gate a centerline derived from the MSCT to the fluoroscopic image following alignment to recognizable landmarks such as the spinal processes and the catheter's tip. This would mean that at all points in the cardiac cycle the centerline will be superimposed on the live fluoroscopic image of the vessel and the advancement of the ablating wire can be safely undertaken. Stereotaxis is now in their final stages of developing a RF ablating magnetic enabled wire (Figure 5). This is a 0.018inch wire having a small RF electrode at its tip with three small magnets protected by a heat sleeve with the RF energy supplied by an external RF generator. The nitinol shaft is electrically insulated with asymmetrically coated PTFE (thinned distally) to provide adequate dielectric strength without affecting the wire's flexibility. The composite metal alloys used in the RF electrode are encased in a polyurethane polymer jacket for smooth transitions between the different components. *In vivo* studies demonstrated good results in artificially created occlusions (5-8cm in length and aged 6-8 weeks) in porcine femoral arteries. The first in man (FIM) study assessing the safety and feasibility will firstly be done in caged coronary CTO 'within stents' and in peripheral vessels.

iii) Stem cell injection

An area in which magnetic navigation is postulated to have an advantage over conventional techniques is intramyocardial injection of stem cells(35). Current methods for delivery remain inexact despite using electromechanically guided injection. This uses NOGA electromechanical

mapping (EMM) of the myocardium to identify the infarction areas for treatment. Appropriate electrical signal strength recorded as the mapping electrode makes a good contact with the myocardium is used as a marker for intramyocardial injection(36). Although this approach is advantageous the mapping of remote areas in the heart can be difficult to access even with very experienced operators. But by using a magnetically enabled MNS-guided NOGA EMM catheter these remote areas can be effectively mapped. Moreover, the magnetic momentum at the catheter tip is supportive enough to allow the use of softer catheters that are less likely to perforate the myocardium. Preclinical studies on a Stereotaxis-compatible NogaStar mapping and MyoStar injection catheters (Biologics Delivery Systems, Cordis Corporation, Diamond Bar, CA) equipped with a small permanent magnet positioned at the tip have been encouraging with a 95.8% success rate for intramyocardial injection of mesenchymal precursor cells (MPC) (37). The NOGA mapping of the myocardium was performed remotely with a computer-controlled catheter advancement system (Cardiodrive unit, Stereotaxis St Louis, MO)(38). This 3-dimensional map was used in Navigant® to create the desired navigational vectors needed for the magnetically enabled MyoStar catheter to follow.

Limitations and Future developments

The ability of the MNS to precisely direct an in-vivo device externally makes it a powerful tool that has the potential to benefit several areas of interventional cardiology. At present it is expensive, technically demanding and has several drawbacks related to both the software and hardware. Both the operator and technician must overcome the learning curve before maximal gains can be achieved. In addition, current methods used to create the 3DRC are time consuming taking up to 30 minutes for the navigational pathway to be displayed on the fluoroscopy image. Moreover, this static image has inherent limitations with co-registration and with the accuracy in directing the vectors on static roadmaps. It therefore means for the full potential of the MNS to be realized there must be continuous improvements in both software and hardware design. Some of the major limitations are already being addressed with the next generation of wires/devices. Current magnetic wires suffer from the lack of sophistication that has become widely accepted through the many generations of standard conventional wire designs. The crudeness of the 2-3mm magnet stuck on to the tip of the wire influences the wire's ability to transit smoothly across a lesion. Planned future generation wires will have multi-magnet designs akin to the RF wire in order to address this particular limitation. Moreover, different alloy composite are being tested to retain the shape of the wire without compromising its ability to deliver a device. However a major limitation is the responsiveness of the hardware in executing the vector change demanded by the Navigant®. In the earlier versions of the software the vectors had to be manually updated by pressing an advancing icon on the touch screen monitor. This meant that the operator had a time delay prior to advancing the magnetic guidewire as the system updated. In the latest version of the Navigant® 2.11 the vectors are automatically updated

at a preset rate – moving at incremental distance of 1-9mm over a chosen time in seconds. Although this is a desirable feature as it frees the operator from performing an additional task he or she still has to wait for the magnets to move to realign their field in the direction of the vector. This time delay makes the magnetic navigation system slower than conventional wire techniques and this may not be easily solved because of the mechanical limitations in moving large external magnets rapidly and accurately. It is also sometimes not fully appreciated that the operator is still required to manually advance the wire with his/her left hand and that the MNS is only steering the tip though the external field. By using a Cardiodrive® unit attached to the distal part of the wire automatic advancement is possible. This system has been extensively used in magnetic guided cardiac electrophysiological procedures and may provide a window for remote control intervention when amalgamated with technologies that can enable accurate device positioning(39). Such technologies exist but require significant investment to make them magnetically field compatible. In the future the potential benefits of steering the tip of a guidewire in a desired direction, driving it externally and accurately knowing the position of a device on the wire will certainly have an impact on the current way of performing PCI (40).

Conclusion

The MNS is a promising technology that when integrated with 3-dimensional information can offer new possibilities in performing percutaneous intervention. Key developments are still however required in both hardware and software to provide a real challenge to conventional approaches. The versatility of the system however in its ability to redirect a device *in vivo* means that there maybe additional benefits in many important aspects of invasive cardiology and patient care.

References

1. Raizner AE. Magnetic navigation: a pivotal technology. Catheter Cardiovasc Interv 2007;69(6):856.
2. Ramcharitar S, Patterson MS, van Geuns RJ, van Meighem C, Serruys PW. Technology Insight: magnetic navigation in coronary interventions. Nat Clin Pract Cardiovasc Med 2008;5(3):148-56.
3. Ernst S, Ouyang F, Linder C, Hertting K, Stahl F, Chun J, Hachiya H, Bansch D, Antz M, Kuck KH. Initial experience with remote catheter ablation using a novel magnetic navigation system: magnetic remote catheter ablation. Circulation 2004;109(12):1472-5.
4. Chu JC, Hsi WC, Hubbard L, Zhang Y, Bernard D, Reeder P, Lopes D. Performance of magnetic field-guided navigation system for interventional neurosurgical and cardiac procedures. J Appl Clin Med Phys 2005;6(3):143-9.
5. Patterson MS, Schotten J, van Mieghem C, Kiemeneij F, Serruys PW. Magnetic navigation in percutaneous coronary intervention. J Interv Cardiol 2006;19(6):558-65.
6. Llander H. Magnetic guidance of a catheter with articulated steel tip. Acta radiol 1951;35(1):62-4.
7. Ram W, Meyer H. Heart catheterization in a neonate by interacting magnetic fields: a new and simple method of catheter guidance. Cathet Cardiovasc Diagn 1991;22(4):317-9.
8. Gillies G.T, Ritter RC, Broaddus WC, Grady MS, Howard MA. Magnetic Manipulation Instrumentation for Medical Physics Research. Rev.Sci.Instrum 1994;65(3):533-562.
9. Kolb C, Luik A, Hessling G, Zrenner B. Magnetic catheter navigation system interference with a dual-chamber pacemaker. J Cardiovasc Electrophysiol 2007;18(8):892-3.
10. Wood BJ, Zhang H, Durrani A, Glossop N, Ranjan S, Lindisch D, Levy E, Banovac F, Borgert J, Krueger S and others. Navigation with electromagnetic tracking for interventional radiology procedures: a feasibility study. J Vasc Interv Radiol 2005;16(4):493-505.
11. Schiemann M, Killmann R, Kleen M, Abolmaali N, Finney J, Vogl TJ. Vascular guide wire navigation with a magnetic guidance system: experimental results in a phantom. Radiology 2004;232(2):475-81.
12. Hertting K, Ernst S, Stahl F, Mathew S, Meulenbrug H, Reimers J, Kuck K.-H, K K. Use of the novel magnetic navigation system Niobe™ in percutaneous coronary interventions; the Hamburg experience Eurointervention 2005;1(336-339).
13. Ramcharitar S, Daeman J, Patterson M, van Guens RJ, Boersma E, Serruys PW, van der Giessen WJ. First direct in vivo comparison of two commercially available three-dimensional quantitative coronary angiography systems. Catheter Cardiovasc Interv 2008;71(1):44-50.
14. Tsuchida K, van der Giessen W, Patterson M, Tanimoto S, García-García H, Regar E, Ligthart J, Maugenest A, Maatrijk G, Wentzel J and others. In Vivo Validation of A Novel Three-Dimensional Quantitative Coronary Angiography System (CardiOp-B): Comparison with A Conventional Two-Dimensional System (CAAS II) and with Special Reference to Optical Coherence Tomography Eurointervention 2007;3:100-108.
15. Hoffmann MH, Lessick J. Multidetector-row computed tomography for noninvasive coronary imaging. Expert Rev Cardiovasc Ther 2006;4(4):583-94.
16. Fishman EK, Horton KM. The increasing impact of multidetector row computed tomography in clinical practice. Eur J Radiol 2007;62 Suppl:1-13.
17. Ramcharitar S, Pugliese F, Patterson M, van Geuns RJ, de Feyter P, Guiliguian D, Serruys PW. Advanced Magnetic Navigation: Multi-slice Computer Tomography-guided Percutaneous Coronary Intervention in a patient with Triple-Vessel Disease. Eurointervention 2008;(will be in print Jan08).
18. Ramcharitar S, Patterson MS, van Geuns RJ, van der Ent M, Sianos G, Welten GM, van Domburg RT, Serruys PW. A randomised controlled study comparing conventional and magnetic guidewires in a two-dimensional branching tortuous phantom simulating angulated coronary vessels. Catheter Cardiovasc Interv 2007;70(5):662-8.
19. Bach RG, Leach C, Milov SA, Lindsay BD. Use of magnetic navigation to facilitate transcatheter alcohol septal ablation for hypertrophic obstructive cardiomyopathy. J Invasive Cardiol 2006;18(6):E176-8.

20. Buergler JM, Alam S, Spencer W, Kleiman NS, Melendez Y, Franklin J, Nagueh SF. Initial experience with alcohol septal ablation using a novel magnetic navigation system. J Interv Cardiol 2007;20(6):559-63.
21. Tsuchida K., García-García H., Tanimoto S., Ong A.T.L., Sehra R., van der Ent M., Sianos G., van der Giessen W.J., Serruys P.W. Feasibility and safety of guidewire navigation using a magnetic navigation system in coronary artery stenoses EuroIntervention 2005;1(329-335).
22. Tsuchida K, Garcia-Garcia HM, van der Giessen WJ, McFadden EP, van der Ent M, Sianos G, Meulenbrug H, Ong AT, Serruys PW. Guidewire navigation in coronary artery stenoses using a novel magnetic navigation system: first clinical experience. Catheter Cardiovasc Interv 2006;67(3):356-63.
23. Atmakuri SR, Lev EI, Alviar C, Ibarra E, Raizner AE, Solomon SL, Kleiman NS. Initial experience with a magnetic navigation system for percutaneous coronary intervention in complex coronary artery lesions. J Am Coll Cardiol 2006;47(3):515-21.
24. Patterson MS, Ramcharitar S, Serruys PW. Magnetically Supported PCI: success after failed surgery and conventional PCI. Cath Lab Digest 2007;15(3):1-14.
25. Ramcharitar S, Patterson MS, van Geuns RJ, Serruys PW. Magnetic navigation system used successfully to cross a crushed stent in a bifurcation that failed with conventional wires. Catheter Cardiovasc Interv 2007;69(6):852-5.
26. Patterson S, Hoeks S, Tanimoto S, Van Mieghem C, Ramcharitar S, Van Domburg R, Serruys PW. A simple score for predicting prolonged crossing times to select patients who would benefit from a magnetic percutaneous coronary intervention. European Heart Journal , 2007; 28 ((Abstract Supplement P4762)):847-848.
27. Kiemeneij F, Patterson MS, Amoroso G, Laarman G, Slagboom T. Use of the Stereotaxis Niobe magnetic navigation system for percutaneous coronary intervention: results from 350 consecutive patients. Catheter Cardiovasc Interv 2008;71(4):510-6.
28. Schneider MA, Hoch FV, Neuser H, Brunn J, Koller ML, Gietzen F, Schamberger R, Kerber S, Schumacher B. Magnetic-guided percutaneous coronary intervention enabled by two-dimensional guidewire steering and three-dimensional virtual angioscopy: initial experiences in daily clinical practice. J Interv Cardiol 2008;21(2):158-66.
29. Di Mario C, Werner GS, Sianos G, Galassi A, Büttner J et al for the EuroCTO Club JS. European perspective in the recanalisation of Chronic Total Occlusions (CTO): consensus document from the EuroCTO Club Eurointervention 2007;3(30-43).
30. Abbas AE, Brewington SD, Dixon SR, Boura JA, Grines CL, O'Neill WW. Intracoronary fibrin-specific thrombolytic infusion facilitates percutaneous recanalization of chronic total occlusion. J Am Coll Cardiol 2005;46(5):793-8.
31. Serruys PW, Hamburger JN, Koolen JJ, Fajadet J, Haude M, Klues H, Seabra-Gomes R, Corcos T, Hamm C, Pizzuli L and others. Total occlusion trial with angioplasty by using laser guidewire. The TOTAL trial. Eur Heart J 2000;21(21):1797-805.
32. Werner GS, Fritzenwanger M, Prochnau D, Schwarz G, Krack A, Ferrari M, Figulla HR. Improvement of the primary success rate of recanalization of chronic total coronary occlusions with the Safe-Cross system after failed conventional wire attempts. Clin Res Cardiol 2007;96(7):489-96.
33. Baim DS, Braden G, Heuser R, Popma JJ, Cutlip DE, Massaro JM, Marulkar S, Arvay LJ, Kuntz RE. Utility of the Safe-Cross-guided radiofrequency total occlusion crossing system in chronic coronary total occlusions (results from the Guided Radio Frequency Energy Ablation of Total Occlusions Registry Study). Am J Cardiol 2004;94(7):853-8.
34. Garcia-Garcia HM, Tsuchida K, van Mieghem C, Daemen J, van Weenen S, Patterson M, van der Ent M, van der Giessen WJ, Meulenbrug H, Sehra R and others. Multi-slice computed tomography and magnetic navigation-initial experience of cutting edge new technology in the treatment of chronic total occlusions. Eurointervention 2007.3, 188-196
35. Perin EC. Stem cell therapy for cardiovascular disease. Tex Heart Inst J 2006;33(2):204-8.

36. Perin EC, Dohmann HF, Borojevic R, Silva SA, Sousa AL, Mesquita CT, Rossi MI, Carvalho AC, Dutra HS, Dohmann HJ and others. Transendocardial, autologous bone marrow cell transplantation for severe, chronic ischemic heart failure. Circulation 2003;107(18):2294-302.
37. Perin E, Silva G, Fernandes M, Munger T, Pandey A, Sehra R, Talcott M, Bichard C, Creed J, J W and others. First experience with remote left ventricular mapping and transendocardial cell injection with a novel integrated magnetic navigation-guided electromechanical mapping system Eurointervention 2007;3:142-148.
38. Pappone C, Augello G, Gugliotta F, Santinelli V. Robotic and magnetic navigation for atrial fibrillation ablation. How and why? Expert Rev Med Devices 2007;4(6):885-894.
39. Mediguide. MPS First in Human MediGuide started its clinical trials in Regensburg University Hospital in Germany. http://www.mediguide.co.il/news/news.asp?newID=43&newsCatID=2.
40. Beyar R, Gruberg L, Deleanu D, Roguin A, Almagor Y, Cohen S, Kumar G, Wenderow T. Remote-control percutaneous coronary interventions: concept, validation, and first-in-humans pilot clinical trial. J Am Coll Cardiol 2006;47(2):296-300.

ASSESSMENT OF SUCCESS IN NATIVE CORONARIES

Integration of 3D reconstruction in the SELection Criteria for Excessive Crossing Times for Magnetically Supported Percutaneous coronary intervention SELECT-MP

Eurointervention 2008 (in press)

Patterson MS, Hoeks SE, Rijkenberg S, **Ramcharitar S**, van Geuns RJ,
Tanimoto S, van Domburg RT, Serruys PW

Objectives:
To develop a clinical prediction rule based on 3D reconstruction of coronary arteries that would prospectively identify lesions that are difficult to cross and could benefit from magnetic navigation.

Material and Results:
The coronary anatomy of a cohort of 120 lesions that had undergone percutaneous coronary intervention (derivation set) was analysed using 3D reconstruction for vessel and lesion characteristics. The crossing time was the total clock time to reach a satisfactory distal position after leaving the guiding catheter. Multivariable logistic regression and linear shrinkage with bootstrapping were used to develop a clinical prediction rule that dichotomised cases into easy or difficult (prolonged crossing time). A prolonged crossing time

(>120s) = 1*Vb + 1*(Vl=1) + 2*(Vl=2) + 2*Vc + (1*Lbb)+1*(Ll=1) + 2*(Ll=2).
(N.B. abbreviations refer to morphological factors, see appendix 1)

A value of 6 was the best cut-off value. This clinical prediction rule was applied to a second independent cohort of patients (validation set) where crossing time was measured. The bootstrapped c-statistic of the model was 0.82 indicating excellent discrimination.

Conclusion:
3D reconstruction helped to develop a simple, accurate clinical prediction rule to identify difficult cases for conventional wires and in whom magnetic navigation may be preferable.

Short Abstract:
We describe the development of a clinical prediction rule, based on 3D reconstruction, to prospectively identify lesions in coronary arteries that are difficult to cross with a conventional angioplasty wire. This clinical prediction rule was developed in a cohort of consecutive patients undergoing angioplasty and validated in a second independent cohort and showed excellent discrimination between long (>120s) and short (<120s) crossing times. The use of these anatomical vessel and lesion characteristics in the clinical prediction rule identifies difficult lesions that may benefit from the precise control given by magnetic navigation.

Introduction

Currently the majority of PCI procedures are performed satisfactorily with conventional wires. However, there is a proportion of PCI procedures where difficulty, or sometimes failure, occurs. As equipment improves and PCI extends into more difficult territories, e.g. smaller, more tortuous, heavily calcified and more distal lesions, there will be an increasing challenge to manual dexterity. The recently introduced magnetic navigation system (MNS) from Stereotaxis uses a magnetic field to precisely steer the wire that utilises a 3D model of the vessel created from angiographic images, and may be of benefit in such problematic procedures. [1] Improved wire delivery may lead to reduced procedural time and complications. [2,3]

However, there is no specific method of identifying those cases where passing the lesion with a wire, or 'crossing', is difficult. The currently available range of lesion classification systems [4-8] is aimed at predicting complications and these have relatively modest accuracies. We have investigated a simple, specific, measurable and crucial part of the PCI procedure, the time to pass the wire from the guiding catheter to a position distal to the culprit lesion. Such prediction may have a number of major benefits. First, better guidance for operators in the assessment of the difficulty of a particular case may help better risk-benefit decision-making. Second, it may allow selection of patients who have difficult morphology for an alternate technique such as magnetic navigation. A clinical prediction rule (CPR) may be a useful method of ultimately comparing magnetic navigation or other navigation technologies to conventional wire manipulation. The aims of this study were two-fold. First, the development of a simple CPR to predict difficult lesions to cross with a conventional wire. Second, the validation of this CPR in lesions that had undergone angioplasty.

Methods

Patient selection

Derivation set

The crossing times of a cohort of 425 consecutive lesions that had elective and semi-urgent PCI performed with a conventional wire at a single centre were noted. Lesions that were excluded from analysis consisted of occluded vessels where a reconstruction could not be produced due to inadequate vessel flow (TIMI flow of 2 or less) such as primary PCI, ACS, and CTOs. ACS patients were generally not excluded. In addition, lesions where special techniques had been used, such as biplane angiography, or magnetic navigation, were excluded. After ranking the crossing times (Figure 1), a random sample of 40 lesions from each tertile was selected for inclusion in the derivation set. The CPR was developed from this set.

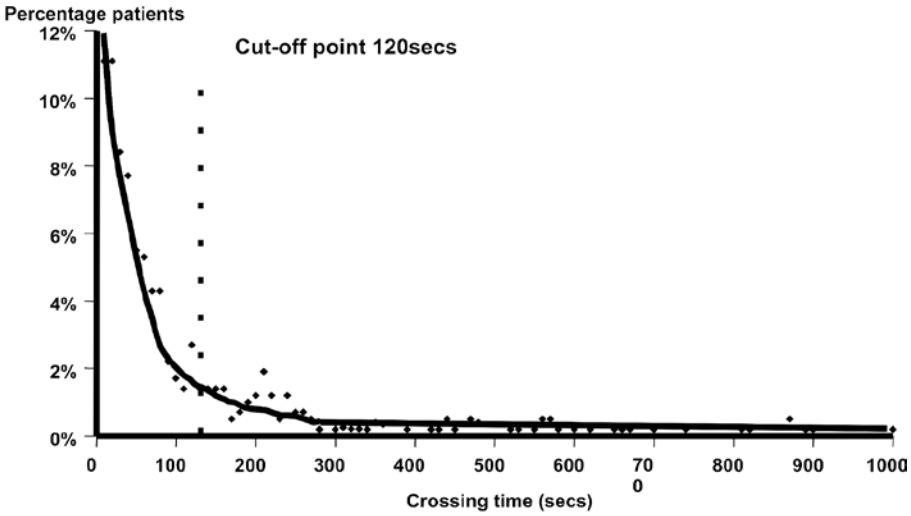

Figure 1. *Graph showing distribution of the total population*

Validation set

The CPR was validated in a second cohort of 415 lesions, the validation set. The same exclusion criteria were used as in the derivation set. 16 lesions were randomly selected from each tertile of the crossing times for further analysis. In order to blind the analysis, the analyst had no knowledge of the results of the crossing time.

Magnetic navigation system

The MNS (Navigant, Stereotaxis, St Louis, USA) has dedicated 3D reconstruction software (CardiOp-B, Paieon Medical Inc., Rosh Ha'ayin, Israel) that produces a virtual model of the entire vessel. With the reconstruction package it is possible to take 2 angiographic views and identify the vessel edges. As the angles of the image intensifier and the position of the table are known, it is possible to triangulate the position of each point of the vessel and make a 3D reconstruction of the vessel that is volume-rendered (Figure 2). All measurements can be made from diagnostic angiography films of suitable quality.

To produce as accurate and reproducible reconstructions as possible, the images were routinely taken in diastole (on or just before the QRS complex). The software has functions that allow measurement of length, diameter and area stenosis with respect to the calculated reference diameter at that point. The model can then be imported into the Navigant program where the angulation of each bend can be measured. The bends were assessed visually and then measured to see whether they fitted the following definition. A bend was considered to be an

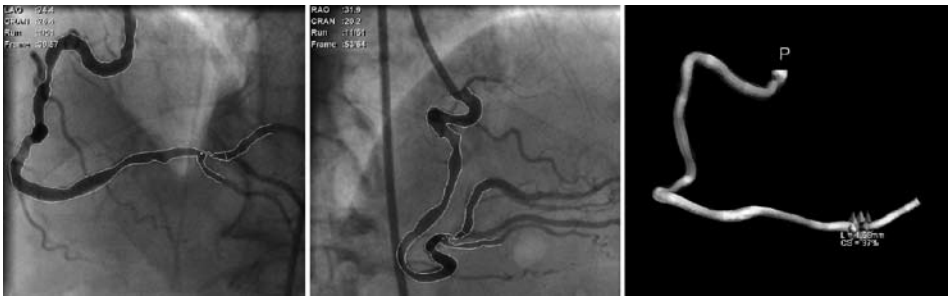

Figure 2. *The left 2 panels show separate angiographic angulations with edges detected and the right panel shows a 2D image of the 3D reconstruction*.

angulation of 45º within 10 vessel diameters (for the purpose of this analysis a standard vessel diameter was considered to be 3mm therefore a bend had to occur within 30mm).

Definition of crossing time

A prolonged crossing time was defined as the absolute time (in seconds) from the initial entry of the wire into the coronary system, out of the guiding catheter, until crossing and reaching a suitable position distal to the target culprit lesion in the coronary artery. The crossing time includes the time required for any and all procedural manoeuvres once the wire has initially left the tip of the guiding catheter, such as the time required to remove and re-shape the conventional wire, re-engagement of the catheter should prolapse occur, or to pass a balloon for support, and implies the placement of the wire in a satisfactory final position for device delivery.

This was a registry where no special techniques of passing a wire were used, and therefore the operators should have been performing normally. While a competitive element may have occurred within an operator's mind, the data once collected was only available to one person. This data was not, and has never been, shown in a fashion that would compare one operator with another and while operators may well have tried to perform their best, this is felt to be an advantage with the 'best' crossing times recorded.

The relevant hypothesised anatomical factors encountered with conventional angioplasty guide-wires can be divided into vessel and lesion characteristics, see appendix 1. We imposed an arbitrary maximum to each factor in order to prevent any specific factor from dominating the grading system.

Vessel characteristics

*Number of bends before the lesion, (Vb), (*Figure *3)*

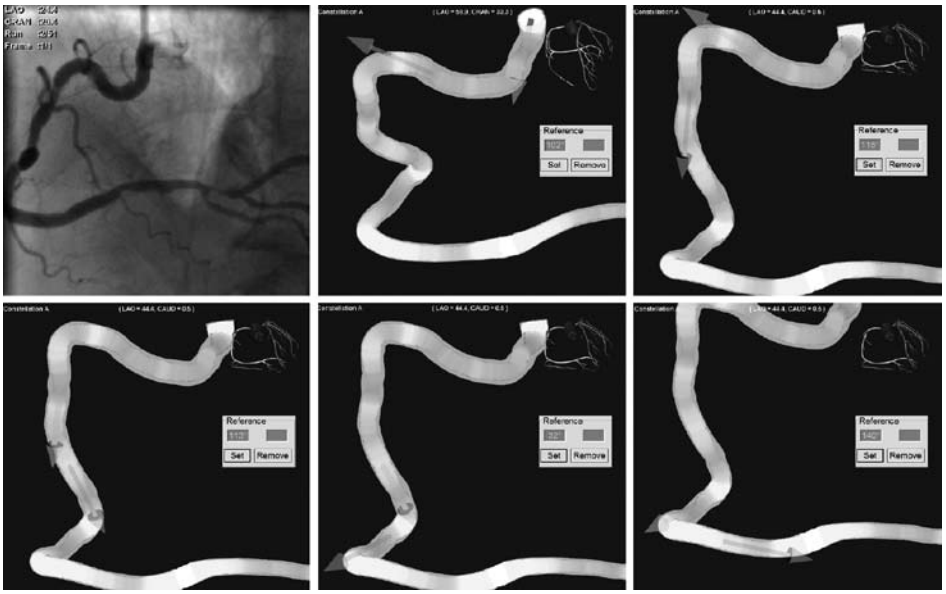

***Figure 3**. Identification of the bends in a vessel and measurement of each angle (possible in the Navigant program) The total angulation of the 5 worst bends, (Vta), (Figure 3)*

Each bend causes deformation of the wire resulting in friction. A greater number of bends leads to increased friction resulting in more difficultly in manipulating the wire. The maximum score is 5.

The greater the cumulative angle, the more the wire is deformed along its course. This results in more friction and produces increased difficulty during manipulation. This has been dichotomised to above and below 45°. The maximum score is 1.

*End-to-end length from the ostium to the lesion, (Vl), (*Figure *4)*
The more distal the lesion is from the ostium, then the greater the chance of encountering problematic bends that impair manipulation, and also the longer the time required to physically pass the wire. This is divided into shorter than 50mm, between 50 and 100 mm and greater then 100mm. The maximum is 2.

Vessel calcification, (Vc).
Calcium may increase friction as the vessel becomes more rigid and less deformable and does not conform to the wire. The frictive effect of a specific angle will be accentuated if deformation cannot occur. The complete angiographic absence of calcium scores 0, mild calcification is 1 and severe calcification is 2. The maximum is 2.

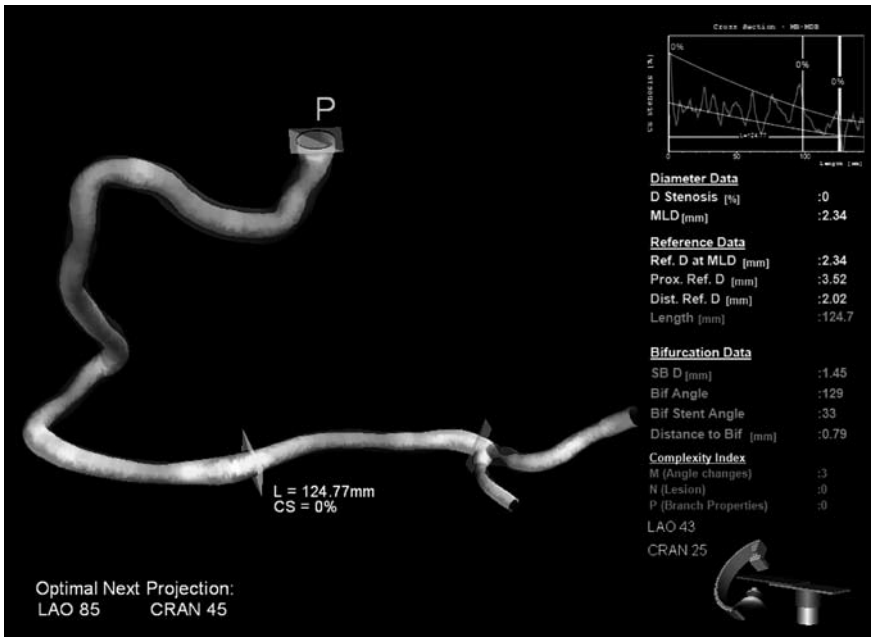

Figure 4. *The measurement of the length from the vessel ostium to the lesion in CardiOp-B (green square indicates proximal marking point and blue square indicates distal marking point)*

*Visible sidebranches before lesion, (Vsb), (*Figure *5)*

Visible sidebranches result in a greater chance of taking a wrong bend. This is dichotomised to 0 or 1.

Lesion factors

Luminal lesion characteristics such as complex and intricate 3D form or tight lesions with little space for manoeuvre affect how quickly and easily a wire can pass. Navigation through complex, intricate, and/or tight lesions may involve a variety of angles that cannot be easily be traversed by a conventional guide-wire with a fixed bend as it has a specific angle of approach.

Lesion characteristics

*Sidebranches within 10mm, (Lbb) (*Figure *5).*

Sidebranches within 10mm of the lesion increase difficultly because, on the approach to a lesion finer control is necessary, the fixed wire-tip angle needed for bends now may have more of a predisposition for sidebranches. This is dichotomised to 0 or 1.

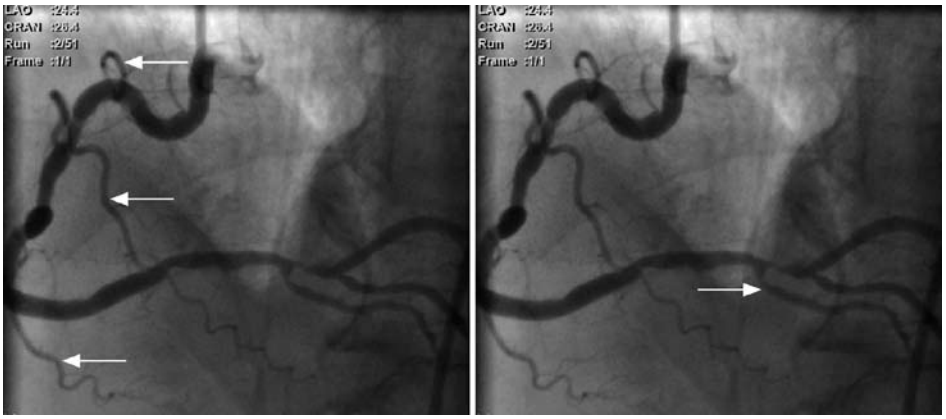

***Figure 5**. The left panel shows visible sidebranches (arrowed) greater then 1mm before the lesion with the right panel showing a branch just before the lesion (within 10mm).*

Sidebranches in lesion, (Lsb).

When the angulated wire tip has to pass through a stenosis, there is a greater chance that the tip will be pushed against the wall and this increases the chance of selecting sidebranches. This is dichotomised to 0 or 1.

Lesion angulation, (La).

The lesion angulation will affect the friction of the wire passing through the lesion. This is dichotomised to 0 or 1.

Lesion calcification, (Lc).

Calcium makes the lesion rigid and reduces deformability, therefore producing more friction. This is dichotomised to 0 or 1.

*Lesion length, (Ll), (*Figure *6).*

Longer lesions produce more friction on the wire. This factor has been divided into <10mm, between 10 and 20mm and greater then 20mm. The maximum is 2.

*Length of severe (greater than 80% area) stenosis, (Lss), (*Figure *6).*

Tighter lesions have greater contact with the wire and this magnifies the effect of bends leading to a greater chance of the wire being forced against the wall. This is dichotomised to into <3mm and >3mm.

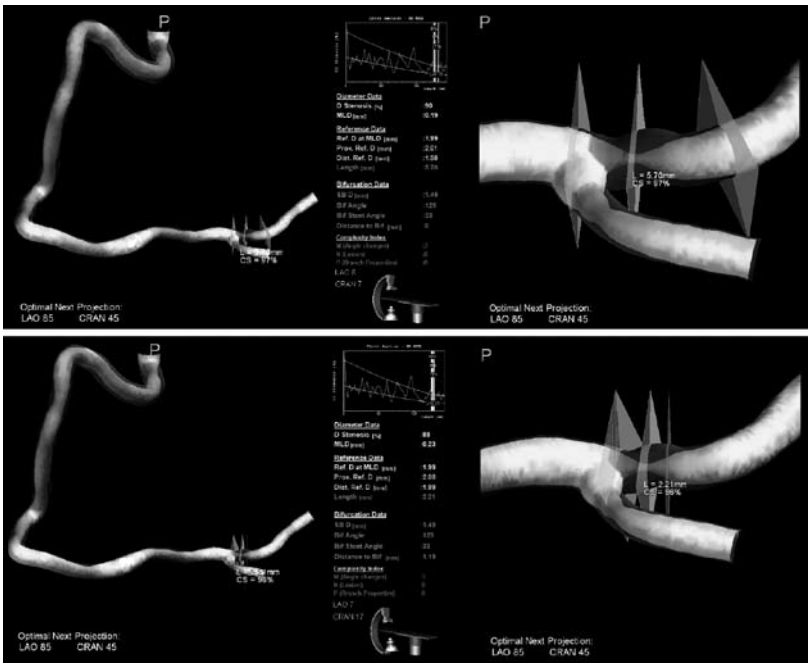

Figure 6. *The top panels show the measurement of the lesion length (green square indicates proximal marking point and blue square indicates distal marking point). The lower panel shows the segment greater than 80% measured in CardiOp-B (green square indicates proximal marking point and blue square indicates distal marking point).*

Statistical analysis

The crossing time was dichotomised with an arbitrary cut-off value of 120 seconds based on the observed crossing times (Figure 1). By the design of the study, one-third of the lesions had the presence of a long crossing time and two-thirds had a normal crossing time.

Statistical modelling

The association between each prognostic factor and the presence or absence of a long crossing time was studied by univariate logistic regression analysis. We applied a stepwise backward selection process (p=0.100) to select the predictors for the final model.

A key problem of regression modelling in small data sets is that the regression coefficients are overestimated for predictive purposes. We calculated a linear shrinkage factor for the regression coefficients with bootstrapping. [9] The difference between performance in the bootstrap samples and the original sample is an estimate of the optimism in the apparent performance (miscalibration). This difference is averaged to obtain a stable estimate of the optimism. 'Shrunk'

***Table 1**. Patient characteristics for test and validation groups*

	Derivation (N=120)	*Validation* (N=48)	*P value*
Baseline patient characteristics			
Age-yr	65.9±10.6	65.5±10.4	0.8
Male sex-no.(%)	74.3	73.3	0.9
Diabetes mellitus-no.(%)	25.7	35.6	0.2
Hypertension-no.(%)	55.7	60.5	0.6
Hypercholesterolemia-no.(%)	94.8	94.8	0.9
History of smoking cigarettes-no.(%)	18.6	11.6	0.3
Previous PCI-no.(%)	32.4	42.2	0.3
Previous CABG-no.(%)	7.6	6.7	0.8
Previous myocardial infarction-no.(%)	38.8	46.7	0.4
Clinical presentation			0.05
Stable angina pectoris	62.1	46.7	
Unstable angina pectoris	37.9	53.3	
CCS class			1.0
I	5.0	5.3	
II	38.3	36.8	
III	53.3	52.6	
IV	3.3	5.3	
LVEF			0.6
Good (>50%)	76.3	66.7	
Moderate (35-50)	15.8	27.8	
Poor (<35)	7.9	5.6	
Vessel disease			0.5
1VD	43.0	31.3	
2VD	30.8	35.5	
3VD	23.4	33.3	

coefficients were calculated by multiplication of the standard coefficients with the shrinkage factor, which might take values between 0 and 1.

The final model was transformed into a CPR. Regression coefficients were rounded to the nearest integer. A score was obtained for each individual lesion by assigning points for each variable and adding the results.

Predictive performance

The prognostic ability of the model, i.e. the power to discriminate between subjects with and without a long crossing time, was estimated with c-statistic. The c-statistic, provides a quantitative summary of the discriminative ability of a predictive model. A value of 0.5 indicates that the model does not have any discriminatory ability, and a value of 1.0 represents perfect discrimination. Calibration refers to whether prediction models agree with the observed probabilities and was assessed with the Hosmer-Lemeshow statistic.

***Table 2**. Results of univariate analysis.*

	Coefficient	P value
Vessel characteristics		
Number of bends before lesion, (Vb)	0.73	<0.001
The total angulation of the 5 worst bends, (Vta)	0.58	0.177
End to end length from the ostium to the lesion, (Vl)		
50-100	1.18	0.009
>100	1.55	0.045
Vessel calcification, (Vc)	2.03	<0.001
Visible sidebranches before lesion, (Vsb)	1.08	0.017
Lesion characteristics		
Sidebranches within 10mm, (Lbb)	0.01	0.985
Sidebranches in lesion, (Lsb)	0.58	0.163
Lesion angulation, (La)	1.00	0.013
Lesion calcification, (Lc)	0.98	0.013
Lesion length, (Ll)	0.75	0.055
Length of severe (> 80% diameter) stenosis, (Lss)	1.01	0.013

Statistical analyses were performed with SPSS and S-plus software (MathSoft, Inc., Seattle WA, version 2000). The authors had full access to the data and take responsibility for its integrity. All authors have read and agree to the manuscript as written.

Results

Mean age was 65 years and 74% were male. All baseline characteristics in the derivation set and the validation set were comparable (Table 1). There was a spread of values for the crossing times showing that 15% of lesions could still not be crossed at 5 minutes (310s) and 10% by 8 min (480s) (Figure 1).

The CPR was derived after applying logistic regression to the sample from the derivation group (results of univariate and multivariate analysis shown in Tables 2 and 3) to provide a relative estimate of crossing complexity:

Procedure with a prolonged crossing time (>120s) = 1*Vb + 1*(Vl=1) + 2*(Vl=2) + 2*Vc + 1*Lbb)+1*(Ll=1) + 2*(Ll=2) .

(N.B. abbreviations refer to morphological factors, see appendix 1)

This dichotomises cases into easy and difficult (prolonged crossing time). A value of 6 was found to be the best cut-off value. The c-index of the standard model was 0.88 and 0.83 for

***Table 3**. Multivariate predictors of the crossing times in the derivation set*

	ß coefficient	Odds Ratio	P-value
Bends to lesion, (Vb)	1.0278	5.06 (1.54-16.66)	<0.001
(end to length from the ostium to lesion (Vl) 50-100mm	1.0495	0.44 (0.12-1.63)	0.119
>100mm	2.7242	3.75 (0.38-37.13)	0.018
Vessel calcification (Vc)	2.9004	9.85 (2.52-38.42)	<0.001
Sidebranches in lesion (Lbb)	1.0622	2.31 (0.78-6.89)	0.057
Lesion length (Ll) 10-20	0.8377	0.52 (0.15-1.76)	0.018
>20	2.0567	2.62 (0.68-10.01)	0.004

the shrunk model used for the CPR. Calibration with the Hosmer-Lemeshow test gave a non-significant p-value. This CPR was then applied to the results from the validation cohort. The cstatistic derived from this group was 0.82 showing good discrimination.

Discussion

We have developed a clinical prediction rule (CPR) that examines the whole vessel that is undergoing PCI and is able to predict which vessels will require more time and contrast to cross. The CPR integrates the use of a 3D reconstruction developed from a combination of lesion and vessel characteristics to give a relative estimate of crossing complexity. It will allow an assessment of the importance of physical factors on wire passage and whether difficult wire passage is related to increased complication rates. This is directly applicable to the decision process of selecting a patient for a magnetically navigated procedure.

This system is fundamentally different from previous classification systems that were developed for the prediction of procedural success and complications. The ACC/AHA guidelines for lesion grading were developed in 1988, [4] modified in 1990, [5] and use 11 simple angiographic factors to help take into account lesion complexity in the comparison of the outcomes of PCI. Further systems, such as the SCAI [6] or the Mayo Risk Score [7] or the SYNTAX score, [8] were subsequently developed in order to improve this predictive ability further. However, the discriminatory power was lower than expected. [5,10] A number of possible reasons may help to explain this shortcoming. First, previous grading systems use a number of coronary factors that have generally been simple, angiographically-defined lesion characteristics. Use of such simple lesion characteristics may underestimate both the lesion complexity itself and also the importance of the rest of the vessel in successfully crossing with a wire. Second, while these factors have a great deal of merit in their simplicity, they are visual estimates from angiographic images and these are known to have poor inter-observer reproducibility. [11-13] Third, some systems include clinical factors, either as an endpoint or in their grading, that are frequently complex and multi-factorial. Difficulty in crossing an individual coronary lesion, that is so problematic

as to result in a clinical complication, may only be indirectly related to a poor clinical state of an acutely sick patient or to the pre-existing clinical diseases. Conversely, a poor clinical state or pre-existing disease may be more closely associated with a complication than the adverse coronary anatomy. Therefore the use of clinical factors, either the pre-existing clinical diseases or the resultant clinical complication, may obscure a clear answer.

A number of factors have been investigated in previous studies. These indicate that increasing complexity of a lesion is associated with an increasing incidence of complications [6,14] and that some anatomical factors of the vessel, such as tortuosity, lesion length or angulation, are associated with decreased success of stent passage. [15-17] The introduction and use of new 3D imaging technology enables a more complete anatomical analysis of the vessel and lesion in a new way. In order to give the clearest idea of factors that might influence passage of the wire we analysed the entire vessel as well as the target lesion. This approach has not been used before.

All the measurements required for the CPR can be obtained from adequate diagnostic angiography films. The CPR can be applied in a matter of minutes and is therefore applicable in general practice. This system is completely independent of the clinical factors that, while important in the broad clinical outcome, are either only loosely related, or even irrelevant, to the passage of a wire through a coronary artery. The analysis aimed to reflect these factors by defining the anatomy of both the coronary vessel and lesion. There are a number of advantages of this system. First, it uses a 3D reconstruction to identify and measure specific vessel factors and to give hard numbers to predict a single, clearly definable endpoint. Second, it examines the anatomy of the entire vessel, a factor that is clearly crucial to the delivery of a wire. Third, it is independent of the clinical factors that obscure the importance of physical factors. Fourth, it has clear applicability in choosing patients who might benefit from a magnetically navigated procedure.

There are a number of limitations. Currently the reconstruction is time-consuming and can take up to 30 minutes to complete. The production of the reconstruction requires angiography of a suitable standard and is not always possible from standard views due to foreshortening or overlapping. The reconstruction that is produced is static and the impact of movement on the measured factors, such as angulation, is unknown. After analysis some factors were not incorporated into the CPR. There may be a variety of reasons for this. Some factors occurred infrequently, such as the presence of a stent. The infrequent occurrence therefore may not reflect the unimportance of the factor but the effect of a small sample size e.g. few patients with stents. Another possible reason for a particular factor not showing significance is the variability of the factor itself. Sidebranches may be cannulated without intention during procedures but this may only occur with sidebranches that come off at a certain angle and not all as measured

in this analysis. Therefore, in general, these factors may play some role, but this may only occur in specific circumstances, or occasionally, and will need further investigation to identify any additional benefit. More generally, there was unselected use of wires and no selection of operators. The limitations of this model therefore also relate to individual operators, techniques and equipment. There were a number of operators and types of wires and this, together with no selection of the target vessel segment, may have led to heterogeneity. In addition, this study examines only one specific aspect of the PCI and deliberately does not address other necessary elements such as the passage and deployment of the balloon and stent. Lastly, this study was performed at a University specialist tertiary referral unit and the case mix might be different to that seen elsewhere.

Despite such limitations, the system could prove useful in application. The ability to predict difficult cases may allow consideration for alternative strategies. In this context, the ability of the MNS to precisely direct the tip of a wire has a clear potential for improving the treatment of patients identified in this way. However the system could potentially be used in other ways. As the number of MNS in an institution is normally limited to one, reconstruction could be performed on selected subsets of patients. Identification of the patients who would most benefit would be not only beneficial for patients but would maximise efficiency. Alternately, an automated system would also allow all patients to be screened in addition to possibly improving reproducibility.

This CPR will be valuable in several ways. First, to identify which anatomical factors are predominant by prospectively identifying difficult cases. Second, this may be a crucial tool in deciding whether a patient should undergo a conventional procedure or rather will benefit from magnetic navigation.

Acknowledgement
The authors are grateful to Joep Maeijer for help with preparation of the images.

Conflicts of interest
The authors have no conflicts of interest.

References

1. Patterson MS, Schotten J, van Mieghem C, Kiemeneij F, Serruys PW. Magnetic Navigation in Percutaneous Coronary Intervention. *Journal of Interventional Cardiology* 2006;**19**(6), 1-6.
2. Patterson MS, Ramcharitar S. Serruys PW. Magnetically Supported PCI: success after failed surgery and conventional PCI. *Cath Lab Digest* 2007;**15(3)**:1-14.
3. Ramcharitar S, Patterson MS, Serruys PW. Randomised controlled study comparing conventional wires with magnetic guided wires in a tortuous phantom. *Cathet Cardiovasc Interv* 2006;**69**:852–855.
4. Ryan TJ, Faxon DP, Gunnar RM, Kennedy JW, King SB 3rd, Loop FD, Peterson KL, Reeves TJ, Williams DO, Winters WL Jr Guidelines for percutaneous transluminal coronary angioplasty. A report for the American College of Cardiology/American Heart Association Task Force on assessment of Diagnostic and Therapeutic Cardiovascular Procedures (Subcommittee on Percutaneous Transluminal Coronary Angioplasty). *Circulation* 1988;**78**:486-502.
5. Ellis SG, Vandormael MG, Cowley MJ and the POSCH Group. Coronary morphologic and clinical determinants of procedural outcome with angioplasty for multivessel coronary disease. Implications for patient selection. Multivessel Angioplasty Prognosis Study Group. *Circulation* 1990;**82**:1193-1202.
6. Krone RJ, Laskey WK, Johnson C, Kimmel SE, Klein LW, Weiner BH, Cosentino JJ, Johnson SA, Babb JD for the Registry Committee of he Society for Cardiac Angiography and Interventions. A simplified lesion classification for predicting success and complications of coronary angioplasty. *Am J Cardiol* 2000;**85**:1179-1184.
7. Singh M, Rihal CS, Lennon RJ, Garratt KN, Holmes DR. Comparison of Mayo Risk Score and American College of Cardiology/American Heart Association Lesion Classification in the Prediction of Adverse Cardiovascular Outcome following Percutaneous Coronary Interventions. *J Am Coll Card* 2004;**44**:357-61.
8. Valgimigli M, Serruys PW, Tsuchida K, Vaina S, Morel MA, van den Brand MJ, Colombo A, Morice MC, Dawkins K, de Bruyne B, Kornowski R, de Servi S, Guagliumi G, Jukema JW, Mohr FW, Kappetein AP, Wittebols K, Stoll HP, Boersma E, Parrinello G; ARTS II Investigators. Cyphering the complexity of coronary artery disease using the syntax score to predict clinical outcome in patients with three-vessel lumen obstruction undergoing percutaneous coronary intervention. Am J Cardiol. 2007;99(8):1072-81.
9. Steyerberg EW, Eijkemans MJ, Van Houwelingen JC, Lee KL, Habbema JD. Prognostic models based on literature and individual patient data in logistic regression analysis. *Stat Med*. 2000;19**(2)**:141-60.
10. Moushmoush B, Kramer B, Hsieh AM, Klein LW. Does the AHA/ACC task force grading system predict outcome in multivessel coronary angioplasty? *Cathet Cardiovasc Diagn* 1992;**27**:97–105.
11. Herrman JPR, Azar A, Umans VAWM, Boersma E, V Es G-A, Serruys PW. Inter- and intra-observer variability in the qualitative categorization of coronary angiograms. *Int J Card Imaging* 1996;**12**:21-30.
12. Botas J, Stadius ML, Bourassa MG, Rosen AD, Schaff HV, Sopko G, Williams DO, McMilliam A, Alderman EL. Angiographic correlates of lesion relevance and suitability for percutaneous transluminal coronary angioplasty and coronary artery bypass grafting in the Bypass Angioplasty Revascularization Investigation Study (BARI). *Am J Cardiol* 1996;**77**:805– 814.
13. Kleiman NS, Rodriguez AR, Raizner AE. Interobserver variability in grading of coronary arterial narrowings using the American College of Cardiology/American Heart Association grading criteria. *Am J Cardiol* 1992;**69**:413– 415.
14. Krone RJ, Shaw RE, Klein LW, Block PC, Anderson HV, Weintraub WS, Brindis RG, McKay CR; ACC-National Cardiovascular Data Registry. Evaluation of the American College of Cardiology/American Heart Association and the Society for Coronary Angiography and Interventions lesion classification system in the current "stent era" of coronary interventions (from the ACC-National Cardiovascular Data Registry). *Am J Cardiol*. 2003;**92(4)**:389-94.
15. Kimmel SE, Berlin JB, Strom BL, Laskey WK, for the Registry Committee of the Society for Cardiac Angiography and Interventions. Development and validation of a simplified predictive index for

major complications in contemporary percutaneous transluminal coronary angioplasty practice. *J Am Coll Cardiol* 1995;**26**:931–938.
16. Ellis SG, Guetta V, Miller D, Whitlow PL, Topol EJ. Relation between lesion characteristics and risk with percutaneous intervention in the stent and glycoprotein IIb/IIIa era: an analysis of results from 10 907 lesions and proposal for new classification scheme. *Circulation* 1999;**100**:1971–1976.
17. Zaacks SM, Klein LW. The AHA/ACC task force criteria: what is its value in the device era? American Heart Association/American College of Cardiology. *Cathet Cardiovasc Diagn* 1998;**43**:9 –10.

Appendix

Grading factors

Vessel characteristics	***range of values***
Number of bends before lesion, (Vb)	
max 5	*(0-5)*
The total angulation of the 5 worst bends, (Vta)	
0:<45,1>45	*(0-1)*
End-to-end length from the ostium to the lesion, (Vl)	
0:<50mm, 1:50-100, 2:>10	*(0-2)*
Vessel calcification, (Vc)	
0:none, 1:yes	*(0-1)*
Visible sidebranches before lesion, (Vsb)	
0 or 1	*(0-1)*
Lesion characteristics	
Sidebranches within 10mm, (Lbb)	
0:no, 1:yes	*(0-1)*
Sidebranches in lesion, (Lsb)	
0:no, 1:yes	*(0-1)*
Lesion angulation, (La)	
0:<45,1:>45	*(0-1)*
Lesion calcification, (Lc)	
0:no, 1:yes	*(0-1)*
Lesion length, (Ll)	
0:<10, 1:10-20, 2:>20	*(0-2)*
Length of severe (> 80% diameter) stenosis, (Lss)	
0:<3mm, 1:>3mm	*(0-1)*

ASSESSMENT OF SUCCESS IN NATIVE CORONARIES

A Randomised Comparison of the Magnetic Navigation System versus Conventional Percutaneous Coronary Intervention

Catheter Cardiovasc Interv ***2008*** (in press)

Ramcharitar S, van Geuns RJ, Patterson MS, van der Ent M,
van der Giessen WJ, van Domburg RT, Serruys PW

Abstract

Objectives:
A randomised comparison of the Magnetic Navigation System (MNS) to conventional guidewire techniques in Percutaneous Coronary Interventions

Background:
The MNS precisely directs a magnetised guidewire *in vivo* through two permanent external magnets.

Methods:
111 consecutive patients were enrolled. Crossing success, crossing/fluoroscopy times and contrast usage were directly compared. Lesions were classified according to the AHA/ACC criteria. Three tertiles of vessel/lesion complexity [low (<5), medium (6-10) and high (>10)] were defined using 3-D reconstructions and angiographic information.

Results:
The crossing success for magnetic and the conventional wires were 93.3% and 95.6% respectively. Crossing and fluoroscopy times were longer with the magnetic wires (72.9 ± 50.3sec vs. 58.1 ± 47.2sec, p<0.001 and 66.2 ± 44.1sec vs. 55.2 ± 44.4sec p=0.03 respectively). In vessels with low and medium complexity the magnetic wires had significantly longer times (p<0.001) but for those with high scores (>10) a trend towards shorter times was observed. The MNS resulted in a small but significant reduction in contrast usage (2.3 ± 3.5ml vs. 4.5 ± 4.4ml p < 0.001). Moreover by superimposing a virtual roadmap of the vessel on the live fluoroscopy image 48% of the lesions were crossed without requiring contrast agents with the MNS

Conclusion:
The MNS has comparable crossing success to conventional PCI. It is relatively slower but there is a trend to support a potential advantage in more complex vessels. By simultaneously employing a virtual roadmap there is a small but significant reduction in contrast usage.

Introduction

Magnetic navigation is an innovative technology that can accurately control the positioning of a guidewire or a catheter *in vivo* (1). To accomplish this, a small (2-3mm) magnet embedded at the tip of the wire or catheter is reoriented by a predetermined and rapidly updated external magnetic field. The field is generated by two permanent external (0.08 Tesla) magnets that can rotate, tilt or translate on movable positioners (2). Within this field a magnetic vector is created through computer driven software to direct the tip of the device (the magnetically enabled wire or catheter). The advantage of *in vivo* control has been previously demonstrated in cardiac electrophysiological procedures whereby inaccessible pathways can be effectively targeted, even remotely (3). In percutaneous coronary intervention (PCI) the initial bend placed on the wire to engage the target vessel might not be ideally suited to cross the target lesion. As such, preliminary studies in patients with complex lesions and tortuous vessels have shown an advantage with magnetic assisted intervention (MAI) in cases that failed with conventional PCI (4). However, to date the only randomised direct comparison of the magnetic navigation system (MNS) to conventional approaches was performed in increasingly tortuous phantom models where it was suggested that the MNS might be advantageous (5). In order to further assess the implication of this novel technology to PCI, it is necessary to include randomised comparisons in native coronary lesions. Areas that warrant investigation include evaluating procedural success, crossing/fluoroscopy times together with contrast media usage. It is perceived that for some of these parameters the MNS may be advantageous as reorienting the wire *in situ* and the navigational road map created from a 3-dimensional reconstructed image - superimposed on real-time fluoroscopy - may indirectly influence the procedure (6). To assess the performance of the MNS we performed the first direct randomised comparison with conventional wire technique in patients presenting with stable and unstable angina.

Material and Methods

Patient Selection and Definitions

In a 12-month period commencing September 2006, 111 consecutive patients admitted with stable and unstable angina were single blinded randomised to cross the culprit lesion twice, either using a conventional or a magnetically enabled guidewire. All patients were appropriately informed about the procedure and gave their consent. Angina was defined according to the Canadian Cardiovascular Society and Braunwald classification respectively (7,8). Patients were excluded if they were haemo-dynamically unstable or had contraindications for magnetic-assisted intervention (MAI) such as a pacemaker. The objectives of the study were the direct evaluation of the crossing success, crossing/fluoroscopy times and contrast usage. This was assessed by measuring the time (sec) and contrast media (ml) required to cross the lesion

having firstly placed the guidewire at the tip of a guiding catheter engaged at the ostium and following the wire passage distal to the lesion. The wire was then withdrawn and the comparative wire was then used to coincide with the start and end position of the first wire. Lesions not crossed within 6 minutes with either wire were labelled as wire failures as previously defined by our published phantom studies (5). Included within the 6 minutes was the time taken for wires to be removed from the catheter and reshaped in order to achieve a successful crossing. Wires that were damaged in crossing could be exchanged for a similar or different conventional or magnetically enabled wire if necessary. The operators (4 in total) had unrestricted access to the choice of either magnetic or conventional guidewires and were interventional cardiologists who were also trained in MAI procedures. The crossing success of each wire was defined as the amount/percentage of successful crossings within 6 minutes. The procedural success was defined as successful crossings without time restrictions using the complementary technique having failed with the first wire technique to cross within 6 minutes.

The Magnetic Navigation System

The Niobe® II Magnetic Navigation System (MNS) (Stereotaxis, St. Louis, M. USA) integrated with a modified C-arm flat-panel detector-fluoroscopic imaging suite (AXIOM Artis dFC, Siemens Medical Solutions, Forchheim, Germany) for angiographic imaging was used throughout this study. The system allows two different modes for navigation by using either 2-Dimensional (2D) such as in the "clockface" method (Figure 1A) or 3-Dimensional (3D) maps of the coronary artery(1). In this study navigation was performed using a 3-dimensional reconstructed (3DRC) virtual vessel roadmap generated from two angiographic images 30° apart (CardiOp-B, Paieon Medical Inc., Rosh Ha'ayin, Israel) (Figure 1B). The 3DRC was first co-registered with the fluoroscopic image (Figure 1C) and a navigational pathway created through the lumen of the 3DRC (Figure 1D). This pathway was then displayed as a fixed centreline on the real-time fluoroscopic image. The operator was then able to manually advance the navigational vectors associated with this centreline at a predetermined distance (1-9mm) by pressing the advance/go button on the touch screen monitor. In cases of complex 3DRC the navigation was performed using the 2-D "clock face" model. In this model navigational vectors are displayed in a circle that looks like the face of a 12hour clock on the touch screen monitor. By pressing points around the perimeter of the circle/clock, the software (Navigant®) calculates vectors to redirect the magnetic field and realign the wire tip to the chosen direction (Figure 1A). In both the 2D and 3D navigational modes the operator manually advances the guidewire once the vector reaches the desired position. As training with the magnetic system requires both an understanding of the software and the hardware on average a novice needs at least 12 hours of practical training to be fully acquainted with all the techniques and tools. In our department, which is a leading center that evaluates the MNS to PCI we feel that after 35 magnetic cases the operator can be

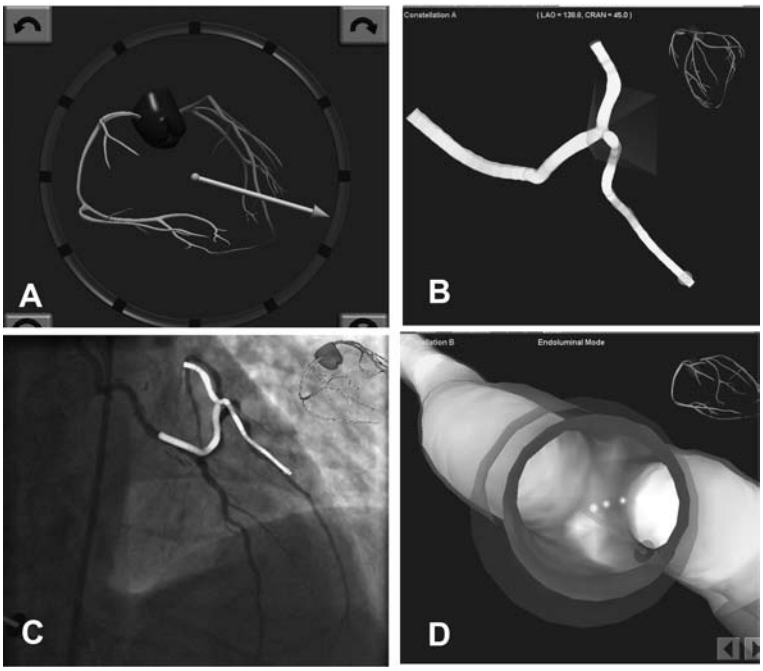

Figure 1. *The clockface navigational mode showing a vector depicted by an arrow that can be repositioned by selecting points around the perimeter of the clock; B) a 3-dimensional reconstruction of a coronary bypass graft to the native left anterior decending artery and C) the registration with the fluoroscopic image; D) navigating at the bifurcation of the virtual reconstructed graft showing a navigational pathway through the lumen*

called an experienced user. In addition, one trained technician is required to operate the system from a control viewing room in the catheterization laboratory.

The Guidewires

The conventional wires used in the study were PT Graphix™ Intermediate, Choice™ PT Floppy (Boston Scientific Corp. Miami Fl, USA), Whisper (Abbott Vascular Devices, Redwood CA, USA) and high torque BMW (Guidant Corp, Santa Clara CA, USA). The magnetic guidewires used were all 180cm long Titan™ Soft Support wires with a 2mm angled and 2mm or 3mm straight magnetic tips attached to a 0.014in/0.36mm stainless steel core (Stereotaxis, St. Louis, M. USA).

Lesions and Vessel Characterisations

Lesions were defined as type A, B1, B2, and C in accordance with the American College of Cardiology/American Heart Association ACC/AHA classifications(9). Type A lesions were generally discrete (<10mm length), concentric, readily accessible non-angulated lesions with little or no calcification and did not involve the ostium or major side branches. Type B1-lesions were longer

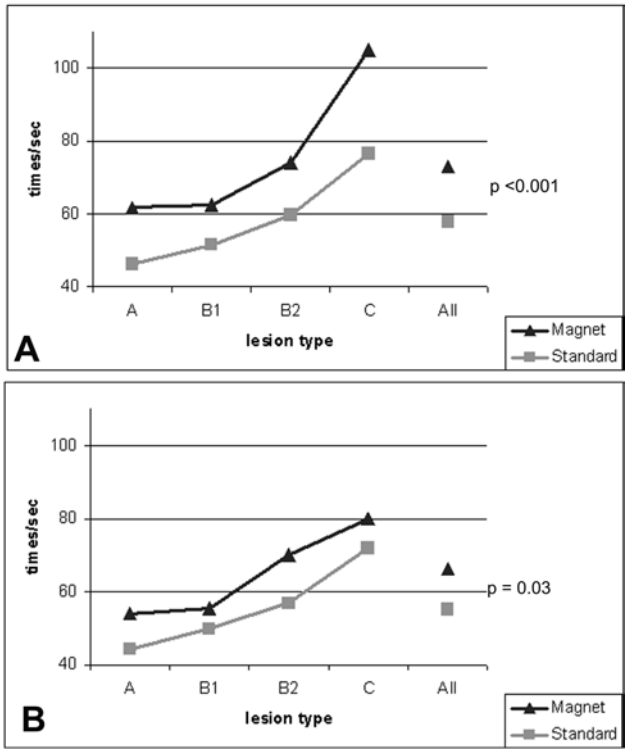

***Figure 2**: Relationship of A) Crossing and B) Fluoroscopy times of both the conventional and magnetic wires to the lesion subtypes*

(10-20mm), or eccentric, or with moderate tortuosity and angulation (45-90°). These lesions might have moderate to heavy calcification and could involve the ostium or a bifurcation. Lesions classed as type B2 had more than one B1 criteria. Type C lesions were diffusely diseased (>2cm in length) with extreme tortuosity and angulations (>90°). When involving a complex bifurcation there is a potential risk of losing the side branch.

Given the limitations of the AHA/ACC classification, namely in not considering the vessel characteristics which may influence the ability to get a wire across our group has developed a simple score system for predicting prolonged crossing times to select patients who would benefit from MAI (10). The score takes into consideration the angulation of the proximal segment, the number of bends to reach the lesion, total vessel angulation, length, calcification, number of side-branches and if there is a stent proximal to the lesion. It also incorporates the following lesion characteristics: side-branch in the lesion or within 10mm of the lesion, lesion angulation and calcification, the lesion length and the length of lesion more than 80% diameter stenosis and also if the lesion is due to instent restenosis (Table 1)(11). The vessel angulations and turns defined as a change in angulation of > 45º were determined using the virtual 3DRC

images created in the CardiOp-B® and integrated in the Navigant®. This scoring system was used to define three tertiles of vessels taking into account the lesion characteristics: - low (<5), medium (6-10) and high (>10) so that the performances of the wires in relation to the vascular anatomy could be evaluated.

Statistical Analysis

Continuous variables are presented as mean ± standard deviation. Student T-test was used to determine if there were significant differences between the parameters assessed using the two techniques. Spearman non-parametric correlation was used to define a trend between the crossing/fluoroscopy times, contrast media usage and lesion/vessel type. Analyses were performed using SPSS 11.5 for Windows (SPSS, Chicago, IL). *P* value < 0.05 was considered statistically significant. Scatter plot distribution was examined correlating complexity score with crossing/fluoroscopy times and contrast media usage for both the magnetic and the conventional wires.

Results

In 93% of the cases magnetic navigation was performed with a 3-dimensional reconstructed (3DRC) virtual vessel roadmap superimposed on the real time fluoroscopy image. The 'clock face' technique was used for the remaining cases. In the 111 patients having 165 lesions there were 7 magnetic wire and 3 conventional wire failures corresponding to a crossing success within 6 minutes of 93.3% and 95.6% respectively. In addition, in another 4 cases (4 lesions) both wires failed in the same patient within 6 minutes. In 3 of these, the lesions were eventually crossed successfully (1 magnetically and 2 conventionally). In one case where both wires failed, the patient proceeded to coronary arterial bypass surgery. The overall procedural success in this study was 99.3% with 91.5% of the lesions crossed within 6 minutes. The direct comparison of successful crossing in the same vessel was performed in 151 lesions (151vessels) corresponding to103 patients.

The patient characteristics are shown in Table 2. The average age of the patients was 64.4 years with three quarters being male. Over one fifth were diabetic, with 3.9% on insulin and almost two-thirds were hyperlipidaemic. Three quarters of the patients presented with stable angina. Nearly, one third of the patients had previous PCI with 6.8% having prior surgery. There was a similar distribution of single and multi-vessel disease within the total population. In 9.7% of the patients a creatinine >100µmol/l was observed. Lesions classified according to the AHA/ACC criteria were 15 Type A (10%), 30 Type B1 (20%), 95 Type B2 (63%) and 11 Type C (7%). The LAD was targeted in 60 patients (40%), followed by the RCA (N=29, 19%), then the diagonal (N=26, 17%), the LCx (N=25, 16%), marginalis (N=9, 6%) and the ramus intermediate (N=2, 1%).

***Table 1**: A scoring system based on vessel and lesion characteristics*

Vessel Characteristics	Score ( )
1st turn (Aorta-Prox vessel angulation)	(0):<90°, (1):90°-135°, (2)>135°
Turns (number) before lesion	1 turn = 1, 2 turns = 2 etc, max (5)
5 worst angulations	(0)<45°, (1):45-90°, (2):90-135°, (3):135-180°, (4)>180°
End to end length ostium-lesion/mm	(0)<50mm (1):50-100mm, (2):>100mm
Visible calcification	(0):none, (1):mild, (2):severe
Visible side branch before lesion	max (2)
Stent before lesion	(0):no, (1):yes
Lesion Characteristics	
Side branch within 10mm	(0):no, (1):yes
Side branch in lesion	(0):no, (1):yes, (2):yes
Lesion angulation	(0)<45°, (1):45-90°, (2):90-135°, (3):135-180°, (4)>180°
Lesion calcified	(0):no, (1):yes
Lesion length/mm	(0):<10mm, (1):10-20mm, (2)>20mm
Length/mm of >80% stenosis	(0):<1mm, (1):1-3mm, (2):3-10mm, (3)>10mm
Through a stent	(0):no, (1):yes (1stent), (2):yes (through struts)
Specific morphological abnormality Eg. aneurysms, fistula etc.	(0):no, (1):yes for each (max 6)

***Table 2**: Patient characteristics*

Patient Characteristics	(N): Patients	%
Age/years	64.4	(45-90)†
Sex	(male)	74.2%
	(N=68)	66.0%
Non/Unknown Smoker	(N=28)	27.2%
Ex-smoker	(N=7)	6.8%
Current Smoker	(N=23)	22.3%
Diabetes	(N=4)	3.9%
Insulin	(N=65)	63.1%
	(N=49)	47.6%
Hyperlipidaemia	(N=47)	45.6%
Hypertension		
Family History		
Indication		
Stable Angina	(N=78)	75.7%
	(N=25)	24.3%
Unstable Angina	(N=30)	29.1%
Previous PCI	(N=7)	6.8%
CABG		
Diseased Vessel		
	(N=49)	47.6%
1 Vessel Disease	(N=43)	41.7%
2 Vessel Disease	(N=11)	10.7%
3 Vessel Disease		
	(N=10)	9.7%
Renal Dysfunction (Creatinine > 100µmol/l)	† Range	

Crossing and Fluoroscopy Times

Overall the crossing times (sec) with the magnetically enabled wires were longer than the conventional standard wire approach (72.9 ± 50.3sec vs. 58.1 ± 47.2sec, p<0.001) especially in AHA/ACC B2 lesions (p=0.01) (Table 3). The crossing times proportionally increased with the lesion complexity (Figure 2A). Simpler type A and B1 lesions were quicker to cross with either wire than the more complex B2 and C lesions, But sub-analyses of the crossing times revealed that the magnetic wires were significantly slower than the conventional wire in both groups.

In the group consisting of type A and B1 lesions the times for magnetic wires compared to the conventional wires were (62.3 ± 42.8sec vs. 50.0 ± 31.9sec, p= 0.02) and in the group containing the lesions B2 and C the times were (77.4 ± 52.9sec vs. 61.5 ± 52.0sec, p= 0.002 respectively). In a comparative assessment of the fluoroscopy times, the conventional approach with the standard wires were overall superior to the magnetic wires although the difference was less (66.2 ± 44.1vs. 55.2 ± 44.4sec, p=0.03) compared to the crossing times (Table 3 and Figure 2B).

The relationship of the Crossing and Fluoroscopy Times to the Complexity score

Scatter plots and correlation of the complexity scores were performed for both the crossing and fluoroscopy times with the standard conventional and magnetic wires. Although there were no obvious correlation a lower slope and R^2 was observed with the magnetic. This may suggests that the magnetic wire had less of an influence on both the crossing and fluoroscopy times in vessels/lesion having high complexity scores – (standard conventional wire's slope and correlation coefficient of the crossing times/sec with complexity score was 7.5 and 0.2 respectively; magnetic wire's slope and correlation coefficient of the crossing times/sec with complexity score was 4.3 and 0.06 respectively; similarly, standard conventional wire's slope and correlation coefficient of the fluoroscopy times/sec with complexity score was 7.2 and 0.21 respectively; magnetic wire's slope and correlation coefficient of the fluoroscopy times/sec with complexity score was 4.0 and 0.07 respectively). When the complexity scores were sub-grouped into tertiles of less than 5 and from 6 to 10 the crossing and fluoroscopy times were significantly prolonged (p<0.001) with the magnetic wires compared to the conventional standard wires (Figure 3). Interestingly, for the tertile greater than 10 both the crossing and fluoroscopy times with the magnetic wire were shorter than that observed with conventional wires although they were not significant (p values of 0.24 and 0.21 respectively).

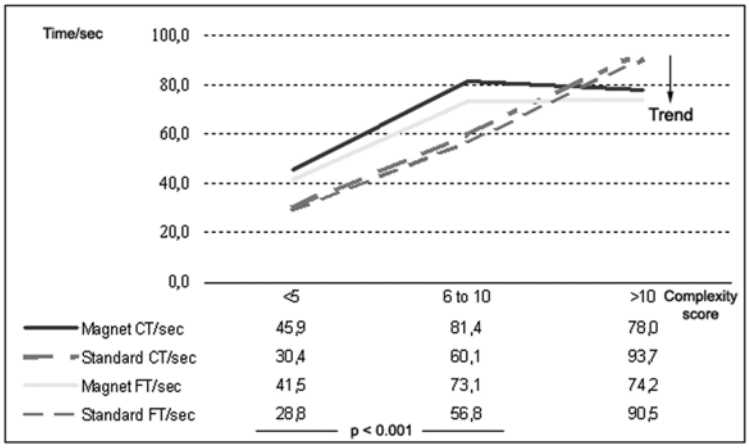

***Figure 3**: Relationship of the Crossing and Fluoroscopy Times to the Complexity score per tertile (FT = fluoroscopy time; CT = crossing time)*

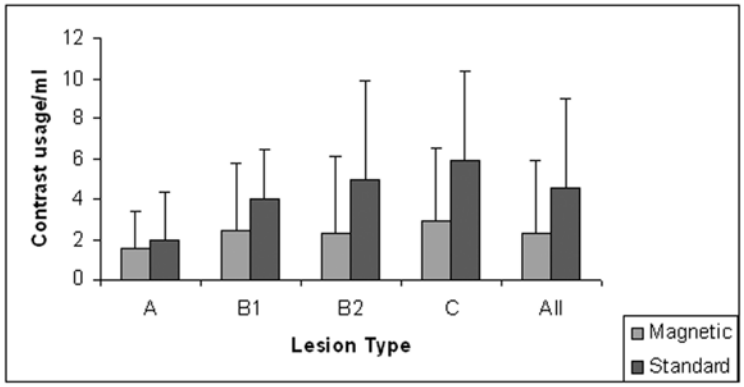

***Figure 4** Comparative contrast usage based on lesion type*

Crossing times and the Minimum Luminal Diameters

Regardless of the studied vessel's minimum luminal diameters (MLD) the magnetic wire was slower. In vessels with a MLD > 2mm the magnetic wire crossing times/sec compared to the standard conventional wires were 52.8 ± 42.9sec vs. 34.2 ± 20.2sec, $p<0.03$. Similarly, in vessels having MLDs of 1-2mm and < 1mm the crossing times/sec were 74.1 ± 52.7sec vs. 56.9 ± 46.1sec, $p<0.004$ and 75.8 ± 49.6sec vs. 63.7 ± 51.1sec, $p<0.05$ respective to that of the standard conventional wires.

Table 4 *The lesions crossed using zero contrast*

Lesion Type	Number of lesions crossed without contrast	
	Magnetic Wire 72	Conventional Wire 31
Type A	8	7
Type B1	14	3
Type B2	47	19
Type C	3	2

Contrast Media Usage

The Spearman non-parametric correlation test demonstrated a positive trend between contrast media usage and lesion complexity with the conventional wire technique (p=0.025). This increase in contrast media usage was eliminated when the MNS was employed (p=0.63) with the Spearman non-parametric correlation for trend. Type A lesions showed no significant difference in contrast usage (ml) in crossing with either the magnetic or conventional wire (1.5 ± 1.8 vs. 1.9 ± 2.3 p = 0.59 respectively) (Figure 4). As lesion complexity increased significantly less contrast (ml) was needed with the MNS:- Type B1 (2.5 ± 3.2 vs. 4.0 ± 2.6 p = 0.01); Type B2 (2.3 ± 3.8 vs. 4.9 ± 4.9 p < 0.001); Type C (2.9 ± 3.4 vs. 5.9 ± 4.9 p = 0.03).

Overall the MNS gave a small but significant reduction in contrast usage (2.3 ± 3.5 vs. 4.5 ± 4.4 p < 0.001) relative to the conventional technique. Interestingly, no contrast was required when crossing in 72 lesions (48%) with the MNS and in 31 lesions (21%) with the conventional approach (Table 4). Moreover, regardless of the vessel crossed, the MNS required less contrast than the conventional wire and this was also observed with increasing complexity scores (Figure

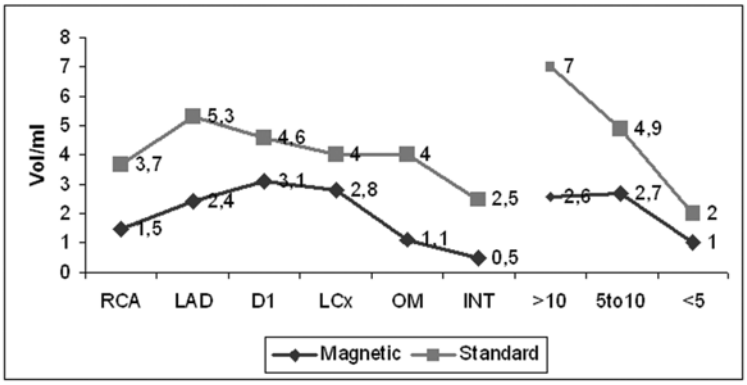

Figure 5 *Comparative contrast usage based on vessel type and complexity score*

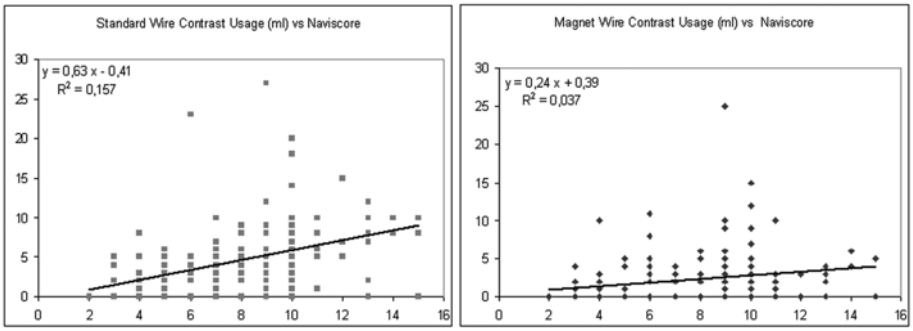

Figure 6 *The scatter plot relationship between contrast and all the complexity scores*

4). Vessels with scores >10 complex vessels had the largest reduction 7.0mls vs. 2.6mls. Vessels with scores 6-10 had almost a two-fold reduction (2.7mls vs. 4.9mls) and those with scores of less than 5 had a limited reduction of 1.0ml. As observed with the crossing and fluoroscopy times a lower slope was recorded with the magnetic wire when the complexity scores were correlated with contrast usage Figure 6.

Discussion

The application of the Magnetic Navigation System to percutaneous coronary intervention is a promising technology(12). There are now over 100 systems installed in catheterisation laboratories worldwide. The system has advantages over traditional PCI techniques with its ability to redirect a magnetised guidewire in-situ. This has been shown to be useful in situations where the ability to cross a lesion with a standard wire failed and in coronary phantom models with increasing tortuosity (5). Even though there is clearly an advantage in precisely controlling the tip of a guidewire, the interventional community has been slow to adopt MNS. There are several reasons why there maybe reservations: a) the presence of a rigid 2-3mm long magnet at the tip of the wire can compromise the performance achievable with conventional wires, b) many conventional wires have achieved a level of sophistication having evolved over several generations to enhance both their trackability and device deliverability c) the 'ocular-hand coordination' seems currently unbeatable because of the delay in responsiveness in the MNS hardware – the speed in moving the large external magnets to align to the desired vectors, d) there is a steep learning curve that must be reached by both the interventionalist and skilled technical staff (6,13), e) together with the additional financial costings for both the MNS and staff training, f) moreover, any gain in crossing time might be compromised by the preparation of the MNS case although in some clinical scenarios this may prove to be beneficial long term eg. MSCT co-integration for CTO, g) but more importantly, there is little randomised data to support the use of the MNS to PCI. Some of these limitations are currently being addressed with

newer generations of wire design together with software updates that can offer automated navigational vector advancement - but many of them are yet to be resolved (14).

In this first randomised study directly comparing the performance of the MNS to conventional PCI techniques we exclusively assessed one system (technique) versus the other. In some studies a 'hybrid' approach can be contemplated whereby the magnetic wire is used initially as a conventional wire technique until a problem of crossing is encountered at which point the external magnets are engaged and then the MNS utilised to facilitate the crossing of the wire through the lesion/vessel (13). This approach was discussed but not acted upon in order to keep the data independent and 'clean' for both techniques. Overall the crossing success of the magnetic wires was comparable to that of the standard guidewires (93.3%vs. 95.6%). Analysis of the four cases that failed to cross with both wires within 6 minutes was in two of the cases subtotal occlusions that failed with the magnetic wires and was eventually crossed with conventional wires. The case that failed with the conventional wire and was crossed with the magnetic wire was in a vessel with an acute angulation. The only case where both wires failed after numerous attempts the patient had an aneurysmal swelling that led into a pinpoint occlusion.

It was not surprising that overall the crossing and fluoroscopy times were longer with the magnetic wire. This is partly because of limitations with the software available at the time of the study that required manual updates of the navigational vectors. This had to be performed by pressing an advancing icon on the touch screen monitor. It meant that the operator had a time delay prior to advancing the magnetic guidewire as the system updated. Newer versions of the software are being developed to address this limitation. But despite this limitation the only significant difference was seen in AHA/ACC B2 lesions as in these cases the operators generally chose smaller incremental distances for the vector to follow. Larger incremental distances were often used in type A and B1 lesions so the differences between the two techniques were less apparent. In type C lesions, the magnetic wire was not significantly slower due to observed limitations with conventional wire techniques in these lesion sub-types (15). In general, the fluoroscopy times were less than the crossing times because manipulations such as reshaping the conventional wire did not require fluoroscopy but was still being timed. Consequently, no significant differences in fluoroscopy times observed between the two systems.

The ACC/AHA criteria was however developed almost 20years ago using 11 simple angiographic factors to define a lesion complexity in the comparison of the outcomes of PCI (16). It is based solely on the lesion and does not take into account the complexity of the vessel as a whole, which can sometimes influence the procedural outcome. In an attempt to circumvent this several other grading systems exist but they are generally based on simple angiographic features and hence fail to take into account the 3-dimensional (3-D) nature of the coronary tree (17,18). Moreover, visual estimates from angiographic images are known to have poor inter-

observer reproducibility (19). By employing dedicated 3-D software more detailed information can be used to define a complexity scoring systems based on both the vessel and lesion characteristics(11). Using this approach and dividing the scores in tertiles of low (5 or less), medium (between 6 and 10) and high complexity (greater than 10) a positive trend for the magnetic wire was observed for crossing and fluoroscopy times in the high complexity group. Both the magnetic wire crossing and fluoroscopy times significantly increased over the conventional methods used in vessels with low and medium complexity scores. But with high complex scores lower times were recorded with the magnetic wire (78.0 vs.93.7sec and 74.2 vs. 90.5sec respectively). This trend does however support anecdotal clinical reports that in selected cases with increased complexity the MNS can be advantageous (20,21). Attempts however to further subcategorise the population with the high complexity scores were unsuccessful because of the size of the study.

To assess measurable differences between the two techniques we quantitatively recorded the amount of contrast media used to cross the lesion. We appreciated the fact that this volume is relatively small in comparison to the total amounts traditionally used in an entire procedure. Nevertheless when assessed as a measurable difference between the two techniques the MNS did reduce the amount of contrast used to cross a lesion primarily because it integrates a 3-dimensional roadmap to provide a visual clue to the position of the wire on the fluoroscopic image. As a result the significant difference between contrast and lesion complexity observed with the conventional wire was effectively eliminated with the MNS. In vessels with complexity scores > 10, there was almost a three fold reduction in amount of contrast used. Moreover 48% of the lesions were crossed without the need of contrast as a direct effect of following a superimposed road map on the live fluoroscopy image. This is an important finding in support of developing technologies aimed at reducing contrast usage that can ultimately affect clinical consequence such as contrast-induced nephropathy (CIN). Already the use of an overlay created from an MSCT co-integration with the MNS can aid the visualisation of CTOs, which may limit the need for retrograde contrast media injection (14). Contrast usage have also been reduced by using 3D reconstruction (3DRC) software to correctly define the optimum angiographic projections needed for stent deployment (22,23). In addition some technologies can accurately localise a wire/device – global positioning - within the coronary artery (24). If these technologies were amalgamated with more sophisticated magnetic wires such as Stereotaxis's multi-magnet design having 3 smaller 1mm interspaced magnets at the tip and furthermore is integrated with a system for automatic wire advancement then an entirely new approach to conventional PCI and contrast usage would be effectively realised (1,25). But for every emerging technology there is a limited period for it to be adopted so it is important that the current limitations and reservations be addressed if the MNS is to succeed in the competitive area of PCI.

Limitations

The 3DRC used in this study was time-consuming and took up to 30 minutes to complete. The production of the reconstruction required angiography of a suitable standard and this was not always possible from standard views due to foreshortening or overlapping. A static road map created from the 3DRC image was superimposed on a dynamic real-time image for magnetic navigation. Only patent vessels were included, as the re-crossing of totally occluded vessels by the comparative wire was avoided because of inherent clinical risk. There were a number of operators and types of wires and this, together with no selection of the target vessel segment, may have led to heterogeneity. The lesion score was also not externally validated. In addition, this study examines only one specific aspect of the PCI related to crossing of lesions and does not address other necessary elements such as the passage and deployment of the balloon and stent. Lastly, this study was performed at a University specialist tertiary referral unit and the case mix might be different to that seen elsewhere.

Conclusions

The Magnetic Navigation System has a comparably crossing success to conventional PCI techniques in crossing lesions as defined by the ACC/AHA criteria. The longer crossing and fluoroscopy times reflect limitations in manually updating the navigational vectors on the roadmap displayed on the live fluoroscopic image. In defining the vessel complexity taking into account the full 3 dimensional characteristics a positive trend was found in support of using MNS in more complex vascular lesions/anatomies. Moreover the incorporation of the 3DRC navigational pathway with the MNS offered a small but significant reduction in the amount of contrast needed to cross a target lesion when compared to a conventional wire approach. Nearly half of the cases required no contrast agent to guide the magnetic wire transit within the vessel.

References

1. Ramcharitar S, Patterson MS, van Geuns RJ, van Meighem C, Serruys PW. Technology Insight: magnetic navigation in coronary interventions. Nat Clin Pract Cardiovasc Med 2008;5(3):148-56.
2. Patterson MS, Schotten J, van Mieghem C, Kiemeneij F, Serruys PW. Magnetic navigation in percutaneous coronary intervention. J Interv Cardiol 2006;19(6):558-65.
3. Pappone C, Vicedomini G, Manguso F, Gugliotta F, Mazzone P, Gulletta S, Sora N, Sala S, Marzi A, Augello G and others. Robotic magnetic navigation for atrial fibrillation ablation. J Am Coll Cardiol 2006;47(7):1390-400.
4. Ramcharitar S, Patterson MS, van Geuns RJ, Serruys PW. Magnetic navigation system used successfully to cross a crushed stent in a bifurcation that failed with conventional wires. Catheter Cardiovasc Interv 2007;69(6):852-5.
5. Ramcharitar S, Patterson MS, van Geuns RJ, van der Ent M, Sianos G, Welten GM, van Domburg RT, Serruys PW. A randomised controlled study comparing conventional and magnetic guidewires in a two-dimensional branching tortuous phantom simulating angulated coronary vessels. Catheter Cardiovasc Interv 2007;70(5):662-8.
6. Tsuchida K, Garcia-Garcia HM, van der Giessen WJ, McFadden EP, van der Ent M, Sianos G, Meulenbrug H, Ong AT, Serruys PW. Guidewire navigation in coronary artery stenoses using a novel magnetic navigation system: first clinical experience. Catheter Cardiovasc Interv 2006;67(3):356-63.
7. Cox J, Naylor CD. The Canadian Cardiovascular Society grading scale for angina pectoris: is it time for refinements? Ann Intern Med 1992;117(8):677-83.
8. Braunwald E. Unstable angina. A classification. Circulation 1989;80(2):410-4.
9. Ellis SG, Vandormael MG, Cowley MJ, DiSciascio G, Deligonul U, Topol EJ, Bulle TM. Coronary morphologic and clinical determinants of procedural outcome with angioplasty for multivessel coronary disease. Implications for patient selection. Multivessel Angioplasty Prognosis Study Group. Circulation 1990;82(4):1193-202.
10. Patterson S, Hoeks S, Tanimoto S, Van Mieghem C, Ramcharitar S, Van Domburg R, Serruys PW. A simple score for predicting prolonged crossing times to select patients who would benefit from a magnetic percutaneous coronary intervention. European Heart Journal , 2007; 28 ((Abstract Supplement P4762)):847-848.
11. Patterson MS, Hoeks SE, Rijkenberg S, Ramcharitar S, van Geuns RJ, Tanimoto S, van Domburg RT, Serruys PW. Integration of 3D reconstruction in the SELection Criteria for Excessive Crossing Times for Magnetically Supported Percutaneous coronary intervention SELECT-MP. Eurointervention 2008;in press.
12. Raizner AE. Magnetic navigation: a pivotal technology. Catheter Cardiovasc Interv 2007;69(6):856.
13. Kiemeneij F, Patterson MS, Amoroso G, Laarman G, Slagboom T. Use of the Stereotaxis Niobe magnetic navigation system for percutaneous coronary intervention: results from 350 consecutive patients. Catheter Cardiovasc Interv 2008;71(4):510-6.
14. Ramcharitar S, Pugliese F, Patterson M, van Geuns RJ, de Feyter P, Guiliguian D, Serruys PW. Advanced Magnetic Navigation: Multi-slice Computer Tomography-guided Percutaneous Coronary Intervention in a patient with Triple-Vessel Disease. Eurointervention 2008;in press.
15. Seshadri N, Whitlow PL, Acharya N, Houghtaling P, Blackstone EH, Ellis SG. Emergency coronary artery bypass surgery in the contemporary percutaneous coronary intervention era. Circulation 2002;106(18):2346-50.
16. Ryan TJ, Faxon DP, Gunnar RM, Kennedy JW, King SB, 3rd, Loop FD, Peterson KL, Reeves TJ, Williams DO, Winters WL, Jr. and others. Guidelines for percutaneous transluminal coronary angioplasty. A report of the American College of Cardiology/American Heart Association Task Force on Assessment of Diagnostic and Therapeutic Cardiovascular Procedures (Subcommittee on Percutaneous Transluminal Coronary Angioplasty). Circulation 1988;78(2):486-502.

17. Singh M, Rihal CS, Lennon RJ, Garratt KN, Holmes DR, Jr. Comparison of Mayo Clinic risk score and American College of Cardiology/American Heart Association lesion classification in the prediction of adverse cardiovascular outcome following percutaneous coronary interventions. J Am Coll Cardiol 2004;44(2):357-61.
18. Valgimigli M, Serruys PW, Tsuchida K, Vaina S, Morel MA, van den Brand MJ, Colombo A, Morice MC, Dawkins K, de Bruyne B and others. Cyphering the complexity of coronary artery disease using the syntax score to predict clinical outcome in patients with three-vessel lumen obstruction undergoing percutaneous coronary intervention. Am J Cardiol 2007;99(8):1072-81.
19. Herrman JP, Azar A, Umans VA, Boersma E, von Es GA, Serruys PW. Inter- and intra-observer variability in the qualitative categorization of coronary angiograms. Int J Card Imaging 1996;12(1):21-30.
20. Schneider MA, Hoch FV, Neuser H, Brunn J, Koller ML, Gietzen F, Schamberger R, Kerber S, Schumacher B. Magnetic-Guided Percutaneous Coronary Intervention Enabled by Two-Dimensional Guidewire Steering and Three-Dimensional Virtual Angioscopy: Initial Experiences in Daily Clinical Practice. J Interv Cardiol 2008.
21. Patterson MS, Ramcharitar S, Serruys PW. Magnetically Supported PCI: success after failed surgery and conventional PCI. Cath Lab Digest 2007;15(3):1-14.
22. Gollapudi RR, Valencia R, Lee SS, Wong GB, Teirstein PS, Price MJ. Utility of three-dimensional reconstruction of coronary angiography to guide percutaneous coronary intervention. Catheter Cardiovasc Interv 2007;69(4):479-82.
23. Green NE, Chen SY, Hansgen AR, Messenger JC, Groves BM, Carroll JD. Angiographic views used for percutaneous coronary interventions: a three-dimensional analysis of physician-determined vs. computer-generated views. Catheter Cardiovasc Interv 2005;64(4):451-9.
24. Mediguide. MPS First in Human! MediGuide started its clinical trials in Regensburg University Hospital in Germany. http://www.mediguide.co.il/news/news.asp?newID=43&newsCatID=2.
25. Beyar R, Gruberg L, Deleanu D, Roguin A, Almagor Y, Cohen S, Kumar G, Wenderow T. Remote-control percutaneous coronary interventions: concept, validation, and first-in-humans pilot clinical trial. J Am Coll Cardiol 2006;47(2):296-300.

Chapter 4

MAGNETIC NAVIGATION IN THE TREATMENT OF BIFURCATING LESIONS

Magnetic navigation system used successfully to cross a crushed stent in a bifurcation that failed with conventional wires

*Catheter Cardiovasc Interv 2007 May 1; 69(**6**):852-5.*

Ramcharitar S, Patterson M, van Geuns RJ, Serruys PW

Abstract

Bifurcation lesions can be technically demanding to manage, and even in the era of drug eluting stents, their procedural success is variable. The use of the crush technique followed by "kissing" balloon postdilatation has been shown to improve the overall outcome. However, crossing the crushed stent is essential to allow performance of a final dilatation with "kissing" balloons and is regarded as the main Achilles' heel of this technique. In this report, we describe the first reported, planned procedure to use a magnetic navigation system to steer a wire through the crushed stent to use "kissing" balloons that had previously failed with conventional wires.

Introduction

Coronary bifurcation lesions are a challenging and frequent problem encountered in patients undergoing percutaneous coronary interventions [[1]]. Their overall long-term success rate is variable but has improved since the introduction of drug eluting stents (DES). A number of stenting techniques are employed in the management of these lesions and they include T-, V-, Y-stenting, the "culotte" and the "crush" technique [[2]]. The latter is a technique that ensures complete coverage of the side branch ostium so as to ensure drug delivery to minimize restenosis at this site [[3]]. This involves wiring both the main vessel and side branch. The proximal part of the stent that is deployed in the side branch protrudes into the main vessel and is crushed with another stent that is deployed in the main vessel [[4]]. Crucial to the success of this technique is the use of "kissing" balloons to ensure complete apposition of both DES to the vessel wall [[5]]. To do this a wire must cross the crushed stent overlying the ostium of the side branch [[6]]. In certain cases this can be difficult and may result in a prolonged procedure with possible complications such as contrast nephropathy and increased radiation exposure. The magnetic navigation system (MNS) can be utilized to steer a wire through the stents' struts to address this limitation of the "crush" technique [[7]]. The MNS has previously been successfully used in chronic total occlusions and in vessels with tortuous anatomy but has not so far been reported as an aid to bifurcation stenting [[8-10]].

We report a planned procedure to use magnetic navigation with an appropriate wire to cross a crushed stent where previous attempts with conventional wires had failed in the emergency setting. This was followed by "kissing" balloon dilatation and led to procedural success in a patient with a bifurcation lesion.

The Magnetic Navigation System

The MNS has been shown to be effective in neurosurgical and cardiac electrophysiological procedures [[11]][[12]]. In percutaneous coronary intervention it is a platform that offers a powerful tool to aid navigation of a guidewire through complex coronary anatomy [[13]]. The Stereotaxis Niobe® MNS has two permanent magnets that can be moved (rotated, translated, or tilted) to produce a uniform magnetic field of 0.08 Tesla within the patient's chest. This field is used to precisely direct a tiny magnet mounted on the tip of a guidewire by changing its magnetic moment. This allows fine control of the orientation of the tip of the guidewire in space. The Titan™ Soft Support coronary guidewire used in this case is a 180-cm moderate support, hydrophilic coated wire with a diameter of 0.014 in./0.36 mm and has a flexible 2 cm distal coiled tip at the end of which is a gold cup attached to a neodynium 2- or 3-mm magnet.

A three-dimensional virtual vessel roadmap is created from the angiographic images using reconstruction software (CardiOp-B, Paieon Medical, Rosh Ha'ayin, Israel). The system computes

a navigation plan from the reconstructed virtual path that supplies all the vectors required to navigate through the coronary artery. By touching a point of interest on this virtual map that is displayed on a touch screen monitor, the Navigant software calculates the best vector and directs the magnetic field to align the wire tip with that direction. This can be performed at anytime during the procedure, in vivo, and without the need for a preshaped wire tip angle.

Case Report

The patient was a 58-year-old man who presented with an anterior ST elevation MI. His risk factors included being a noninsulin-dependent diabetic and being on treatment for hypertension.

The Primary PCI

Angiography revealed an occluded LAD that, once open, showed a bifurcation lesion at LAD/D1. This was managed by placing PT Graphix wires into each vessel. A Taxus Liberte 3.0 × 16 mm stent in the LAD was used to crush the proximal end of a Taxus Liberte 2.5 × 12 mm stent in the diagonal. Both stents were deployed without predilatation of the lesion at 16 atmospheres. To perform the "kissing" balloon technique it was necessary to cross the crushed stents' struts to gain entry into the diagonal. This was unsuccessful despite the various techniques employed,

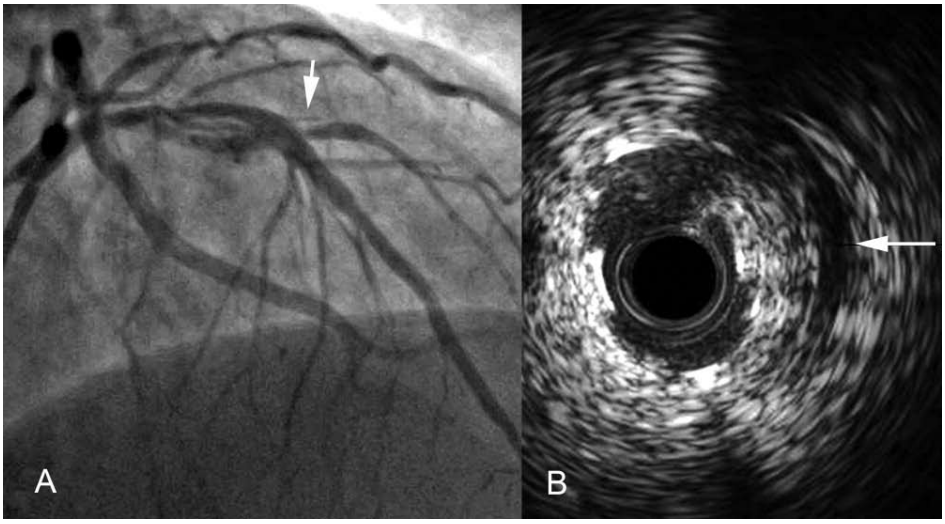

Figure 1. *(A) The results of crushing the proximal end of the stent in D1 with a stent in the LAD and a dissection of D1 (arrowed) created iatrogenically by inflating a balloon between the D1 stent and the vessel wall. (B) An IVUS image of the deployed crushed stent showing the dissection (arrowed)*

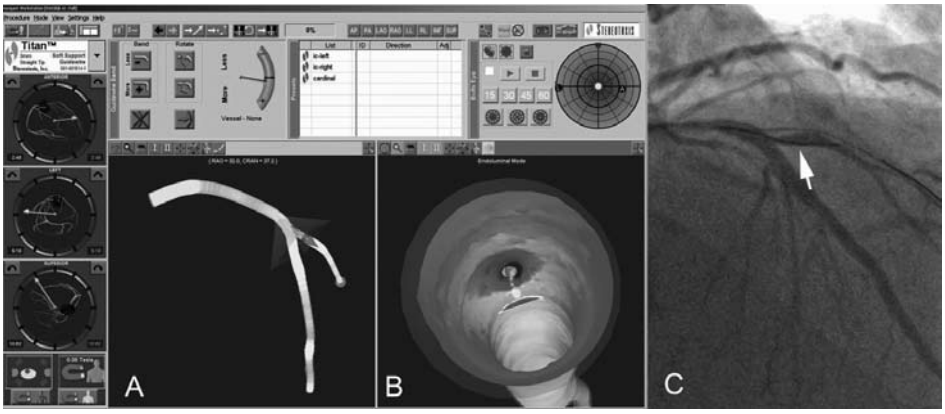

Figure 2. *The 3D reconstruction (A) and the endoluminal view of the LAD/diagonal bifurcation (B). The magnetically guided TitanTM Soft Support wire (arrowed) successfully crosses the stent strut into the true lumen and the Graphix Intermediate wire preferentially chose the false lumen of the dissection (C).*

such as an over the wire balloon (OTW), to support the wire or by changing the angle of the wire tip manually.

When a stiffer wire (PT Graphix Super Support) was used, it did not enter the true lumen but went subintimally. This was apparent after dilatation with a Maverick 1.5 × 15 mm OTW balloon as it resulted in a dissection at the proximal end of the deployed stent in the diagonal (Fig. 1A and B). Consequently, it was even more imperative to use "kissing" balloons in this case to fully appose the diagonal stent against the dissected vessel so as to improve the overall outcome. Attempts were made to finish the procedure and, having tried to cross the stent struts for almost an hour, and in the presence of TIMI 3 flow down both the LAD and D1, the operator elected to leave the sheath in situ and use magnetic navigation in the morning.

The Magnetic Navigation Assisted PCI

The left coronary artery was cannulated with a Mach 1 CLS 3.5 6F guide catheter. The first attempt was with another PT Graphix intermediate wire but this again preferentially chose to follow the tract of dissection, outside the stent before re-entering the true lumen. Therefore, a three-dimensional virtual vessel roadmap was created from the angiographic images by using reconstruction software (Fig. 2A). A vector was then created that navigated a Titan^{TM} Soft Support angled magnetic tip wire between the crushed stents' struts and avoid the false lumen (Fig. 2C). Subsequent use of "kissing" balloons, Maverick 2.5 × 15 mm in the diagonal and Maverick 3.0 × 15 mm in the LAD at 16 atmospheres (Fig. 3A), resulted in full apposition of the diagonal stent (Fig. 3B). The patient tolerated the procedure well and his cardiovascular status was stable as monitored via an arterial line.

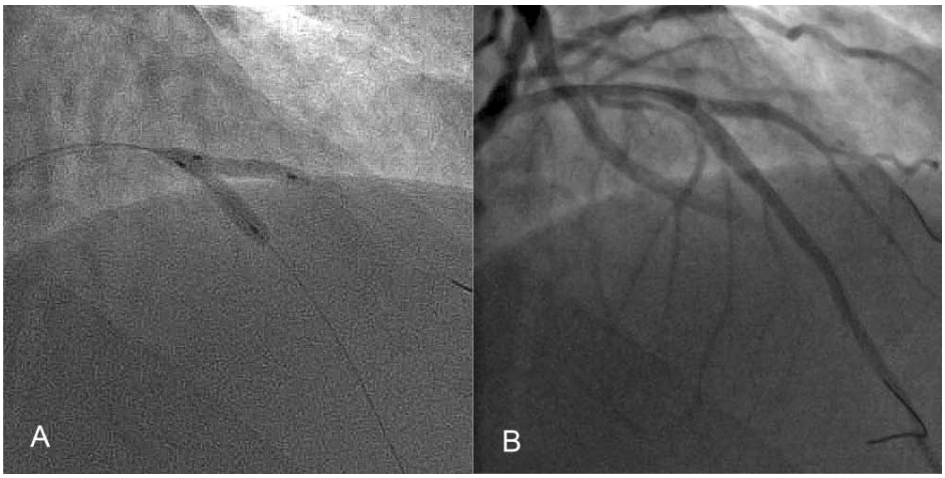

Figure 3. *(A) The postdilatation with "kissing" balloons using a Maverick 2.5 × 15 mm in the diagonal and a Maverick 3.0 × 15 mm in the LAD at 16 atmospheres. (B) The final angiographic result of the crush.*

Discussion

Magnetic navigation is a novel technique that was successfully used to cross a crushed stent where traditional methods had failed. The tip of the steerable wire employed can rotate in three-dimensions depending on the programmable vector created by the magnetic field. This has the advantage that it can be performed within the coronary artery itself and is aided by a digitally reconstructed image of the coronary vessel. This technique was crucial to the success of this case as it was necessary to fully appose the crushed stent against the dissection using the "kissing" balloons technique.

Conclusions

This is the first report of the use of the MNS to successfully cross a crushed stent in the management of a bifurcation lesion. The advantage of this technology is that it produces a three-dimensional digitally constructed visual map and can precisely direct a guide wire along a chosen path. This can potentially reduce the time of the procedure, the amount of contrast needed, and radiation exposure.

Acknowledgements

We thank S. van Weenen for technical support, J.M.R. Ligthart for image preparation, and Dr. C. van Mieghem for advice.

References

1. Colombo A. Bifurcation lesions. *Ital Heart J* 2005; **6**: 475-488.
2. Hoye A,Iakovou I,Ge L,van Mieghem CA,Ong AT,Cosgrave J,Sangiorgi GM,Airoldi F,Montorfano M,Michev I,Chieffo A,Mauro Carlino M,Corvaja N,Aoki J,Rodriguez Granillo GA,Valgimigli M,Sianos G,van der Giessen WJ,de Feyter PJ,van Domburg RT,Serruys PW,Colombo A. Long-term outcomes after stenting of bifurcation lesions with the "crush" technique: Predictors of an adverse outcome. *J Am Coll Cardiol* 2006; **47**: 1949-1958.
3. Hermiller JB. Bifurcation intervention: Keep it simple. *J Invasive Cardiol* 2006; **18**: 43, 44.
4. Sianos G,Vaina S,Hoye A,Serruys PW. Bifurcation stenting with drug eluting stents: Illustration of the crush technique. *Catheter Cardiovasc Interv* 2006; **67**: 839-845.
5. Ge L,Airoldi F,Iakovou I,Cosgrave J,Michev I,Sangiorgi GM,Montorfano M,Chieffo A,Carlino M,Corvaja N,Colombo A. Clinical and angiographic outcome after implantation of drug-eluting stents in bifurcation lesions with the crush stent technique: Importance of final kissing balloon post-dilation. *J Am Coll Cardiol* 2005; **46**: 613-620.
6. Ge L,Iakovou I,Cosgrave J,Agostoni P,Airoldi F,Sangiorgi GM,Michev I,Chieffo A,Montorfano M,Carlino M, et al. Treatment of bifurcation lesions with two stents: One year angiographic and clinical follow up of crush versus T stenting. *Heart* 2006; **92**: 371-376
7. Atmakuri SR,Lev EI,Alviar C,Ibarra E,Raizner AE,Solomon SL,Kleiman NS. Initial experience with a magnetic navigation system for percutaneous coronary intervention in complex coronary artery lesions. *J Am Coll Cardiol* 2006; **47**: 515-521.
8. Garcia-Garcia HM,Tsuchida K,van Mieghem C,Daemen J,van Weenen S,Patterson M,van der Ent M,van der Giessen WJ,Meulenbrug H,Sehra R,de Feyter P,Serruys PW. Multi-slice computed tomography and magnetic navigation - Initial experience of cutting edge new technology in the treatment of chronic total occlusions. *Eurointervention* , in press.
9. Garcia-Garcia HM,Tsuchida K,Meulenbrug H,Ong ATL,Van der Giessen WJ,Serruys PW. Magnetic navigation in coronary phantom: Experimental results. *Euro Interv* 2005; **1**: 321-328.
10. Tsuchida K,Garcia-Garcia HM,van der Giessen WJ,McFadden EP,van der Ent M,Sianos G,Meulenbrug H,Ong AT,Serruys PW. Guidewire navigation in coronary artery stenoses using a novel magnetic navigation system: First clinical experience. *Catheter Cardiovasc Interv* 2006; **67**: 356-363.
11. Bach RG,Leach C,Milov SA,Lindsay BD. Use of magnetic navigation to facilitate transcatheter alcohol septal ablation for hypertrophic obstructive cardiomyopathy. *J Invasive Cardiol* 2006; **18**: E176-E178
12. Thornton AS,Janse P,Theuns DA,Scholten MF,Jordaens LJ. Magnetic navigation in AV nodal re-entrant tachycardia study: Early results of ablation with one- and three-magnet catheters. *Europace* 2006; **8**: 225-230.
13. Patterson M,Schotten J,van Mieghem C,Kiemeneiji F,Serruys PW. Magnetic navigation in percutaneous coronary intervention. *J Interv Cardiol* 2006; **19**: 558-565.

MAGNETIC NAVIGATION IN THE TREATMENT OF BIFURCATING LESIONS

A Randomised Comparison of the Magnetic Navigation System versus Standard wires in the treatment of Bifurcations

Submitted

Ramcharitar S, van Geuns RJ, van der Giessen WJ, van der Ent M, de Feyter PJ, Serruys PW

Abstract

Objectives:
A randomised comparison of the Magnetic Navigation System (MNS) to standard guidewire techniques in the treatment of bifurcations

Background:
Optimal treatment of bifurcations requires kissing balloon post-dilatation. By precisely directing a magnetised guidewire *in vivo* the MNS may facilitate the recrossing of stents struts.

Methods:
31 consecutive patients with bifurcating lesions were randomised to cross the bifurcating vessels prior to treatment and subsequently the struts of deployed stents with either magnetic or standard guidewires. All bifurcations were categorised according to the Medina classification. Crossing success, crossing/fluoroscopy times and contrast usage were directly compared.

Results:
The majority of bifurcations were in LAD/diagonal (80.6%). The side branch was involved in 87% and was treated with the crush (54.8%), provisional (22.6%) or culotte technique (22.6%). The magnet wires had a greater crossing success (96.8% vs. 90.0%) and salvaged two cases as a direct result of false lumen formation with standard wires. Crossing times were longer with the magnetic wires in crossing untreated vessels (75.2 ± 53.4sec vs. 62.1 ± 56.1sec, p=0.03) and those covered with a single layer of struts (78.6 ± 63.6sec vs. 64.1 ± 45.8sec p=0.03) but was shorter in crossing double layers as in the 'crush' technique (132.9 ± 106.4sec vs. 137.1 ± 135.5sec p=0.45). There was no significant difference between the wires in reducing fluoroscopy time. A small but a significant reduction in contrast usage was noted with the magnetic wires.

Conclusion:
In routine bifurcation the MNS had greater crossing success despite being slower and was useful in managing failed standard wire cases.

Introduction

Treatment of coronary bifurcation lesions represents a challenging area in interventional cardiology[1]. They have lower procedural success rate, higher procedural costs and longer hospitalization with higher clinical and angiographic restenosis rates compared to their non-bifurcating counterparts. The introduction of drug eluting stents has radically changed the management of these lesions by limiting the restenotic rates of complex stenting at the bifurcation carina[2]. But to ensure adequate apposition of the stent to the wall or to improve the blood flow in the side branch kissing balloon post-dilatation of the stent(s) is desirable[3]. This means that if the "crush" bifurcation technique is employed 2 layers of the stent must be crossed in order to gain access to the side branch whilst in others (T-stent, provisional or culotte) recrossing a single layer is required. Gaining access to the side branch can be the Achilles heel of the entire procedure and has resulted in the development of dedicated stents designed to protect abrupt side branch closure[4]. We first reported that the magnetic navigation system (MNS) could be used to steer a wire through the layers of crushed stent into a side branch that had previously failed to access with standard wires[5]. This was possible because of the system's ability to precisely control the wire tip externally so as to avoid the wire entering a false lumen in a dissected vessel. It was therefore speculated that the MNS may be advantageous in the recrossing of stents struts by negotiating through the overlapping layer(s) or vessel dissections that may result through standard guidewire manipulations. To evaluate this hypothesis we performed a randomised comparative assessment of the MNS to conventional percutaneous intervention (PCI) with standard wires in the management of routine bifurcating lesions.

Material and Methods

Patient Selection and Definitions

In a 12 months period 31 consecutive patients diagnosed with having coronary disease involving a bifurcating vessel were managed with the Stereotaxis MNS (Stereotaxis, St. Louis, M. USA). They presented with either stable or unstable angina defined according to the Canadian Cardiovascular Society and Braunwald classification respectively. The bifurcations were classified according to the Medina classification[6]. All patients were single blinded- randomised to cross both limbs of the bifurcation twice, either using a standard/conventional or a magnetically enabled guidewire. Firstly, following a treatment strategy for the bifurcation determined by the operator the layer of stent(s) covering the ostium of a vessel had to be recrossed so that kissing balloon dilatation could be performed. The crossing of the overlaying stent struts were randomised to be crossed twice either using a standard/conventional or a magnetically enabled guidewire first. The crossing success, crossing/fluoroscopy times and contrast usage for both techniques was determined and compared. The times (sec) and contrast media (ml) required to

cross was measured from the transit of the guidewire at the tip of a guiding catheter engaged at the ostium to a pre-defined point in a distal vessel. Inability to cross within 6 minutes with either wire was defined as a failure in accordance to previously published phantom studies[7]. Included within the 6 minutes was the time taken for wires to be removed from the catheter and reshaped in order to achieve a successful crossing. Wires that were damaged in crossing could be exchanged for a similar or different standard/conventional or magnetically enabled wire if necessary. The operators had unrestricted access to the choice of either magnetic or conventional guidewires and were all interventional cardiologists who were also trained with the MNS. The study was locally approved; all patients were appropriately informed about the procedure and gave their written consent. Patients were excluded if they were haemodynamically unstable or had contraindications for magnetic-assisted intervention (MAI) such as having a pacemaker.

The Magnetic Navigation System

The Niobe® II Magnetic Navigation System (MNS) (Stereotaxis, St. Louis, M. USA) is an innovative technology that can accurately steer a guidewire or a catheter *in vivo* [8]. To accomplish this, a small (2-3mm long) magnet embedded at the tip of the guidewire or catheter is reoriented by a predetermined and rapidly updated external magnetic field. The field (0.08Tesla) is generated and focused by tilting and rotating two permanent magnets and is directed by means of navigational vector created through computer driven software (Navigant®) (Figure 1). To do this the Navigant® can directly incorporate 2-dimensional angiographic films to create a navigational pathway. But a more accurate roadmap depicted as a centreline through a virtual vessel can be created by employing dedicated 3-Dimensional Reconstruction (3-DRC) software (Figure 2A). This can allow precise wire steering through a virtually created lumen (Figure 2B) once co-registered with the fluoroscopic image (Figure 2C). As a visual aid the vectors together with a virtual navigational centerline is displayed on the live fluoroscopic image on the radiographic X-ray monitor (Figure 2D).. The vectors along the centreline can be automatically updated or manually controlled by a touch sensitive monitor situated at arm's length from the operating table.

In this study the navigation was performed using a 3DRC virtual vessel roadmap generated from two angiographic images 30° apart (CardiOp-B, Paieon Medical Inc., Rosh Ha'ayin, Israel) and displayed as a fixed centreline on the real-time fluoroscopic image. The operator had the choice to manually advance or to use the automatic updates of the navigational vectors when deemed advantageous to facilitate the crossings.

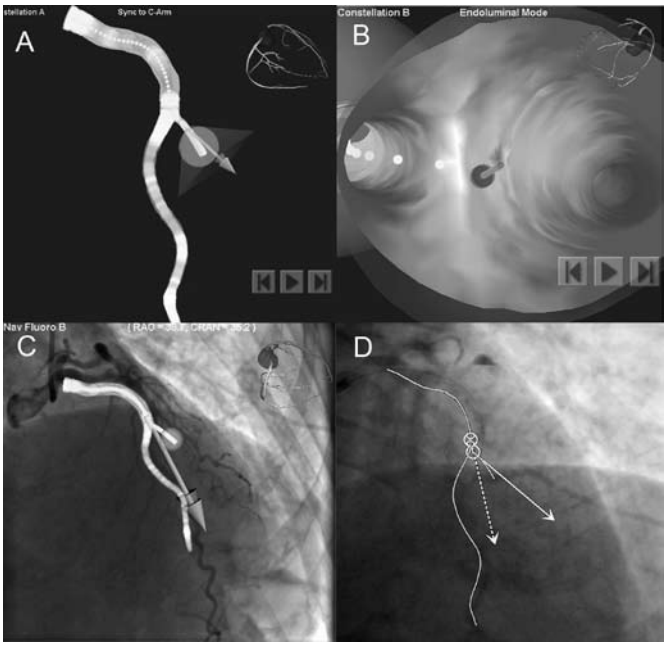

Figure 1. *A) A virtually reconstructed bifurcation using the Paeion software displaying a directional vector created in the Navigant; B) The endoluminal view of the virtual carina at the bifurcation showing the navigational path in one of the branches; C) Co-registration of the virtual vessel to the angiographic image; D) The navigational vectors and centrelines displayed on the live fluoroscopic image.*

The Guidewires

The standard/conventional wires used in the study were PT Graphix™ Intermediate, Choice™ PT Floppy (Boston Scientific Corp. Miami Fl, USA), Whisper, Pilot 50 and high torque BMW (Abbott Vascular Devices, Redwood CA, USA). The magnetic guidewires used were all 180cm long Titan™ Soft Support wires with a 2mm angled or 3mm straight magnetic tips attached to a 0.014in/0.36mm stainless steel core (Stereotaxis, St. Louis, M. USA

Bifurcation Classification and Treatment Strategies

In the Medina classification diseased vessels that comprise the bifurcation are given the numerically identified as 1 and those free of disease 0[6]. The nomenclature is designated further by labelling the proximal main vessel followed by the distal main vessel and then the side branch. The treatment strategies employed were based on established techniques- the crush, T-stent, culotte, provisional and the Tryton™ Side Branch Stent[4]. The crush, T-stent, culotte and the Tryton™ uses two stents to refashion the bifurcation[9]. In the crush technique the side branch stent in allowed to protrude into the main vessel and In the crush technique the side branch stent is allowed to protrude into the main vessel and is crushed against the vessel wall with the main

vessel stent. This results in two layers of struts covering the side branch ostium. The provisional technique is a single stent approach and as with the T-stent, culotte and the Tryton™ only one layer of stent's struts is required to be crossed for kissing balloon optimisation.

Statistical Analysis

Continuous variables are presented as mean ± standard deviation. Student T-test was used to determine if there were significant differences between the parameters assessed using the two techniques. Non-continuous variables are presented as median, 25-75% interquartile ranges (IQR). Analyses were performed using SPSS 11.5 for Windows (SPSS, Chicago, IL). *P* value < 0.05 was considered statistically significant.

Results

Of the 31 patients the percentage of stable and unstable angina was 81% and 19% respectively. The majority were males (68%) and 23% had a previous PCI procedure. The highest risk factor was smoking (ex or current) 45% and one fifth were diabetic. Over a third was on medication to control either hypertension or cholesterol. Bifurcating lesions were found to involve the left anterior decending (LAD)/diagonal (D) branches in 25 cases (81%), the left circumflexus (LCX)/obtuse marginal (OM) arteries in 5 cases (16%) and the right coronary (RCA) /posterior decending artery (PDA) in one case (3%). Based on the Medina classification the bifurcation were characterised as 13 cases of (1,1,1), 8 cases of (0,1,1), 6 cases of (1,1,0) and 4 cases of (1,0,1). This translated into disease involving 74% (23 cases) of the proximal main vessel, 87% (27 cases) the distal main vessel and 81% (25 cases) the side branch. Drug eluting stents (DES) were used in all the treatment strategies that comprised of 17 cases (54.8%) the crush, 2 cases (6.5%) each for the culotte and T-stent technique together with 5 cases (16.1%) each for the provisional and Tryton™ stenting approach. The majority of stents used in the crush technique were Taxus™ (41%) and Xience™ V (47%). Only Taxus™ was used for culotte and the T-stenting methods. In addition to these stents Cypher™ and Biometrix™ stents were used for the provisional approach and in combination with the Tryton™ Side Branch stent.

Analysis of the crossing profiles revealed that in all cases both wire successfully crossed both branches of the (non stented) bifurcation within 6 minutes. However the magnetic wire was significantly slower in crossing compared to the standard/conventional wires (Table 1). The comparative crossing and fluoroscopic times of the magnetic wires to that of the standard/conventional wires were 75.2 ± 53.4sec vs. 62.1 ± 56.1sec (p=0.03) and 68.9 ± 48.1sec vs. 57.5 ± 48.0sec (p=0.04) respectively. Contrast media usage in crossing both limbs of the bifurcation was significantly better with the magnetic wires [median, 25-75% IQR, 2ml, 0 - 5mls vs. 4.5ml, 0 -7mls (p<0.001)] respectively (Table 2). In the recrossing of the stents overlying the carina

Table 1 *Comparative assessment of crossing/fluoroscopy times with the magnetic and standard/conventional wires in different bifurcation stenting strategies*

	Crossing time/sec Mean ± SD		**Fluoroscopy time/sec Mean ± SD**	
	Magnet wire	**Standard wire**	**Magnet wire**	**Standard wire**
Native untreated bifurcation N = 31	75.2 ± 53.4	62.1 ± 56.1	68.9 ± 48.1	57.5 ± 48.0
	p = 0.03		p = 0.04	
Culotte and Tryton N= 7 (22.6%)	57.0 ± 38.3	57.0 ± 36.6	52.3 ± 36.9	51.4 ± 38.5
	p = 0.5		p = 0.44	
T-stent and Provisional N= 7 (22.6%)	100.1 ± 78.8	71.1 ± 55.6	95.6 ± 73.3	67.9 ± 51.6
	p = 0.02		p = 0.02	
Crush/three layers of struts N= 17 (54.8%)	132.9 ± 106.4	137.1 ± 135.5	121.9 ± 95.0	130.3 ± 127.1
	p = 0.45		p = 0.38	
One layer of struts N = 14	78.6 ± 63.6	64.1 ± 45.8	73.9 ± 60.1	59.6 ± 44.6
	p = 0.03		p = 0.45	
Overall treated bifurcation N= 31	108.4 ± 92.5	104.1 ± 109.9	100.2 ± 83.5	98.4 ± 103.7
	p = 0.4		p = 0.45	

the magnetic wires were more successful achieving 96.8% vs. 90% success over the standard/conventional wires. Failure to recross within the 6 minutes was observed in only 4 cases (1 magnetic and 3 standard/conventional) but interestingly they all occurred only in cases involving the crush stent technique and all employed Taxus™ stents in reconstructing the carina. In the single magnetic wire failure the bifurcation in the LCX/OM had a Medina classification of 1,1,1 and was treated with a Taxus™ 3.0x12mm in the main branch and a Taxus™ 2.75x28mm in the side branch. The 3mm long magnetic tip wire took over 6minutes to recross as the tip caught between in the struts resulted in the wire 'buckling' and unable to penetrate the two layers of struts. Recrossing was eventually successful by using the software to increase the gain of the angle at the wires' tip so that it was able to negotiate through an alternative set of overlying stent cells. A similar situation was encountered with one of the failed standard/conventional wire cases. Here the bifurcation involved the LAD/D and was also classified as Medina 1,1,1. Two Taxus™ stents (3.0x24mm and 2.25x12mm) were employed in the crush. The Pilot 50 guidewire (Abbott Vascular Devices) used in crossing was caught between the struts and could not be

Table 2 *The assessment of contrast used in crossing the native vessels, all stents overlying the carina and one versus three layers of struts. Values are given as median, 25-75% interquartile range (IQR*

	Native untreated bifurcation N = 31	Overall treated bifurcation N= 31	One layer of struts N = 14	Crush/three layers of struts N= 17 (54.8%)
	median, 25-75% IQR	median, 25-75% IQR	median, 25-75% IQR	median, 25-75% IQR
Contrast/ml used with magnet wire	2ml, 0 – 5ml	0ml, 0 – 5ml	0ml, 0 – 3ml	2ml, 0 – 5ml
Contrast/ml used with standard wire	4.5ml, 0 -7ml	5ml, 0 – 9ml	4.5ml, 0 - 6.8ml	5ml, 0 – 15ml

advance distally. When the damaged wire was exchanged for another guidewire with a different angulated bend created manually at the tip so that an alternative cell could be engaged then the crossing and subsequent kissing balloon dilatation was successful. In the other two failed standard/conventional wire cases kissing balloon dilatations were only salvageable because of the magnetic wire. Both cases involved the LAD/D with diseased side branches, Medina 1,0,1 and 0,1,1 respectively. Stents used were Taxus™ (3.5x24mm and 2.25x16mm) and Taxus™ stents (3.0x16mm and 2.5x12mm) respectively. In both cases a false lumen was created by the wire dissecting between the layers of the vessel and the underlying stent and thus prevented the standard/conventional wires from entering the true ostium (Figure 3). Only by using the magnetic wires to circumnavigate away from the dissected false lumen was the wire successfully tracked within the true lumen.

Comparative assessment of the times taken in recrossing the stent overlying the carina revealed that overall the magnetic wires were slower than the standard/conventional wires. The differences was however non-significant with averages of 108.4 ± 92.5sec vs. 104.1 ± 109.9sec p= 0.4 for the crossing times and 100.2 ± 83.5sec vs. 98.4 ± 103sec p=0.45 for the fluoroscopy times (Table 1). Grouped together by virtue of being technically similar the culotte and the Tryton™ Side Branch stent together had nearly identical times with either wire. This was unlike the group comprising of provisional and T-stent techniques where shorter times were observed with the standard/conventional wires (Table 1). When further categorised into the recrossing of single versus double layers of struts a significant difference in times was only observed with the crossing of the former. Both the crossing and fluoroscopy times were longer in recrossing a single layer of struts with the magnetic wire when compared to the standard/conventional wire (78.6 ± 63.6sec vs. 64.1 ± 45.8sec p=0.03 and 73.9 ± 60.1sec vs. 59.6 ± 44.6sec p=0.02 respectively) (Table 1). In recrossing two layers of stent struts (crush technique) there was no significant difference (132.9 ± 106.4sec vs. 137.1 ± 135.5sec p=0.45 and 121.9 ± 95.0sec vs.

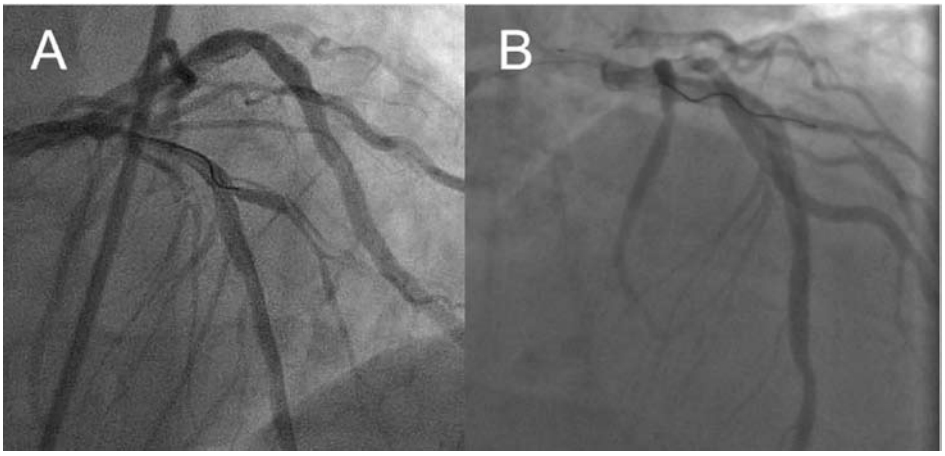

***Figure 2**: The two cases (A and B) where the MNS successfully entered the true lumen of dissections created conventional/standard wires in crossing stents used in the crush technique.*
Noninvasive cardiac computed tomography: an interventional cardiologist's perspective

130.3 ± 127.1sec p=0.38 respectively) although the magnetic wire was slightly faster. Contrast media usage was significantly reduced with the magnetic wire regardless of the layers of stent crossed (Table 2).

Discussion

The Magnetic Navigation System offers an innovative way of steering a device/guidewire which has already been adopted in cardiac electrophysiological procedures whereby inaccessible pathways can be effectively targeted, even remotely[10]. In percutaneous coronary interventions such ability to precisely redirect a guidewire within the coronary tree can potentially have a major advancement over traditional techniques[11]. This is because in the initial bend placed on the wire to engage the target vessel might not be ideally suited to cross the target lesion. Indeed early studies demonstrated that patients having complex lesions and tortuous vessels the MNS was successful in crossing lesions that had failed conventionally [12,13]. However, to date the only published randomised direct comparison of the MNS to conventional approaches was performed in increasingly tortuous phantom models where it was suggested that the MNS might be advantageous [7]. In addition, technical limitations with the current system curtail its potential advantage over conventional wires approaches in all rather than selective PCI procedure [8]. One major limitation is the rigid 2-3mm magnetic tip wires, which restrict the degree of flexibility when compared with the smoother transition of the tip with the shaft, found in the more sophisticated standard conventional wires. Moreover the 'ocular-hand coordination' of the 'seasoned' conventional PCI operator seems currently unbeatable since time is loss in

moving the large external magnets to realign with the desired vectors [14]. It is also an expensive technology that has a learning curve for both the operator and the technical staff.

The complexity of bifurcating lesions means that there remain technical issues on the best treatment approach to achieve optimal procedural outcomes and, more importantly, long-term success with low restenosis rates and MACE rates[15]. The adoption of a simple strategy of stenting only the main vessel with provisional stenting of the side branch or a more complex strategy of stenting both vessels are still fiercely debated[16]. The "crush" technique was developed to improve ostial side branch coverage without compromising access to the side branch[3]. However several investigators have shown higher overall restenosis rate (main and side branch) although this can be dramatically reduced from 37.9% to 11.1% in the side branch with a final kissing balloon dilatation[17]. But even with a final kiss, the crushed portion of the stent is often not fully apposed thus increasing the risk of stent thromboses. In addition, the minimum residual stenosis within in the main branch is nearly always at the site of the crush[18]. It is therefore not surprising that several studies have failed to demonstrate an advantage of more complex double-vessel two-stenting strategies over a simple one stent or provisional stenting strategy. Further progress in this lesion subset will depend on developing effective bifurcation-specific stent platforms. Currently in development or in trials are side branch access systems, which allow continued access with modest ostial branch scaffolding, devices that allow for continued access and 1–2 mm of side branch scaffolding at the ostium and self-expanding modular systems[19]. But until these dedicated bifurcating stents have shown a definitive advantage recrossing the struts to perform final kissing balloon especially in the crush technique is essential to limit restenosis and stent thrombosis. Moreover even with a simple single stent strategy almost one third of all angiographically significant side branch lesions are hemodynamically significant by fractional flow reserve analysis and importantly flow can be improved following provisionally opening the overlying strut at the ostium[20].

In this randomised study directly comparing the performance of magnetic and standard conventional wires in routine bifurcation lesion treatment the MNS had a greater overall procedural success. More importantly it permitted the safe crossing into the side branch by avoiding entering the false lumen of dissected vessels in selected failed standard wire. But to rationale the use of the MNS to treat all bifurcations based on these limited success cannot be currently justified when the whole PCI procedure is taken into account. In the crossing of the branches of the pre-treated bifurcating vessel the magnetic wires were significantly slower than the conventional wires. This is partly because of limitations with the software available at the time of the study that required manual updates of the navigational vectors on the touch screen monitor. It meant therefore that the operator had a time delay prior to advancing the magnetic guidewire as the system updated. Despite the slowness of vector updates the software had a direct effect on the contrast through the displayed navigational centerline on the live fluoroscopic image (Figure

2). Following the various stenting strategies there was no significant difference in the overall crossing and fluoroscopic times with either wire. Understandably for the same reasons as in the untreated vessels the magnetic wire was also significantly slower in crossing a single layer of stents. With no recrossing failures and only minor benefits with contrast media reduction the magnetic wires offer no additional advantage over the conventional wires in this subgroup. A better performance was observed with the magnetic wires compared to the standard wire in recrossing the two layers of stents in the crush technique although it did not achieve statistical significance. The failure of the magnetic wire could have been due to the lack of pushability to force a trapped magnetic tip between the overlapping cells. But the fact that the wire was retracted and the tip direction changed within the proximity of the carina to allow the wire to engage an alternative set of cells led to a safe recrossing without causing vessel trauma. This was the reason why the standard wire failed in two cases involving crushed stents as the operator unknowingly forced the wire between the struts and the vascular wall to form a false lumen. With a better-designed magnetic wire having a more gentle transition of the magnetic tip with the shaft such as the proposed multi-magnet where smaller magnets are beaded together in manufacturing the tip the current problems encountered in crossing the stents struts might be reduced. Moreover it may allow better targeting of selective stents cells such as those closest to the carina due to smaller curves to optimize some bifurcation stenting techniques[21].

Limitations

The study was limited by the small number of patients with bifurcating lesions admitted into the magnetic room over the study period. The 3D-reconstruction required angiography of a suitable standard and this was not always possible from standard views due to foreshortening or overlapping. The 3DRC used in this study was time-consuming taking upto 30 minutes to complete. The static road map created from the 3DRC image was superimposed on a dynamic real-time image for magnetic navigation and this meant that only in one phase the wire tip was perfectly aligned. There were a number of operators and types of wires and this, together with no selection of the target vessel segment, may have led to heterogeneity. This study was performed at a University specialist tertiary referral unit and the case mix might be different to that seen elsewhere.

Conclusions

In this randomised study the Magnetic Navigation System had greater crossing success to conventional PCI techniques in managing bifurcations. It is relatively slower in crossing a single layer of stent struts and there is no real difference in the crossing or fluoroscopy times in crossing two layers of stents. But importantly, in selected failed standard wire cases of the crush technique the system can permit safe crossings to complete final kissing balloon dilatation.

Furthermore, by employing a navigational road map superimposed on the live fluoroscopic image the system offers a small but significant reduction in the amount of contrast media usage.

References

1. Louvard Y, Lefevre T, Morice MC. Percutaneous coronary intervention for bifurcation coronary disease. *Heart* 2004;90:713-22.
2. Colombo A, Moses JW, Morice MC, Ludwig J, Holmes DR, Jr., Spanos V, Louvard Y, Desmedt B, Di Mario C, Leon MB. Randomized study to evaluate sirolimus-eluting stents implanted at coronary bifurcation lesions. *Circulation* 2004;109:1244-9.
3. Hoye A, Iakovou I, Ge L, van Mieghem CA, Ong AT, Cosgrave J, Sangiorgi GM, Airoldi F, Montorfano M, Michev I, Chieffo A, Carlino M, Corvaja N, Aoki J, Rodriguez Granillo GA, Valgimigli M, Sianos G, van der Giessen WJ, de Feyter PJ, van Domburg RT, Serruys PW, Colombo A. Long-term outcomes after stenting of bifurcation lesions with the "crush" technique: predictors of an adverse outcome. *J Am Coll Cardiol* 2006;47:1949-58.
4. Kaplan A, Ramcharitar S, Louvard Y. Tryton I, First-In-Man (FIM) Study: acute and 30 day outcome. A preliminary report. *EuroIntervention* 2007;3 54-59.
5. Ramcharitar S, Patterson MS, van Geuns RJ, Serruys PW. Magnetic navigation system used successfully to cross a crushed stent in a bifurcation that failed with conventional wires. *Catheter Cardiovasc Interv* 2007;69:852-5.
6. Medina A, Suarez de Lezo J, Pan M. [A new classification of coronary bifurcation lesions]. *Rev Esp Cardiol* 2006;59:183.
7. Ramcharitar S, Patterson MS, van Geuns RJ, van der Ent M, Sianos G, Welten GM, van Domburg RT, Serruys PW. A randomised controlled study comparing conventional and magnetic guidewires in a two-dimensional branching tortuous phantom simulating angulated coronary vessels. *Catheter Cardiovasc Interv* 2007;70:662-8.
8. Ramcharitar S, Patterson MS, van Geuns RJ, van Meighem C, Serruys PW. Technology Insight: magnetic navigation in coronary interventions. *Nat Clin Pract Cardiovasc Med* 2008;5:148-56.
9. Movahed MR. Coronary artery bifurcation lesion classifications, interventional techniques and clinical outcome. *Expert Rev Cardiovasc Ther* 2008;6:261-74.
10. Pappone C, Vicedomini G, Manguso F, Gugliotta F, Mazzone P, Gulletta S, Sora N, Sala S, Marzi A, Augello G, Livolsi L, Santagostino A, Santinelli V. Robotic magnetic navigation for atrial fibrillation ablation. *J Am Coll Cardiol* 2006;47:1390-400.
11. Raizner AE. Magnetic navigation: a pivotal technology. *Catheter Cardiovasc Interv* 2007;69:856.
12. Patterson MS, Ramcharitar S, Serruys PW. Magnetically Supported PCI: success after failed surgery and conventional PCI. *Cath Lab Digest* 2007;15:1-14.
13. Atmakuri SR, Lev EI, Alviar C, Ibarra E, Raizner AE, Solomon SL, Kleiman NS. Initial experience with a magnetic navigation system for percutaneous coronary intervention in complex coronary artery lesions. *J Am Coll Cardiol* 2006;47:515-21.
14. Ramcharitar S, van Geuns RJ, Patterson MS, van der Giessen WJ, van der Ent M, van Domburg RT, Serruys PW. A Randomised Comparison of the Magnetic Navigation System versus Conventional Percutaneous Coronary Intervention. *Catheter Cardiovasc Interv* 2008;in press.
15. Pendyala L, Jabara R, Hou D, Shinke T, Li J, Gadesam R, Robinson K, Chronos N, Chen JP. Review of percutaneous therapy for bifurcation lesions in the era of drug-eluting stents. *Minerva Cardioangiol* 2008;56:89-105.
16. Steigen TK, Maeng M, Wiseth R, Erglis A, Kumsars I, Narbute I, Gunnes P, Mannsverk J, Meyerdierks O, Rotevatn S, Niemela M, Kervinen K, Jensen JS, Galloe A, Nikus K, Vikman S, Ravkilde J, James S, Aaroe J, Ylitalo A, Helqvist S, Sjogren I, Thayssen P, Virtanen K, Puhakka M, Airaksinen J, Lassen JF, Thuesen L. Randomized study on simple versus complex stenting of coronary artery bifurcation lesions: the Nordic bifurcation study. *Circulation* 2006;114:1955-61.
17. Ge L, Airoldi F, Iakovou I, Cosgrave J, Michev I, Sangiorgi GM, Montorfano M, Chieffo A, Carlino M, Corvaja N, Colombo A. Clinical and angiographic outcome after implantation of drug-eluting stents

in bifurcation lesions with the crush stent technique: importance of final kissing balloon post-dilation. *J Am Coll Cardiol* 2005;46:613-20.
18. Costa RA, Mintz GS, Carlier SG, Lansky AJ, Moussa I, Fujii K, Takebayashi H, Yasuda T, Costa JR, Jr., Tsuchiya Y, Jensen LO, Cristea E, Mehran R, Dangas GD, Iyer S, Collins M, Kreps EM, Colombo A, Stone GW, Leon MB, Moses JW. Bifurcation coronary lesions treated with the "crush" technique: an intravascular ultrasound analysis. *J Am Coll Cardiol* 2005;46:599-605.
19. Abizaid A CR, Alfaro VJ, Feres F, Staico R, Mattos LA, Maldonado G, Sousa JE. Bifurcated Stents: giving to Caeser what is Caeser's. *Eurointervention* 2007:518-525.
20. Koo BK, Park KW, Kang HJ, Cho YS, Chung WY, Youn TJ, Chae IH, Choi DJ, Tahk SJ, Oh BH, Park YB, Kim HS. Physiological evaluation of the provisional side-branch intervention strategy for bifurcation lesions using fractional flow reserve. *Eur Heart J* 2008;29:726-32.
21. Laborde JC, Borenstein N, Behr L, Ramcharitar S. Stentys Coronary Bifurcated Stent. *Eurointervention* 2007;3:162-165

Chapter 5

THE INTEGRATION OF MULTISLICE COMPUTER TOMOGRAPHY WITH MAGNETIC NAVIGATION

Noninvasive cardiac computed tomography: an interventional cardiologist's perspective

Submitted

Van Mieghem CAG, **Ramcharitar S**, Mc Fadden E; Serruys,PW, de Feyter, PJ

Introduction

The in-vivo assessment of the coronary arteries was feasible by the end of the 1950s and quickly revolutionized the practice of cardiology.[1] Forty years later a noninvasive alternative in the form of computed tomography coronary angiography (CTCA) became available.[2,3] The high diagnostic accuracy of CTCA for the detection and exclusion of significant (> 50% stenosis) coronary artery disease has repeatedly been demonstrated. Important upgrades in scanning technology have resulted in the current generation of 64-slice CT scanners ability to accurately assess clinically relevant segments of the coronary tree (vessels with a diameter of 1.5 mm or greater) within 10 seconds, a time comfortable to most patients. Even though there are limitations and it does not provide yet the same spatial and temporal resolution as its invasive counterpart. Also the 3-dimensional nature offers a hitherto underappreciated and added value in determining both the lesion and vessel characteristics that is vastly superior to conventional 2-D angiography.

In many countries, a patient that qualifies for coronary revascularisation usually undergoes a 2-step imaging procedure, consisting of diagnosis and therapy. In the initial diagnostic phase an accurate assessment of all segments of the coronary arterial tree is performed. The patient that harbors significant coronary artery disease that is deemed appropriate for revascularisation, ideally undergoes an ad hoc percutaneous coronary intervention (PCI), but more often due to logistical reasons will be scheduled for an elective PCI or coronary bypass surgery (CABG) at another day. Aside from the inherent risks that arise when cannulating the peripheral arterial system and manipulating the catheter alongside the aorta, the intubation of the coronary arteries itself can be time-consuming and is not entirely devoid from complications. (Figure 1) Furthermore, it requires a meticulous operator to provide the interventional cardiologist or cardiac surgeon with precise information regarding the lesion site and its relation with side branches. Not infrequently however, additional projections are needed at the moment of the planned PCI. Moreover in some instances the cardiac surgeon asks for a repeat catheterization because of suboptimal projections at the initial diagnostic angiogram.

The purpose of this article is to discuss the inherent limitations of conventional coronary angiography (CCA) and highlight the advantages of cardiac CT in this regard. Furthermore, the information as provided with CTCA might prove to be essential in certain circumstances before attempting coronary revascularization or percutaneous valvular procedures.

Diagnostic coronary imaging

CCA plays a central role in the management of patients with coronary artery disease and is regarded as the gold standard for confirming or excluding the presence of coronary obstructive

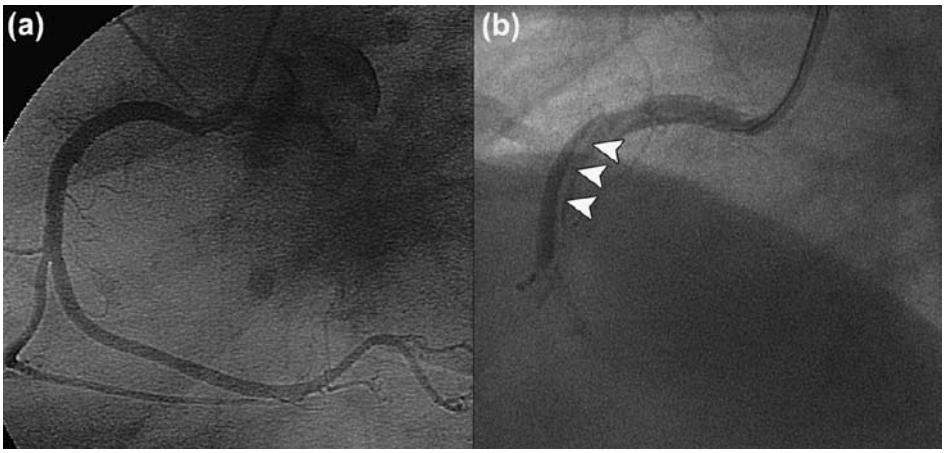

Figure 1. *Invasive coronary angiogram of the right coronary artery. (a) Normal appearance of the vessel at initial catheterization. (b) In order to perform an intravascular ultrasound of the vessel, the artery was intubated again 2 weeks later, which resulted in a proximal dissection of the vessel. The dissection flap is clearly visible (arrowheads).*

disease. Due to its invasive nature, this procedure should ideally be confined to patients in whom the likelihood of proceeding to coronary revascularization is high. Current guidelines recommend the use of noninvasive stress testing as a first-line test before proceeding to a catheter-based assessment of the coronary anatomy.[4] In daily practice however our approach to patients with suspected or proven coronary artery disease is different. The majority of patients that undergo coronary revascularization do not have objective proof of ischemia.[5] Recent surveys demonstrate that normal CAs account for up to 20% of all coronary angiograms.[6] Also, the proportion of patients that proceed to a coronary intervention is only one third of the number of patients catheterized.[7] These data confirm that even today CA is still widely performed for excluding the presence of coronary atherosclerosis, as was concluded by Mason Sones 35 years ago, and not as a prelude to coronary revascularization.[8] It is not surprising therefore that diagnostic uncertainties that often persist when faced with a normal noninvasive stress test in a patient with unexplained chest pain.[9] Furthermore, the favorable prognostic value of a normal nuclear scan or dobutamine stress echocardiogram (DSE) often is not sufficient to confidently finalize the diagnostic work-up and to reliably exclude the presence of coronary artery disease This is because standard SPECT and PET imaging rely on normalization of acquired data to the region of the myocardium with maximal perfusion, even if this area of perfusion may be abnormal. As a result, this method may underestimate the extent of disease, particularly in patients with significant three-vessel or left main disease. [10,11] Stress echocardiography has limited sensitivity for the detection of single-vessel disease, which explains the good prognostic value of a normal DSE but at the same time its inaccuracy for clarifying the possible ischemic origin of a patient's symptoms.[12]

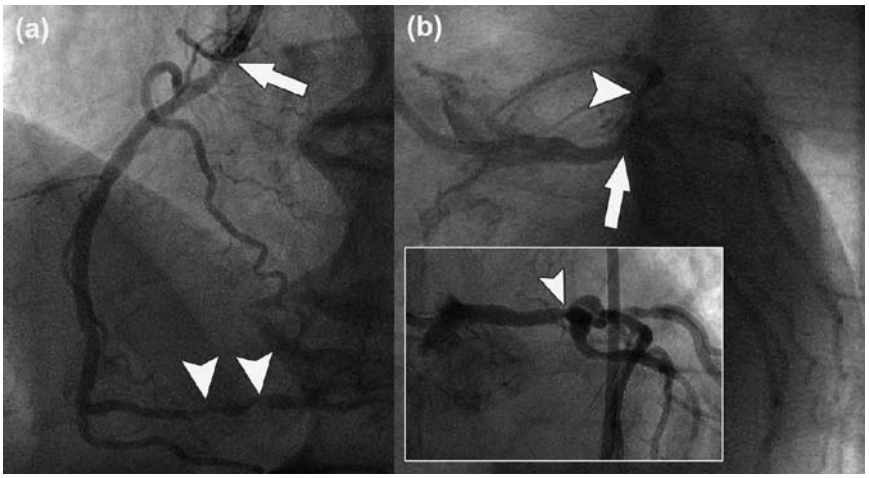

Figure 2. *(a) Invasive coronary angiogram of the right coronary artery (RCA). The diagnostic catheter (arrow) is obscuring the ostium of the vessel. The distal segment shows 2 consecutive significant stenoses (arrowheads). (b) Invasive coronary angiogram of the left coronary artery. The initial angiogram only revealed a significant narrowing in the proximal left anterior descending coronary artery (arrowhead). The distal part of the left main coronary artery (arrow) appears unaffected. A straight anteroposterior view (inset), which was performed when the patient was scheduled for a percutaneous coronary intervention, clearly shows a severe stenosis at this level (arrowhead).*

Current 64-slice CT scanners are particularly useful for excluding the presence of significant coronary artery disease with a a normal scan result having a favorable prognosis.[13,14] As a result, a CT-based approach seems most useful in patients with a low to intermediate likelihood of coronary artery disease, in whom it is deemed necessary to evaluate the coronary anatomy.[15] Most clinicians would advocate catheter-based CA as the preferred strategy in patients with a high pre-test likelihood of CAD primarily because of the option to perform an ad hoc therapeutic intervention. Nevertheless, such an ad-hoc approach has several disadvantages when compared to a stepwise approach: the latter strategy allows time to inform the patient about risks, benefits, and possible therapeutic alternatives and allows optimally preparation of the patient before before the procedure by ensuring adequate pre-hydration if necessary and pre-treatment with oral anti-platelet agents. [16] These issues are now vitally important in the current climate of late stent thrombosis with drug eluting stents.[17] In addition, an ad-hoc approach does not allow general discussion between the general cardiologist, interventional cardiologist, and cardiac surgeon to reach consensus about the most optimal treatment strategy.

Importantly, only when adequately performed and interpreted can CCA reveal the exact location and relative severity of obstructive lesions in branches of the coronary tree. Contrary to the general belief, CCA may not always prove to be the gold standard technique for the visualization of the coronary anatomy even in very experienced hands. Indeed, the intrinsic limitations of a

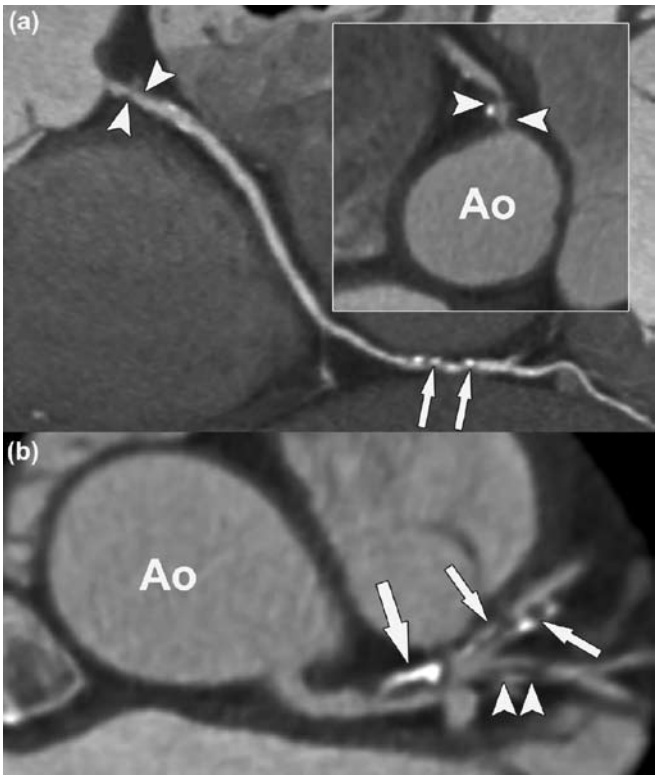

Figure 3. *Corresponding CT coronary angiogram (a) Curved multiplanar reconstruction of the right coronary artery confirming the 2 consecutive stenoses in the distal segment (arrows). The ostium (inset) also shows a high-grade stenosis (arrowheads), which initially was not visualized by the invasive coronary angiogram. (b) Multiplanar reconstruction of the proximal segments of the left coronary artery, clearly showing significant stenoses in the distal part of the left main coronary artery (large arrow), the proximal left anterior descending coronary artery (small arrows) and the large intermediate branch (arrowheads). Ao, indicates ascending aorta.*

2-dimensional projectional imaging technique may sometimes be difficult to appreciate in the presence of a coronary narrowing especially in cases of complex anatomy[18] (Figures 2 and 3). The lack of adequate contrast media opacification within the vessel can lead to inaccuracies in determining the true diameter stenosis at the minimal luminal diameter that may result in inappropriate management. Moreover, limitations due to vessel overlapping and foreshortening can have an impact on stent usage when compared to computer generated virtual 3-D vessel reconstructions.[19] It should be borne in mind that CTCA is not a virtual 3-D *reconstructed* (3DRC) image *but an accurate representation of the heart in different views. Furthermore unlike a 3DRC image and conventional 2-D luminography it allows the direct visualization of the* atherosclerotic disease process. It may therefore have and important role in the future in indentify the so-called 'high risk' plaques. [20]

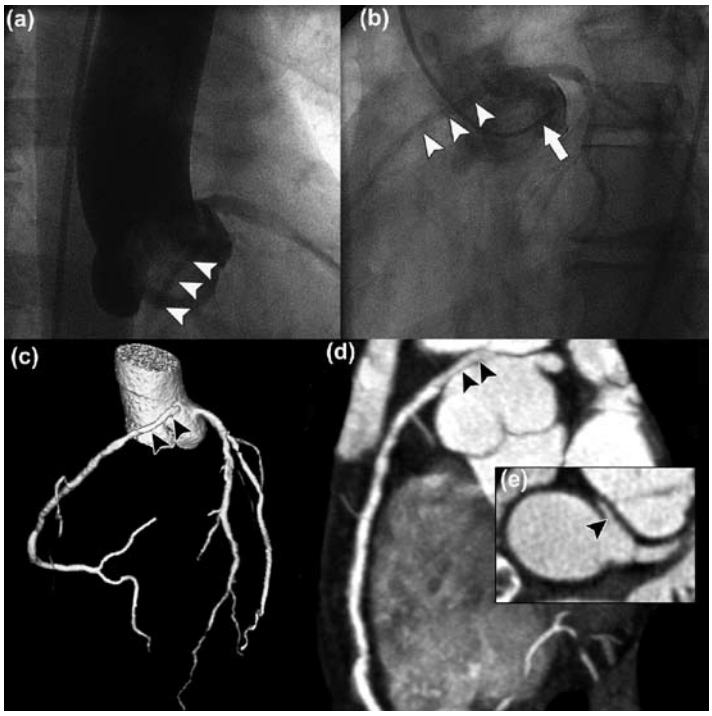

***Figure 4**. Anomalous origin of the right coronary artery (RCA). (a) An aortogram was performed to localize the origin of the RCA, whose contours are faintly visible (arrowheads). (b) Non-selective injection confirms its origin (arrowheads) out of the left coronary cusp. (c, d, e) CT coronary angiogram clearly showing the anomalous origin (arrowheads) and course of the RCA*

Complex anatomy

Failure to visualize or to understand the course of a coronary artery has become a frequent reason to refer a patient for an alternative imaging technique. Coronary anomalies are the prototype example where the cardiac catheterization findings often are inconclusive or result in a prolonged procedure with excessive use of contrast material. (Figure 4) In this regard, cardiac CT is becoming the investigation of choice to demarcate complex 3D coronary artery anatomies and the relationship to the surrounding structures.[21,22] The favorable experience when assessing anomalous coronary arteries with cardiac CT, can be extended to other difficult coronary anatomy, such as ostial lesions, lesions at bifurcations or within the left main artery, and chronic total occlusions. Cardiac CT can provide important information in all the above complex anatomical lesion subsets in order to target the most appropriate modality for treatment.

Ostial lesions

Catheter-based imaging of coronary ostial disease can be technically challenging because of difficulties in obtaining adequate contrast media opacification through non-selectively

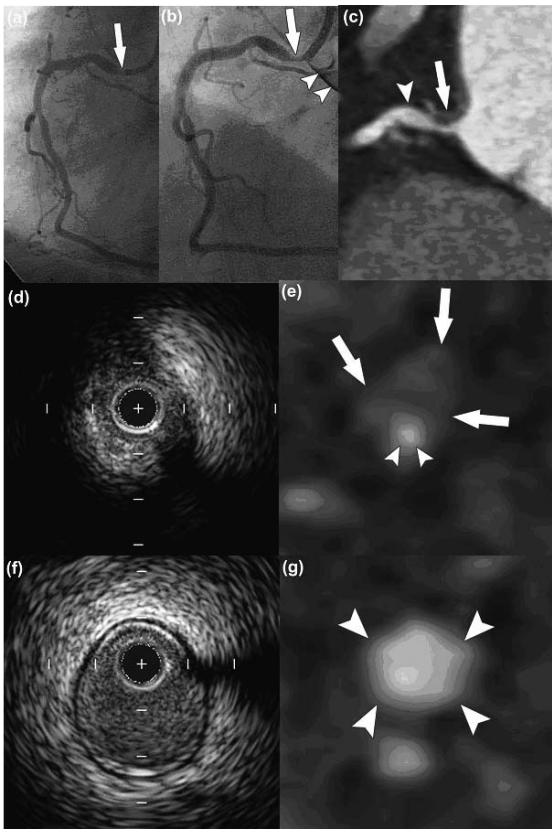

Figure 5. *Patient with a true ostial stenosis of the right coronary artery (a) Initial invasive coronary angiogram showing the stenosis (arrow). (b) These findings are confirmed (arrow) when the patient was rescheduled to undergo a percutaneous coronary intervention. The contrast injection this time was non-selective, as is obvious from the appearance of contrast in the right coronary cusp (arrowheads), to minimize the chances of catheter-induced spasm. (c) Corresponding CT coronary angiogram clearly showing the ostial involvement (arrow). (d, e, f, g) Cross-sectional intravascular ultrasound (d and f) and CT (e and g) images, clearly showing the significant narrowing of the lumen (d and e). The extent of disease (e, arrows) in the vessel wall is quite obvious on CT, the residual lumen area (arrowheads) is very small. (f, g) Corresponding cross-sections at the reference site (panel c, arrowhead), distal to the stenosis.*

engaging the catheter outside the ostium and in the coronary cusp. By virtue of the technique itself CA poorly assessed ostium especially so if the catheter is deeply intubated. (Figure 5) Misinterpretation with possible inappropriate therapeutic handling can be a possible consequence of failure to recognize catheter-induced spasm, a condition that typically affects the right coronary artery. (Figure 6) These caveats are effectively avoided by using cardiac CT which in our experience is the preferred imaging tool in re-assessing patients with suspected coronary ostial disease in whom the initial CA was inconclusive.

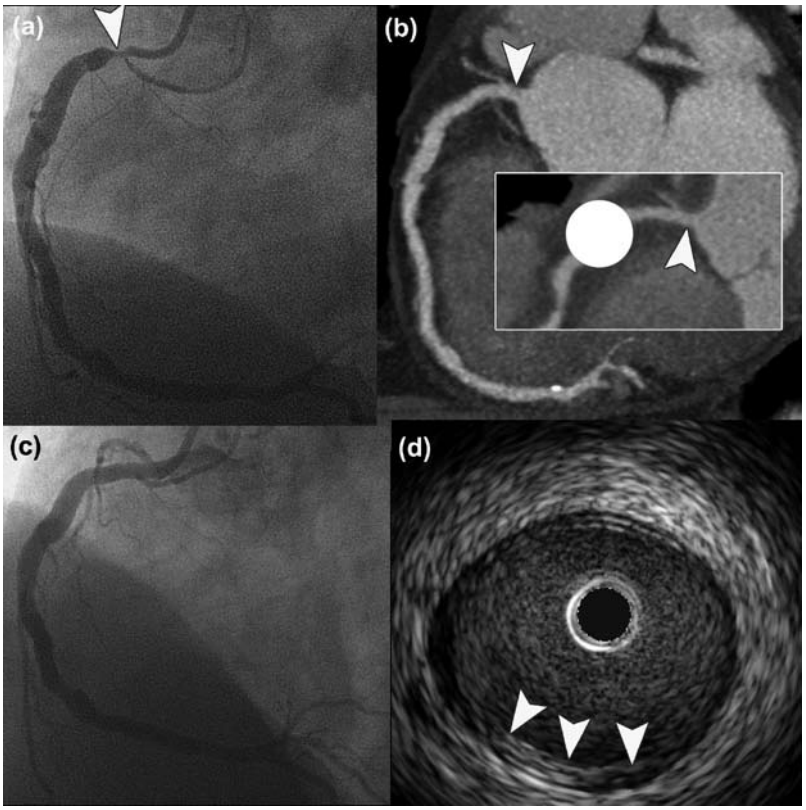

Figure 6. *Patient who was referred to undergo a percutaneous coronary intervention for an ostial stenosis of the right coronary artery. (a) Initial angiographic image showing the coronary narrowing (arrowhead). (b, with inset) On cardiac CT the vessel had a normal appearance. (c) A repeat coronary angiogram confirmed the CT findings. (d) On intravascular ultrasound the ostium was indeed widely patent with only minimal intimal thickening (arrowheads).*

Bifurcations

Coronary atherosclerosis exhibits a predilection for areas of low shear stress, typically at bifurcation sites. Plaque build-up usually is already extensive in these areas before becoming angiographically visible. In today's practice, percutaneous coronary intervention (PCI) for bifurcation pathology entails up to 20% of attempted lesion subsets.[23] PCI of bifurcation lesions remains quite challenging and the most effective treatment strategy remains as yet undefined. Important determinants of the chosen approach are the distribution of plaque in main vessel and side branch, as well as the degree of angulation between both branches. Coronary bifurcations are notoriously difficult to examine completely by CCA despite multiple angiographic projections, due to factors such as vessel overlap and foreshortening. Cardiac CT offers accurate three-dimensional information and is not subject to the limitations of conventional angiography. (Figure 7) CTCA reliably assesses the plaque distribution across the bifurcation and in contrast

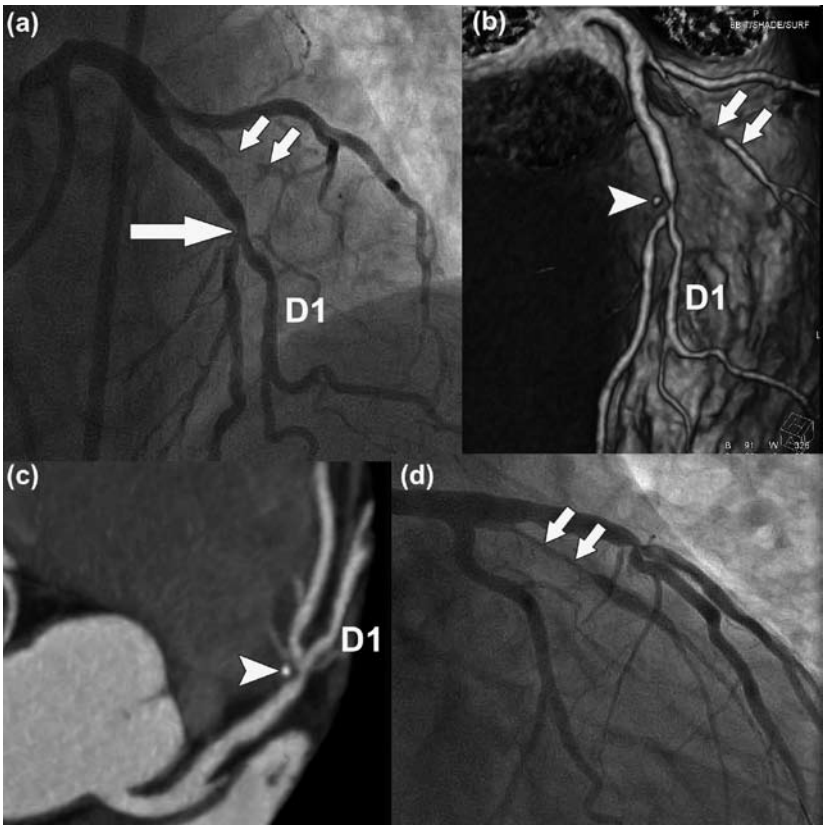

Figure 7. *(a) Invasive coronary angiogram showing a significant bifurcation lesion (large arrow) of the left anterior descending coronary artery with the first diagonal branch (D1). Also note the limited contrast enhancement (small arrows) in what looks like a small side branch. (b) Three-dimensional reconstruction of the heart with CT showing the bifurcation lesion. The dense spot within the lesion (arrowhead) corresponds to calcification. The branch that was faintly visible angiographically, can now be clearly recognized without interference of overlapping vessels as the intermediate branch (arrows). (c) 3-mm thick maximum intensity projection clearly showing the calcified (arrowhead) and non-calcified plaque components causing the lumen narrowing. (d) After wiring the intermediate branch its true dimension can be well appreciated (arrows).*

to CCA allows a more precise assessment of coronary bifurcation angles.[24,25] These advantages might be of benefit for deciding on an adequate treatment strategy.

Left main coronary artery

The left main (LM) coronary artery combines the difficulties that arise when assessing ostial and bifurcational disease. Indeed, ostial lesions of the left anterior descending or circumflex artery frequently involve the distal LM bifurcation. Despite its clinical significance, LM disease may not be accurately evaluated by CCA alone.[26,27] CTCA overcomes the limitations of CCA and can be a clinically useful, adjunctive method to evaluate LM coronary artery disease. (Figure 8)

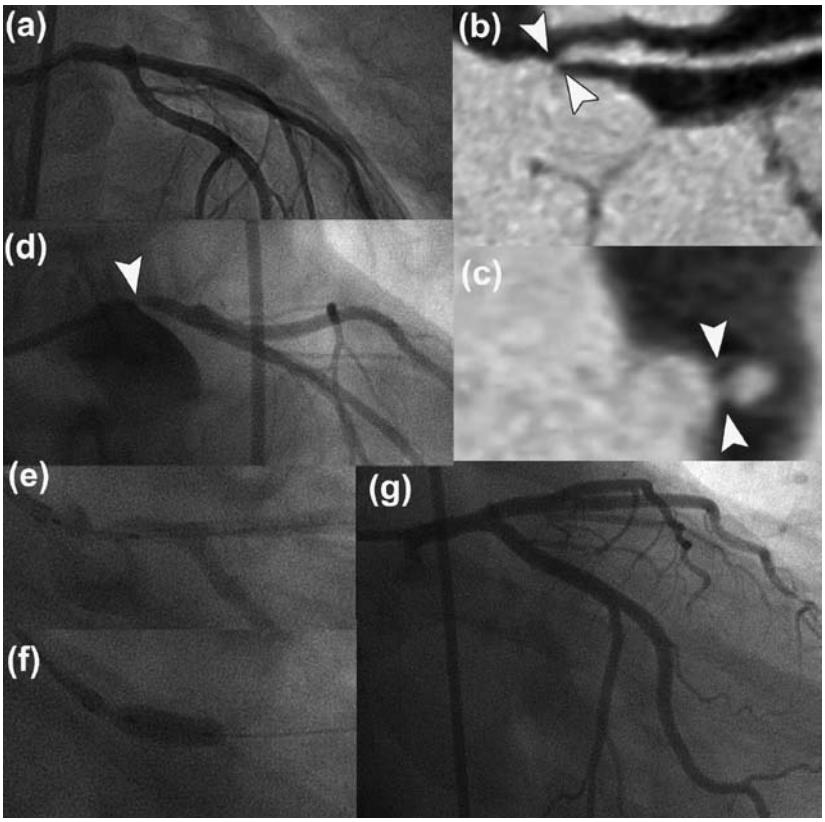

Figure 8. *(a) Diagnostic coronary angiogram of the left coronary artery in a female patient with atypical chest pain who presented with ventricular fibrillation during a bicycle stress test. Although not visible there was a suspicion of ostial left main disease because of the absence of contrast back flow in the coronary sinus. (b and c) The CT coronary angiogram clearly shows a severe ostial narrowing (arrowheads). (d) A non-selective repeated invasive coronary angiogram confirms the CT findings (arrowhead). (e and f) A percutaneous coronary intervention was performed: shown are the positioning and deployment of the stent. (g) Postprocedural coronary angiogram.*

Chronic total occlusions

Coronary chronic total occlusions (CTOs) are found in up to 50% of patients with significant coronary artery disease, but PCI is attempted in only a fraction of these lesions.[28] The relatively low procedural success rate compared to PCI of non-occluded coronary arteries and the higher risk of procedural-related complications in case of failed recanalization, explain the rather low referral rates for PCI.[29] Several angiographic features have been identified as predictors for successful recanalization, and the presence or absence of these can influence the decision regarding whether PCI is attempted or the patient is referred for coronary artery bypass surgery.[30] CTCA not only assesses the luminal impact of atherosclerosis, but also visualizes the disease process in the coronary artery wall and by consequence in occluded parts of the coronary arteries. (Figure 9) Independent predictors of PCI failure for CTOs, are the length of the

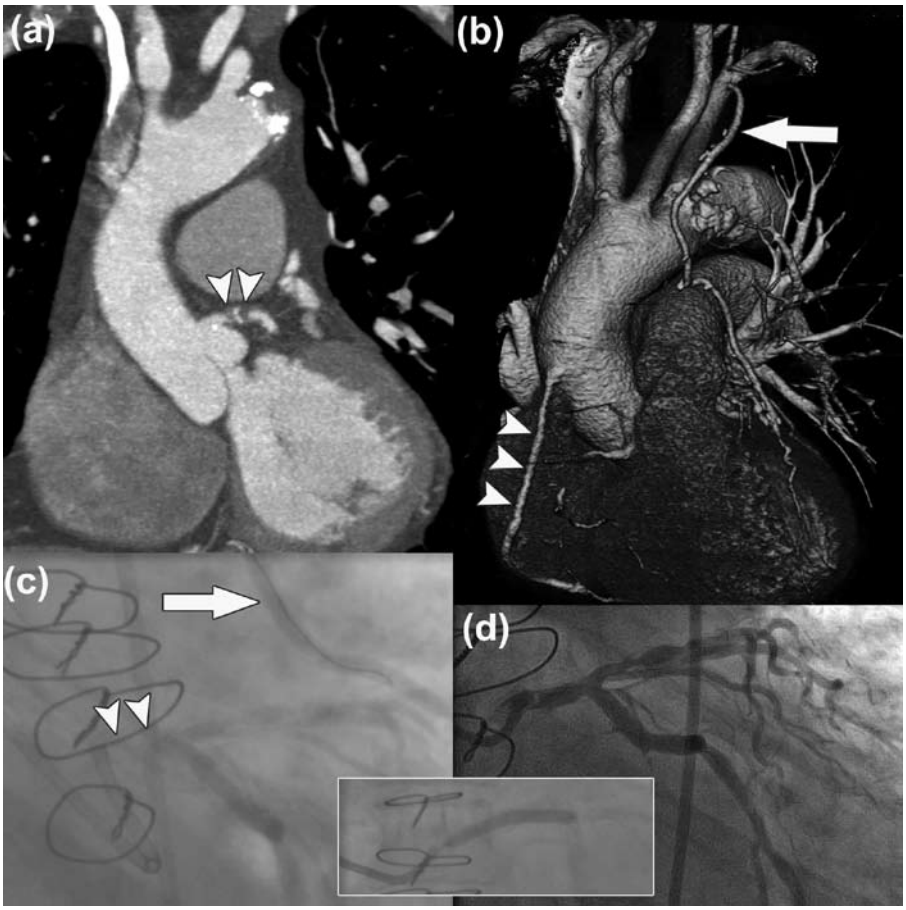

***Figure 9**. Patient with recurrent angina after previous coronary bypass graft surgery, including a venous graft to the right coronary artery (RCA) and left internal mammary artery (LIMA) to the left anterior descending coronary artery. At initial invasive catheterization the origin of the left coronary artery appeared occluded. (a) Cardiac CT scan, coronal view, indeed showing a short occlusion (arrowheads) of the left main stem. (b) Three-dimensional reconstruction of the heart showing the patent LIMA (arrow) and venous graft to the RCA (arrowheads). (c) Contrast injection after wiring of the LIMA (arrow) results in opacification of the native coronary artery up to the distal part of the left main stem. (d) Six-month angiographic result after successful PCI (inset) of the left main stem.*

occlusion and the presence of heavy calcifications within the occluded segment: both variables are more precisely defined by CTCA as compared to CCA.[31] Preprocedural evaluation of CTOs by means of CTCA is becoming routine in several institutions as it provides the interventional cardiologist a roadmap that appears to be helpful in the selection of the devices to facilitate a successful crossing of the occlusion.[32,33] Moreover differentiating the nature of the occluding plaque whether it is soft (lipid-rich) or hard (fibrocalcific), can influence thedevice selection and clinical outcome. [34] Retrograde or contralateral cannulation can often be avoided since the 3-dimensional visualization of the course of the occluded vessel oprovides visual landmarks for

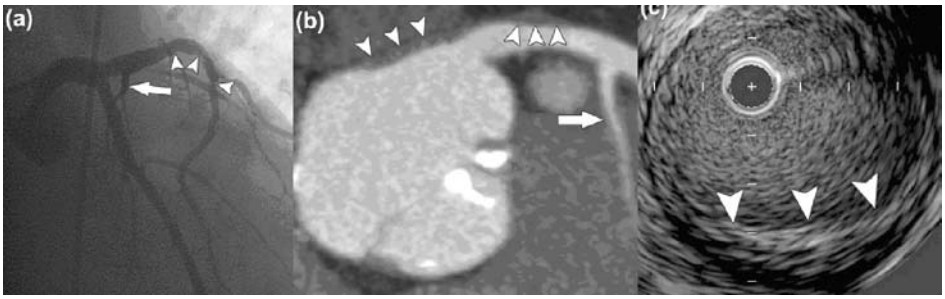

Figure 10. *(a) Invasive coronary angiogram showing "wall irregularities" (arrowheads) and thus indirect signs of atherosclerosis distal to the origin of the first septal branch (arrow). (b) Corresponding CT coronary angiogram, maximum intensity projection, showing atherosclerosis (arrowheads) in its earlier stages, i.e.outward remodeling of the vessel without lumen impairment, proximal to the take-off of the first septal branch (arrow). (c) Intravascular ultrasound of the left main stem clearly showing plaque build-up in the intimal layer (arrowheads).*

the interventional cardiologist to steer the guidewire towards the direction of the distal vessel beyond the occlusion.

Plaque imaging

CTCA confirms what surgeons and pathologists have emphasized in the past- that angiography underestimates the extent of atherosclerotic disease in general and can be greatly misleading in predicting the distribution of plaque in any given portion of the vessel wall. The fundamental difference between CCA and CTCA is the basic image format: while CCA provides high-resolution imaging, it is limited to the luminal surface. CTCA overcomes the limitations of silhouette imaging and reveals details of the distribution and composition of atheroma within the vessel wall. (Figure 10) It could be of considerable value to be able to identify lipid-rich plaques and, ideally, identify morphological factors influencing the likelihood of plaque rupture. Visualization and characterization of coronary plaques with CTCA is feasible and provides us new dimensions of information on the coronary atherosclerotic disease process. However, data are not available yet that show a patient benefit when using CTCA as a tool for risk stratification of asymptomatic individuals.

Therapeutic use of cardiac CT imaging

Guidance during complex percutaneous coronary interventions

In addition to its diagnostic value, cardiac CT images might also facilitate the actual process of PCI. This is currently being realised by integration of the CTCA with the Stereotaxis Niobe® Magnetic Navigation System (St Louis, MO, USA). [35] In this novel technology two permanent external magnets situated at either side of the patient can be rotated, translated or tilted to produce a uniform magnetic field of 0.08 Tesla within the patient's chest. This field is used to precisely direct a tiny magnet mounted on the tip of a guidewire by changing its magnetic moments.

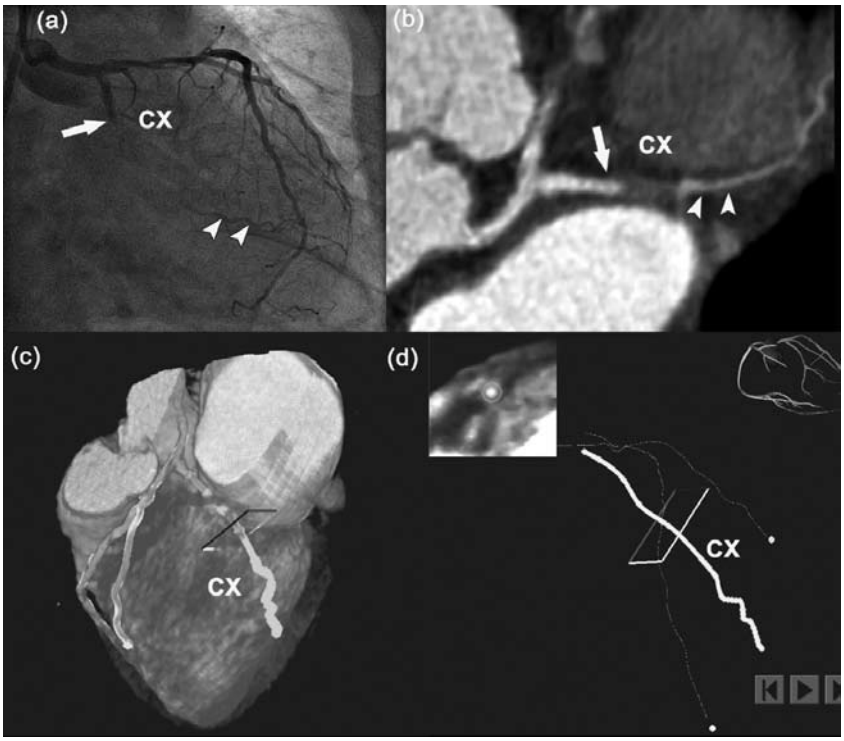

Figure 11. *(a) Invasive coronary angiogram, showing a chronic total occlusion (arrow) of the circumflex artery (CX). Only the very distal part of the vessel is visible through collaterals (arrowheads) (b) Corresponding CT image (curved multiplanar reconstruction): compared to the angiographic information the occlusion appears much shorter and consists of non calcified tissue. (c) The CT dataset has been uploaded in the navigation software; the course of the CX, including the path of the occlusion, is marked by a green line overlay. (d) The course of the CX has been marked as a yellow line. The rectangular which is present in panel c and d marks the location of the wire tip in the vessel. The inset in panel d represents the perpendicular cross-sectional view of the vessel to allow the steering of the guidewire in the desired direction.*

This allows fine control of the orientation of the tip of the guidewire in space achieving a full 360ºomni rotation. This unique ability to manipulate a guidewire in vivo facilitates easier wire transit across otherwise difficult lesions and tortuous vessels. [36,37] Moreover it can potentially reduce vessel trauma in addition to reducing radiation exposure and contrast usage. In preliminary assessment it is feasible to perform coronary intervention without contrast media in patients having prior CTCA when the dataset is co-integrated in the Navigant® software and the derived roadmap is co-registered with the tip of the guiding catheter in the coronary sinus.

In addition, the integration of CTCA and MNS may provide a novel route to improving the success rate in treating CTOs. By co-registering the occluded coronary segment of the volume rendered image in the Navigant® software to the fluoroscopy live image an accurate virtual

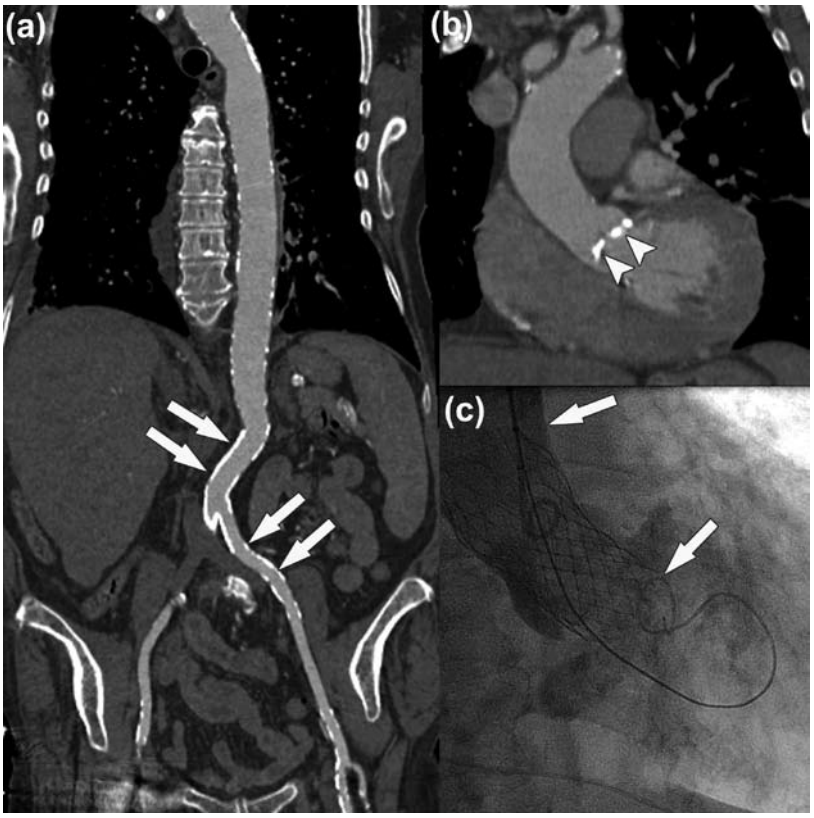

Figure 12. *Eighty-three year-old woman with symptomatic severe aortic valve stenosis who was considered a candidate for percutaneous aortic valve replacement. (a) The thoraco-abdominal CT scan revealed severe calcifications (arrows) of the abdominal aorta and iliac arteries. (b) CT image, coronal view, showing the severe calcifications of the aortic valve (arrowheads). (c) Because of the expected difficult femoral access, the valve replacement was successfully performed through the left subclavian artery. The arrows are showing the borders of the freshly implanted aortic valve, which consists of a equine pericardial valve mounted on a stainless steel bioprosthesis.*

road map through the vessel lumen can be achieved. (Figure 11) This can be used to guide a magnetically aided radio-frequency ablating wire through the occlusion.

Percutaneous therapies for valvular heart disease

In addition to the investigation of the coronary arteries, cardiac CT is well suited to assess valvular anatomy and disease of the large extra-cardiac arteries. Percutaneous aortic valve replacement (PAVR) is an emerging technology in the management of patients with severe aortic stenosis unsuitable for surgical management. [38,39] These percutaneous heart valves are routinely implanted via a transfemoral arterial access using large diameter sheaths (18 to 24 French). Limited experience with this technology means that there is restricted knowledge of how these percutaneous devices impact on the often challenging cardiac anatomy and general

haemodynamics post implantation. In the few centres that offer this therapeutic option, CT scans are routinely used to evaluate the size of the aortic annulus and iliac arteries to ensure adequate patient selection and feasibility of passage of a 18-to-24 French system. (Figure 12).

In the future, cardiac surgeons and interventional cardiologists will increasingly rely on this noninvasive imaging modality to plan the specific intervention and to assess the results on follow-up

Limitations of CTCA: a word of caution

Subsequent improvements in CT scan technology have brought this cardiac imaging tool to the stage where accurate and noninvasive evaluation of the coronary anatomy is feasible. As is true for any new technology that is being considered for clinical use, the final hurdle to take is to determine the incremental information offered by this new test in comparison to existing standard assessments. Continuing rises in the costs of health care and the increasing use of cardiac imaging tests in particular, underscribe the need for a test to be cost-effective before changing existing diagnostic pathways. [40,41]Awaiting further scientific evidence, several societies have issued guidelines describing the optimal use of cardiac CT in an appropriate clinical context. [15,42] In general, cardiac CT proves most valuable for clinical situations where one seeks to confidently establish the absence of coronary artery disease. Initial studies have highlighted the potential of CTCA to be cost-effective in this regard.[43] Determination of the right clinical scenario is just one of the determinants of a succesful cardiac CT program. Other factors, such as adequate heart rate control, body mass index of the patient and amount of coronary artery calcification, are equally important and contribute to the " readability" of a scan.[44,45] A cardiac CT scan is not entirely limited to the heart, but also includes the adjacent thoracic structures. Non-cardiac findings requiring clinical or radiological follow-up are reported in up to 25% of patients undergoing cardiac CT and are a good reason to liaise with other specialists, in particular the radiology department.[46] The potential increase in cancer risk due to CT-related ionizing radiation is an important limiting factor and is spurring the search towards dose-saving algorithms and new scanning protocols that allow to bring down the patient's effective radiation dose in the range of that of ICA.[47-49] Finally, state-of-the-art cardiac CT imaging and interpretation requires adequate training in cardiovascular diseases and radiology imaging and ideally requires a sufficiently long interaction period of at least 6 months within a cardiology and radiology department of a dedicated teaching hospital.[50,51]

Conclusion

Cardiac CT holds great promise for cardiovascular imaging. This relatively new technology alters the way in which we diagnose CAD and provides diagnostic opportunities that may potentially be beneficial for many individuals with known or suspected cardiovascular disease. As a diagnostic test the use of CTCA is considered appropriate for clinical scenarios where one seeks to confidently exclude the presence of CAD. By substituting more costly diagnostic imaging modalities, in particular invasive coronary angiography and nuclear imaging studies, it is expected that CTCA will result in substantial cost savings for the health care system. The cost-effectiveness of cardiac CT is currently being evaluated in large clinical trials.

Invasive coronary angiography remains the preferred test for the patient with typical angina as it provides the option for immediate intervention. As illustrated in this review, improved coronary imaging using CTCA might be of value in certain circumstances to complement the invasively obtained angiographic data and thus might improve the safety and efficacy of the subsequent therapeutic action taken. This complementary role of cardiac CT imaging already results in so-called "reverse referrals", i.e. patients initially referred for an invasive CCA are subsequently sent for a cardiac CT to detect significant features of vascular pathology that are inaccessible by conventional angiography.

More and more, cardiac CT is finding its place as a diagnostic tool in clinical cardiology. To prove valuable in the long-run a high professional standard needs to be maintained by providing adequate training in cardiac CT and through strict adherence to guidelines issued by professional societies.

References

1.. Sones FM, Shirey EK, Proudfit WL, et al. Cine coronary arteriography. Circulation 1959; 20:773-775
2. Achenbach S, Moshage W, Ropers D, et al. Value of electron-beam computed tomography for the noninvasive detection of high-grade coronary-artery stenoses and occlusions. N Engl J Med 1998; 339:1964-1971
3. Nieman K, Oudkerk M, Rensing BJ, et al. Coronary angiography with multi-slice computed tomography. Lancet 2001; 357:599-603
4. Scanlon PJ, Faxon DP, Audet AM, et al. ACC/AHA guidelines for coronary angiography. A report of the American College of Cardiology/American Heart Association Task Force on practice guidelines (Committee on Coronary Angiography). Developed in collaboration with the Society for Cardiac Angiography and Interventions. J Am Coll Cardiol 1999; 33:1756-1824
5. Topol EJ, Ellis SG, Cosgrove DM, et al. Analysis of coronary angioplasty practice in the United States with an insurance-claims data base. Circulation 1993; 87:1489-1497
6. Uretsky BF, Wang FW. Implementation and application of a continuous quality improvement (CQI) program for the cardiac catheterization laboratory: one institution's 10-year experience. Catheter Cardiovasc Interv 2006; 68:586-595
7. Togni M, Balmer F, Pfiffner D, et al. Percutaneous coronary interventions in Europe 1992-2001. Eur Heart J 2004; 25:1208-1213
8. Sones FM, Jr. Indications and value of coronary arteriography. Circulation 1972; 46:1155-1160
9. Fleischmann KE, Hunink MG, Kuntz KM, et al. Exercise echocardiography or exercise SPECT imaging? A meta-analysis of diagnostic test performance. Jama 1998; 280:913-920
10. Lima RS, Watson DD, Goode AR, et al. Incremental value of combined perfusion and function over perfusion alone by gated SPECT myocardial perfusion imaging for detection of severe three-vessel coronary artery disease. J Am Coll Cardiol 2003; 42:64-70
11. Ragosta M, Bishop AH, Lipson LC, et al. Comparison between angiography and fractional flow reserve versus single-photon emission computed tomographic myocardial perfusion imaging for determining lesion significance in patients with multivessel coronary disease. Am J Cardiol 2007; 99:896-902
12. Elhendy A, van Domburg RT, Bax JJ, et al. Accuracy of dobutamine technetium 99m sestamibi SPECT imaging for the diagnosis of single-vessel coronary artery disease: comparison with echocardiography. Am Heart J 2000; 139:224-230
13. Pundziute G, Schuijf JD, Jukema JW, et al. Prognostic value of multislice computed tomography coronary angiography in patients with known or suspected coronary artery disease. J Am Coll Cardiol 2007; 49:62-70
14. Min JK, Shaw LJ, Devereux RB, et al. Prognostic value of multidetector coronary computed tomographic angiography for prediction of all-cause mortality. J Am Coll Cardiol 2007; 50:1161-1170
15. Budoff MJ, Achenbach S, Blumenthal RS, et al. Assessment of coronary artery disease by cardiac computed tomography: a scientific statement from the American Heart Association Committee on Cardiovascular Imaging and Intervention, Council on Cardiovascular Radiology and Intervention, and Committee on Cardiac Imaging, Council on Clinical Cardiology. Circulation 2006; 114:1761-1791
16. Smith SC, Jr., Feldman TE, Hirshfeld JW, Jr., et al. ACC/AHA/SCAI 2005 guideline update for percutaneous coronary intervention: a report of the American College of Cardiology/American Heart Association Task Force on Practice Guidelines (ACC/AHA/SCAI Writing Committee to Update 2001 Guidelines for Percutaneous Coronary Intervention). Circulation 2006; 113:e166-286
17. Waksman R. Late stent thrombosis--the "vulnerable" stent. Catheter Cardiovasc Interv 2007; 70:54-56
18. Topol EJ, Nissen SE. Our preoccupation with coronary luminology. The dissociation between clinical and angiographic findings in ischemic heart disease. Circulation 1995; 92:2333-2342
19. Gollapudi RR, Valencia R, Lee SS, et al. Utility of three-dimensional reconstruction of coronary angiography to guide percutaneous coronary intervention. Catheter Cardiovasc Interv 2007; 69:479-482

20. Motoyama S, Kondo T, Sarai M, et al. Multislice computed tomographic characteristics of coronary lesions in acute coronary syndromes. J Am Coll Cardiol 2007; 50:319-326
21. Berbarie RF, Dockery WD, Johnson KB, et al. Use of multislice computed tomographic coronary angiography for the diagnosis of anomalous coronary arteries. Am J Cardiol 2006; 98:402-406
22. Datta J, White CS, Gilkeson RC, et al. Anomalous coronary arteries in adults: depiction at multi-detector row CT angiography. Radiology 2005; 235:812-818
23. Lemos PA, Serruys PW, van Domburg RT, et al. Unrestricted utilization of sirolimus-eluting stents compared with conventional bare stent implantation in the "real world": the Rapamycin-Eluting Stent Evaluated At Rotterdam Cardiology Hospital (RESEARCH) registry. Circulation 2004; 109:190-195
24. Pflederer T, Ludwig J, Ropers D, et al. Measurement of coronary artery bifurcation angles by multidetector computed tomography. Invest Radiol 2006; 41:793-798
25. Van Mieghem CA, Thury A, Meijboom WB, et al. Detection and characterization of coronary bifurcation lesions with 64-slice computed tomography coronary angiography. Eur Heart J 2007; 28:1968-1976
26. Hermiller JB, Buller CE, Tenaglia AN, et al. Unrecognized left main coronary artery disease in patients undergoing interventional procedures. Am J Cardiol 1993; 71:173-176
27. Fisher LD, Judkins MP, Lesperance J, et al. Reproducibility of coronary arteriographic reading in the coronary artery surgery study (CASS). Cathet Cardiovasc Diagn 1982; 8:565-575
28. Christofferson RD, Lehmann KG, Martin GV, et al. Effect of chronic total coronary occlusion on treatment strategy. Am J Cardiol 2005; 95:1088-1091
29. Hoye A, van Domburg RT, Sonnenschein K, et al. Percutaneous coronary intervention for chronic total occlusions: the Thoraxcenter experience 1992-2002. Eur Heart J 2005; 26:2630-2636
30. Puma JA, Sketch MH, Jr., Tcheng JE, et al. Percutaneous revascularization of chronic coronary occlusions: an overview. J Am Coll Cardiol 1995; 26:1-11
31. Mollet NR, Hoye A, Lemos PA, et al. Value of preprocedure multislice computed tomographic coronary angiography to predict the outcome of percutaneous recanalization of chronic total occlusions. Am J Cardiol 2005; 95:240-243
32. Soon KH, Selvanayagam JB, Cox N, et al. Percutaneous revascularization of chronic total occlusions: review of the role of invasive and non-invasive imaging modalities. Int J Cardiol 2007; 116:1-6
33. Van Mieghem CA, van der Ent M, de Feyter PJ. Percutaneous coronary intervention for chronic total occlusions: value of preprocedural multislice CT guidance. Heart 2007; 93:1492
34. Garcia-Garcia HM, Van Mieghem CA, Gonzalo N, et al. Computed Tomography in Totally Occluded lesions (CTTO Registry): Focus on Conventional Angiography and Computed Tomography Angiography Predictors of Success and Radiation Exposure. J Am Coll Cardiol 2008; submitted
35. Ramcharitar S, Patterson MS, van Geuns RJ, et al. Technology Insight: magnetic navigation in coronary interventions. Nat Clin Pract Cardiovasc Med 2008; 5:148-156
36. Patterson MS, Schotten J, van Mieghem C, et al. Magnetic navigation in percutaneous coronary intervention. J Interv Cardiol 2006; 19:558-565
37. Atmakuri SR, Lev EI, Alviar C, et al. Initial experience with a magnetic navigation system for percutaneous coronary intervention in complex coronary artery lesions. J Am Coll Cardiol 2006; 47:515-521
38. Webb JG, Pasupati S, Humphries K, et al. Percutaneous transarterial aortic valve replacement in selected high-risk patients with aortic stenosis. Circulation 2007; 116:755-763
39. Grube E, Schuler G, Buellesfeld L, et al. Percutaneous aortic valve replacement for severe aortic stenosis in high-risk patients using the second- and current third-generation self-expanding CoreValve prosthesis: device success and 30-day clinical outcome. J Am Coll Cardiol 2007; 50:69-76
40. Lucas FL, DeLorenzo MA, Siewers AE, et al. Temporal trends in the utilization of diagnostic testing and treatments for cardiovascular disease in the United States, 1993-2001. Circulation 2006; 113:374-379
41. Redberg RF. Computed tomographic angiography: more than just a pretty picture? J Am Coll Cardiol 2007; 49:1827-1829
42. Hendel RC, Patel MR, Kramer CM, et al. ACCF/ACR/SCCT/SCMR/ASNC/NASCI/SCAI/SIR 2006 appropriateness criteria for cardiac computed tomography and cardiac magnetic resonance imaging: a

report of the American College of Cardiology Foundation Quality Strategic Directions Committee Appropriateness Criteria Working Group, American College of Radiology, Society of Cardiovascular Computed Tomography, Society for Cardiovascular Magnetic Resonance, American Society of Nuclear Cardiology, North American Society for Cardiac Imaging, Society for Cardiovascular Angiography and Interventions, and Society of Interventional Radiology. J Am Coll Cardiol 2006; 48:1475-1497
43. Goldstein JA, Gallagher MJ, O'Neill WW, et al. A randomized controlled trial of multi-slice coronary computed tomography for evaluation of acute chest pain. J Am Coll Cardiol 2007; 49:863-871
44. Leschka S, Wildermuth S, Boehm T, et al. Noninvasive coronary angiography with 64-section CT: effect of average heart rate and heart rate variability on image quality. Radiology 2006; 241:378-385
45. Brodoefel H, Reimann A, Burgstahler C, et al. Noninvasive coronary angiography using 64-slice spiral computed tomography in an unselected patient collective: Effect of heart rate, heart rate variability and coronary calcifications on image quality and diagnostic accuracy. Eur J Radiol 2007
46. Onuma Y, Tanabe K, Nakazawa G, et al. Noncardiac findings in cardiac imaging with multidetector computed tomography. J Am Coll Cardiol 2006; 48:402-406
47. Einstein AJ, Henzlova MJ, Rajagopalan S. Estimating risk of cancer associated with radiation exposure from 64-slice computed tomography coronary angiography. Jama 2007; 298:317-323
48. Hausleiter J, Meyer T, Hadamitzky M, et al. Radiation dose estimates from cardiac multislice computed tomography in daily practice: impact of different scanning protocols on effective dose estimates. Circulation 2006; 113:1305-1310
49. Husmann L, Valenta I, Gaemperli O, et al. Feasibility of low-dose coronary CT angiography: first experience with prospective ECG-gating. Eur Heart J 2008; 29:191-197
50. Budoff MJ, Achenbach S, Berman DS, et al. Task force 13: training in advanced cardiovascular imaging (computed tomography) endorsed by the American Society of Nuclear Cardiology, Society of Atherosclerosis Imaging and Prevention, Society for Cardiovascular Angiography and Interventions, and Society of Cardiovascular Computed Tomography. J Am Coll Cardiol 2008; 51:409-414
51. Schroeder S, Achenbach S, Bengel F, et al. Cardiac computed tomography: indications, applications, limitations, and training requirements: report of a Writing Group deployed by the Working Group Nuclear Cardiology and Cardiac CT of the European Society of Cardiology and the European Council of Nuclear Cardiology. Eur Heart J 2008; 29:531-556

THE INTEGRATION OF MULTISLICE COMPUTER TOMOGRAPHY WITH MAGNETIC NAVIGATION

Navigant® software facilitates Magnetically Assisted Percutaneous Interventions by directly co-integrating the Multi-Slice Computer Tomography Scan

EuroIntervention(in press)

Ramcharitar S, Pugliese F, van Geuns RJ, de Feyter PJ, Guiliguian D, Serruys PW

Description

Multi-slice computed tomography (MSCT) is a rapidly evolving technology in the field of coronary artery imaging(1). Current 64-slice MSCT allows the delineation of coronary lumen and the visualization of the plaque burden through the attenuation of soft-tissue contrast and its high sensitivity for vessel calcification(2). At present, this technology is utilized for its diagnostic potential. However, it is now possible to couple a MSCT scan with the Niobe® Magnetic Navigation System (MNS) through its dedicated software Navigant® (Stereotaxis, St Louis, MO, USA) and to use it for performing percutaneous coronary intervention (PCI)(3).

History

Magnetic navigation is a technology that allows the accurate guidance of a magnetically enabled guidewire through the use of external magnets that generate a precisely directed magnetic field. The coupling of this technology with MSCT was initially introduced in the Navigant® 2.10 software as an innovative approach to manage chronic total occlusions (CTOs)(4). It allowed the user to segment out the 3D rendered MSCT volume and to identify the diseased vessel by manually marking points on the vessel surface. This generated a pathway used as a baseline to produce directional magnetic vectors, tangent to the pathway at the point where the guide-wire magnetic tip is placed.

With the recent upgrade to Navigant® 2.11, a segmented MSCT volume that only shows the coronary tree (Siemens Medical Solutions, Forchheim, Germany) can be imported into the software. The pathway of the diseased coronary arteries can automatically be traced, even through CTOs. The interventional cardiologist can hence request magnetic vectors that truly correspond to the patient anatomy. In addition, the operator has access to the endoluminal view (5) that simulates looking through the vessel lumen and simultaneously to the corresponding Multi-Planar Reconstruction (MPR) slice, as well as an automated update of the magnetic vector as the wire is advanced. In this technical report we have illustrated the first use of this innovation - in a complex patient with triple-vessel disease.

Technical specifications

Pathway Planning and Crossing

This is done in three steps:

1. Extraction of the coronary tree from the raw MSCT DICOM dataset (Siemens)
2. Automatic vessel centerline computation (Stereotaxis)
3. Sequenced magnetic guidewire navigation (Stereotaxis)

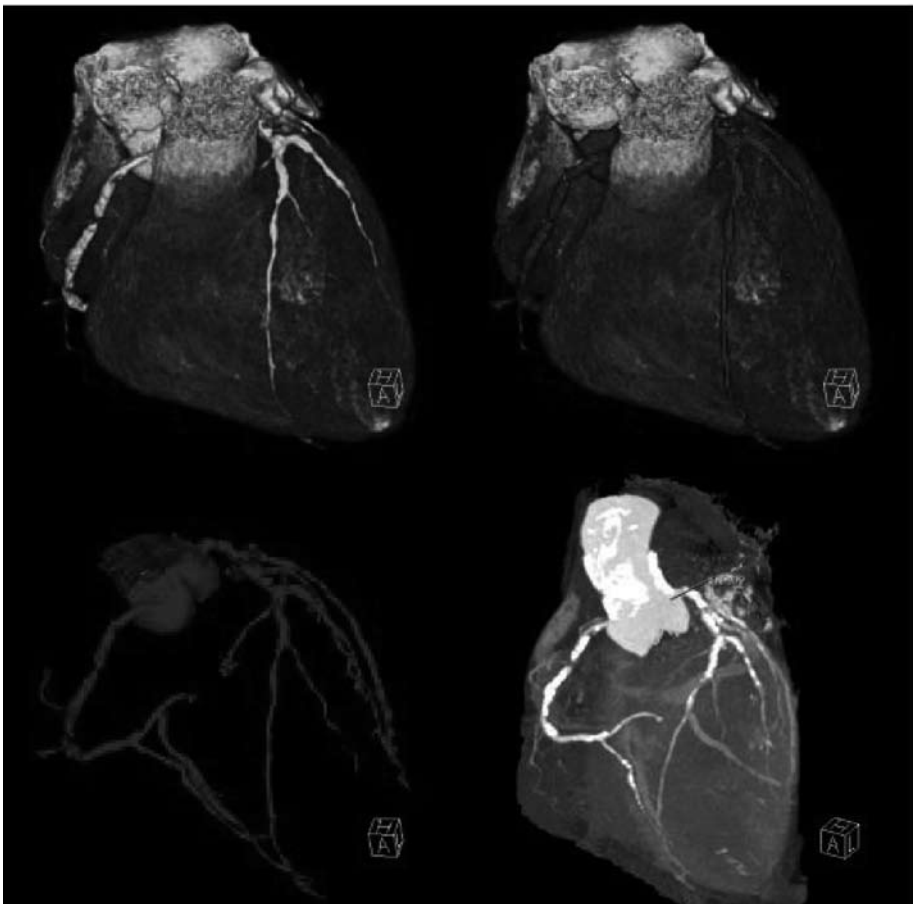

Figure 1 *Volume-rendered MSCT image with coronary segmentation is displayed in blue with vessel calcification shown in bottom right image*

Coronary Tree Extraction

The Siemens Circulation™ (Circulation, version syngo CT 2007A, Siemens, Forchheim, Erlangen, Germany) allows the identification of the coronary tree from an MSCT angiogram (Figure 1). The package then performs a semi-automatic segmentation of the coronary tree based on a single seed point. This post-processing of the DICOM dataset can be imported into the Navigant® 2.11 software.

Pathway Planning

Once the coronary tree is imported into Navigant® 2.11, the user assesses the diseased vessels and asks the software to compute their centerlines: the trajectory in the middle of each vessel. This results in a pathway based on which the magnetic field – critical for directing the guide-wire tip – will be generated. The magnetic vector will be tangent to the point in the vessel

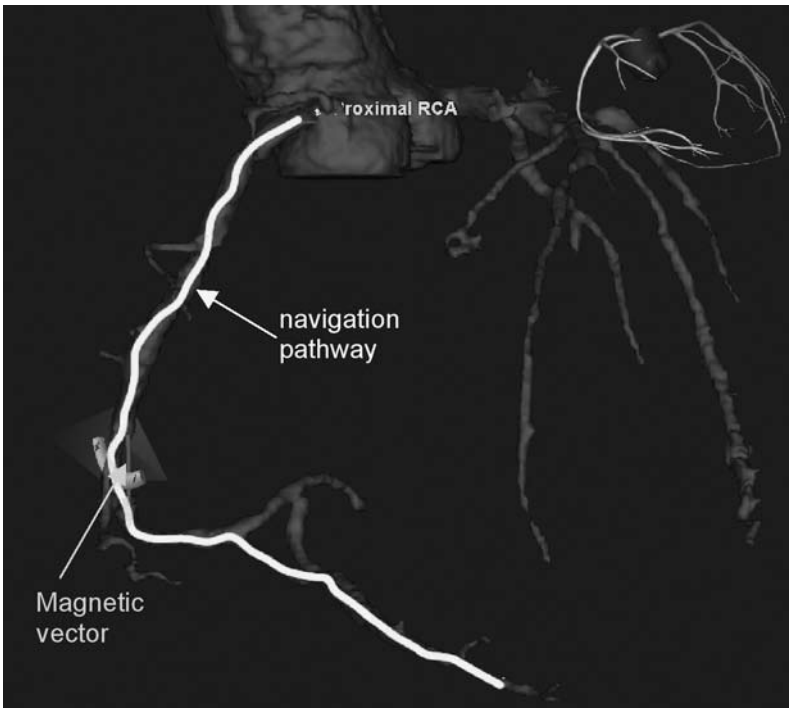

Figure 2 *Coronary tree with the automatically computed pathway and the tangent magnetic vector*

where the operator has chosen to navigate. It therefore defines the instantaneous advancement direction (Figure 2). In addition to this, Navigant® 2.11 uses the data from the MSCT to generate an endoluminal view and an MPR slice. Hence, the interventionalist is provided with a forward-looking representation of the inside walls of the diseased coronaries. At the same time, the Hounsfield map of the transversal MPR slice is shown.

Magnetic Navigation

The navigation is performed after co-registration of the MSCT to two Xray images that are at least 30° apart and aligning the centerline/navigational path to the live fluoroscopy image. At each position along the navigational path all three corresponding magnetic vector, endoluminal view and MPR slice can be shown on a touch screen monitor. A novel feature that is unique to Navigant® 2.11 is that after registering a magnetic wire the physician is able to choose a step size (1 to 9mm) and a so-called sequencing rate (1 to 60sec) for the vector to automatically update along the vessel. This means that the operator can fully concentrate on the wire advancement guided by the moving vectors on the live fluoroscopy image (Figure 3). As the vector is sequentially updated so too are the MPR slices together with the endoluminal views.

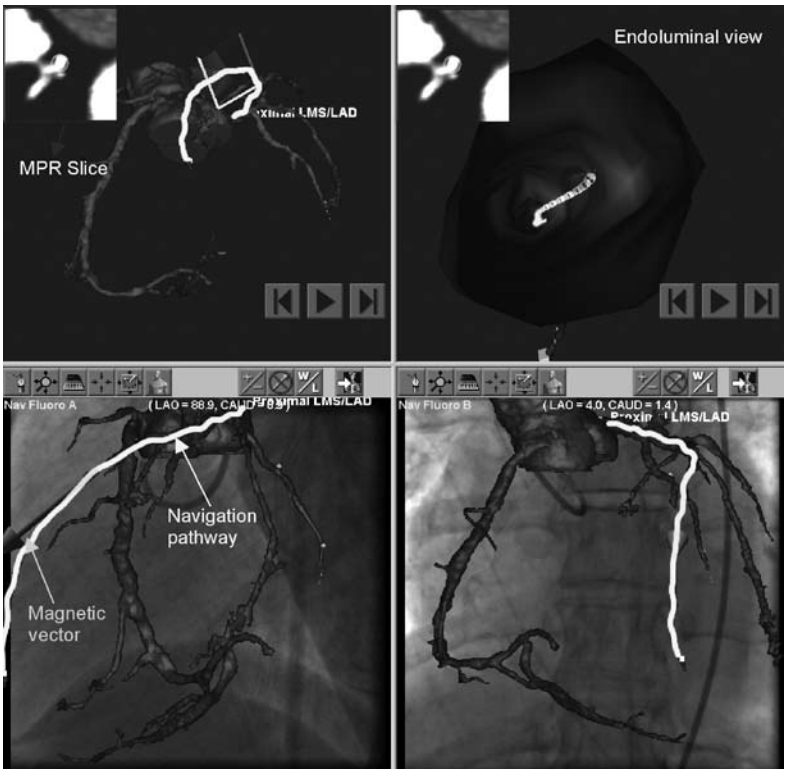

Figure 3 *Navigation and tools for the operator*

This automated sequencing can however be temporarily stopped at any desired time (Figure 4)

Clinical experience

The Case

A 56-year old diabetic woman presented unstable angina. Angiography performed at her referring hospital revealed significant three-vessel disease (Figure 5 a-c). Lesions were identified in the proximal segments of both the right coronary artery (RCA) and the left anterior descent (LAD) as well as diffuse disease in the obtuse marginal (MO). Percutaneous Coronary Intervention was planned following a clinical consultation with our surgical colleagues. Standard six French catheters (4.0 Judkins Right and 3.5 CLS) were used to facilitate the MSCT guided Magnetic Assisted Intervention (MAI). The procedure of integrating the MSCT in Navigant® 2.11 (Pathway Planning) and crossing the lesion is detailed above.

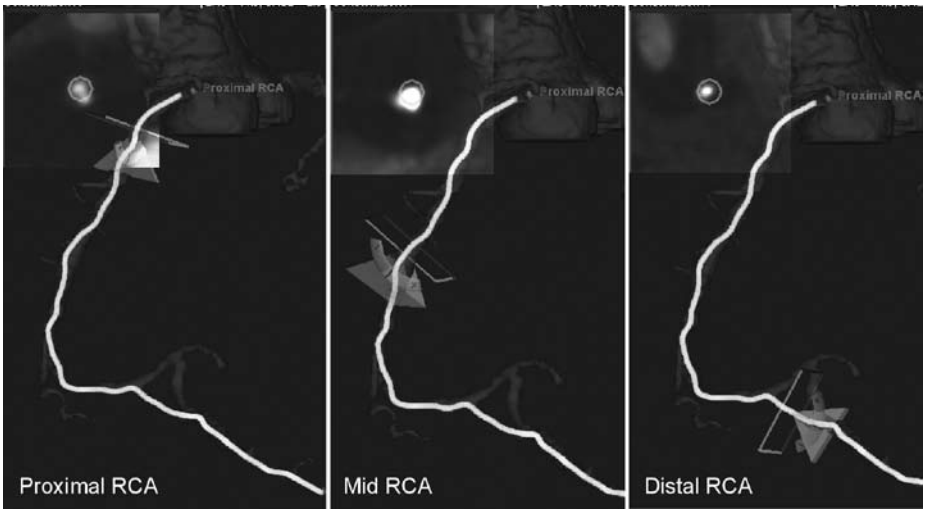

Figure 4 *Automated vessel sequencing MPR slices upper left quadrant*

Clinical Outcome

Using the approach of automated wire advancement, the proximal lesion in the RCA was crossed with a Titan 3mm straight tip magnetic wire in 30 seconds with minimal contrast (8ml). The lesion was predilated with a Voyager 2.5x20mm balloon at 8 atmospheres following which a Xience™ V stent (2.5x20mm) was implanted at 20 atmospheres. A similar magnetic wire was used to cross the lesions in the MO (20sec, 2ml contrast) and in the LAD (20sec, 2ml contrast) to permit the direct implantation of Xience™ V stents (2.5x15mm and 3.5x15mm) respectively. There was TIMI 3 flow in all three coronary arteries on angiography (Figure 5d-e) and she was discharged home after an uncomplicated 48h stay in hospital. She is requested to continue dual anti-platelet medication for one year.

Discussion

The MNS allows a full omni directional (360º) movement of a 2-3mm Neodymium magnet attached to the tip of a 0.014mm guide wire. Magnetic vectors created in Navigant® precisely control this movement so as to follow a 3-dimensional navigational path or road map of the coronary artery. The use of MSCT to create such a road map not only gives useful information about the plaque composition and eccentricity but more importantly it enables the direct visualization of occluded segments in a CTO. It is reported that the success in treating CTO can depend not only on the length of the occlusion but also on the amount of calcium within the occlusion. As such, the ability to directly visualize the MPR slices whilst simultaneously being aligned to the position of the vector that guides the wire is an extremely useful tool. This paper describes the first ever PCI where an interventionalist can visualize exactly what is being

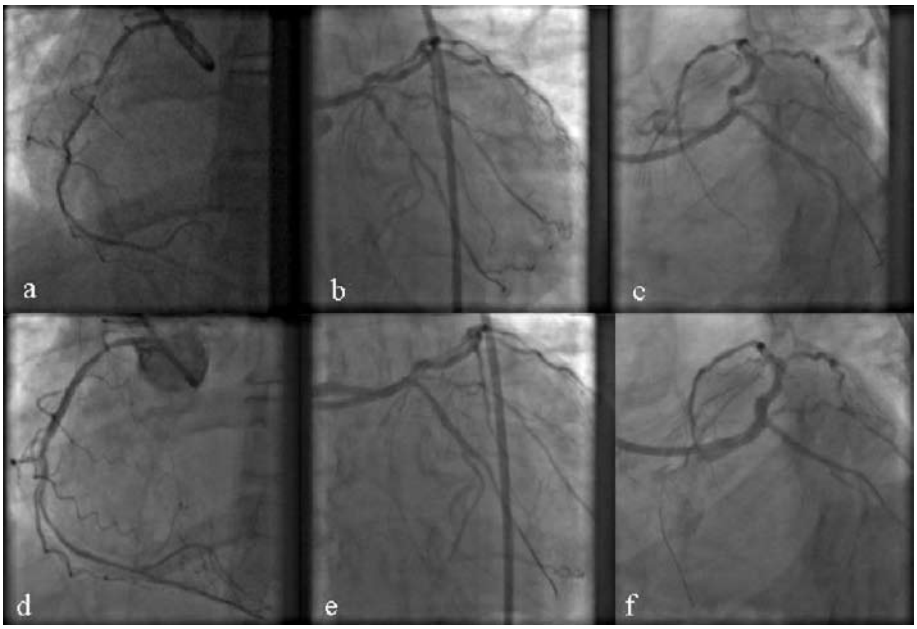

Figure 5 *Angiographic views of the three diseased vessels pre- (a-c) and post (d-f) treatment*

encountered ahead of a guidewire. The link with MNS gives the wire the ability to steer around eccentric plaque as highlighted in this case or to channel microvessels within an occlusion. It is worth pointing out that the endoluminal view is a display tool and the vectors generated are the same with or without this additional feature. However, by manually adjusting the vector to take into account subtle changes in the vascular anatomy while looking in the endoluminal view can offer a higher degree of navigational accuracy. The overall complexity of the case demonstrates that MAI is safe and feasible in patients with multi-vessel disease.

Conclusion

The incorporation of MSCT extracted coronary arteries in Navigant® 2.11 provide an innovative approach to facilitate PCI with its potential advantages of visualizing the MPR slice, the endoluminal view and automated segmental vector advancement.

References

1. Van Mieghem CA, Cademartiri F, Mollet NR, Malagutti P, Valgimigli M, Meijboom WB, Pugliese F, McFadden EP, Ligthart J, Runza G and others. Multislice spiral computed tomography for the evaluation of stent patency after left main coronary artery stenting: a comparison with conventional coronary angiography and intravascular ultrasound. Circulation 2006;114(7):645-53.
2. Sanz J, Dellegrottaglie S, Fuster V, Rajagopalan S. Calcium scoring and contrast-enhanced CT angiography. Curr Mol Med 2006;6(5):525-39.
3. Patterson MS, Schotten J, van Mieghem C, Kiemeneij F, Serruys PW. Magnetic navigation in percutaneous coronary intervention. J Interv Cardiol 2006;19(6):558-65.
4. Garcia-Garcia HM, Tsuchida K, van Mieghem C, Daemen J, van Weenen S, Patterson M, van der Ent M, van der Giessen WJ, Meulenbrug H, Sehra R and others. Multi-slice computed tomography and magnetic navigation-initial experience of cutting edge new technology in the treatment of chronic total occlusions. Eurointervention 2007.
5. Patterson M, Tanimoto S, Tsuchida K, Serruys PW.. Magnetic Navigation with the Endo-Luminal View and the X-ray overlay - Major advances in novel technology. Eurointervention 2007;in press.

THE INTEGRATION OF MULTISLICE COMPUTER TOMOGRAPHY WITH MAGNETIC NAVIGATION

Integration of Multislice Computer Tomography with Magnetic Navigation facilitates Percutaneous Coronary Interventions without contrast agents – A proof of concept

Submitted

Ramcharitar S, Pugliese F, Schultz C, Ligthart J, de Feyter P. J., Li, H., Mollet N., vd Ent M, Serruys P.W.J.C., van Geuns. R.J.M.

Abstract

Introduction:
We investigated invasive percutaneous coronary investigations and interventions based directly on multislice computer tomography coronary angiography (CTCA) integration into the magnetic navigation system (MNS) to avoid using contrast agents during the procedure.

Methods:
Fifteen patients scheduled for invasive investigation with an intention to treat were included. Based on diagnostic non-invasive workup CTCA centerlines of the target vessels were created, co-registered and overlaid on real-time fluoroscopic images. Using a guidewire with a magnetic tip the vessels were manually wired with the assistance of variable local magnetic fields. The severity of the lesion was determined by fractional flow reserve (FFR) or intravascular ultrasound (IVUS) with stent sizing determined by IVUS measurements. Locations of IVUS catheter along the lesion were incorporated in software to facilitate stenting without contrast agents.

Results:
Using magnetically enabled wires the lesions were crossed in 105.3±35.5sec with an average fluoroscopic time of 83.4±38.6sec. In 11 of the 15 patients no contrast agents were used in crossing the target vessel. In all cases FFR or IVUS measurements were successfully used to identify the culprit lesion. Out of 10 patients in whom an IVUS was performed only in one patient was any contrast agent needed. In 4 patients the complete percutaneous intervention (lesion crossing, stent sizing, positioning and deployment) was performed following subsequent co-registration of the IVUS probe position in the MNS.

Conclusion:
The integration of pre-procedural CTCA within the MNS allowed percutaneous coronary investigations and interventions (stenting) without using contrast agents.

Introduction

The number of percutaneous coronary artery interventions (PCI) has steadily increased ever since Gruentzig performed the first angioplasty in 1975[1]. Improved interventional devices supported by novel pharmacological agents together with an understanding of the pathogenesis of atherosclerosis have established both the safety and efficacy of PCI in numerous clinical settings. This has resulted in widespread adoption with more than 2 million procedures performed annually worldwide[2]. But despite these major advances the general method of performing a PCI has remained unchanged for over a quarter of a century, relying primarily on the manual dexterity of the operator and the use of radiographic X-rays with selective injections of potentially harmful contrast agents into the coronary arteries to visualize the anatomy and guide appropriate stent placement. But there are several limitations with such an approach since representing 3-dimensional (3-D) information with a 2-D X-ray lumenogram leads to inaccuracies in lesion evaluation and subsequent stent sizing. This is because vessel foreshortening and overlap can hinder the full lesion characterization while plaque eccentricity can lead to inaccurate luminal measurements.

For diagnostic purposes contrast enhanced multislice computer tomography coronary angiography (CTCA) has achieved a quality standard nearly comparable to invasive selective coronary angiography (CAG) for initial lesion evaluation provided that the amount of calcium in the arterial wall is low[3]. This has led to a sharp increase in the number of CTCA performed within the last few years primarily as a screening tool to rule out significant coronary artery disease (CAD)[4]. Therefore we feel that in the not too distant future most elective PCI patients will have a CTCA at some point in their diagnostic work-up. This is because, in addition to being non-invasive, CTCA provides important information on the extent of the atherosclerotic plaque and provides unique 3-D information of the nature of coronary arterial tree, which can serve as a tentative roadmap to guide a PCI procedure. Moreover, recent technological advancements has allowed a visible static 3-D road map (a centerline) of the CTCA dataset to be superimposed on the live fluoroscopic. This can be used to precisely direct magnetically enabled guidewires in the coronary artery when incorporated within the Magnetic Navigation System (MNS)[5]. The system has the ability to change the direction of tip of the wire without the need for externally reshaping[6]. By integrating both systems it means therefore, that a further contrast filled lumenogram at the start of the procedure can be effectively skipped so reduce the amount of contrast needed for the procedure. Furthermore, the notable inaccuracies of 2-D lumenography can be avoided by functionally characterizing the lesion with fractional flow reserve (FFR) and by using intravascular ultrasound (IVUS) measurements to choose the appropriate stent length[7]. Our aim therefore was to demonstrate that following such a strategy - PCI without contrast media could be feasible provided that CTCA and IVUS information could be effectively integrated within the MNS (Figure 1).

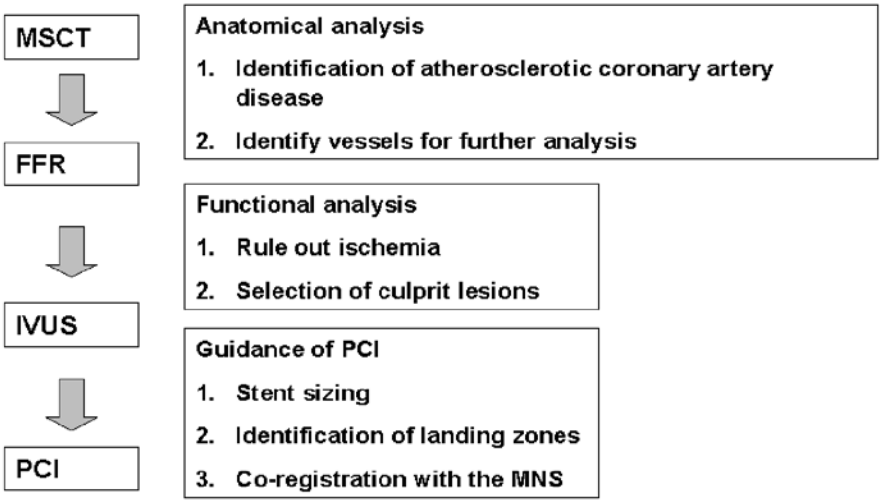

Figure 1 *The Concept of performing a non-contrast PCI from a pre-procedural CTCA*

Methods

Patients

To investigate the feasibility of this concept, CTCA was initially performed on 5 patients with single vessel disease diagnosed on coronary angiograms undertaken at referring hospitals. Following this initial evaluation phase, 10 additional patients with more complex multivessel disease where recruited in whom a CTCA was performed in accordance with local clinical protocols. All 15 patients included in the study were subsequently scheduled for Magnetic Assisted Intervention (MAI) using the Niobe® II magnetic navigation system (Stereotaxis, St. Louis, M. USA). During the PCI procedure indeterminate lesions seen on CTCA were further characterized by IVUS or FFR measurements[8]. Patients were excluded if they were haemodynamically unstable, presented with an acute infarction or an acute coronary syndrome or had contraindications for a MAI such as a pacemaker or Intracardiac Defibrillator (ICD). Other exclusion criteria were left main or ostial right coronary artery disease, significant amount of calcium on CTCA or if the patient had other medical condition preventing a prolonged PCI procedure. The institutional review board approved the study. All patients were consented to undergo the CTCA studies prior to conventional coronary angiography.

Computer Tomography Coronary Angiography Acquisition

CTCA was performed using the newest generation dual source 64-slice CT scanner (Somatom Sensation 64 Cardiac Configuration Siemens, Erlangen, Germany). Images were reconstructed

by using a monosegmental electrocardiographically gated reconstruction algorithm[9]. One experienced observer interpreted the lesion on the CTCA in accordance to the conventional coronary angiogram algorithm used in the 17-segment modified American Heart Association classification model[10]. This was performed off-line (Leonardo VB30A; Siemens) with the images visually classified for the presence of significant stenosis using both the multiplanar reconstruction and curved multiplanar reconstruction. Blood vessels with diameters of 2 mm or larger were considered significant because of their clinical relevance and because they are amenable to revascularization.

Magnetic Guidewire Navigation using CTCA co-integration

Magnetic navigation was achieved through two permanent external magnet situated at either side of the operating table capable of generating a 0.08 Tesla magnetic field to accurately redirect a tiny 2 or 3mm long magnet at the tip of the guidewire (Titan™, Stereotaxis, St. Louis, M. USA). In our laboratory, the Niobe® II the system is integrated with a modified C-arm flat-panel detector-fluoroscopic imaging suite (AXIOM Artis dFC, Siemens Medical Solutions, Forchheim, Germany) for angiographic imaging. Before the start of a procedure the CTCA - DICOM images were uploaded into a MNS dedicated guidance software called Navigant®. These images were create using the Leonardo Circulation post-processing software (Siemens Medical Solutions, Forchheim, Germany) Figure 2A. A minimal cost algorithm was used to create a navigational pathway through the extracted vessels Figure 2B which was co-registered to the live fluoroscopic image. This was achieved by firstly recording two orthogonal non-contrast filled images of the guiding catheter tip during suspended breathing after engaging the ostium of either the left or right coronary artery. On these images the tip of the catheter in end diastole was identified as a registration point in the three dimensional space. Using this point and software that prompts the identical point on the extracted CTCA coronary arteries the dataset were aligned and co-registered to the actual position of the patient Figure 2C. From this moment onwards the centerlines/navigational pathway from the CTCA could be overlaid on every live fluoroscopic image in any desired orientation. Along the entire length of this centreline/navigational pathway Navigant® created navigational vectors to instruct the two large external permanent magnets to rotate, tilt and translate about their axes to redirect a 0.08Tesla external magnetic field Figure 2D. The navigational vectors associated with this centreline were automatically updated at a predetermined distance (1-9mm) every second and when correctly positioned the operator manually advanced the guidewire. By continuously repeating this process of wire steering through automated vector updates and manual wire advancement the magnetically enabled guidewire was allowed to cross the lesion and be advanced distally along the vessel using minimal or no contrast agents.

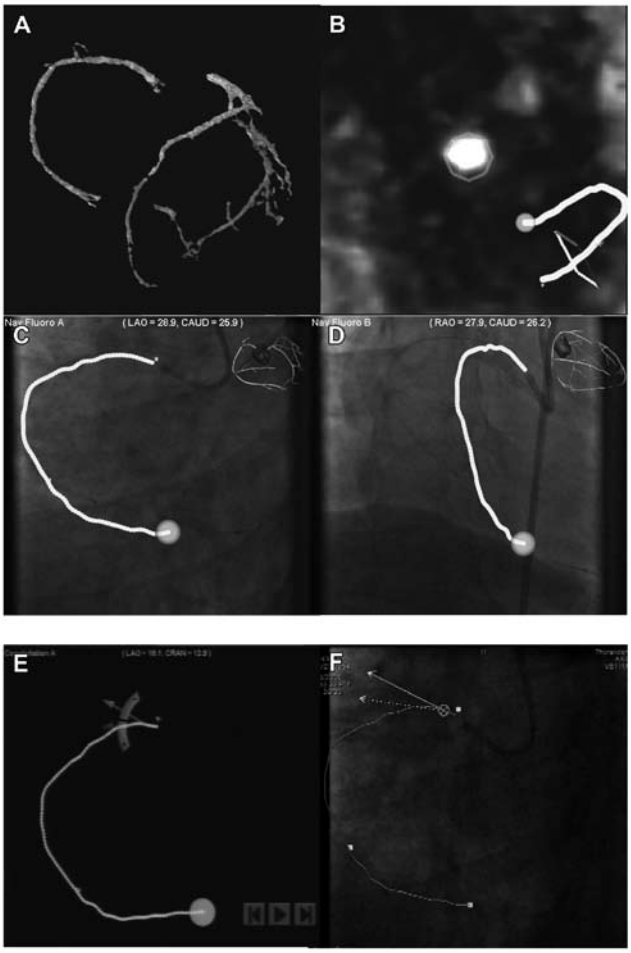

Figure 2 *A) Extracted coronaries arteries from the CTCA dataset to be introduced directly into the MNS; B) slice through a navigational pathway (depicted by yellow line) simultaneously showing the corresponding MPR cross-section at that position; C and D) Co-registration of the navigational pathway to the guiding catheter in two orthogonal planes; E) the navigational pathway with a directional vector and F) it being displayed on the live fluoroscopic image*

Fractional Flow Reserve Analysis

Fractional flow reserve (FFR) was measured with a sensor-tipped 0.014-inch angioplasty guidewire (WaveWire/WaveMap, Volcano Therapeutics, Inc, Rancho Cordova, CA or PressureWire, Radi Medical Systems, Uppsala, Sweden). After crossing the target lesion a two lumen multifunctional probing catheter (Boston Scientific, Corporation, Santa Clara, CA) was used to replace the magnetic wire with the pressure wire. Hyperaemia was induced by intravenously infusing 120µg/min adenosine (Adrecar, Sanofi, Munich, Germany). The maximum pressure gradient was used to calculate the FFR, which was defined as the ratio of the mean post-stenotic pressure to the

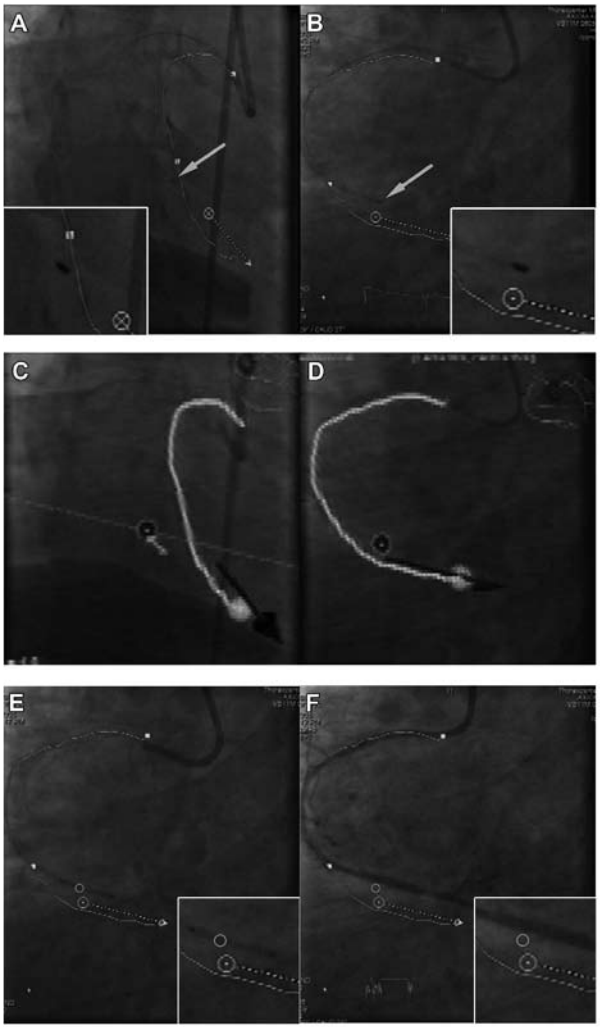

Figure 3 *A and B) Radiographic recordings of two orthogonal images IVUS probe positioned in the middle of the lesion and C and D) these two points co-registered as a new reference point (green circle) in the 3D space of Navigant®; E) the overlay of the location of this point (open white circle) on the live fluoroscopic was used to position the stent on the middle of the lesion; F) The stent being deployed following a single "safety check" angiogram.*

mean aortic pressure, measured by the guiding catheter, during maximal hyperaemia. A FFR of ≥0.75 was considered functionally not significant.

Intravascular Ultrasound Analysis

IVUS was performed using CVIS Atlantis™ SR Pro 2.5F 40-MHz catheter (Boston Scientific Corporation, Santa Clara, CA) with an automated pullback device (0.5 mm/sec) after the lesion was crossed with the magnetically enabled wire. All measurements were made off-line at end

diastole following intracoronary administration of isosorbide dinitrate. These measurements included the minimum luminal and proximal reference diameters. Reference vessel measurements were made before a major branch in the least diseased section. Stent apposition was visually assessed with incomplete apposition defined as at least one stent strut not apposed to the vessel wall, with clear blood flow behind it.

Performing an entire PCI procedure without contrast

This was achieved following appropriate stent sizing. The IVUS catheter was re-advanced to the distal landing zone as visible on tip of IVUS catheter and the position of the piezoelectric crystal recorded on two different angiographic projections (Figure 3A and B) to locate it within the 3 dimensional space of the Navigant® (Figure 3C). These angiographic images were uploaded into the Navigant® and the position of this point identified as an additional overlay point on the live fluoroscopic navigational centerline derived from the CTCA (Figure 3D). The stent was then advanced to this new point on the live fluoroscopic overlay and deployed without using any contrast agent (Figure 3E) apart from a protocol driven safety check for placement accuracy.

The accuracy of placement

Although the study was designed to test the feasibility of PCI without contrast agents a measure of safety was introduced in the protocol by the co-operator. As such, after positioning of the stent using the overlay a short angiographic film was taken to check the position. If this position was ideal no correction was undertaken and the stent deployed. If this was adjudged as being incorrectly positioned then the co-operator made the necessary readjustments prior to deployment. The film was also used for ACC/AHA lesion characterization.

Assessment of lesion lengths and reference diameters by IVUS and CTCA

The assessment of IVUS and CTCA measurements was performed off-line and independently by an IVUS trained technician and a radiologist experienced in interpreting CTCA data. The lesion length, the MLD, proximal diameter stenosis (DS) and the % DS were analyzed. The absolute differences were calculated by the numerical summation of the over and underestimated values relative to both techniques.

Statistical Analysis

Continuous variables are presented as mean ± standard deviation. Student T-test was used to determine if there were significant differences between the parameters assessed. Analyses were performed using SPSS 11.5 for Windows (SPSS, Chicago, IL). *P* value < 0.05 was considered statistically significant.

Results

Assessment of lesion with FFR and IVUS measurements

In all 15 patients the magnet wire was successfully navigated using a CTCA derived overlay. The average contrast media usage of 0.5ml, with an average crossing and fluoroscopic time of 105.3±35.5sec and 83.4±38.6sec respectively. Notably in 11 of the 15 patients no contrast agent was used in crossing the target vessel Table 1. The largest volume of contrast needed was 3mls in a patient who was enrolled in the initial phase. In this particular case the contrast agent was needed to reenter the main vessel following advancement of the magnetic wire in a small side branch almost parallel to the main branch. No contrast agent was needed in 5 out of the 8 patients where FFR measurements were made. Moreover only in one patient was contrast agent used amongst the 10 patients in whom IVUS measurements were performed. In the first phase (patient 1-5) one patient with a negative FFR (0.87) had the entire procedure performed without an additional lumenogram with a control angiogram only done at the very end for safety control and documentation. The four other patients in this first series underwent stenting with conventional PCI techniques.

In the second phase multivessel FFR was used to identify the culprit lesion/vessel since exercise ECG testing confirmed ischemia but no conclusive localization could be made (patients 6-8). Out of the six vessels assessed, three were found to have functionally significant disease and were subsequently treated. Furthermore, in three additional cases, lesions characterized by FFR had IVUS performed to accurately determine the stent size and length (patient 9-11) without needing further contrast agents. The average stent length in these patients was found to be 17.6mm with an average diameter of 3.3mm.

Complete PCI without additional contrast agents

In the last four patients the entire PCI procedure from lesion crossing to stent sizing, positioning and deployment was performed without additional contrast agents relying exclusively on CTCA datasets and IVUS measurements incorporated in the Navigant®. It should be noted that in only one of these cases following a check angiogram to determine the accuracy for placement did the co-operator required performing a 2mm adjustment in stent repositioning. After stent deployment repeat IVUS measurements demonstrated satisfactory stent apposition and no post dilatation was performed. In one case IVUS did reveal a type A distal edge dissection not visible at control angiography. No additional stent placement was necessary. In keeping with the hospital's angiographic recording policy the final results were documented using two different angiographic views. These control angiograms showed no additional abnormalities in all 15 patients.

Table 1 Vessels and lesions characterized by FFR and IVUS. Stent dimensions and deployment performed without contrast agents (patients 9-15); LAD, left anterior descending, LCx, Left circumflex, IM, intermediate and RCA, right coronary arteries

Patient	Gender	Age	Vessel	Procedure	Contrast/ ml	Crossing/sec Fluoro/time	Lesion Type
1	Female	56	LAD	IVUS	1	110/53	B1
2	Male	67	IM	IVUS	0	123/121	A
3	Male	56	RCA	IVUS	0	71/67	B1
4	Male	61	LCX	FFR No PCI	3	136/111	B1
5	Male	69	LCX	FFR	0	89/87	B1
6	Male	72	LAD + RCA	FFR both + PCI LAD	0	136/123	B1
7	Male	78	LAD + LCX	FFR both + PCI LAD	1	93/84	B1
8	Female	74	LAD + LCX	FFR both + PCI LCX	2	84/71	A
9	Male	61	LAD	FFR+IVUS chose stent	0	64/63	A
10	Female	56	LAD	FFR+IVUS chose stent	0	130/100	A
11	Male	67	LCX	FFR+IVUS chose stent	0	92/84	B1
12	Male	58	LCX	IVUS + place stent	0†	104/98	B1
13	Male	73	LCX	IVUS + place stent	0	200/165	B1
14	Male	66	LAD	IVUS + place stent	0	105/87	A
15	Female	53	RCA	IVUS + place stent	0	42/42	A

Analysis of IVUS and CTCA measurements

The off-line analysis of the IVUS and CTCA revealed that although longer lesion lengths were determined by CTCA measurements (19.2±13.3mm vs. 14.5±5.6mm) overall the difference was non-significant, p = 0.19 (Table 2). There was little differences observed in measuring the MLD and %DS. However, a significant difference was recorded with the proximal reference diameter measurements 3.6±0.6mm vs. 4.2±0.8mm p=0.05) which was overall smaller with CTCA. In terms of the absolute difference CTCA measurements would have resulted in one stent size smaller (absolute difference = 0.8mm) and longer (absolute difference = 6.6mm) than that determined through IVUS analysis.

Table 2 Analysis of lesion dimensions with CTCA and IVUS

	CTCA (n = 10) Mean ± SD	IVUS (n = 10) Mean ± SD	Absolute Difference	Student's t-Test
Lesion length/mm	19.2±13.3	14.5±5.6	6.6mm	0.19
Minimum Luminal Diameter/mm	1.5±0.8	1.4±0.3	0.6mm	0.87
Proximal. Reference Diameter/mm	3.6±0.6	4.2±0.8	0.8mm	0.05
% Diameter Stenosis	62.4±19	64.9±9.1	16.9%	0.71

Discussion

In this paper we described a new concept for non-contrast agent driven percutaneous coronary investigation and subsequent intervention. By integrating a diagnostic CTCA which is increasingly used as a screening tool for CAD [11] with the MNS it was possible at a later date to guide magnetically enable wires safely though a lesion without contrast agent. Moreover lesions were functionally characterized without contrast agents when the magnetic wire was exchanged with FFR wires. Although reduction of contrast agent usage is important because of its associated nephrotoxicity, this is the first reported study to demonstrate the extension of pre-procedural 3-D information to directly guide a PCI procedure. The MNS has recently been shown to incorporate 3D information to cross the target vessel[12]. But in this study the reduction in contrast agent was relatively small (2-7 ml) over conventional wire PCI approaches and does not affect significantly the total amount of contrast agents necessary to the complete procedure. This is because large amounts of contrast agents are needed for the initial angiographic assessment of the lesion, stent/balloon sizing, stent positioning and deployment.

It is generally believed that CTCA is predicted to supersede diagnostic CAG in patients without a history of PCI or previous bypass surgery[13]. Presently radiation dose exposure is more than diagnostic CAG and it is hopeful that the faster CTCA systems in development with increased spatial resolution and single heart beat imaging will address this limitation[14]. Nevertheless with the satisfactory image quality obtained with the modern 64-slice scanners it seems illogical to start a PCI procedure with an additional lumenogram that exposes the patient to more radiation and more contrast agents[15]. This is particularly so in light of the well recognized limitations of conventional angiography in lesion characterization (plaque eccentricity, vessel foreshortening) and the trial and error approach in determining the best angiographic views for stent deployment[16]. It is not surprising therefore the potential advantages in using the CTCA dataset to guide a PCI procedure are attractive. But as a word of caution, CTCA is currently insufficient to guide the actual stent selection and placement due to its limited spatial resolution[4]. This was

apparent in our study where stent selection based on CTCA alone would have recommended one stent length longer and having smaller diameters. Consequently, the incorporation of an intermediate step using IVUS was crucial in accurately determining the appropriate stent dimension [17].

We choose to use an FFR guided strategy to characterize the lesion because evaluating coronary stenosis with CTCA alone does not provide additional relevant functional diagnostic information[18]. Moreover, FFR guided therapy in multivessel disease has been proven to be a successful strategy in reducing the number of stents implanted so is cost effective[19]. In addition, in our patients where multivessel disease was identified on CTCA, 50% of the lesions were effectively ruled out by FFR measures without subjecting the patients to more contrast agents.

The novelty of stent placement without contrast is based on an identifiable positioning of reference point along a navigational centerline derived from CTCA. But currently there is a limitation with this methodology because the navigational pathway is derived for only one cardiac phase. In the future however, with increased computation power and algorithms to provide an electrocardiography (ECG) gated CTCA centerline superimposed on the live fluoroscopy image such a limitation might be overcome. But also needing consideration will be the patient voluntary movements and those linked with respiration, which may be more difficult to control. Already some compensation can be achieved through respiratory/movement sensors located on the sternum/diaphragm that adjust the centerline to the live radiographic image accordingly[20]. With newer technologies such as those based on a 'GPS-like' navigational system to accurately locate the catheter/wire position within the coronary tree many these movement artifacts may be eventually be eradicated[21]. When such a system is introduced within a magnetically enabled wire then more accurate positioning following the CTCA derived navigational centerline will be possible and this will pave the way for the truly remote non-contrast PCI procedure in the future.

Limitations

This was study to evaluate the concept of stenting without contrast agent so the patient population was small. Selection was not based on particular patient demographics, but rather on the availability of the 64-slice CT scanner for the examination of cardiac patients. The study was not designed to directly compare the precision and accuracy of CTCA and IVUS, which has been validated by several groups, but purely to describe our finding with the parameters assessed[4]. Integration of the CTCA in the MNS was time consuming and can take up to 30mins prior to starting the PCI procedure. Apart from the check angiogram prior to stent deployment a final film was required for documentation. Therefore to be truly independent of contrast agents a validation study base solely on 3 D imaging techniques (such as 3D-IVUS) may be required.

Conclusions

Although percutaneous coronary intervention has revolutionized the management of coronary artery disease the general methodology has remained unchanged ever since the work of the early pioneers. In this concept paper we have shown that by merging modern imaging technologies in particular CTCA with the ability to use a magnetic field to precisely guide a wire within the coronaries, the potential exist to radically change this process. The integration of pre-procedural 3-D information and intravascular ultrasound in the magnetic navigation system allowed PCI without the use of contrast agents with optimal results.

References

1. Serruys PW. Fourth annual American College of Cardiology international lecture: a journey in the interventional field. *J Am Coll Cardiol* 2006;47:1754-68.
2. Serruys PW, Kutryk MJ, Ong AT. Coronary-artery stents. *N Engl J Med* 2006;354:483-95.
3. Nieman K, Oudkerk M, Rensing BJ, van Ooijen P, Munne A, van Geuns RJ, de Feyter PJ. Coronary angiography with multi-slice computed tomography. *Lancet* 2001;357:599-603.
4. Bruining N, Roelandt JR, Palumbo A, La Grutta L, Cademartiri F, de Feijter PJ, Mollet N, van Domburg RT, Serruys PW, Hamers R. Reproducible coronary plaque quantification by multislice computed tomography. *Catheter Cardiovasc Interv* 2007;69:857-65.
5. Ramcharitar S, Patterson MS, van Geuns RJ, van Meighem C, Serruys PW. Technology Insight: magnetic navigation in coronary interventions. *Nat Clin Pract Cardiovasc Med* 2008;5:148-56.
6. Ramcharitar S, Patterson MS, van Geuns RJ, van der Ent M, Sianos G, Welten GM, van Domburg RT, Serruys PW. A randomised controlled study comparing conventional and magnetic guidewires in a two-dimensional branching tortuous phantom simulating angulated coronary vessels. *Catheter Cardiovasc Interv* 2007;70:662-8.
7. Hanekamp CE, Koolen JJ, Pijls NH, Michels HR, Bonnier HJ. Comparison of quantitative coronary angiography, intravascular ultrasound, and coronary pressure measurement to assess optimum stent deployment. *Circulation* 1999;99:1015-21.
8. Fearon WF, Luna J, Samady H, Powers ER, Feldman T, Dib N, Tuzcu EM, Cleman MW, Chou TM, Cohen DJ, Ragosta M, Takagi A, Jeremias A, Fitzgerald PJ, Yeung AC, Kern MJ, Yock PG. Fractional flow reserve compared with intravascular ultrasound guidance for optimizing stent deployment. *Circulation* 2001;104:1917-22.
9. Pugliese F, Mollet NR, Hunink MG, Cademartiri F, Nieman K, van Domburg RT, Meijboom WB, Van Mieghem C, Weustink AC, Dijkshoorn ML, de Feyter PJ, Krestin GP. Diagnostic performance of coronary CT angiography by using different generations of multisection scanners: single-center experience. *Radiology* 2008;246:384-93.
10. Austen WG, Edwards JE, Frye RL, Gensini GG, Gott VL, Griffith LS, McGoon DC, Murphy ML, Roe BB. A reporting system on patients evaluated for coronary artery disease. Report of the Ad Hoc Committee for Grading of Coronary Artery Disease, Council on Cardiovascular Surgery, American Heart Association. *Circulation* 1975;51:5-40.
11. Goldstein JA, Gallagher MJ, O'Neill WW, Ross MA, O'Neil BJ, Raff GL. A randomized controlled trial of multi-slice coronary computed tomography for evaluation of acute chest pain. *J Am Coll Cardiol* 2007;49:863-71.
12. Ramcharitar S, van Geuns RJ, Patterson MS, van der Giessen WJ, van der Ent M, van Domburg RT, Serruys PW. A Randomised Comparison of the Magnetic Navigation System versus Conventional Percutaneous Coronary Intervention. *Catheter Cardiovasc Interv* 2008;in press.
13. Fishman EK, Horton KM. The increasing impact of multidetector row computed tomography in clinical practice. *Eur J Radiol* 2007;62 Suppl:1-13.
14. Husmann L, Valenta I, Gaemperli O, Adda O, Treyer V, Wyss CA, Veit-Haibach P, Tatsugami F, von Schulthess GK, Kaufmann PA. Feasibility of low-dose coronary CT angiography: first experience with prospective ECG-gating. *Eur Heart J* 2008;29:191-7.
15. Budoff MJ, Achenbach S, Blumenthal RS, Carr JJ, Goldin JG, Greenland P, Guerci AD, Lima JA, Rader DJ, Rubin GD, Shaw LJ, Wiegers SE. Assessment of coronary artery disease by cardiac computed tomography: a scientific statement from the American Heart Association Committee on Cardiovascular Imaging and Intervention, Council on Cardiovascular Radiology and Intervention, and Committee on Cardiac Imaging, Council on Clinical Cardiology. *Circulation* 2006;114:1761-91.
16. Topol EJ, Nissen SE. Our preoccupation with coronary luminology. The dissociation between clinical and angiographic findings in ischemic heart disease. *Circulation* 1995;92:2333-42.

17. Tanabe K, Serruys PW, Degertekin M, Grube E, Guagliumi G, Urbaszek W, Bonnier J, Lablanche JM, Siminiak T, Nordrehaug J, Figulla H, Drzewiecki J, Banning A, Hauptmann K, Dudek D, Bruining N, Hamers R, Hoye A, Ligthart JM, Disco C, Koglin J, Russell ME, Colombo A. Incomplete stent apposition after implantation of paclitaxel-eluting stents or bare metal stents: insights from the randomized TAXUS II trial. *Circulation* 2005;111:900-5.
18. Meijboom WB, van Mieghem CA, Mollet NR, Pugliese F, Weustink AC, van Pelt N, Cademartiri F, Nieman K, Boersma E, de Jaegere P, Krestin GP, de Feyter PJ. 64-slice computed tomography coronary angiography in patients with high, intermediate, or low pretest probability of significant coronary artery disease. *J Am Coll Cardiol* 2007;50:1469-75.
19. Sant'Anna FM, Silva EE, Batista LA, Ventura FM, Barrozo CA, Pijls NH. Influence of routine assessment of fractional flow reserve on decision making during coronary interventions. *Am J Cardiol* 2007;99:504-8.
20. Timinger H, Krueger S, Dietmayer K, Borgert J. Motion compensated coronary interventional navigation by means of diaphragm tracking and elastic motion models. *Phys Med Biol* 2005;50:491-503.
21. Mediguide. MPS First in Human! MediGuide started its clinical trials in Regensburg University Hospital in Germany. http://www.mediguide.co.il/news/news.asp?newID=43&newsCatID=2.

Chapter 6

MAGNETIC NAVIGATION IN CHRONIC OCCLUDED VESSELS

The Magnetic Navigation Wire

"Chronic Total Occlusions: A Guide to Recanalization"

Ramcharitar S and Serruys PW

Editors Ron Waksman and S Saito

Wiley-Blackwell 2008

Introduction

Magnetic Navigation System (MNS) is a rapidly growing technology with nearly 100 systems globally installed(1). It was first utilized in the field of neurosurgery and cardiac electrophysiology (2)and is now being extended to percutaneous coronary interventions (PCI). In PCI, the Niobe®, MNS (Stereotaxis, St Louis, MO, USA) offers a novel approach to cross a lesion by precisely controlling of the tip of a magnetically enabled wire *in vivo*(3,4). The system comprises of four key components: i) two permanent adjustable magnets mounted on mechanical positioners situated at either side of the fluoroscopy table ii) a navigation software (Navigant®) that creates a virtual roadmap and vectors after inputting imaging data, iii) a real time fluoroscopy system to display a virtual roadmap on the live image and iv) a sterile touch screen monitor ideally placed at the operating table for the operator to control the system. The magnetic guide wire used together with this system has a nominal diameter of 0.014inch/0.36mm and a nominal length of 185cm or 300cm(5). The wire is configured with a 2 or 3mm embedded gold encapsulate neodynium iron boron magnet at the distal tip. The first generation wires called the Cronus™ was hydrophilically coated with a tapering end that led to a 2cm floppy or 3mm intermediate coiled segment to which the magnet was attached (Figure 1)(6). These tiny magnets when placed in the magnetic field generated by the MNS aligned themselves in the direction of the applied field(7). nce the tip direction is aligned in the desired direction then the wire can be manually advanced until another change of direction is required(8). This basic principle of wire guidance is retained in the newer generation wires and towards the development of a radiofrequency enabled magnetic wire aimed at coronary and peripheral occlusion.

The Current and Future Magnetic Navigation Wires

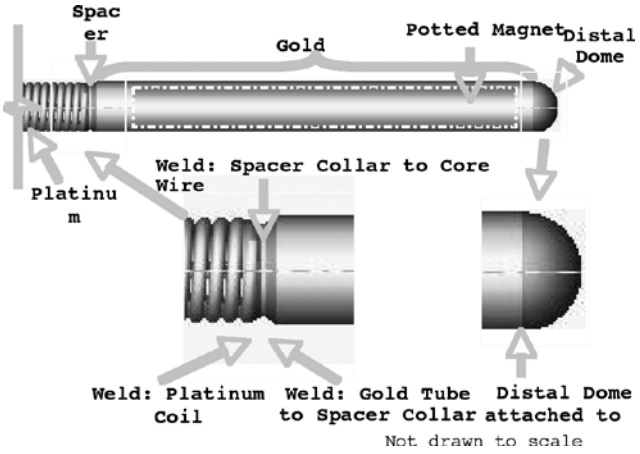

Figure 1 *The basic design at the tip of a magnetically enabled wire*

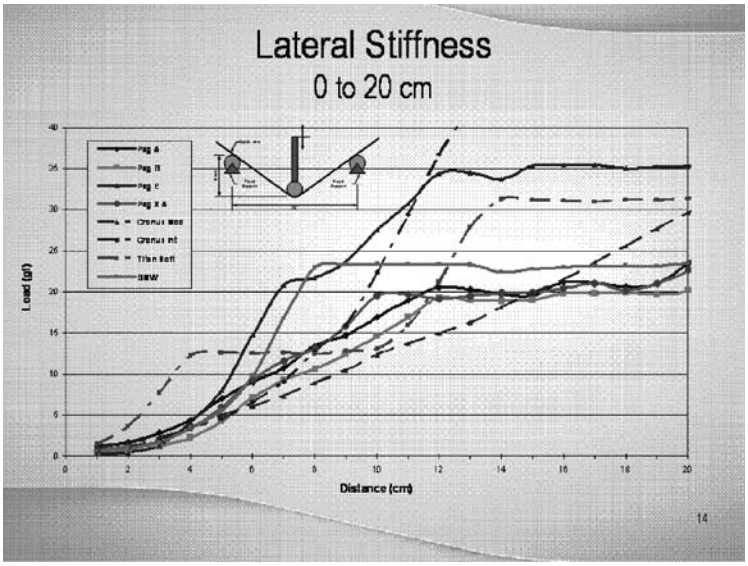

***Figure 2**: The lateral stiffness of magnetically enabled wire as determined by three point testing*

The newest family of magnetic wires that is currently commercially available is the Titan™ range. Like the Cronus™ wires they are available in either angled or straight 2 or 3mm magnetic tips. Although the basic design of the wires is the same as the Cronus™ these wires are superior in their ability to deliver a device. Three point deflection testing performed by supporting the wires at two points and measuring the force required to deflect the mid-point to 4mm showed that they stiffen quicker in order to improve device delivery. It gives the Titan™ wires a profile more similar to that of a Balance Medium Weight (BMW, Abbott Vascular Devices, Redwood, CA, USA) moderate support wire. At present the Titan™ wires are used in the majority of magnetic assisted PCI and these can include chronic total occlusions (CTOs) provided that the occlusion is short and not very old. However, when a stiffer wire that has greater pushability is desirable then the Titan™ Assert wire can be used as the shaft and tip load has similar characteristics to a Miracle 3 gram (Asahi Intecc,. Nagoya, Japan). The tip load measures the force to buckle the guidewire with 1 cm of extension. The new Pegasus™ wires will soon supersede The Titan™ range. These wires are different as they are manufactured using nitinol in the distal shaft allowing a greater retention in the shape during the magnetic assisted PCI. The proximal shaft is stainless steel to provide pushability. As with other magnetic wires they are hydrophilically coated to facilitate a smooth wire transit. At the tip of the wire is attached the 2 or 3mm magnet. Various degrees of wire stiffness (moderate or intermediate) are possible by varying the diameter of the nitinol shaft under the coil. The three-point deflection test pattern shows that the Pegasus™ Moderate and Assert have similar support profiles. However, the very distal 2cm of the Assert is stiffer to transmit more force when crossing tight or total occlusions. There are a number of

Tip Load @ 1cm Extension	
Guidewire	Tip Load (gf)
Cronus Soft	1.0
Cronus Moderate	1.8
Cronus Assert	3.5
Titan Soft	1.3
Titan Super Support	1.8
Titan Assert	3.5
BMW	0.6
Asahi Miracle 3	3.3

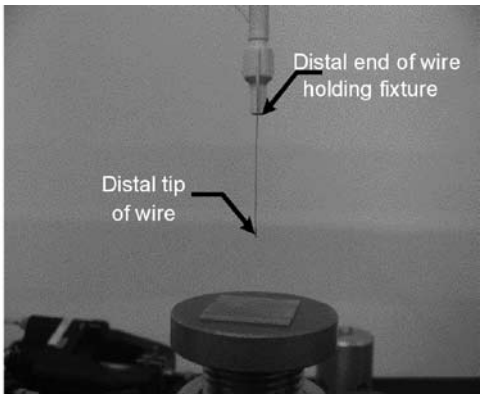

***Figure 3**: The tip load comparison of magnetically enabled and conventional wires*

improvements scheduled in the near future to the magnetic wires beyond Pegasus™. These include having smaller, but more, magnets embedded in a polymer tipped wire so as to have smoother transitions and larger, sharper magnetic deflections.

Navigational Modes to Orientate the Magnetic Tip

The magnets when correctly positioned and iso-centered interact to produce a uniformly spherical 15cm magnetic field of 0.08 Tesla called the magnetic volume. Within this volume any applied magnetic field vector precisely directs the tiny magnet mounted on the tip of a wire. Preset vectors of major vessels can be selected by the operator and advanced via the touch screen monitor. In doing so the magnets rotate, tilt or translate to align the magnetic field to the orientation of the vector. The desired vector is displayed on the live fluoroscopy image and as the magnets move a second vector is displayed that eventually assumes the same orientation of the desired vector confirming the desired magnetic orientation is reached. In addition to the preset, vectors can also be created from two-dimensional maps of angiographic images or by using dedicated three-dimensional reconstruction software to generate a virtual road map of the vessel lumen. This virtual road map is displayed as a static centre white line on the live fluoroscopy image. The latter programme has the ability to create an endoluminal view of the

***Table 1**: Characteristics of the Stereotaxis Guidewire Family*

Stereotaxis Guidewire Family Comparison				
Guidewire	Distal Core	Proximal Core	Magnet Tip Length	Distal Hydrophilic Coating
Cronus	Nitinol	Nitinol	2 & 3 mm	25 cm
Titan	Stainless Steel	Stainless Steel	2 & 3 mm	10-34 cm
Pegasus	Nitinol	Stainless Steel	2 & 3 mm	40 cm

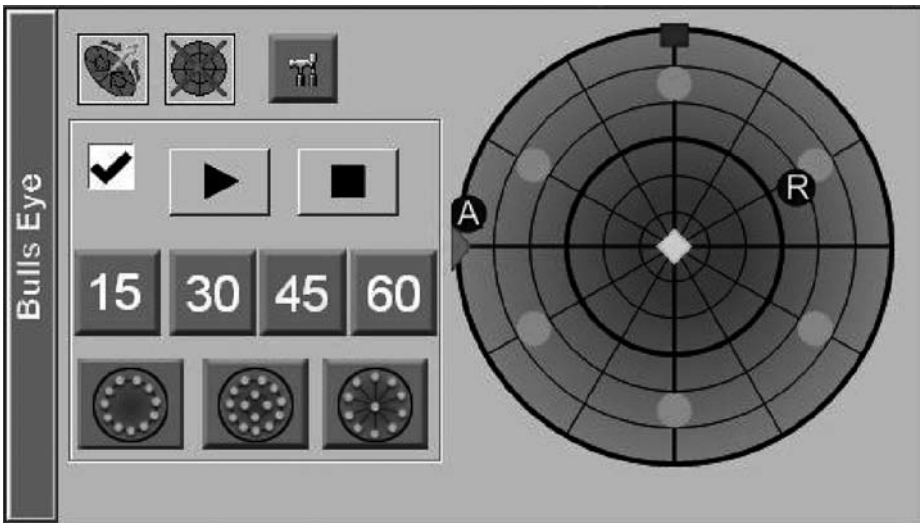

Figure 4: *The Bulls Eye Navigational mode depicting the various interrogation patterns and tip angulations that can be utilized in searching for a micro channel in a CTO*

coronary artery that can accentuate subtle changes in the direction of the vectors(9). In the initial experience to extend MNS to CTOs it was described that the 'Bulls Eye View' that allows navigation around a central axis was a particularly useful technique(6). In this approach the tip of the guidewire can be automatically or manually orientated to follow points that mimics a bulls eye used for target shooting. In doing so microchannels within the CTO can be locate through which the magnetic wire can enter (Figure 4).

The Theory of Radiofrequency (RF) Ablation in CTO

An attractive strategy for CTOs using the following concepts has been postulated by Serruys(10): first, using magnetic navigation to steer a guidewire towards the occlusion; second: a technology to look forward within the vessel, either through the use of an optical coherence tomography or an IVUS system or MSCT cross-sections to ensure ideal positioning of the wire in the true lumen; finally, some ablative power is needed at the tip of the wire to recanalize the CTO. Radiofrequency ablation has previously been reported with the Safe-Cross RF wire (Intraluminal Therapeutics, Carlsbad, CA., USA) uses optical reflectometry to verify the intraluminal position of the wire prior to radiofrequency ablation(11). In the treatment of CTOs using RF ablation the first step required is energy delivered through mono or bipolar electrodes in order to generate a current that travels between the active electrode and the ground electrode (or dispersive electrode). In addition, continuous RF energy of frequencies greater than 100 kHz is desirable as this avoids neuromuscular stimulation without compromising the ablating potential. The distribution of this current is dictated by the size of the ablating active electrodes and the characteristics of the tissues surrounding the electrodes. The potential difference

between the active electrode and the ground electrode determines the impedance and when low is the preferred pathway for current flow. When an RF voltage is applied to the electrodes, the polarity of the electrodes alternates at a given frequency. Polar molecules are alternatively attracted to the active electrode and then to the ground electrodes during each cycle of RF current, resulting in the generation of heat. The bioheat equation is used to describe how the temperature changes as a result of RF current delivery(12):

$$T = \frac{1}{\sigma \rho c} J^2 t + T_C$$

where T= final temperature (K)
σ= electrical conductivity (S/m)
p= tissue density (kg/m^3)
J= magnitude of the current density (A m^2)
t = duration of activation (s)
T_0 = initial temperature (K)
c = specific heat (J/kg/K)

Furthermore, if the electric field between the tissue and electrode is large enough, arcing can occur. Electrical arcs are focused very high energy sparks that are thought to vaporized cells in front of the active electrode and in so doing disrupt the tissue layer for effective ablating/cutting. Theoretical calculations show arcs can heat tissue from 37 °C to 100 °C in microseconds. Studies of electrical characteristics along with observation of the tip during cutting with the RF guidewire indicate two distinct phases in the cutting/ablation process(13):

Phase 1 - water around the active electrode heats up and vaporizes. A capacitive vapour layer (dielectric layer) separates the electrode and the tissue.
Phase 2 – along the points on the electrode where the voltage potential is sufficient to break down the dielectric layer, an arc jumps from the electrode to the tissue.
Each arc quickly vaporizes water within the occlusion on contact, disrupting the tissue to allow easy passage of the electrode. If the vapour layer is maintained, then continuous arcing and steady cutting occurs.

The Magnetically enabled RF wire

At present this wire is still being developed by Stereotaxis with the final testing due to be completed later this year. The latest prototype (Figure 5) consists of an insulated core wire, 3 spaced magnets in a polymer jacket and a heat shield surrounded by a heat sleeve attaching the RF electrode. Its electrically conductive nitinol core wire is supportive on the proximal end whilst being flexible and durable on the distal end. For safe delivery of the RF energy to the electrode tip of the wire, the length of the core is electrically insulated with a PTFE coating. The degree

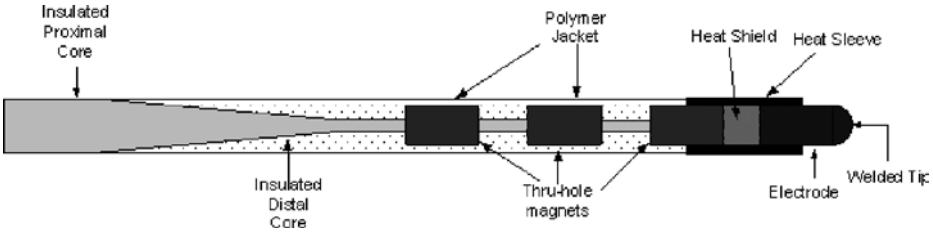

Figure 5: *The magnetically enabled RF wire*

of insulation of the distal and the proximal section takes into account the wires function. In the distal section only very thin insulation is used so as to provide adequate dielectric strength without affecting the wire's flexibility. In the proximal section the insulation has a higher dielectric strength than the distal section since it is to be handled by the operator. As PTFE is naturally lubricious it avoids the need for an additional coating. Different designed magnets ('thru-hole magnets') having hollow central cores are placed proximally along the distal tip of the wire and are specially treated to prevent corrosion. A heat shield and sleeve protects them as since the intense heat generated can result in their demagnetization. The RF electrode is manufacture from the composite metal alloy and the entire wire is encased in a polyurethane polymer jacket for smooth transitions between the different components. In house *in vivo* studies were performed in porcine models having artificially created occlusions of the femoral arteries. The occlusions were typically 5-8cm in length and aged 6-8 weeks to form the tough end caps and induce collateral formation. The device proved capable of engaging and perforating the proximal cap and entering the occlusion. It also proved capable of progressing within the occlusion, traversing the entire occlusion and exiting the distal cap into the distal patent section of artery.

Magnetic Navigation and MSCT Co-integration in CTOs

In a CTO the inability to image the artery with contrast media means that an alternative imaging modality is require to create the 3-D roadmap. Multislice Computer Tomography (MSCT) offers the ability to visualize the occluded coronary artery and can provide a full 3-D roadmap of the coronary tree in Navigant®(14). In the newest version (Navigant® 2.11) a segmented MSCT volume that only shows the coronary tree (Siemens Medical Solutions, Forchheim, Germany) can be imported into the software. In addition, the operator has access to the endoluminal view that simulates looking through the vessel lumen and simultaneously to the corresponding Multi-Planar Reconstruction (MPR) slice, as well as an automated update of the magnetic vector as the wire is advanced. The latter means that the operator can fully concentrate on the wire advancement guided by the moving vectors on the live fluoroscopy image. Moreover, as the vector is sequentially updated so too are the MPR slices together with the endoluminal views so that the operator can always have prior knowledge of the lesion in front of the wire

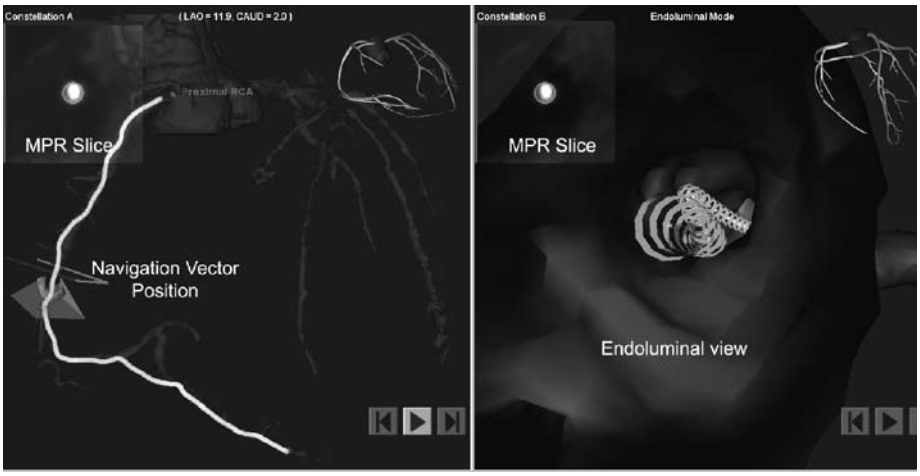

Figure 6: *Navigation through MSCT co-integration demonstrating the MPR cross-section slice (left upper quadrant at the site of the navigational vector and the corresponding endoluminal view in the right panel.*

(Figure 6). Clinical evaluation of the magnetically enabled RF wire with MSCT co-integration of chronically occluded stents is in the final stages of preparation.

Limitations

One major limitation with current wire designs is that the magnet is stuck on to the tip of the wire and this can influence the wire's ability to transit smoothly across a lesion. In the future generation wires the multi-magnet design as used in the RF wire will try to accommodate this limitation. Another limitation with the current technology in that the uploaded MSCT dataset for managing CTO creates a static roadmap of the vessel, while the heart is a beating dynamic organ. In the future a dynamic roadmap created from the MSCT will be needed so that the wire advancement can be appropriately gated to the image to maximize the probability that it will be within the true lumen.

Conclusion

Magnetic Navigation is a promising technology in the management of CTOs. Over the past 5 years the improvement in magnetic guide wire designs has led to wires with comparable characteristics to conventional wires. The development of the magnetically enabled RF ablating wire together with the recent upgrades in MSCT co-integration software has brought the MNS closer to realizing its full potential to the CTO field.

References

1. Patterson MS, Schotten J, van Mieghem C, Kiemeneij F, Serruys PW. Magnetic navigation in percutaneous coronary intervention. J Interv Cardiol 2006;19:558-65.
2. Ernst S, Ouyang F, Linder C, et al. Initial experience with remote catheter ablation using a novel magnetic navigation system: magnetic remote catheter ablation. Circulation 2004;109:1472-5.
3. Faddis MN, Chen J, Osborn J, Talcott M, Cain ME, Lindsay BD. Magnetic guidance system for cardiac electrophysiology: a prospective trial of safety and efficacy in humans. J Am Coll Cardiol 2003;42:1952-8.
4. Hertting K, Ernst S, Stahl F, et al. Use of the novel magnetic navigation system Niobe™ in percutaneous coronary interventions; the Hamburg experience Eurointervention 2005;1:336-339.
5. Atmakuri SR, Lev EI, Alviar C, et al. Initial experience with a magnetic navigation system for percutaneous coronary intervention in complex coronary artery lesions. J Am Coll Cardiol 2006;47:515-21.
6. Tsuchida K, Garcia-Garcia HM, van der Giessen WJ, et al. Guidewire navigation in coronary artery stenoses using a novel magnetic navigation system: first clinical experience. Catheter Cardiovasc Interv 2006;67:356-63.
7. Ramcharitar S, Patterson MS, van Geuns RJ, et al. A randomised controlled study comparing conventional and magnetic guidewires in a two-dimensional branching tortuous phantom simulating angulated coronary vessels. Catheter Cardiovasc Interv 2007;70:662-668.
8. Ramcharitar S, Patterson MS, van Geuns RJ, Serruys PW. Magnetic navigation system used successfully to cross a crushed stent in a bifurcation that failed with conventional wires. Catheter Cardiovasc Interv 2007;69:852-5.
9. Patterson M, Tanimoto S, Tsuchida K, Serruys PW. Magnetic Navigation with the Endo-Luminal View and the X-ray overlay - Major advances in novel technology. Eurointervention 2007;in press.
10. Serruys PW. Fourth annual American College of Cardiology international lecture: a journey in the interventional field. J Am Coll Cardiol 2006;47:1754-68.
11. Werner GS, Fritzenwanger M, Prochnau D, et al. Improvement of the primary success rate of recanalization of chronic total coronary occlusions with the Safe-Cross system after failed conventional wire attempts. Clin Res Cardiol 2007;96:489-96.
12. Pearce JA. Electrosurgery London. Chapman and Hall, 1986;Chapter 4.
13. Honig WM. The mechanism of cutting in electrosurgery. IEEE Trans. Biomed. Eng 1975;January:58-62
14. Garcia-Garcia HM, Tsuchida K, van Mieghem C, et al. Multi-slice computed tomography and magnetic navigation-initial experience of cutting edge new technology in the treatment of chronic total occlusions. Eurointervention 2008, in press.

MAGNETIC NAVIGATION IN CHRONIC OCCLUDED VESSELS

Single Center Experience in applying the Magnetic Navigation System to manage Chronically Occluded Vessels

Submitted

Ramcharitar S, van Geuns RJ, van der Giessen W.J, van der Ent M, de Feyter P, Serruys PW

Objective:
Applying the Magnetic Navigation System (MNS) to manage Chronic Total Occlusions (CTOs)

Background:
The MNS precisely directs a magnetised guidewire *in vivo* through two permanent external magnets.

Methods:
Single center experience on the first 43 consecutive MNS treated CTOs was evaluated. Computed tomography coronary angiography (CTCA) co-integrated within the MNS provided a virtual road map through the occlusion. Failed MNS cases were intervened with bailout conventional CTO guidewires. Experienced CTO and MNS operators had unrestricted access to devices and equipments.

Results:
Crossing success rose from initially 40% to a maximum of 56% over 52 months. The overall MNS crossing success was 44.2% (19/43patients). Conventional wires were successful in 14 out of the 24 failed MNS cases (58.3%). Overall procedural success was acceptable (76.6%) and complication rates low (4.6%). 1.8±0.9 stents (lengths 44.7±21.4mm and diameter 2.8±0.4mm) were implanted. Procedures were lengthy (125.0±35.3mins) with high dose area product (DAP) (11980.2±6457.9 Gy/cm^2) and contrast media usage (388.8±170.2mls). Operators persevered less with magnetic wires (20.9±12.4min vs. 27.7±24.4mins) and used softer ones preferentially (1st choice, 53.5%). OTW balloons were used in 70% of the cases. Similarly weighted 3gram wires were terminated earlier in the MNS. CTCA co-integration did not influence procedural outcome but higher magnetic wire success was observed in low calcified lesions, those with a central stump and without bridging collaterals.

Conclusion:
In unselected CTOs the magnetic wires is safe, but the modest success rates and relatively high procedural bailouts means currently there is no additional advantage over the more sophisticated conventional CTO wires.

Introduction

Chronic total occlusions (CTO) are encountered in over 25% of patients undergoing percutaneous coronary interventions (PCI)[1,2]. Their importance stems from the fact that treatment relieves symptoms, increases exercise tolerance and improves left ventricular function[3]. Moreover, recanalization reduces the need for coronary artery bypass surgery and leads to better long-term survival [4]. But despite a high proportion of CTOs having recanalized lumen, crossing the occlusion remains a challenge[5]. This is because factors such as calcification, the occlusion length, age, the nature of the stump, the presence of collaterals and the immediate anatomical environment of the CTO can all influence the outcome[6]. These vessel characteristics together with ability of the skilled operator in responding to tactile feedback prior to advancing sophisticated conventional guidewires can be critical to the overall procedural success[7].

The magnetic navigation system (MNS) has the ability to steer through a vessel by changing the tip of a magnetically enabled guidewire without the need to removing it from the patient[8]. It has been reported that this ability can aid the search for micro-channels to effectively negotiate through the occlusion[9]. Moreover, by co-integrating data obtained from computed tomography coronary angiography (CTCA) into the MNS software a navigational pathway can be derived from the inherent radio-opacity of the occluded segment tissue that is non delineated by contrast media to be used in the guidewire navigation[10]. In this study we report on the feasibility and safety of this novel approach and our experience on the factors that influenced the procedural outcome with the MNS.

Material and methods

Study patients

In a 52month study period from February 2004 to May 2008, forty-three consecutive patients presenting with symptomatic coronary artery disease due to a chronic total occlusion were managed with the MNS. The selection criteria for a chronic occlusion was defined as either an occlusion on angiography with no antegrade filling of the distal vessel other than via collaterals or minimal antegrade flow (TIMI flow 0 or 1). All patients included had a native vessel occlusion estimated to be at least one month's duration, defined according to previously published studies and based on either a history of sudden chest pain, a previous acute myocardial infarction in the same target vessel territory, or the time between the diagnosis made on coronary angiography and PCI[6,7]. The type of CTO was either *de novo* or in-stent restenosis. The protocol was locally approved and all patients gave written informed consent. In total 5 cardiologist experienced in CTO had unrestricted access to the choice of either magnetic or conventional guidewires. Importantly the cardiologists were also trained with the MNS. In addition, one experienced MNS technician was required to operate the navigational software. Patients were

excluded if they were haemodynamically unstable or had contraindications for magnetic-assisted intervention (MAI) such as having a pacemaker.

CTCA acquisition

CTCA was performed on 64-slice CT (Sensation 64, Siemens, Forchheim, Germany) using a bolus of 100 ml contrast fluid (iomeprol, Iomeron 400, Bracco, Milan, Italy) intravenously injected at a rate of 5ml/sec. ECG-gating dataset were reconstructed during the mid-to-end diastolic phase (–300 to –450 ms before the next R-wave or 60% to 70% of the R-R interval). The coronary artery was automatically extracted off-line using dedicated post processing software (Leonardo VB30A; Siemens) and incorporated directly in the MNS navigational software called the Navigant®.

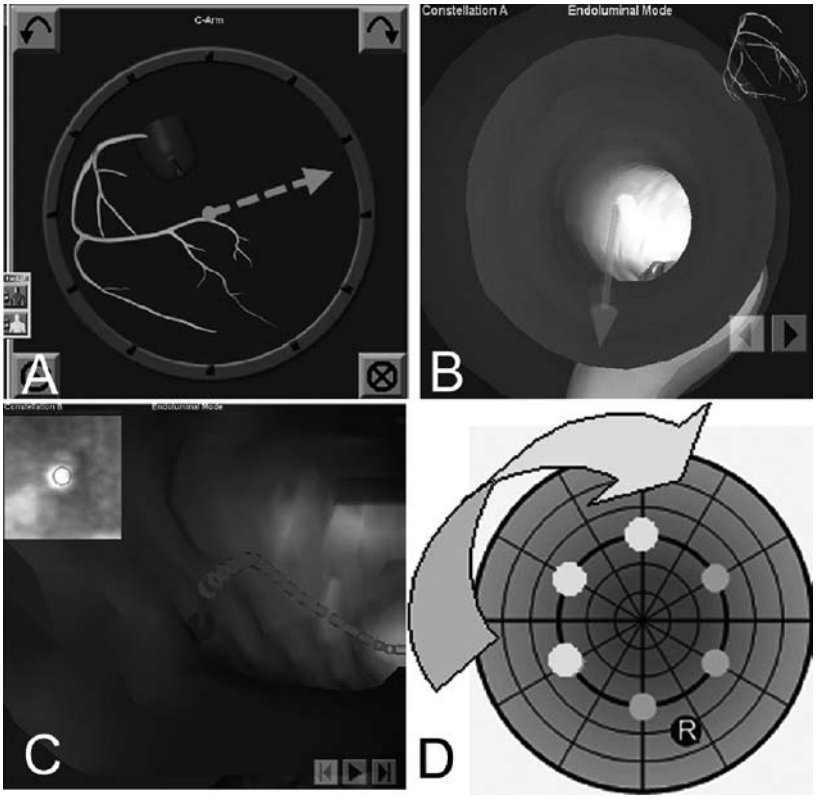

Figure 1: A) Clockface navigation mode vectors are orientated by through a touch sensitive monitor; B) CardiOpB® virtual 3DRC vessel showing fly-through endoluminal view for navigation; C) extracted CTCA virtual fly-through endoluminal view with MPR slice in the top left corner; the Bull's eye navigational mode demonstrating the ability to reorient wire tip in a systematic manner.

The Magnetic Navigation System

The Niobe® II Magnetic Navigation System (MNS) (Stereotaxis, St. Louis, M. USA) has been previously described[8]. Briefly two permanent magnets generate a field (0.08Tesla) that can be focused to follow navigational vectors created in Navigant®. The vectors are derived through various navigational modes based on 2-Dimensional or 3-Dimensional information. In addition, they can be automatically updated or manually controlled via a touch sensitive monitor situated at arm's length from the operating table.

Navigational modes used in this study

i) The clockface navigation

In the clockface navigation mode vectors are orientated through a touch sensitive monitor that mimics the dial of a clock (Figure 1A). The vectors move in the X-Y axis and there is an option for a third dimension (Z axis). Full 360ºomni rotation of the magnetically enabled wire is therefore possible but to be effective a spatial understanding of coronary anatomy is required.

ii) Three-dimensional (3-D) virtual reconstruction (3DRC)

The CardiOpB® (Paieon Medical Inc., Rosh Ha'ayin, Israel) uses 2 orthogonal Xray images that are at least 30° apart to create a virtual 3DRC vessel. A navigational path associated with vector created in Navigant® is then overlaid on the live fluoroscopic image after alignment with the tip of a guiding catheter. The system also incorporates a fly-through endoluminal view for navigation (Figure 1B).

iii) The co-integration of CTCA

Incorporating the extracted CTCA into Navigant® allows both the mapping and co-registration of the occluded segment. Superimposing the derived navigational pathway on the fluoroscopic images enables navigation to be performed in a similar manner to a 3DRC. But in addition to providing an endoluminal view the system can simultaneously display the multi-planer reconstructed (MPR) slices through the occlusion thus allowing the operator to visualize upfront the morphology of the occlusion (Figure 1C).

iv) The Bull's Eye view

Regardless of the 2D or 3D navigational mode, the Bull's Eye can be additionally employed to search for micro-channels in a systematic way. To achieve this the wire tip can be automatically or manually re-orientated in a systematic fashion to mimic the contours of a dartboard or a bull's eye (Figure 1D).

Special CTO Techniques

In this study over-the-wire balloons (OTW) provided additional back up for the guidewires. It also facilitated the rapid exchange of various guidewires though its lumen without losing the original wire position. Subsequent removal of the OTW required inflation of an indeflator containing saline to roughly 16 atmospheres connected to the lumen.

Employing two guidewires to search for the true lumen was used in the parallel wire technique: -one that has entered the vessel subintimally and left in this position with another usually a stiffer wire used to find the true lumen from a different entry point. In a somewhat similar technique, the see-saw technique used two guidewires, but instead of leaving one of them in the false lumen, both are used sequentially to reenter in the true lumen[11].

The Guidewires

The first generation Cronus™ and second generation Titan™ Soft Support coronary guidewire (Stereotaxis, St. Louis, M. USA) are 180cm moderate support, hydrophilic coated 0.014in wires with a flexible 2cm distal coiled tip having a 2mm or 3mm long gold cup neodynium magnet attached. The Pegasus™ guidewire is similar to the Titan™ Soft Support coronary guidewire except the distal 30cm of the stainless steel distal shaft is replaced by nitinol. All 3 generations are available in the stiffer Assert™ wires ranges The conventional wires used in this study were PT Graphix™ Intermediate, Choice™ PT Floppy (Boston Scientific Corp. Miami Fl, USA); Pilot™ 50, 150, Whisper™ and high torque BMW (Abbott Vascular Devices, Redwood CA, USA); Miracle bros™ 3G, 4.5G, 6G, 12G, Fielder and Confianza (ASAHI, INTEC, Co, Japan); Crosswire NT (Terumo Inc, Tokyo, Japan).

Statistics

Continuous variables are presented as means and standard deviation. T-test and one-way ANOVA (Bonferoni) were used to determine if there were significant differences in the procedural time and fluoroscopic times. Analyses were performed using SPSS 11.5 for Windows (SPSS, Chicago, IL). *P* value < 0.05 was considered statistically significant.

Results

Demographics and CTO characteristics

The baseline characteristics of the 43 patients enrolled in this single center registry on magnetically managed chronic total occlusion are given in Table 1. The mean age of patients were 67.1±9.8 years and the majority was male (76.7%). One fifth was diabetics and the most common cardiovascular risk factors were hypertension (60.5%) and hyperlipidaemia (76.7%).

Table 1 Baseline characteristics	n = 43
Age, years (mean+SD)	67.1 ± 9.8
Male (%)	76.7
Diabetes mellitus (%)	20.9
Insulin Dependent (%)	14.0
Hypertension (%)	60.5
Family history of CHD (%)	27.9
Ex smoking (%)	48.8
Hypercholesterolaemia (%)	76.7
Previous PCI (%)	41.7
Previous CABG (%)	14.0
Vessel disease (%)	
One vessel disease	34.9
Two vessel disease	39.5
Three vessel disease	25.6
Attempts to reopen the CTO (%)	
First	93.0
Second	7.0

SD = standard deviation; CHD = cardiovascular heart disease;

CABG = coronary artery bypass graft;

PCI = percutaneous coronary intervention;

Interestingly, a significant number of patients had a previous PCI (41.7%) or CABG (14.0%) at presentation. On diagnostic angiographic images there was roughly equal distribution of one, two and three vessel disease. The majority of patients (93.0%) underwent first attempt to revascularize the CTO. Most CTOs were *de novo* lesions (95.3%) frequently involving the left anterior decending artery (LAD, 32.6%) and to a lesser extent the circumflex coronary artery (LCX, 25.5%) and the right coronary artery (RCA, 18.6%). The angiographic characteristics are also shown in Table 2. Of note the characteristic in stump morphology was equally distributed[12]. Over three-quarters had significant contra-lateral collateralization and 30% had calcific vessels on coronary angiography. In addition to the occluded vessels nearly one third of patients had a second single vessel treated at the indexed procedure and in a smaller number (9.3%) two vessels.

The overall crossing success using the full armamentarium of all possible choices of magnetically enabled wires and navigational modes was 44.2% (19/43patients). Bail-out conventional wires were successful in 14 of the failed 24 magnetic cases (58.3%) giving an overall procedural success of 76.6%. In the majority of cases the 2nd generation Titan™ wires were used (72.1%).

Table 2 CTO Characteristics	
Type of CTO (%)	De novo 95.3
In-stent restenosis	4.7
Target vessel (%)	
Left anterior descending	32.6
Left circumflex	25.5
Right coronary artery	18.6
Intermediate/Obtuse Marginal	14.0
Diagonal	9.3
Stump morphology (%)	
Central	32.6
Eccentric	37.2
Blunt	30.2
Ostial involvement (%)	30.2
Side branch at entry (%)	81.3
Bridging collaterals (%)	37.2
Collateral filling [Rentrop Classification (%)]	
0/1	20.9
2	41.9
3	37.2
Angiographic Calcification (%)	
None/mild	69.8
Moderate	23.2
Severe	7.0
PCI in at least one additional (non-occluded) major vessel during the index procedure (%)	
One arteries	32.6
Two arteries	9.3
Treated CTO	
Number of stents in treated occluded vessel	1.8±0.9
Average target vessel stent length (mm)	44.7±21.4
Average target vessel stent diameter (mm)	2.8±0.4
Contrast used (ml)	388.8±170.2
Procedure time (min)	125.0±35.3
Fluoroscopic time for entire procedure (min)	42.1±19.7
Radiation exposure, dose area product (DAP) Gy/cm^2	11980.2±6457.9

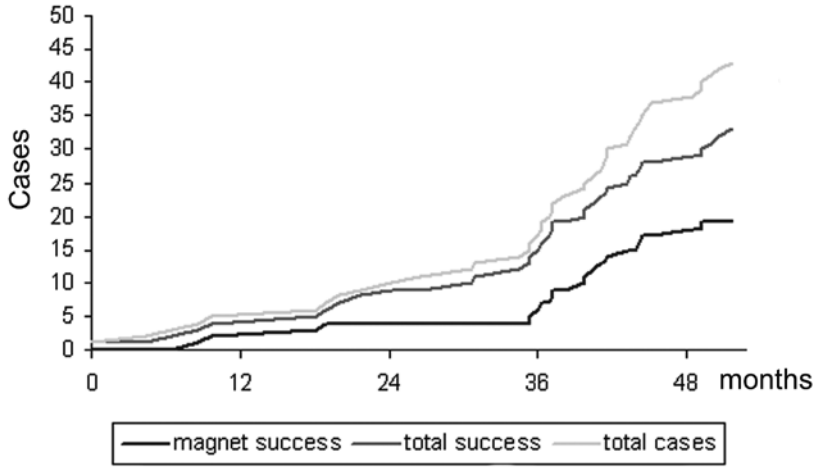

Figure 2 Cumulative curve of CTO success with the MNS with respect to the total success and cases.

These wires had a greater overall crossing success over the 1st generation Cronus™ range (36.4% vs. 48.4%). A significant proportion (44.2%) of patients had CTCA co-integration into Navigant® to create vectors along a navigational path through the occlusion. Surprisingly, the overall success in patients where the CTCA was co-integrated and navigated upon was nearly identical to those managed without CTCA co-integration (73.6% vs. 75% respectively). Moreover, CTCA co-integration only marginally improved the magnetic wire success (47.3%) when compared to the overall success achieved with this system (44.2%).

In total 1.8±0.9 stents with an average length of 44.7±21.4mm and diameter of 2.8±0.4mm were implanted in the occluded vessels. The average procedural time was 125.0±35.3mins with an overall contrast media usage of 388.8±170.2mls. Additionally, patients were exposed to lengthy radiation times 42.1±19.7mins and periods of exposure 11980.2±6457.9 Gy/cm^2. The overall procedural complication was low (4.6%) with two patients needing pericardial drainage insertions resulting from bail out conventional wire exits and subsequent ballooning. One of these patients later proceeded to emergency surgery following an extra-vascular balloon dilatation.

Analysis of Magnetic Navigation System Performance in Crossing the Occlusion

Following the installment of the MNS in 2004 the feasibility of managing CTO was performed initially in 5 patients using the 1st generation wires (Cronus™) with a success rate of 40%. The low patient recruitment observed in the subsequent 2 years improved following the integration of the CTCA extracted coronary artery into the Navigant®. In year 3 there was a dramatic rise in

the patient enrolment accounting for 53% of all the magnetically managed CTO (Figure 2) and with the availability of the 2nd generation wires (Titan™) the success rate to increased 56%.

In terms of the wire performances, the average time for wiring the CTO whether successful or not regardless of the technique (magnetic or bail-out) was 34.5±28.4mins. Within this period the magnetic wire was used for average of 18.2±11.7mins. In the 19 successful magnetic cases the average crossing time was 14.8±9.8mins and in the 24 failed cases the average trial time was 20.9±12.4mins. Longer wiring times 27.7±24.4mins (p=0.22) was required in the 14 failed magnetic cases that were eventually successful using bailout conventional wire techniques. In the 10 cases (23.3%) were both wires failed, wiring was continued for over an hour (69.5±32.9). Analysis of these cases revealed that the majority (6 cases) was due to vessel dissections after several trials with the conventional wire. The inability to penetrate the cap or re-enter the true lumen distally each accounted for 2 failed cases. Analysis of the lesion characteristics revealed that the magnetic wires were more successful if the stump was central (76.6%) and if there were low levels (none/mild) of calcification (60.0%). Limited magnetic wire successes were observed in vessels having moderate/severe calcification (7.7%) or in cases where there was angiographically bridging collaterals (11.8%), Table 3.

Assessment of wire usage

In total twenty different types of guidewires (7 magnetic and 13 conventional) were used in this study (Table 4). 70% of the cases involved the use in of an OTW balloon. Overall operators were less inclined to use stiffer magnetic wires early in the procedure. They also gave up similarly weighted magnetic wire (the 3 gram Assert range) relatively earlier (4th choice) in favor to the 3 gram Miracle wires, which was employed as far as a 9th choice. Amongst the 1st generation magnetic wires the Cronus™ Moderate was the 1st choice (20.9%) with stiffer Cronus™ 3 gram Assert guidewires used as a 2nd choice only in one case (Table 4). Surprisingly, softer 2nd generation wire (Titan™ Soft Support) where used as 1st choice in over fifty percent of cases. Only in a relatively small number of procedures (21%) were the stiffer Titan™ Moderate or Asset wires used as the 1st choice. In a somewhat similar fashion to the MNS, softer conventional wires (PT choice, Hi Torque Whisper, Hi Torque BMW) were preferentially used as the 1st choice (36.5%) in bailout MNS cases. More hydrophilic (PT Graphic Intermediate and Crosswire NT) and stiffer wires (Miracle 3gram and Confianza) were more often used as a 3rd choice (47.6% and 28.6% respectively). The prevalence of the stiffer conventional wires increased over time.

Table 3 Wires, Success, Times and Complications	
Wires/cases (%)	
Cronus	25.6
Titan	72.1
Pegasus	2.3
Special technique (%)	
Over the wire balloon	69.8
Parallel wire	30.0
See Saw	4.7
MSCT co-integration	44.2
Success (%)	
Overall success rate (33/43)	76.6
Magnetic wire success rate (19/43)	44.2
Standard wire success in failed Magnetic cases (14/24)	58.3
Cronus (4/11)	36.4
Titan (15/31)	48.4
Pegasus (0/1)	0
Magnetic success with MSCT co-integration (9/19)	47.3
Overall success with magnetic and bail-out standard wires in patients with MSCT co-integration (14/19)	73.6
Overall success with magnetic and bail-out standard wires in patients without MSCT co-integration (18/24)	75.0
Magnetic wire Success in Lesion Subset (%)	
Moderate/Severe calcification (1/13)	7.7
None/Mild calcification (18/30)	60.0
Central stump (11/14)	76.6
Eccentric stump (4/16)	25.0
Blunt stump (4/13)	30.8
Bridging collaterals (2/17)	11.8
Crossing Times/min; (mean+SD)	
Overall crossing time	34.5±28.4
Magnetic wire (successful and unsuccessful cases)	18.2±11.7
Magnetic wire (successful cases)	14.8±9.8
Magnetic wire (unsuccessful cases)	20.9±12.4
Standard wire times in magnetic unsuccessful cases	27.7±24.4
Magnetic and standard wire failures	69.5±32.9
Complications (%)	
Pericardial Drains	4.6
Surgical repair	2.3

Table 4: Choice of wires used in chronological order from 1st attempt with magnetically enabled wires to 9th choice with conventional wires.

	1st	2nd	3rd	4th	5th	6th	7th	8th	9th
Number and % patients	n=43 100.0	n=24 55.8	n=21 48.8	n=16 37.2	n= 8 18.6	n=7 16.3	n=2 4.7	n=2 4.7	n=1 2.3
Magnetic wires %									
Cronus Soft	2.3								
Cronus Moderate	20.9								
Cronus Assert	2.3	4.2							
Titan Soft	51.2	12.5	4.8						
Titan Moderate	14.0								
Titan Assert	7.0	4.2		6.3					
Pegasus Intermediate	2.3								
Standard Wires %									
Choice PT		8.3							
PT Graphix Intermediate		29.2	28.6	18.7	12.5				
Crosswire NT		4.2	19.0	18.7		14.3			
Hi-torque Whisper		4.2							
Hi-torque pilot 50		25.0	19.0	12.5	12.5	14.3			
Hi-torque pilot 150								50.0	
Hi-torque BMW wire		4.2							
ASAHI Fielder					12.5	14.3			
ASAHI Miracle 3g		4.2	23.8	37.5	25.0	28.6	100.0	50.0	100.0
ASAHI Miracle 4.5g					12.5				
ASAHI Miracle 6g					12.5				
ASAHI Miracle 12g						14.3			
ASAHI Confianza			4.8	6.3	12.5	14.3			

Discussion

The variability in success rates in crossing CTO provides the impetus for seeking alternative therapeutic options for managing this interesting but complex lesion subset[10]. Apart from

being gratifying for the operator the successful treatment is prognostically significant to the patient. As such the wealth of tools and devices bears testament to the determination amongst the interventional cardiology community in succeeding. But in this quest, several key elements are occasionally overlooked. Patients are subjected to lengthy procedures, high volumes of contrast media impacting on renal function, and high levels of radiation exposure[13,14]. Moreover, the high procedural cost can have repercussions on budgets and resources[15].

It is not surprising therefore that the application of the magnetic navigation system to managing CTOs has been warmly received[10]. The technology has been shown to be effective in crossing complex vascular anatomies in patent vessels[16]. Moreover, it can reduce contrast media usage and successfully manage selected cases that failed to cross conventionally[17]. In occluded vessels however, there is limited data from only two recent registries and no randomized studies. In one having 30 patients, 3 out of the 5 magnetically failed cases was due to subtotal chronic occlusion and this included 1 patient who required surgical intervention[18]. In the other registry containing 439 lesions in 350 consecutive PCI patients, 25 out of the 35 failed crossing where CTOs[19].

In this paper we report in detail our experience as a leading center in the MAI treatment of chronic total occlusions starting form the initial installation of the system in 2004 [9]. The data demonstrated that the MNS has limited success but can be safely used in unselected occlusions. Over this period a learning curve was demonstrable as with the initial low success rates improved over time. Several coronary and non-coronary groups using the MNS have previously reported similar learning curves[19-21]. The overall success rate with the MNS was lower than that historically reported from our center[6]. Following bailout conventional wire strategy a good overall success rate achieved. Moreover, complication rates were low and restricted to the bailout group. These findings are not surprising if one considers the wiring times and choice in wire usage in the MNS. In general, operators were more inclined to use the softer magnetic wires and gave up much earlier in preference to the traditionally dedicated CTO standard wires. These dedicated CTO were more often stiffer, used for longer periods and were exchanged for increasingly stiffer ones in the more difficulty cases. The reason for this could be explained in part to the initial novelty and lack of familiarity with the magnetic wires to this lesion subset. But more so, in our experience we felt that even though the ability to steer using a 2-3mm long attached magnetic tip has been proved to be effective for patent vessels, this tip profile may not be ideally suited for total occlusions. The notion of searching for micro-channels using the bull's eye is limited by the blunt and straight nature of the wire tip restricting the wire from engaging small-angulated channels within the occluded segment[22]. Furthermore the transition of the magnetic tip to the shaft lends itself to "buckling" when "push force" is applied to the wire. Operators were therefore more likely to resort to the conventional wires that had smoother transition of the tip to the shaft without compromising the applied force. Using the magnetic wire in an OTW balloon does not solve this crucial limitation. This is because although

like conventional wires the shaft is equally support, the advancement of the balloon to support the tip incapacitates the steering ability and furthermore changes the profile of the wire to such an extent that the tactile responsiveness of the tip is completely lost.

These results provide further evidence that for the magnetic system to be effective in the all CTOs and not restricted to those with central stumps, low calcium or collateralization a completely different wire with a different procedural strategy is required. Non-steerable radiofrequency and laser-guided wires have been previously used to manage CTOs with limited success[10]. Enabling such devices to steer can potentially improve the outcome in managing CTOs. But in order to be safe and effective precision mapping of the occluded segment and real time feedback positioning of the device within a fraction of a millimeter is required. This report demonstrates that real time knowledge of the navigational path through the occlusion did not influence the success in patients who had a CTCA overlaid on the fluoroscopy images and those treated without. This suggest that for the co-integration of a CTCA roadmap to be clinically effective it needs to be used with dedicated CTO devices such as the magnetically enabled RF ablating wire (Stereotaxis Corp) in development[8]. It is also necessary to simultaneously update the CTCA roadmap to the changing vessel anatomy of the cardiac cycle (dynamic road mapping) since currently the static overlay based only on one diastolic image will not guarantee that the device will be optimally positioned when the energy is delivered. Additional factors such as patient and respiratory movement will need to be adequately compensated and overcome.

Limitations

The level experiences with the two strategies may have influence the period of time operators were willing to persevere with each system. There was no written or universal approach to deal with the various complexities encountered. The study was not powered to assess the influence of guiding catheters, which could have influence procedural outcome. Contrast media usage and fluoroscopic times were assessed for the whole procedure so included treatment of other vessels. The age of the occlusion could not be precisely determined, relying primarily on the patient's clinical history and previous angiographic films. This was a single-center's experience in a University specialist tertiary referral unit and the case mix might be different to that seen elsewhere.

Conclusions

In unselected chronically occluded vessel the magnetic navigation system is safe. The modest success and relatively high procedural bailouts does not currently confer an advantage with the MNS over the more sophisticated conventional CTO wires. The limited success is related to the operator's reluctance to persevere because of the inherent limitations with the current magnetic wire technology. At present CTCA co-integration did not influence procedural outcome.

References

1. Stone GW, Kandzari DE, Mehran R, Colombo A, Schwartz RS, Bailey S, Moussa I, Teirstein PS, Dangas G, Baim DS, Selmon M, Strauss BH, Tamai H, Suzuki T, Mitsudo K, Katoh O, Cox DA, Hoye A, Mintz GS, Grube E, Cannon LA, Reifart NJ, Reisman M, Abizaid A, Moses JW, Leon MB, Serruys PW. Percutaneous recanalization of chronically occluded coronary arteries: a consensus document: part I. *Circulation* 2005;112:2364-72.
2. Stone GW, Reifart NJ, Moussa I, Hoye A, Cox DA, Colombo A, Baim DS, Teirstein PS, Strauss BH, Selmon M, Mintz GS, Katoh O, Mitsudo K, Suzuki T, Tamai H, Grube E, Cannon LA, Kandzari DE, Reisman M, Schwartz RS, Bailey S, Dangas G, Mehran R, Abizaid A, Moses JW, Leon MB, Serruys PW. Percutaneous recanalization of chronically occluded coronary arteries: a consensus document: part II. *Circulation* 2005;112:2530-7.
3. Hannan EL, Racz M, Holmes DR, King SB, 3rd, Walford G, Ambrose JA, Sharma S, Katz S, Clark LT, Jones RH. Impact of completeness of percutaneous coronary intervention revascularization on long-term outcomes in the stent era. *Circulation* 2006;113:2406-12.
4. Prasad A, Rihal CS, Lennon RJ, Wiste HJ, Singh M, Holmes DR, Jr. Trends in outcomes after percutaneous coronary intervention for chronic total occlusions: a 25-year experience from the Mayo Clinic. *J Am Coll Cardiol* 2007;49:1611-8.
5. Di Mario C., Werner G., Sianos G., Galassi A., Büttner J., Dudek D., Chevalier B., Lefèvre T., Schofer J. European perspective in the recanalisation of Chronic Total Occlusions (CTO): consensus document from the EuroCTO Club. *EuroIntervention* 2008; 3:30-43.
6. Hoye A, van Domburg RT, Sonnenschein K, Serruys PW. Percutaneous coronary intervention for chronic total occlusions: the Thoraxcenter experience 1992-2002. *Eur Heart J* 2005;26:2630-6.
7. García-García HM, Kukreja N, Daemen J, Tanimoto S, van Mieghem C, Gonzalo N, van Weenen S, van der Ent M, Sianos G, de Feyter P, Serruys P.W. Contemporary treatment of patients with chronic total occlusion: critical appraisal of different state-of-the-art techniques and devices. *EuroIntervention* 2007;3:188-196.
8. Ramcharitar S, Patterson MS, van Geuns RJ, van Meighem C, Serruys PW. Technology Insight: magnetic navigation in coronary interventions. *Nat Clin Pract Cardiovasc Med* 2008;5:148-56.
9. Tsuchida K, Garcia-Garcia HM, van der Giessen WJ, McFadden EP, van der Ent M, Sianos G, Meulenbrug H, Ong AT, Serruys PW. Guidewire navigation in coronary artery stenoses using a novel magnetic navigation system: first clinical experience. *Catheter Cardiovasc Interv* 2006;67:356-63.
10. Weisz G, Moses JW. New percutaneous approaches for chronic total occlusion of coronary arteries. *Expert Rev Cardiovasc Ther* 2007;5:231-41.
11. Stone GW, Colombo A, Teirstein PS, Moses JW, Leon MB, Reifart NJ, Mintz GS, Hoye A, Cox DA, Baim DS, Strauss BH, Selmon M, Moussa I, Suzuki T, Tamai H, Katoh O, Mitsudo K, Grube E, Cannon LA, Kandzari DE, Reisman M, Schwartz RS, Bailey S, Dangas G, Mehran R, Abizaid A, Serruys PW. Percutaneous recanalization of chronically occluded coronary arteries: procedural techniques, devices, and results. *Catheter Cardiovasc Interv* 2005;66:217-36.
12. Katsuragawa M, Fujiwara H, Miyamae M, Sasayama S. Histologic studies in percutaneous transluminal coronary angioplasty for chronic total occlusion: comparison of tapering and abrupt types of occlusion and short and long occluded segments. *J Am Coll Cardiol* 1993;21:604-11.
13. Suzuki S, Furui S, Isshiki T, Kozuma K, Koyama Y, Yamamoto H, Ochiai M, Asakura Y, Ikari Y. Patients' skin dose during percutaneous coronary intervention for chronic total occlusion. *Catheter Cardiovasc Interv* 2008;71:160-4.
14. Mehran R, Aymong ED, Nikolsky E, Lasic Z, Iakovou I, Fahy M, Mintz GS, Lansky AJ, Moses JW, Stone GW, Leon MB, Dangas G. A simple risk score for prediction of contrast-induced nephropathy after percutaneous coronary intervention: development and initial validation. *J Am Coll Cardiol* 2004;44:1393-9.

15. Lemos PA. Recanalization of chronically occluded coronaries: a step forward in understanding its impact. *Catheter Cardiovasc Interv* 2008;71:E5-6.
16. Ramcharitar S, van Geuns RJ, Patterson MS, van der Giessen WJ, van der Ent M, van Domburg RT, Serruys PW. A Randomised Comparison of the Magnetic Navigation System versus Conventional Percutaneous Coronary Intervention. *Catheter Cardiovasc Interv* 2008;in press.
17. Atmakuri SR, Lev EI, Alviar C, Ibarra E, Raizner AE, Solomon SL, Kleiman NS. Initial experience with a magnetic navigation system for percutaneous coronary intervention in complex coronary artery lesions. *J Am Coll Cardiol* 2006;47:515-21.
18. Schneider MA, Hoch FV, Neuser H, Brunn J, Koller ML, Gietzen F, Schamberger R, Kerber S, Schumacher B. Magnetic-guided percutaneous coronary intervention enabled by two-dimensional guidewire steering and three-dimensional virtual angioscopy: initial experiences in daily clinical practice. *J Interv Cardiol* 2008;21:158-66.
19. Kiemeneij F, Patterson MS, Amoroso G, Laarman G, Slagboom T. Use of the Stereotaxis Niobe magnetic navigation system for percutaneous coronary intervention: results from 350 consecutive patients. *Catheter Cardiovasc Interv* 2008;71:510-6.
20. Krings T, Finney J, Niggemann P, Reinacher P, Luck N, Drexler A, Lovell J, Meyer A, Sehra R, Schauerte P, Reinges M, Hans FJ, Thron A. Magnetic versus manual guidewire manipulation in neuroradiology: in vitro results. *Neuroradiology* 2006;48:394-401.
21. Ernst S, Ouyang F, Linder C, Hertting K, Stahl F, Chun J, Hachiya H, Bansch D, Antz M, Kuck KH. Initial experience with remote catheter ablation using a novel magnetic navigation system: magnetic remote catheter ablation. *Circulation* 2004;109:1472-5.
22. Saito S, Tanaka S, Hiroe Y, Miyashita Y, Takahashi S, Satake S, Tanaka K. Angioplasty for chronic total occlusion by using tapered-tip guidewires. *Catheter Cardiovasc Interv* 2003;59:305-11.

Chapter 7

MAGNETIC NAVIGATION FOR NON-CORONARY INTERVENTIONS

Magnetically guided left ventricular lead implantation base on virtual 3D reconstructed image of the coronary sinus

EuroPACE 2008 Sep;10(9):1042-7.

Rivero-Ayerza M, Jessurun E, **Ramcharitar S** , van Belle Y, Serruys PW, Jordaens LJ

Abstract

Background:
Left ventricular lead (LV) implantation is feasible using remote magnetic navigation of a guidewire (Stereotaxis, St. Louis, MO, USA). A novel software that performs a 3-D reconstruction of vessels based on 2 or more angiographic views has recently been developed (CardiOp-B system™, Paeion Inc, Haifa, Israel).

Objectives:
To evaluate 1) the performance of the 3D reconstruction software to reproduce de anatomy of the coronary sinus (CS) and 2) the efficacy of remotely navigating a magnetic guidewire within the CS based on this reconstruction.

Methods:
In patients undergoing CRT implantation a 3D reconstruction of the CS was performed using CardiOp-B™ system. Accuracy of the reconstruction was evaluated as compared to the CS angiogram. This reconstruction was imported into the Stereotaxis system. Based on the reconstruction magnetic vectors to navigate within the CS were automatically selected and manually adjusted if needed. Feasibility of deploying the guidewire and LV lead into the selected side branch, fluoroscopy time (FT) required for cannulation of the target side branch (SB) and total FT were also evaluated.

Results:
Sixteen patients were included. In one case the software could not reconstruct the CS. The quality of the reconstruction was graded as good in 13 and poor in 2. In 10 cases manual adjustments to the traced edges of the CS was required to perform the 3-D reconstruction and in 5 no adjustments were needed. In 13 patients the target SB was engaged based on the automatically selected vectors. In 2 cases manual modification of the vector was required. Mean total FT was 23 ± 14 min and FT required to cannulate the target SB was 1.7 ± 1.3 min.

Conclusion:
A 3D reconstruction of the CS can be accurately performed using 2 angiographic views. This reconstruction allows precise magnetic navigation of a guidewire within the CS.

Introduction

Despite the technological progress aimed at improving success and reducing complication rates during cardiac resynchronization therapy (CRT) device implantation, in a proportion of cases delivery of a left ventricular (LV) pacing lead through the coronary sinus (CS) still fails. As recently demonstrated transvenous implantation of a LV pacing lead is safe and feasible using remote magnetic navigation of a guidewire (1,2). However, we encountered certain limitations in order to reach the ultimate goal of reproducibly implanting the LV lead remotely. Among these limitations was the lack of having a real-time three-dimensional (3D) CS model to facilitate more accurate navigation of the guidewire. A novel imaging system (CardiOp-B system, Paeion Inc, Haifa, Israel) is becoming an established technique for the 3D reconstruction of vessels using data obtained from standard vascular angiography (3). The reconstructed vessel can subsequently be imported to the Niobe™ (Stereotaxis, St. Louis, USA) magnetic navigation system and magnetic vectors can be selected based on this virtual model of the vessel.

Our purpose was to test the feasibility of reconstructing the anatomy of the CS using this software and evaluate the accuracy of navigating within the CS based on this 3D model.

Material and Methods

Patient Population

Sixteen consecutive patients who underwent CRT device implantation were included in this study. These patients met the standard criteria for CRT comprising of advanced heart failure refractory to medical therapy, low ejection fraction (EF) (<35 %), and a broad QRS (≥120 msec) on the electrocardiogram (ECG) with a left bundle branch block (LBBB)-like morphology. All patients gave informed consent.

Implantation Procedure:

All procedures were performed in the room equipped for magnetic navigation (Niobe™ II, Stereotaxis, St. Louis, MO, USA). In all patients the left cephalic vein was dissected. An RV shock lead (model 1580 Riata, St. Jude Medical, Sylman,CA, USA or model 6947 Sprint Quattro Secure, Medtronic Inc., Minneapolis, MN, USA) was introduced and actively fixed to the right ventricular apical wall. After a double left subclavian venous puncture, a right atrial active fixation lead (model 5076, Medtronic, Inc.) was introduced and positioned in the right atrial appendage. Pacing and sensing properties of these leads was assessed.

CS angiography and 3D reconstruction

A 9 F long guiding sheath (model Attain 6216, Medtronic, Inc.) was introduced, in order to cannulate the CS. Angiograms of the CS were performed using 30˚ LAO, AP and 30˚ RAO projec-

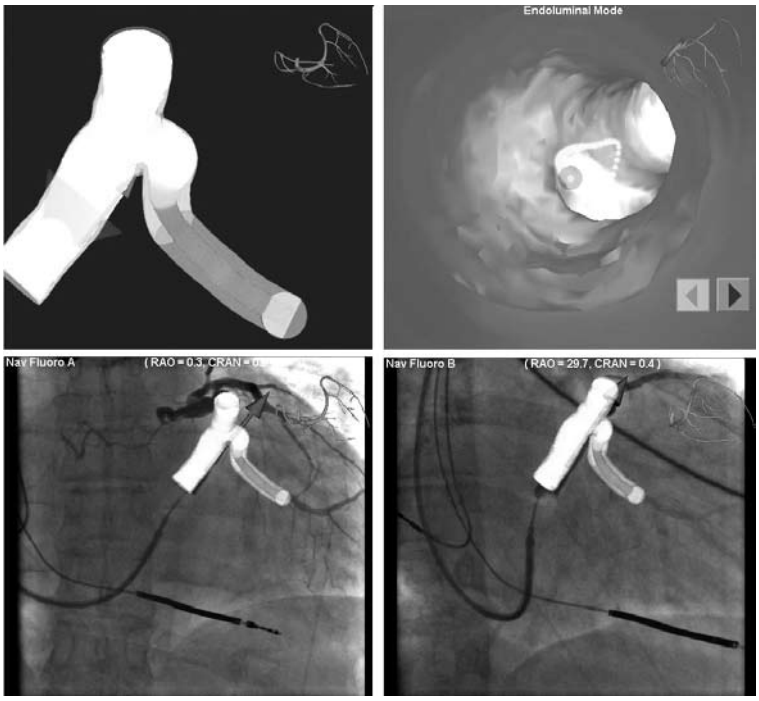

Figure 1. *Top: at the left, 3D reconstruction of the coronary sinus with one side branch in an antero-posterior view. Note the marked angulation of the lateral side-branch. At the right, a flythrough image of the reconstruction. Bottom: Reconstructed model aligned to the fluoroscopic view in LAO projection (left panel) and AP projection (right panel). In green, the automatically selected vector.*

tions (projections allowed when the magnets are in navigate position). These angiograms were imported to the CardiOp-B System™ (Paeion Inc.).

An automatic algorithm detects the vessel edges in each of the projections used for the reconstruction. In case edge detection was inaccurate (not exactly superimposed to the angiographic edge), manual adjustments could be made so as to obtain the best reconstruction possible. Based on the traced edges, and using a minimum of two complementary angiographic views, a 3D reconstruction of the vessel was performed. The system allows reconstructing the body of the vessel and one bifurcation or side branch at a time. The reconstructed 3D model of the CS and its side branch can then be imported to the Niobe™ (Stereotaxis, St. Louis, MO, USA) where, after alignment to the real time fluoroscopic views, flythrough images of the model can be used to navigate (Figure 1). The quality of the reconstruction was assessed by two operators performing the procedure and graded as i) not possible to be reconstructed, ii) poor or iii) good, after superimposing and aligning it to the real-time angiography in the LAO, AP and RAO projections (Figure 2). The need of manual adjustment of the traced edges in order to improve the quality of the reconstruction was also evaluated.

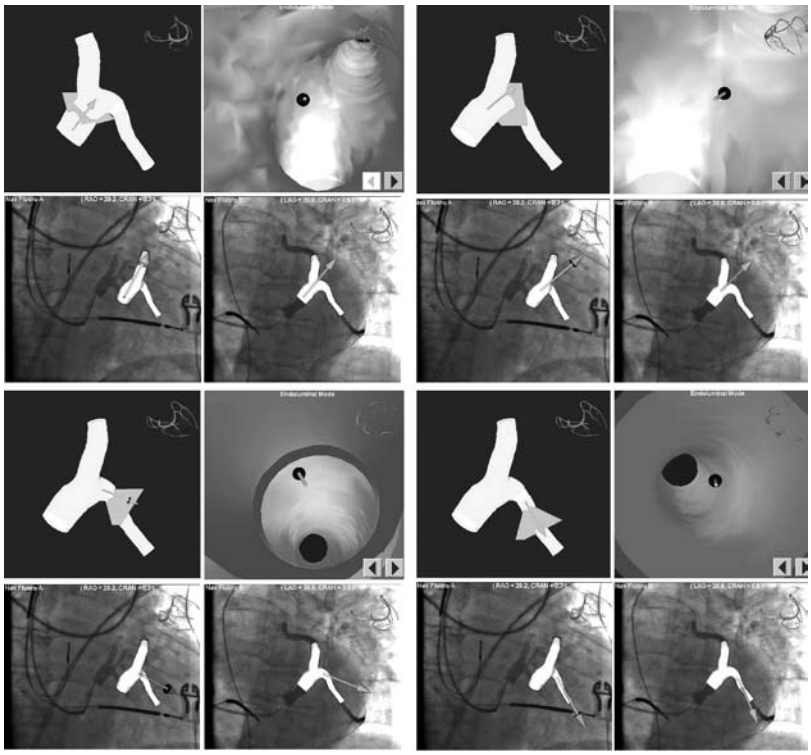

Figure 2. *Four panels, as seen in real time, showing the different automatically selected vectors (green arrows) chosen to navigate within the reconstructed coronary sinus (CS) model. In each panel, at the top left: 3D reconstruction of the CS; top right: endovascular view; bottom left: RAO projection and not aligned 3D model to facilitate visualization of the side branch; bottom right: LAO projection with aligned 3D model. Note how the vector changes according to the portion of the vessel it is aiming at.*

Magnetic navigation based on the virtual 3D image of the CS

Magnetic navigation is performed by positioning two external magnets (Stereotaxis) at each side of the table in order to generate a 0.08 Tesla magnetic field within the patient. The orientation of the magnetic field is established by the interaction the two external magnets exert with each other and can be automatically determined or specified by an operator working remotely in the viewing room. A single 2 mm neodymium iron boron magnet attached at the tip of a 0.014 guidewire (Cronus™ Soft support Endovascular Guide wire, Stereotaxis) aligns itself to the direction of the magnetic vector. In this way, by changing the orientation of the magnets, the resultant magnetic vector changes and the tip of the guidewire aligns itself in the direction of the newly applied vector. A dedicated software package, the Navigant™ (Stereotaxis) allows the full integration of the Niobe™ system and the imported CardioOp® 3D reconstruction (Paeion). In this way the vectors needed to navigate within the reconstructed vessels and to access the desired portion of the vessel, can be automatically determined by the system (Figure

2). In case the vectors suggested by the system are not accurate enough to allow access to the desired side branch, manual adjustments can be performed. In this study the guidewire was manually advanced after each modification of the magnetic field (every 3 to 5 mm steps) in order to access the ideal side branch (as previously defined by the operators). Once the target side branch was engaged an over-the-wire LV pacing lead, (Medtronic Attain, Medtronic, Inc. or QuickSite, St. Jude Medical, Sylmar, CA, USA) was introduced and lodged in the vessel. Feasibility of i) deploying the guidewire and LV lead into the selected side branch (SB) using the automatically determined vectors, ii) need of manual adjustments of these vectors, iii) fluoroscopy time (FT) required for cannulation of the target SB, iv) total FT and v) procedure time were assessed.

Results

The procedural outcome of the 16 consecutive patients included in the study is detailed in Table 1. All had a LBBB-like broad QRS complex on the ECG, a severely depressed LV ejection fraction and advanced symptoms of heart failure (NHYA functional class 3 ± 1). The mean procedure time was 99 ± 26 min, the mean FT was 23 ± 14 min and the mean FT required to position the LV lead into the target CS side branch was 1.7 ± 1.3 min.

3D reconstruction of the coronary sinus

In 15 patients (93 %) the 3D reconstruction of the CS was successfully performed. In case number 4 the software was unable to reconstruct the CS and consequently the LV lead implantation was conventionally performed. In 10 cases minor manual adjustments to the traced edges of the CS was required in order to obtain a 3-D reconstruction of good (in 8 cases) or poor (2 cases) quality. In the remaining 5 patients no manual adjustments were required in order to obtain a good reconstruction (Figure 1). Overall, the quality of the reconstruction was considered to be good in 13 cases (81 %) and poor in 2 (12 %).

LV lead implantation

In all 15 patients in whom magnetic navigation based on the reconstructed CS was performed the target side branch was successfully engaged with the magnetically steered guidewire. In 13 patients (87%) this was possible based only on the automatically selected vectors; in 2 cases (13%) manual modification of the automatically selected vectors was required in order to navigate distally in the target vessel. In one case the lead had to be definitively deployed in an anterior side branch due to lack of acceptable pacing thresholds in other locations. However, navigation all through the CS was feasible in this patient using the automatically selected vectors. In 2 other cases the LV lead had to be deployed in a different side branch than that initially targeted because they could not be engaged with the selected leads. It is interesting to note that in patient 1 after CS angiography no further fluoroscopy was required to engage the target

Table 1 – Procedure characteristics and left ventricular lead position

Patient number	Procedure Time (min)	Fluoroscopy Time (min)	LVL Fluoroscopy (min)	Target SB accessed w/ guidewire	Final LVL Location	Pacing Threshold (mV)
1	150	18,4	0,2	Yes	PL	1
2	85	36,7	3	Yes	AL	0,4
3	75	23,3	2,36	Yes	PL	0,5
4	-	-	-	Yes	PL	1.1
5	95	23,2	1,64	Yes	PL	0,7
6	140	46	0,13	Yes	Ant	1,6
7	96	14,48	4,5	Yes	L	1
8	101	19,2	0,33	Yes	L	1,2
9	75	18,4	0,26	Yes	PL	0,7
10	70	7,5	2,26	Yes	L	0,8
11	85	27,35	1,05	Yes	L	0,9
12	110	9,41	0,18	Yes	Ant	4,8
13	98	16,21	2	Yes	PL	2
14	60	8,7	3,05	Yes	L	1,5
15	110	21,42	2,4	Yes	PL	1,1
16	130	58	2,2	Yes	L	0,4
Mean (SD)	98.6 (25)	23.2 (14)	1.7 (1.3)			1.2 (1)

AL=anterolateral, Ant= anterior, LVL= left ventricular lead, L=lateral, PL= postero-lateral side, SB= coronary sinus side branch, SD= standard deviation.

Table 2 – Quality of reconstruction and Navigation

Patient number	Quality of 3D reconstruction	Edge adjustment needed	Type of navigation
1	Good	Yes	Automatic
2	Good	Yes	Automatic
3	Good	Yes	Automatic
4	Not done	-	-
5	Good	Yes	Automatic
6	Good	Yes	Automatic
7	Good	Yes	Automatic
8	Good	No	Automatic
9	Good	Yes	Automatic + Manual
10	Good	No	Automatic
11	Poor	Yes	Automatic
12	Good	No	Automatic
13	Poor	Yes	Automatic + Manual
14	Good	No	Automatic
15	Good	Yes	Automatic
16	Good	No	Automatic

side branch and position the lead. One patient suffered from diaphragmatic stimulation at high pacing output (10 V) but the lead required no repositioning because of lack of diaphragmatic capture with lower output (7.5 V). No other complications were observed during or after the procedure.

Discussion

To the best of our knowledge, this is the first reported use of 3D reconstruction software to create an accurate real-time virtual map of the CS. We demonstrate that this virtual 3D model can be integrated with the magnetic navigation system in order to allow reliable navigation within the CS. Based on the reconstructed image, the system allows automatic vector selection to guide a magnetically enabled wire to its desired position within the CS in order to later advance the LV pacing lead.

3D reconstruction of the coronary sinus

Transvenous LV lead implantation is sometimes time consuming, it may require prolonged fluoroscopy times and can eventually fail. Local complications generated by the delivery system and the occlusive angiogram of the CS (dissection of the vessel, spasm or even rupture) may lead to implantation failure. However, the main reason of implantation failure remains the sometimes challenging anatomical properties of the CS. Valvular structures, stenosis, lack of side branches, highly angulated side branches and tortuous vessels are common findings during CRT implantation. Despite continuous innovations and technological improvement of the delivery systems, guidewires and LV leads, approximately 10% of implantations attempts still fail (4).

Implantation procedures are conventionally guided by the use of fluoroscopy which offers a two dimensional view of the vessel of interest. In this way, tortuous side branches can appear foreshortened or overlapped (5) resulting in inaccurate interpretations of the anatomy and making decisions regarding selection of the appropriate material and manoeuvres needed to reach certain vessels more difficult. Magnetic navigation of guidewires was meant to help overcome these difficulties and allow access to places that using conventional technology is very challenging (6,7). The possibility of performing an accurate 3D reconstruction of a vessel that is integrated to the magnetic navigation system allows more reliable and effective navigation as compared to that guided only by fluoroscopy. The advantage of this reconstruction is that it is performed with the patient in the same position and under the same circumstances (heart rate, rhythm, hemodynamic status, etc.) than that during the implantation. This should allow more precise navigation than using imported pre-operative 3D images obtained under different circumstances than during implantation.

In our experience it was not possible to obtain a 3D model of the CS, in only one case probably due to the fact that the diameter of this particular vessel was larger than conventionally encountered. It should be borne in mind that this software was developed to reproduce the anatomy of coronary arteries which are narrower and less tortuous than the CS and its side-branches. In 2 other cases the final result was a poor reconstruction. Here, the sizes of the vessels were no different than those that were more accurately reconstructed. Probably the particular anatomy of these vessels required other fluoroscopic projections than the ones used (LAO 30˚, AP and RAO 30˚) to create the model. Nevertheless, these reconstructions were good enough to allow navigation and deployment of the guidewire into the desired side branch. In the remaining 13 cases a good quality reconstruction was obtained. In 10 cases the automatically traced contour of the vessel had to be manually modified in order to correct for inaccuracies in the interpretation of the vessel's edge. However, in most of them the end result of the reconstruction was satisfactory. Performing the 3D reconstruction, importing it to the magnetic navigation system and aligning it to the fluoroscopic views required only a few minutes and did not significantly delay the procedure. The reconstruction of the CS was performed while the implanting physician was selecting the appropriate lead, preparing it and introducing it into the guiding sheath.

This software, and its integration to the magnetic navigation system, offers a reliable 3D view of the CS and its side branches allowing precise navigation within the vessel. In all patients were reconstruction of the CS was feasible the target side branch was successfully engaged by the guidewire. In 87% of these cases this was achieved only using the automatically selected vectors and in 2 cases manual modifications were required. Using the 3D reconstruction as a model for navigation provides much more information than the fluoroscopic views and allows the system (and the operator) to more precisely interpret the side-branch location, direction, angulation and length. It is this model that is used to guide the implant, consequently potentially reducing the use of fluoroscopy and limiting the amount of projections (and contrast injections) needed to interpret the angiograms. In all the patients in whom the CS was successfully reconstructed, navigation within the CS was only based on the reconstruction irrespective of whether vectors were automatically selected or manually adjusted.

Limitations

One limitation of this technique is that the 3D model of the vessel is obtained from static images from a beating heart. Even though the fluoroscopic images used to perform the reconstruction were ECG gated, it remains a static model that is being used to guide an implantation performed in a beating heart. Also respirator movements are also not compensated for by this system. Consequently, inaccuracies of magnetic navigation based on this 3D reconstructed model may also be due to a lack of compensation for respiratory movements and cardiac cycle. Whether

developments as rotational angiography will serve as better models for magnetic navigation is another step to investigate (8). Nonetheless, these same limitations would be applicable also for this technique. However, nowadays it is not possible to integrate rotational angiography to the magnetic navigation system.

Another limitation of the present version of the software is that it allows reconstruction of the body of the vessel and only one side branch or bifurcation. In this way, in order to navigate to a different side branch than the initially selected, a new reconstruction using the second side branch was needed.

In our view, once the guiding sheath and the guidewire can be remotely advanced using an advancer system similar to the one used for radiofrequency ablation catheters (9-12), this software will allow remote LV lead implantations with minimal fluoroscopic exposure. One example is the patient in whom navigation using the reconstructed CS image was enough to engage the desired side branch without the use of fluoroscopy.

Conclusion

A reliable 3D reconstruction of the coronary sinus can be performed using at least two complementary angiographic views. This reconstruction, when integrated into the magnetic navigation system, allows accurate navigation within the vessel of a magnetically steered guidewire to perform left ventricular lead implantations.

References

1. Rivero-Ayerza M, Thornton AS, Theuns DA, Marcoen F. Scholten, Joris Mekel, Jan Res, and Luc J. Jordaens. Left ventricular lead placement within a coronary sinus side branch using remote magnetic navigation of a guidewire: a feasibility study. *J Cardiovasc Electrophysiol. 2006 Feb;17(2):128-33.*
2. Gallagher P, Martin L, Angel L and Tomassoni G. Initial clinical experience with cardiac resynchronization therapy utilizing a magnetic navigation system. *J Cardiovasc Electrophysiol. 2007 Feb;18(2):174-80.*
3. Ramcharitar S, Daeman J, Patterson M, van Guens RJ, Boersma E, Serruys PW and van der Giessen WJ. First direct in vivo comparison of two commercially available three-dimensional quantitative coronary angiography systems. *Catheter Cardiovasc Interv 2008;71:44-50*
4. DeRose JJ, Ashton RC, Belsley S, Shaw R and Ashton RC Jr. Robotically assisted left ventricular epicardial lead implantation for biventricular pacing. *J Am Coll Cardiol. 2003;41:1414-9.*
5. Rivero-Ayerza M, Jessurun E, Theuns D and Jordaens L. A grateful heart. *Europace. 2007 Jul;9(7):533*
6. Rivero-Ayerza M, van Belle Y, Mekel J and Jordaens L. Left ventricular lead implantation assisted by magnetic navigation in a patient with a persistent left superior vena cava. *Int J Cardiol. 2007 Mar 2;116(1):e15-7.*
7. Ramcharitar S, Patterson MS, van Guens RJ and Serruys PW. Magnetic navigation system used successfully to cross a crushed stent in a bifurcation that failed with conventional wires. *Catheter Cardiovasc Interv 2007;69:852-855.*
8. Mansour M, Reddy VY, Singh J, Mela T, Rasche V, Ruskin J. Three-dimensional reconstruction of the coronary sinus using rotational angiography. *J Cardiovasc Electrophysiol. 2005;16(6):675-6.*
9. Thornton AS, Janse P, Theuns DA, Scholten MF, Jordaens LJ. Magnetic navigation in AV nodal reentrant tachycardia study: early results of ablation with one- and three-magnet catheters. *Europace. 2006 Apr;8(4):225-30.*
10. Thornton AS, Rivero-Ayerza M, Knops P, Jordaens LJ. Magnetic navigation in left-sided AV reentrant tachycardias: preliminary results of a retrograde approach. J *Cardiovasc Electrophysiol. 2007 May;18(5):467-72.*
11. Ernst S, Ouyang F, Linder C, Hertting K, Stahl F, Chun J, Hachiya H, Bansch D, Antz M, Kuck KH. Initial experience with remote catheter ablation using a novel magnetic navigation system: magnetic remote catheter ablation. Circulation. 2004;109:1472-5.
12. Ernst S, Ouyang F, Linder C, Hertting K, Stahl F, Chun J, Hachiya H, Krumsdorf U, Antz M, Kuck KH. Modulation of the slow pathway in the presence of a persistent left superior caval vein using the novel magnetic navigation system Niobe. Europace. 2004;6:10-4.

MAGNETIC NAVIGATION FOR NON-CORONARY INTERVENTIONS

Magnetically Supported Procedures and Cardiac Regeneration

EuroIntervention Supplement B 2007; 2, B42-B46

Patterson MS, Duckers E, **Ramcharitar S**, Meliga E, van Weenen S, Maugenest AM, Perin E, Serruys PW,

Introduction

Cardiac failure secondary to ischaemic heart disease is a leading cause of morbidity and mortality[1]. Infarction leads to cell loss by oxidative stress and reperfusion injury. Chronic ischaemia and myocyte loss produces progressive expansion of the infarct area, fibrous replacement of the myocardium and predisposes to dilation of the left ventricle[2], a major factor in survival[3]. Progenitor/stem cell therapy has potential for promoting structural and functional repair of the myocardium.

Progenitor/stem cells may stimulate either angiogenesis[4,5] by the release of growth factors and anti-apoptotic factors (including Akt, VEGF and FGF), and/or vasodilation (by VEGF) with an increase in iNOS bioavailability that may help maintain cell viability and encourage blood flow. More controversially, progenitor/stem cells from the bone marrow, circulating blood or embryonically-derived, may lead to myocardial cell regeneration[6,7]. However to date, improvements in cardiac function and structure have been modest[8,9].

Current delivery techniques include 2-D angiographically-guided endocardial injection and catheter-based intracoronary release. However, these techniques have general limitations that include imprecise on-table identification of the best areas to target, poor ability in targeting a specific area, and mediocre identification of the treated area at follow-up. In addition, intracoronary release has specific drawbacks such as induction of ischaemia, or the 'shedding' of cells into the general circulation. Two particular clinical settings that appear particularly appropriate for progenitor/stem cell therapy are those of recent anterior myocardial infarction that results in reduced LV function and of chronic, ischaemic, and dilated cardiomyopathy.

The development and integration of electromechanical mapping technology, NOGA® XP (Biologics Delivery Systems™, Cordis Corporation, Diamond Bar, California, USA) with the development of a magnetically navigable injection catheter, the MyoStar™ Injection Catheter (Biologics Delivery Systems™), could transform cell delivery.

This article will review the principles of magnetic navigation with the forthcoming technology; consider how localisation, delivery and follow-up might potentially be improved compared with current techniques; discuss the relevance to two of the clinical settings that might derive the most benefit; and mention the possibilities of improved percutaneous revascularisation that might be used to optimise the local *milieu* for progenitor/stem cell survival. The purpose of this article is to suggest and speculate upon how this technology might allow integration of the real-time visualisation of target tissue with site-directed deliverability in order to reduce procedure times and irradiation, and to simultaneously improve efficacy and follow-up.

Magnetic navigation system

The magnetic navigation system (Niobe®, Stereotaxis, St Louis, MO, USA) consists of two adjustable permanent magnets on either side of the fluoroscopy table (Figure 1). In essence the system does three things. Firstly, the system operates using a 3-D reconstruction that is either produced from angiographic images (as in the case of coronary arteries) or, alternatively, an imported 3-D reconstruction from an external system e.g. NOGA® XP. Secondly, the spatial orientation and location of this reconstruction is matched to the real-life patient's internal cardiac anatomy i.e. coronary artery or cardiac chamber. Thirdly, the model gives the real-time, on-line vectors to direct an external magnetic field to orientate a magnet on an intravascular device to match the direction required for navigation through the 3-D reconstruction. The result is the ability to use 3-D information in real-time in patient therapy.

The magnetic navigation system has been described in detail previously[10,11]. Briefly, the interacting magnetic field produces a 15 cm uniform magnetic field of 0.08 Tesla that can be increased to 0.1 Tesla. Computer-controlled movements of the magnets allow re-direction of this externally applied magnetic field vector in 360° in all planes. For cardiac chambers a 3-D volume-rendered reconstruction is imported and aligned for navigation. For coronary artery use, the 2-D locations of points on X-ray images are known in relation to the image intensifier, angiography system and table and this allows production of a 3-D reconstruction from 2 views separated by at least 30°. The result is real-time, on-table localization of the reconstruction within the chest of a patient during a procedure to allow direction of therapy. Adjustment

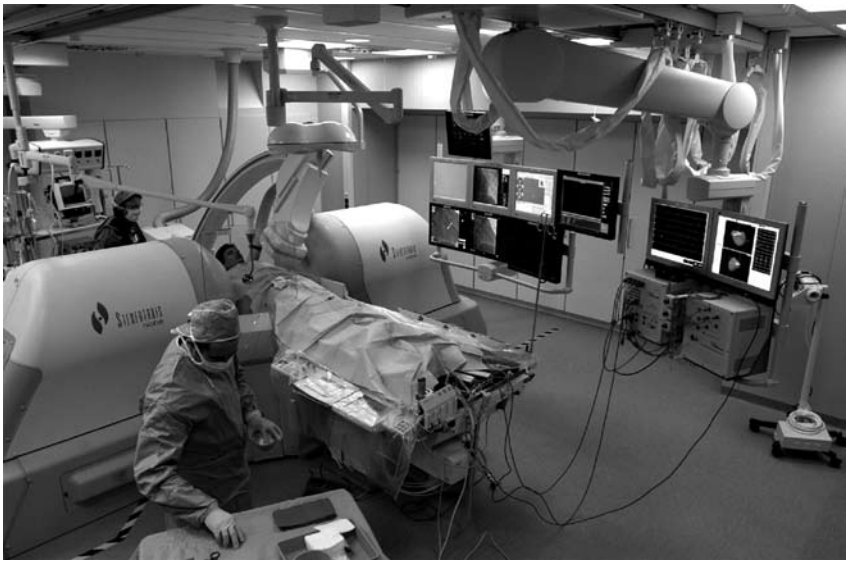

Figure 1. *Magnetic navigation system is shown with the magnets in position on either side of the patient.*

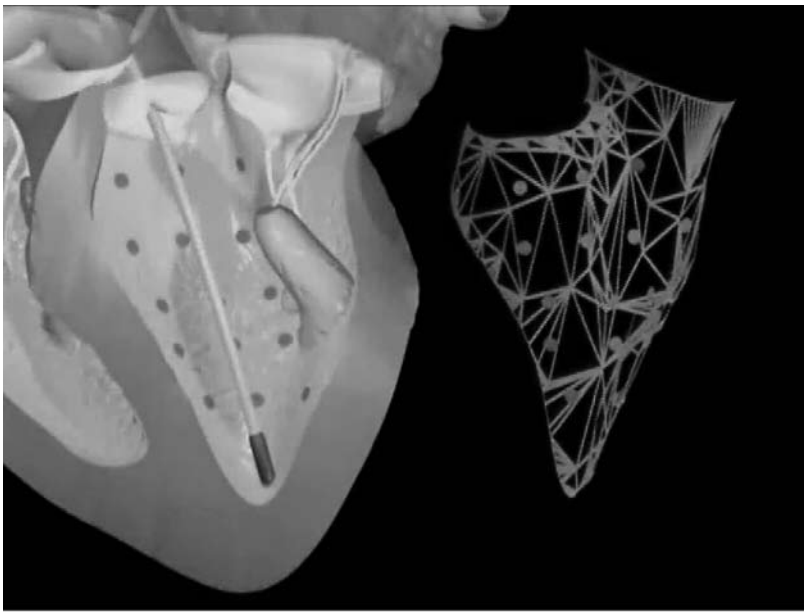

Figure 2. *Graphic showing reconstruction of LV mapping*

of the magnetic vectors from the model synchronized to the X-ray system adjusts tip-magnet direction in the patient to produce deflection of the wire. This gives reproducibly precise steering of the tip of the intravascular device and this steering is independent of the factors that can restrict conventional procedures such as poor transmission of manipulation.

New technology for progenitor/stem cell delivery

Previous methods for endocardial stem cell delivery had several drawbacks in identification, cell delivery and therapy. Identification of the sites for injections was poor and depended on strategies such as marking acetate sheets overlaid on the X-ray screen, delivery was time-consuming with poor targeting, and follow-up was hampered by imprecise knowledge of where the injections had been and therefore depended on generalised LV measurements rather then the region of interest.

The magnetic navigation system can integrate other 3-D volume rendered information such as MSCT, MRI or the NOGA® XP mapping system, (Figure 2) to give precise steering /direction of injections. Infarct localisation is possible by current techniques such as MSCT, which is capable of identifying infarcted areas of myocardium[12], and integration can provide a 3-D volume rendered map of the damaged myocardium. However this information is not real-time and was of limited use in treating the patient on the table. New technology is under current development. The NOGA® XP mapping system gives information on the functional and electrical properties

Figure 3. *MYOSTAR™ Injection Catheter to have electromechanical guidance provided by the NOGA® XP.*

of the myocardium simultaneously with real-time, precise localisation by producing a map of the left ventricle, Figure 2. This may allow differentiation between the extent of the infarct and peri-infarct regions as well as giving valuable information for follow-up. This, together with the MyoStar™ Injection Catheter to allow magnetically enabled cell delivery, Figure 3, may not only allow areas to be identified by electrical and mechanical mapping measurements but also deliver injections of cell therapy.

Potentially, this could give several major advantages. Firstly, integration of real-time electromechanical mapping would give a real-time, on-table 3-D LV map for exact localisation. Secondly, electromechanical mapping may discriminate between viable and non-viable infarcted areas e.g. identifying electrically active but non-contractile areas such as stunned myocardium. Therefore this combination of detection methods could enable new strategies that tailor delivery of cell therapy to particular areas. Thirdly, a magnetically navigable injection catheter could precisely direct cell injection and simultaneously integrate spatial and electrical information. Fourthly, an electromechanical map could aid follow-up both to identify the region on the map that was previously treated, and also to give quantifiable information for specific locations on the map. Definable delivery of stem cells would allow investigation of specific locations or patterns of cell delivery. As different parts of an infarcted area may have discordant electrical and mechanical properties, the effect of injection of penumbral regions with intact electrical but poor mechanical activity that might indicate stunned myocardium may be easier to clarify. Additionally, current estimates of the resolution of the new system suggest that this could localise positions to within 1mmthat would represent a major improvement. An idea of the type of the information that may be available with this system for diagnosis and follow-up is seen in Figure 4.

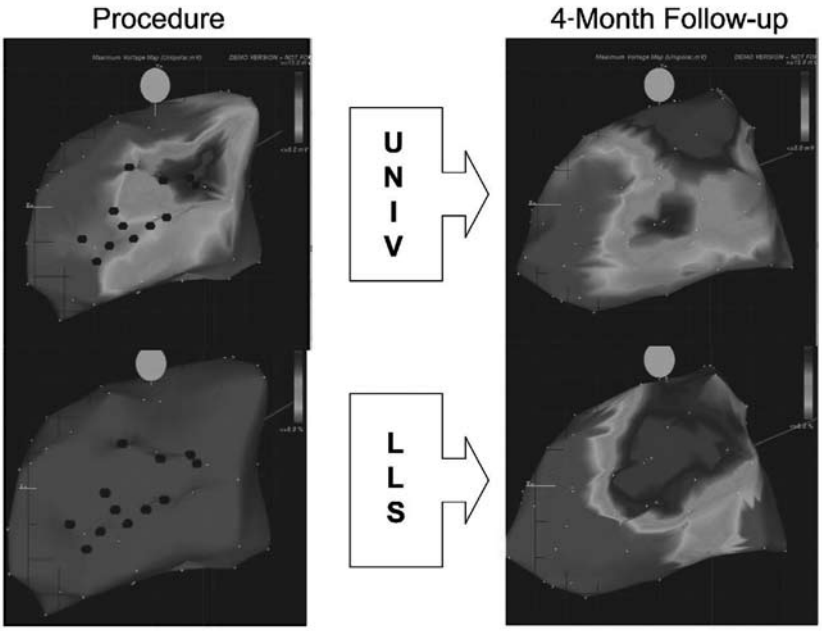

***Figure 4**. NOGA™ electrical (UNIV, at top) and mechanical (LLS, at bottom) maps from a human patient in the stem cell treatment group. The maps on the left are those performed at the time of injection and maps at right are those at 4-month follow-up. An area of viability, showing normal electrical activity, can be noted on the upper-right map. The maps on the right show improvement in both electrical and mechanical function. LLS = linear local shortening; UNIV = unipolar voltage.*

Limitations of current cell delivery techniques

The strategy of endocardial injection has suffered from a number of limitations. The current technique of LV angiography gives mediocre localisation as the entire LV volume is seen only in 2-D pictures from different views. This technique gives little idea of the location of the watershed or penumbral area that might contain stunned rather then necrotic cells. Injection sites, and particularly areas that might be particularly susceptible to improvement with cell therapy, are poorly identifiable in real-time, and are difficult to access with current equipment. Intracoronary injection has been the other widely used technique and has its' own limitations. Release of cells depends on haematogenous spread and this may be poor in areas that are poorly revascularised or are still occluded, therefore reducing the effectiveness in these areas. This inhomogeneous delivery may prevent delivery to salvageable areas that have competitive flow from a neighbouring territory that is, however, insufficient for long-term survival. As intracoronary injection often uses occlusion of the proximal vessel this results in further ischaemic insult with further, possibly irreversible, damage and cell loss and reduced perfusion pressure leading to collapse of pinched microvasculature. Additionally, loss of cells that do pass through

the microvasculature into the general circulation, also known as 'shedding', may lead to the drawback of these progenitor cells reaching areas where conditions favourable for angiogenesis are present but clinically unwanted, e.g. neoplastic neovascularisation or ischaemic areas such as retinopathy.

Implications for the clinical situation of cell delivery

Two particular situations may be particularly appropriate for treatment of cell therapy; these are recent anterior infarction with significant LV impairment and non-revascularisable chronic ischaemic cardiomyopathy. While these situations have some similarity such as extensive cell loss, unattractiveness for cardiothoracic surgery, there are specific reasons why precisely directed endocardial injection may hold particular advantages. These have advantages over and above the general advantages of improved diagnosis with two modalities, precise site-directed delivery and follow-up discussed above. The purpose of using cell therapy in the treatment of recent acute MI is to prevent maladaptation or remodelling and so preserve LV contractile function and thus exercises tolerance. This group may be the most effective group to treat with cell therapy in order to maximise myocardial cell salvage. As discussed above endocardial injection may be advantageous over intracoronary delivery as it delivers cells to areas that have a restricted or absent blood supply. This direct delivery via the endocardium overcomes the problem of tissue swelling related to ischaemic damage that may cause pinching of the microvasculature to reduce haematogenous delivery to peripheral sections of the infarct territory i.e. to the penumbral areas that may be particularly suitable for salvage. In addition, endocardial injection decreases shedding of cells into the circulation since cells are injected within the tissue thus placing decreased numbers of cells into the bloodstream

.

In the treatment of chronic heart failure there has already been tissue loss and often, this is combined with severe ischaemic coronary disease. Cell therapy aims to reverse the chronic changes by improving the vascular bed and salvaging as much myocardium as possible. This situation would particularly benefit from addition of new myocardial cells, although the ability to produce new myocytes remains controversial. Precise delivery to electrically and mechanically definable areas could allow uniform coverage or other distributions to target specific areas. In addition the risk of perforation of a thin myocardium may be minimised by use of electrical signals via the adjustable and retractable needle providing exact depth control together with monitoring of the ECG for reverse potentials.

Revascularisation

A further option enabled by the magnetic navigation system is the ability to treat complex coronary disease. As the predominant cause of LV dysfunction is ischaemic heart disease, the

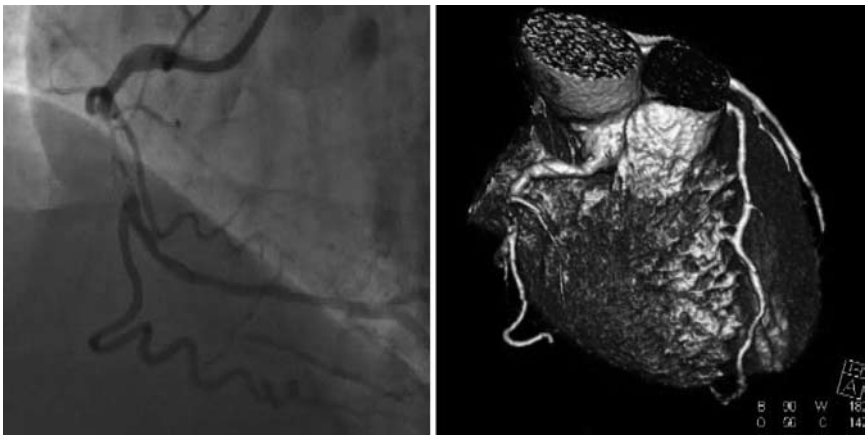

Figure 5. *The panel on the left shows the raw data from angiography and the panel on the right shows the reconstructed MSCT.*

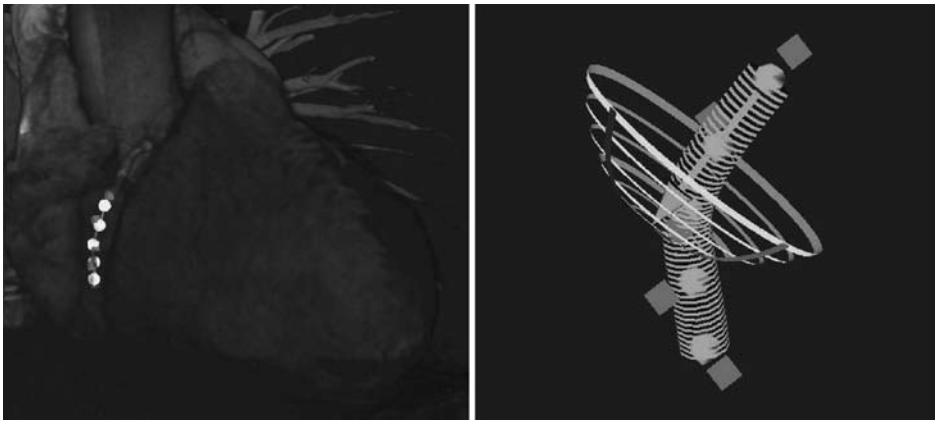

Figure 6. *The panel on the left shows the co-registered points applied to the MSCT image that was imported into Navigant and the panel on the right shows the computer reconstructed pathway that is derived from CT and projected onto the reconstruction in Navigant.*

partial or complete recovery of the native coronary circulation may encourage both recovery of native myocytes and provide a milieu for better uptake and differentiation of stem cells.

The ability of the system to support PCI has been demonstrated in a number of scenarios from simple to complex lesions[13] and evidence suggests that this system may be particularly advantageous in more difficult anatomy[14] and is capable of successfully treating CTOs[15]. The integration of MSCT data, Figure 5, allows the missing segment of the vessel to be judged, Figure 6, and the superimposition of this data by co-registration gives an indication of the pathway.

Conclusion

Magnetic navigation may aid the performance of cardiac stem cell transplantation by allowing integration of spatially-localised, 3-D volume-rendered information with real-time tissue visualisation in multiple modalities to give site-directed deliverability to reduce procedure times and irradiation, and improve efficacy simultaneously. The development of the NOGA® XP system and the magnetically navigable MyoStar™ Injection Catheter may lead to improved detection of non-functional myocardium, better delivery and more precise follow-up.

Acknowledgement

The authors are grateful to Joep Maeijer for his help in the preparation of the images.

References

1. World Health Organization (WHO). The atlas of heart disease and stroke. Geneva: World Health Organization; 2004.
2. Pfeffer, J.M., Pfeffer, M.A., Fletcher, P.J. & Braunwald, E. Progressive ventricular remodeling in rat with myocardial infarction. *Am. J. Physiol.* 1991 260; H1406–1414.
3. White HD ,Norris RM ,Brown MA ,Brandt PW, Whitlock RM ,Wild CJ. Left ventricular end systolic volume as the major determinant of survival after recovery from myocardial infarction. *Circulation* 1987 76; 44–51.
4. Kocher AA, Schuster MD, Szabolcs MJ, Takuma S, Burkhoff D, Wang J, Homma S, Edwards NM, Itescu S. Neovascularization of ischemic myocardium by human bone-marrow– derived angioblasts prevents cardiomyocyte apoptosis, reduces remodeling and improves cardiac function. *Nat Med*. 2001 7:430–436.
5. Tse HF, Kwong YL, Chan JK, Lo G, Ho CL, Lau CP. Angiogenesis in ischaemic myocardium by intramyocardial autologous bone marrow mononuclear cell implantation. *Lancet*. 2003 361:47–49.
6. Tomita S, Li RK, Weisel RD, Mickle DA, Kim EJ, Sakai T, Jia ZQ. Autologous transplantation of bone marrow cells improves damaged heart function. Circulation 1999 100: 247–256.
7. Makino S, Fukuda K, Miyoshi S, Konishi F, Kodama H, Pan J, Sano M, Takahashi T, Hori S, Abe H, Hata J, Umezawa A, Ogawa S. Cardiomyocytes can be generated from marrow stromal cells in vitro. J. Clin. Invest. 1999 103: 697–705.
8. Assmus B, Schachinger V, Teupe C, Britten M, Lehmann R, Dobert N, Grunwald F, Aicher A, Urbich C, Martin H, Hoelzer D, Dimmeler S, Zeiher AM. Transplantation of progenitor cells and regeneration enhancement in acute myocardial infarction. (TOPCARE-AMI). *Circulation*. 2002;106:3009–3017.
9. Meyer GP, Wollert KC, Lotz J, Steffens J, Lippolt P, Fichtner S, Hecker H, Schaefer A, Arseniev L, Hertenstein B, Ganser A, Drexler H Intracoronary bone marrow cell transfer after myocardial infarction: eighteen months' follow-up data from the randomized, controlled BOOST (BOne marrOw transfer to enhance ST-elevation infarct regeneration) trial. Circulation. 2006 113; 10:1272-4.
10. Tsuchida K, Garcia-Garcia HM, van der Giessen WJ, McFadden EP, van der Ent M, Sianos G, Meulenbrug H, Ong AT, Serruys PW. Guidewire navigation in coronary artery stenoses using a novel magnetic navigation system: first clinical experience. Catheter Cardiovasc Interv. 2006 Mar;67(3):356-63.
11. Patterson MS, Schotten J, van Mieghem C, Kiemeneij F, Serruys PW. Magnetic Navigation in Percutaneous Coronary Intervention. Journal of Interventional Cardiology. 2006;19:558–565.
12. Nieman K, Cury RC, Fecencik M, Nomura CH, Abbara S, Hoffman U, Gold HK. Jang I-K, Brady TJ. Differentiation of recent and chronic myocardial infarction by cardiac computed tomography. AJC 2006; doi:10.1016/j.amjcard.2006.01.101.
13. Patterson MS, van Geuns RJ, Tanimoto S, Tsuchida K, Serruys PW. Magnetic Navigation with the Endo-Luminal View and the X-ray overlay - Major advances in novel technology. Eurointervention in press
14. Ramcharitar S, Patterson MS, Serruys PW. Randomised controlled study comparing conventional wires with magnetic guided wires in a tortuous phantom. Submitted for publication.
15. García-García HM, Tsuchida K, van Mieghem C, Daemen J, van Weenen S, Patterson M, van der Ent M, van der Giessen WJ, Meulenbrug H, Sehra R, de Feyter P, Serruys PW. Multi-Slice Computed Tomography and Magnetic Navigation - Initial experience of cutting edge new technology in the treatment of Chronic Total Occlusions. *Eurointervention in press.*

Chapter 8

SELECTED CASES

Magnetically Supported PCI: Success after failed surgery and conventional PCI

Cath Lab Digest 2007 (15) 03,1-14

Patterson M, **Ramcharitar** S, Serruys PW

Introduction

Magnetically supported PCI is starting to deliver on its potential to improve and extend several aspects of percutaneous cardiac treatment. In particular, the ability to control tip direction more accurately and independently of bends or friction has allowed increased utilization. We present a patient in whom both surgery and previous conventional PCI failed to produce a satisfactory long-term result. The use of magnetic navigation allowed for successful revascularization of an extremely tortuous conduit, restoring blood supply to a large territory of myocardium.

The System

The Niobe® II magnetic navigation system (MNS: Stereotaxis, St Louis, Missouri) has two external magnets that produce a 15-cm uniform magnetic field. Through computer-controlled magnet movements, the magnetic field can be directed 360˚ in all planes. When the field is changed, the deflection of the magnet at the wire tip also changes, resulting in reproducibly precise steering. The system has an adjustable touch screen at the lab table that is the interface between the operator and the MNS (Figure 1). The current system has three main advantages with regards to tortuosity. First, it produces a 3-D, volume-rendered reconstruction from angiographic images, providing better morphological information about the artery. Second, the spatial coordinates, or location, of the reconstruction within the patient are known. Third, the model gives real-

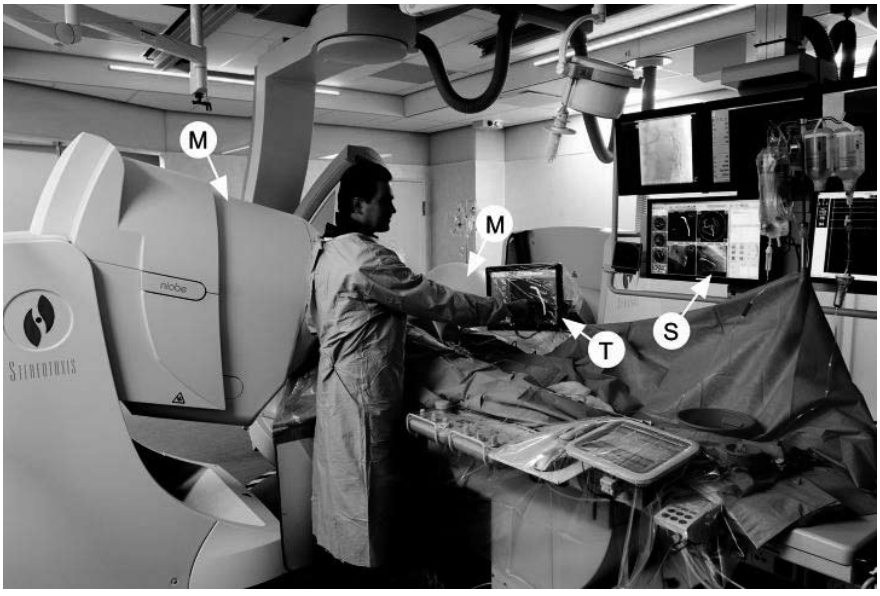

Figure 1. *System in position for PCI. M indicates magnets in tilt position for better lateral movement of the image intensifier. T indicates touch screen interface to give real-time instruction to the MNS. S indicates in-lab main screen monitor.*

time, on-line vectors, which direct the external magnetic field to navigate the wire through the 3-D reconstruction. As a result, operators have the ability to utilize 3-D information in real-time patient therapy.

System costs. The current list price for the Stereotaxis Magnetic Navigation System is $1.9 million. The size of a typical modern Stereotaxis cath lab room is 770 square feet (72 square meters). The cost of magnetic shielding generally ranges from $50,000–$100,000 and consists of minimal common steel shielding in the walls, ceiling and floor.

There is a range of magnetically enabled Stereotaxis 0.014" guidewires that are priced at a marginal premium over conventional wires. All other PCI equipment is standard and compatible with the Stereotaxis guidewires and MNS. No additional consumable items are required. All third-party billing occurs as part of a standard PCI intervention; therefore, all current reimbursement applies and there is no effect on current billing practices

Case Report

This report describes a 60-year-old man with multiple medical pathologies and a burdened cardiac history. Past medical history included severe airways disease (FEV1 of 1 litre), ulcerative colitis with chronic iron deficiency anemia despite iron therapy, previous GI bleeding, gout, hypertension and hypecholesterolaemia, and a family history of ischemic heart disease and peripheral vessel disease.

The patient had undergone an aortic valve replacement 8 months earlier for significant calcific aortic stenosis. At that time, he received a jump saphenous vein graft (SVG) that anastomosed to the obtuse marginal branch (OM) and then the right posterior descending coronary artery (RDP). At the time of the operation, the cardiothoracic surgeon had noted that although the RCA had been grafted, it was heavily calcified, of poor quality and not suitable for further surgical treatment. The patient had a difficult recovery after the coronary artery bypass graft (CABG) operation with persistent hypotension, in part due to episodes of arrhythmia such as sinus bradycardia that was externally paced, and also atrial fibrillation (AF), for which he was later cardioverted. He had some generalized oedema and, once extubated, dyspnoea that resolved slowly.

Unfortunately, 2 months after surgery, the patient again began to suffer with chest pains (despite a satisfactory Hb) that could not be fully controlled with medication. Angiography showed the proximal end of the graft was occluded but a section of graft between the OM and the RDP was still patent. However, this remaining section of the SVG was compromised by severe lesions at both anastomoses with an adversely acute angle in the stenosis just before the OM anastomosis (Figure 2). .

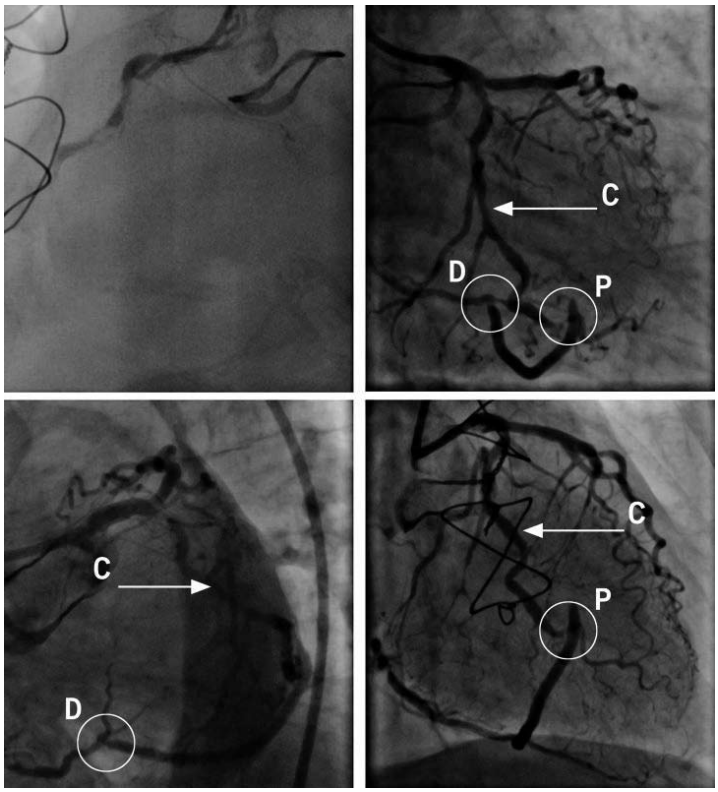

***Figure 2**. The top left panel shows the occluded RCA that could not be opened anterogradely. The other three panels are different views showing Cx tortuousity and severe lesions at proximal and distal anastomoses of the SVG. C indicates the Cx. P indicates the proximal anastomosis. D indicates the distal anastomosis*

Further surgery was refused and conventional PCI using biplane angiography was attempted, with a view to reopening the RCA or if unsuccessful, intervening on the tortuous Cx-OM-SVG-RDP (Cx: circumflex artery). The RCA was heavily calcified. Despite the use of stiff occlusion wires and a variety of balloons for support, a wire could not be passed and the attempt was stopped due to the presence of dissection. An attempt to pass the wire into the SVG via the left coronary artery (LCA) was unsuccessful due to tortuosity and despite the use of multiple catheters and wires. For the attempts on both vessels, a total of 5 guiding catheters and 7 angioplasty guide wires, including Asahi Miracle 3, Asahi Miracle 6 (Abbott Vascular Devices, Redwood City, CA) and Crosswire NT (Terumo Medical Corporation, Somerset, NJ), were used.

The Magnetic Procedure

Reconstruction. A decision was made to attempt a further procedure with the MNS. A 3-D reconstruction (Figures 3–4) showed that the sum of all the angles from the LMS to the RCA was over 1180˚ (equivalent to over 3 complete turns of a corkscrew). Currently, an analysis of the reasons for prolonged procedures (with respect to wire passage across a lesion) is ongoing. Both the

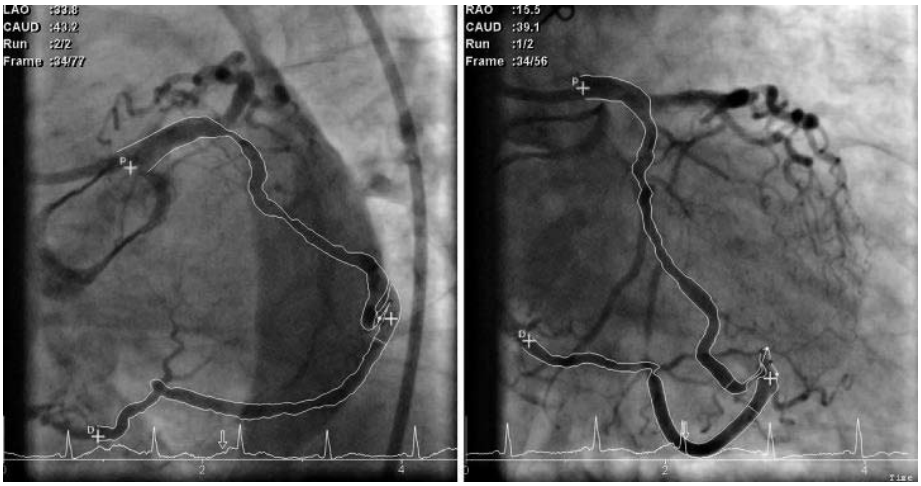

Figure 3. *Panels showing different fluoroscopy views with vessel edges marked by edge detection software (CardiOp-B, Paieon Medical Inc., Rosh Ha'ayin, Israel) before reconstruction. P indicates proximal point. D indicates distal point*

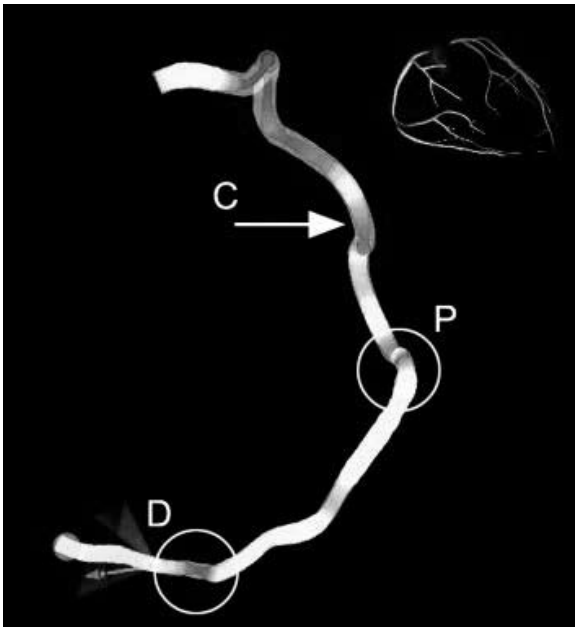

Figure 4. *Three-dimensional reconstruction of target pathway. C indicates the tortuous Cx. P indicates the proximal anastomosis. D indicates the distal anastomosis*

number of bends and the degree of angulation seem to be strongly related to a prolonged crossing time. Each bend adds friction to conventional wire rotation and therefore steering, and this friction becomes greater as the angulation increases (as the wire is more deformed and

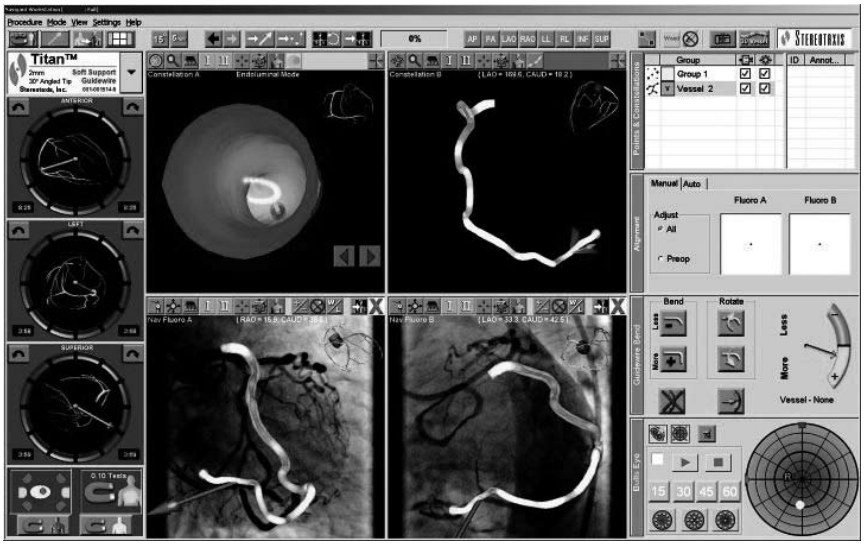

Figure 5. *Screen of Stereotaxis Navigant program during procedure, showing top left panel with endoluminal view. The top right panel shows the reconstruction. The bottom 2 panels are static-captured fluoroscopy images with the reconstruction for that angle superimposed.*

may also be pushed more forcefully against the vessel wall). Thus, the cumulative angulation may be extremely relevant to procedural duration and success.

Navigation. One of the prime benefits of the MNS 3-D reconstruction is that it provides an endoluminal view with a computed 3-D center line (Figure 5). This view offers a tailored direction for the magnetic field vector at every point in the vessel. There is also a white-line overlay that is a roadmap on the fluoroscopy screen. Tip advancement is shown on the white-line overlay in tandem with operator advancement of the wire. The 3-D vector changes simultaneously to keep the wire pointing down the chosen path. The Titan™ Soft Support 2 mm angled tip wire (Cordis Corp., Miami, FL) was navigated through the tortuous LMS, Cx and OM using the vectors as far as the stenosis before the first anastomosis (with the adverse angle). At this stage, finer navigation was required to reach the SVG. Careful interrogation, by changing the angulation using the endoluminal view (the vector can be changed in the endoluminal view by double-tapping the screen at any point), and increasing the magnetic field strength to 0.1 Tesla, managed to get the wire tip to angulate enough to pass into the body of the graft. At this point, a 1.5 mm Maverick over-the-wire balloon (Boston Scientific Corp., Natick, MA) was passed to the graft body and used for support. The wire was then advanced through the graft using vector control and then into the RDP. In order to maximize support, the balloon was advanced to the RDP and an Iron Man support wire (Abbott Vascular) exchanged.

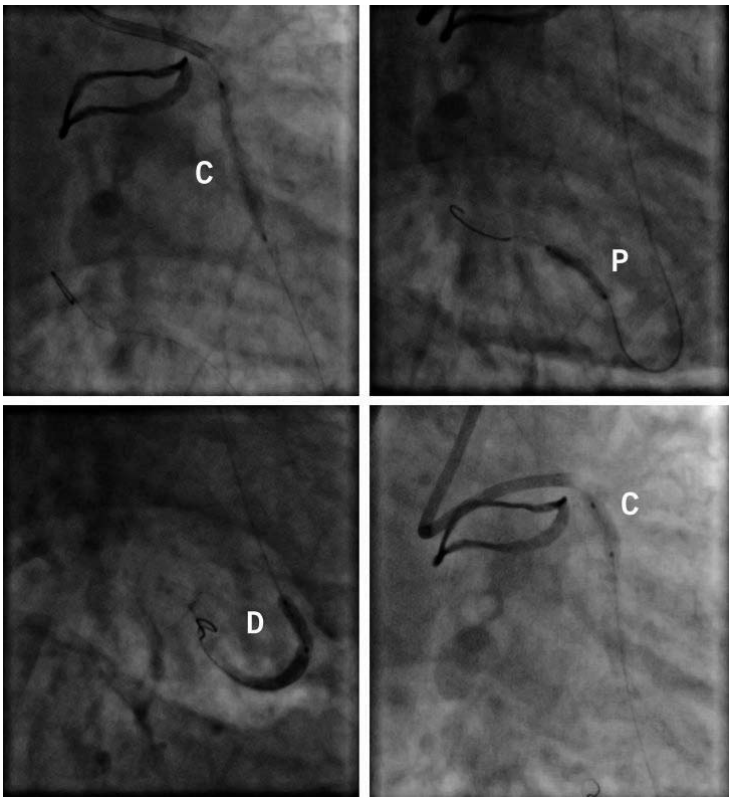

***Figure 6**. Interventions. The top left panel shows predilation of Cx. The top right panel shows stent placement in distal anastomosis. The bottom left panel shows stent deployment at the proximal anastomosis. The bottom right panel shows one of the stents being deployed in the Cx. C indicates the Cx. P indicates the proximal anastomosis. D indicates the distal anastomosis.*

Intervention. Both anastomoses were predilated. However, on the first attempt to pass a stent, there was excess resistance in the Cx that nearly caused wire retraction. The Cx was predilated, and both the anastomoses and the Cx were then stented (Figure 6). There was a good result, with TIMI-3 flow at the conclusion of the procedure (Figure 7).

Discussion

The potential advantages of magnetic navigation are especially relevant to excessively tortuous vessels. It is in these cases where the advantages of magnetic steering are most obvious over conventional procedures:

1) A conventional procedure has to use the same tip shape throughout. While appropriate for some angles, it is not ideal for multiple bends of varying angulation.

2) Once inside the patient, the tip shape of a conventional wire cannot be changed without retrieving the wire and losing position or exchanging through a support catheter.

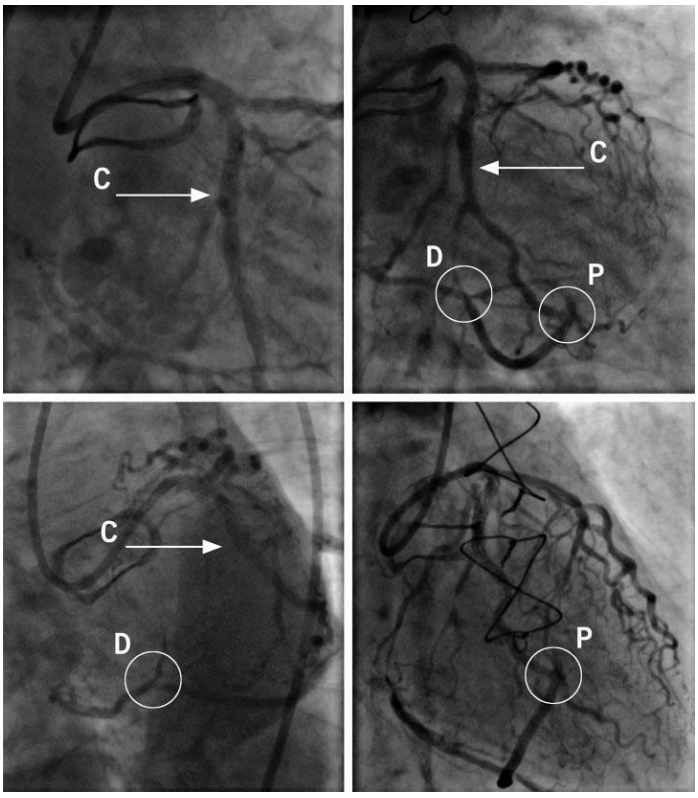

Figure 7. *Results of stenting form different views. C indicates the Cx. P indicates the proximal anastomosis. D indicates the distal anastomosis.*

3) After a conventional wire has been passed distally, there may be resistance when trying to rotate the wire tip for manipulation.

In contrast, the tip of a magnetically-enabled wire can be directed at will in any direction. Therefore, the tip shape is variable at will, is adjustable in situ for a particular bend and is independent of rotation of the wire (and thus friction from the bends in the vessel). Such abilities may be of significant benefit in challenging cases.

While the system is relatively intuitive and usable after minimal experience, we are finding that further improvement continues steadily as the range of additional features is explored. The experience at our institutions is a little over 350 cases and rising. A variety of randomization studies and registries are currently ongoing or under analysis.

Future Directions

The MNS has other potentially valuable capabilities. For PCI, the integration of other 3-D, volume-rendered imaging such as multislice computed tomography (MSCT) as well as the possibility of other useful functions such as magnetically-navigable ablation or remote control

navigation, may prove advantageous. In addition, the integration of data such as the electromechanical maps from the Carto RMT™ system (Cordis) may enhance procedures such as stem cell therapy.

Limitations

Software. While 3-D imaging represents improved appreciation of coronary anatomy compared to the 2-D black-and-white x-ray images that have been the standard manner of visualizing coronary arteries, the current reconstructions are static. Dynamic road-mapping is an area under development.

Hardware. The internal guide wire magnets are currently rigid 3 mm wire tips, with a 2 mm option. While the rigidity can potentially restrict the movement of the magnet tip in a lesion of less than 3 mm diameter, to date, there has been only a mild clinical impact, mainly when attempting to enter side branches that may come off at right angles within a tight lesion. A flexible tip (with several magnets) is under development for enhanced navigation.

Strategies. The range of options within the system translate into a number of possible strategies that may develop in an evolutionary fashion. One example of a hybrid strategy is the manipulation of an angled wire without a magnetic field, bringing in the magnets as necessary. The use of presets and the 2-D clockface allow for relatively speedy use of the system, and may better suit procedures in simple lesions or where time plays a role, such as primary PCI. Performing a 3-D reconstruction may give a better idea of the anatomy and provide more individually tailored pre-calculated vectors for navigation. Bringing together reconstructions from diagnostic images and using navigation with the white-line overlay and minimal contrast may be helpful when it is necessary to reduce contrast volume. Additionally, 3-D reconstruction may be especially useful in extremely long and tortuous segments.

Conclusions

MNS has been shown to aid PCI of complex and tortuous vessels. System capabilities, together with other current and forthcoming options, indicate that MNS could have a major impact on the performance of PCI. In our opinion, the finer wire tip control, the extended anatomical information, the potential for integration in using other 3-D sources such as MSCT in real-time, together with forthcoming developments such as flexible wire-tips, ablative wire-tips and navigable injection catheters, may produce a formidable system.

SELECTED CASES

Primary Percutaneous Coronary Intervention using Magnetic Navigation

Eurointervention 2007, 12,

Riezebos RK, Patterson MS, Braat JH, **Ramcharitar S**, Serruys PW, Kiemeneij F

Abstract

Primary percutaneous coronary intervention is a situation that can benefit from the advantages of magnetic navigation. This case describes the use of this novel system to rapidly perform a complex primary PCI. Magnetic navigation has distinct advantages including the guidance of wire orientation on 3D information such as preset vectors, precise deflection that obviates the need for wire rotation. In addition magnet navigation offers the possibility to reconstruct a tailored 3D model that can be used to facilitate complex procedures.

Introduction

The rapid restoration of full TIMI 3 flow is crucial in primary percutaneous coronary intervention (PCI) (1). However, angiographic success is not always obtained (2-6). Magnetic navigation might facilitated primary PCI by allowing more accurate manipulation. However, there has been concern that the use of this procedure could delay reperfusion. The magnetic navigation system (MNS: Stereotaxis, St Louis, Missouri, USA) can be used immediately by using the preset vector control or freestyle navigation with the 2D clockface view, Figure 1. The system allows for precise navigation without the need for excessive wire rotation. In case of more complex anatomy, a 3D reconstruction can be used (Software: CardiOp-B: Paieon Medical Inc., Rosh Ha'ayin, Israel) for individualized navigation (7). This report describes the feasibility of the MNS to quickly and successfully complete a complex primary PCI that involved aspiration thrombectomy and a bifurcation procedure.

Case report

A 48 year old man presented to the Emergency Department with an evolving STEMI requiring immediate reperfusion. Angiography showed a proximal occlusion of the Left Circumflexus (LCx) with an obvious filling defect and TIMI 0 distal flow, see Figure 2. A Titan™ 3mm angled Soft Support wire was chosen. While the wire and an aspiration catheter were brought and prepared, the patient was put in the magnetic isocenter position by visualizing the catheter tip and cardiac silhouette on X-ray in 2 orthogonal views. Navigation was performed using preset

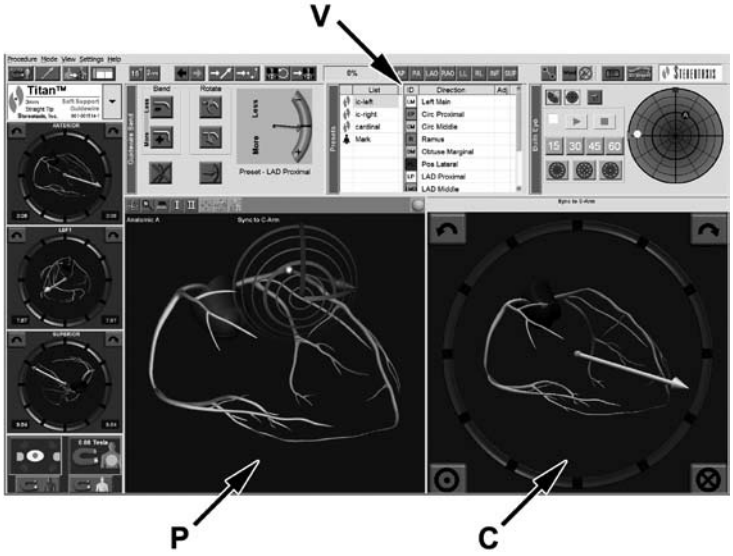

Figure 1. *The screen of the Navigant workstation, the panel (P) shows virtual coronary tree of the preset navigation with the list of preset vectors (V) seen above. The panel (C) shows the 2D clockface.*

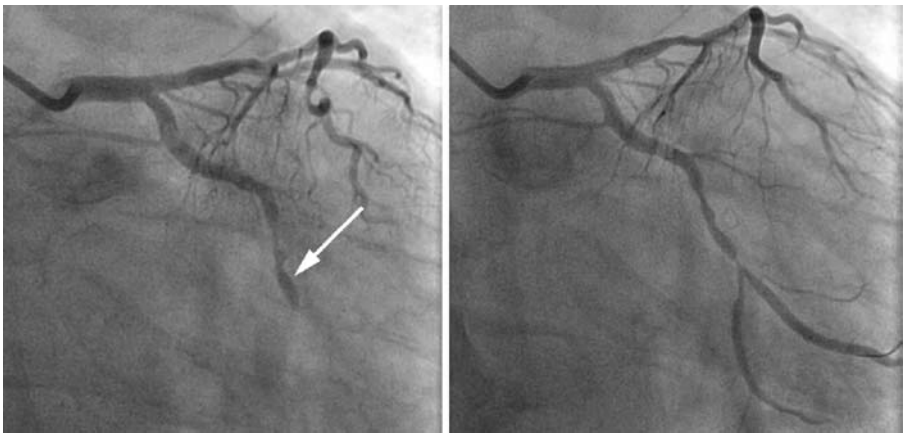

Figure 2. *The left panal shows the occluded OM branch with an eccentric lesion, more irregular on the superior aspect, before the occlusion, the right panel shows the restoration of flow to 2 distal branches after aspiration thrombectomy.*

vectors through the Left Main Stem (LMS) and proximal LCx to reach the lesion. The lesion was eccentric and more irregular on the superior aspect, see figure 2. An inferior vector was selected on the 2D clock freestyle navigation to cross this section in order to reduce contact and possible dislodgement of material. The crossing time from the tip of the catheter was 28 seconds and 2 ml of contrast was given. Contrast injection confirmed TIMI 1 flow and an aspiration catheter removed a large portion of the thrombus to produce TIMI 3 flow in 2 branches but with obvious residual stenoses, see Figure 2. A 3.0 x 25mm Skylor™ produced a good result in the main branch, but there was pinching of the ostium of the sidebranch, see Figure 3.

It was decided to fenestrate the stent into the sidebranch. The passage of a second Titan™ 3mm angled Soft Support wire into the sidebranch took 8 seconds with no contrast used. Kissing balloons produced a good result with TIMI 3 flow in both vessels, see Figure 4.

Discussion

There is strong evidence that swift restoration of flow in the obstructed infarct artery after the onset of symptoms of a STEMI is key determinant of short – and long term outcome. (3-7) Therefore, current guidelines advocate rapid evaluation for reperfusion therapy and the prompt implementation of a reperfusion therapy at presentation. (1) PCI is a very effective method for re-establishing coronary perfusion and is suitable for approximately 90% of patients. (2-6) In cases with more complex anatomy the magnetic navigation system may provide extra benefits such as 3D reconstruction. (7) The magnetic navigation system uses two permanent magnets, mounted on mechanical positioners, on either side of the fluoroscopy table. (7) These magnets create an interacting magnetic field to produce an approximately spherical 15 cm uniform

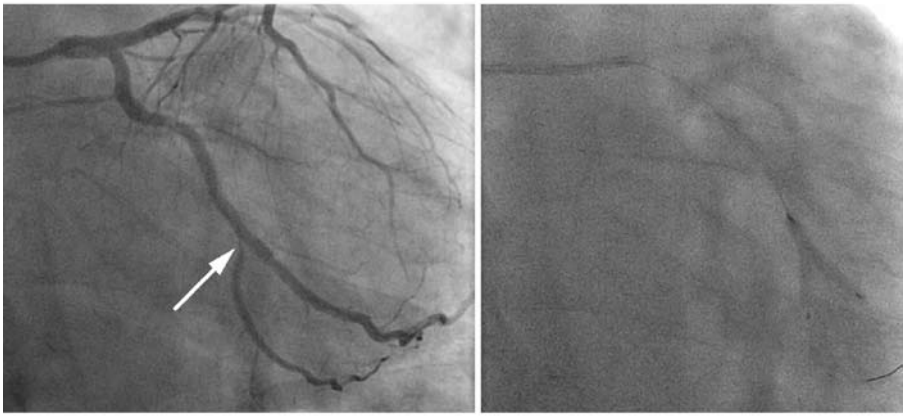

Figure 3. *The left panal shows the result of the stent with pinching of the ostium (arrowed) to the inferior branch, the right panel shows the deployment of kissing balloons*

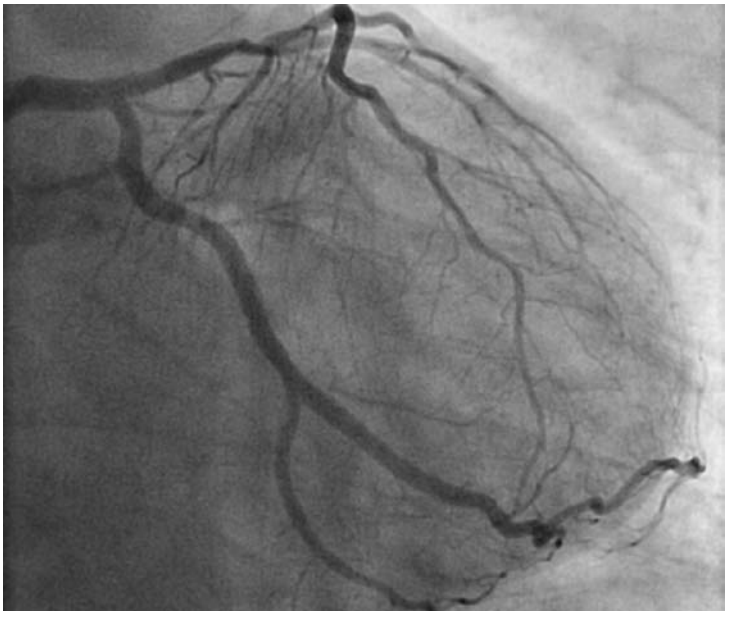

Figure 4. *The final result showing TIMI 3 flow in both distal branches*

magnetic field of 0.08 T. The movement of the magnets allows the direction of the applied magnetic field vector to be orientated in 360° on all planes. The result is control of direction of the wire tip, *in vivo,* without the need for a preshaped wire tip angle.

The current case demonstrates that the procedure can be performed rapidly during primary PCI with the use of 2D controls such as the use of preset vectors or the 2D clockface. However, should more complex anatomy be uncovered, then an interactive 3D coronary model can be

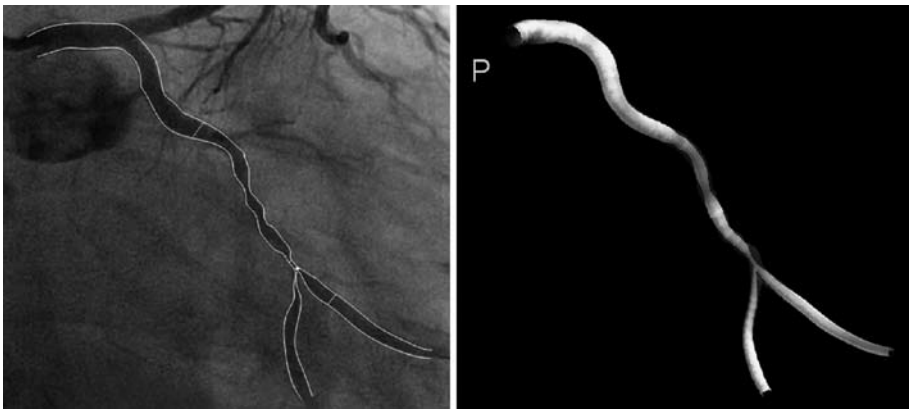

Figure 5. *The left panel shows the edges detected on the fluoroscopy image (2 views required), the right panel shows the 3 dimensional reconstruction of the infarct related coronary artery.*

created from two views allowing accurate individualized navigation, see Figure 5. Theoretically, the MNS may have two particular benefits in primary PCI. First, precise control of the magnetic tip needs less movement when compared with conventional wires that must be rotated to steer. This improves not only the navigation to, but also past an eccentric thrombus-laden lesion. Possibly this may help to reduce thrombus dislodgement and subsequent distal embolization. (8) Second, the lack of rotation of a second wire reduces the risk of wire entwinement that could both impair steering and smooth balloon delivery.

Conclusion

Primary PCI is not only feasible with the MNS but may give procedural advantages. Furthermore, the option of 3D reconstruction is available when complex anatomy is uncovered. This case demonstrates the feasibility of the MNS to rapidly perform primary PCI and support complex procedures that sometimes occur in this emergent situation.

Acknowledgement

The authors are grateful to Joep Maeijer for help with preparation of the images.

References

1. Antman EM, Anbe DT, Armstrong PW, Bates ER, Green LA, Hand M, Hochman JS, Krumholz HM, Kushner FG, Lamas GA, Mullany CJ, Ornato JP, Pearle DL, Sloan MA, Smith SC Jr. ACC/AHA guidelines for the management of patients with ST-elevation myocardial infarction: executive summary: a report of the ACC/AHA Task Force on Practice Guidelines (Committee to Revise the 1999 Guidelines on the Management of Patients With Acute Myocardial Infarction). J Am Coll Cardiol 2004;44:671–719.
2. Weaver WD, Simes RJ, Betriu A, Grines CL, Zijlstra F, Garcia E, Grinfeld L, Gibbons RJ, Ribeiro EE, DeWood MA, Ribichini F. Comparison of primary coronary angioplasty and intravenous thrombolytic therapy for acute myocardial infarction: a quantitative review. JAMA 1997;278:2093-8. [Erratum, JAMA 1998;279:1876.]
3. Zijlstra F, Hoorntje JC, de Boer MJ, Reiffers S, Miedema K, Ottervanger JP, van 't Hof AW, Suryapranata H. Long-term benefit of primary angioplasty as compared with thrombolytic therapy for acute myocardial infarction. N Engl J Med 1999;341:1413-9.
4. The Global Use of Strategies to Open Occluded Coronary Arteries in Acute Coronary Syndromes (GUSTO IIb) Angioplasty Substudy Investigators. A clinical trial comparing primary coronary angioplasty with tissue plasminogen activator for acute myocardial infarction. N Engl J Med 1997;336:1621-8. [Erratum, N Engl J Med 1997;337:287.]
5. Keeley EC, Boura JA, Grines CL. Primary angioplasty versus intravenous thrombolytic therapy for acute myocardial infarction: a quantitative review of 23 randomised trials. Lancet 2003;361:13-20.
6. Boersma E, Primary Coronary Angioplasty vs. Thrombolysis Group. Does time matter? A pooled analysis of randomized clinical trials comparing primary percutaneous coronary intervention and inhospital fibrinolysis in acute myocardial infarction patients. Eur Heart J 2006;27: 779-88.
7. Patterson M, Schotten J, van Mieghem C, Kiemeneiji F, Serruys PW. Magnetic Navigation in Percutaneous Coronary Intervention: J Interven Cardiol 2006;19:558–565

SUMMARY AND CONCLUSIONS

Magnetic Navigation in Percutaneous Coronary and Non-Coronary Interventions

SUMMARY

Interventional cardiology has embraced many novel technologies to push the frontiers in managing more complex lesions. As such, the evolution of the drug stents with the ability to limit restenosis has radically changed the way we approach a lesion, enabling the latent creativity entwined in our minds to be effectively realized. But one area that has resisted change thus far has been technologies aimed specifically at lesion crossing and in particular the co-integration of 3 dimensional imaging modalities to guide a procedure. The magnetic navigation system (MNS) addresses both these issues by its ability to redirect wires without externally reshaping the tip and by creating a 3 dimensional road map that also can be view endoluminally. The aim of this Thesis was to critically evaluate the current technology within the field of interventional cardiology.

Following an introduction, Chapter 2 evaluated both the current hardware and the software. We were able to show that the MNS significantly reduces both the crossing and fluoroscopy times in tortuous coronary phantom models achieving excellent success rates with dramatic reductions in guidewire usage. Operators with prior MNS experience had an advantage over the inexperienced thus effectively demonstrating the need for a learning curve. In evaluating the software we found that an alternative 3 dimensional reconstruction software, the CAAS 5 3D QCA system had a greater degree of accuracy and precision in both the luminal and area measurements than the Navigant® CardiOp-B 3D QCA system. We identified weakness in the system such as the catheter based calibration methodology.

Concentric phantoms used for the validation are however not representative of the eccentricity of the plaque or the natural complexity in a dynamically beating heart. So in Chapter 3 we identified the types of patients most likely to benefit from the magnetic navigation system. Multivariable logistic regression and linear shrinkage with bootstrapping were used to develop a clinical prediction rule that dichotomised cases into easy or difficult (prolonged crossing time). A relationship was demonstrable between complexity that took into account both the vessel and lesion characteristics (so called Naviscore) and prolongation of crossing times with conventional wires. When investigated in routine cases the MNS had overall longer crossing and fluoroscopy times than conventional wires (72.9 ± 50.3sec vs. 58.1 ± 47.2sec, $p<0.001$ and 66.2 ± 44.1sec vs. 55.2 ± 44.4sec $p=0.03$ respectively. But, there was a trend to support a potential advantage in more complex vessels as identified by the Naviscore. Interestingly, by simultaneously employing a virtual roadmap there was a small but significant reduction in contrast usage.

We proceeded in Chapter 4 to evaluate selective complex lesions. We found that in routine bifurcation the MNS had greater crossing success despite being slower and was useful in

managing failed standard wire cases. It was more effective in crossing double rather than single layers of stent struts by retracting and changing the tip direction at the proximity of the carina to engage an alternative set of cells. As a prelude to investigating chronically occluded vessels in Chapter 5 we showed that it was possible to directly co-integrate a CTCA scan and create a road map for the angiographically "missing segment". This led to a concept paper demonstrating the possibility of using a pre-procedural CTCA scan to directly perform an intervention without contrast agents. It opened the possibility to effectively move away from the use of 2-dimensional radiographic imaging which has inherent limitations in both lesion and vessel characterizations.

In assessing the Thoraxcenter's overall experience in using magnetically enabled wires to manage CTOs we reported in Chapter 6 that crossing success rose from initially 40% to a maximum of 56% over 52 months. But there were relatively high procedural bailouts with conventional PCI techniques, which meant that currently there was no additional advantage of the MNS over the more sophisticated conventional CTO wires. Importantly we were able to show that CTCA co-integration did not influence procedural outcome but found that higher magnetic wire successes were observed in low calcified lesions, those with a central stump and without bridging collaterals. In Chapter 7, the system was shown to be effective in guiding left ventricular lead implantation based on the virtually 3D reconstructed image of the coronary sinus. The chapter also examined the methodology and equipment required for a magnetically enabled injection needle to facilitate precise stem cell implantation within the myocardium.

CONCLUSIONS

The magnetic navigation system can be safely applied to non-selective percutaneous coronary and non-coronary interventions. But technical limitations with the current system curtail its potential advantage over conventional wires approaches in a PCI setting. The rigid 2-3mm long magnetic tip wires restricts the degree of flexibility achieved with the smoother transition of the tip and the shaft apparent in the more sophisticated standard conventional wires. Moreover the 'ocular-hand coordination' of the 'seasoned' conventional PCI operator seems currently unbeatable since time is loss in moving the large external magnets to realign with the desired vectors. It is also an expensive technology that has a learning curve for both the operator and the technical staff. But its novel approach of redirecting a device in the body together with the ability to effectively co-integrate 3-dimensional information within its software has the potential to revolutionise the manner in which percutaneous intervention is currently performed.

SAMENVATTING EN CONCLUSIE

Magnetische Navigatie in Percutane Coronaire en Niet-Coronaire Interventies

SAMENVATTING

Interventie cardiologie heeft vele nieuwe technologieën omhelst om de grenzen te verkennen van complexe lesies. Het gebruik van drug eluting stents heeft niet alleen geresulteerd in een afname van in-stent stenose, maar ook de wijze waarop wij lesies benaderen. Echter, de wijze waarop stenoses gepasseerd worden tijdens een procedure zijn tot op heden aan innovatieve ontwikkelingen ontsnapt, in het bijzonder het integreren van 3 dimensionale beeldweergave tijdens de procedure. Het magnetische navigatiesysteem (MNS) heeft de potentie om beide problemen op te lossen daar de voerdraden opnieuw te richten zijn zonder deze handmatig te vervormen alsmede de mogelijkheid om gebruik te maken van een 3D weergave van de coronairarteriën samen met een virtueel lumen. Het doel van dit proefschrift is de huidige technologie binnen de interventie cardiologie kritisch te evalueren.

Na een inleiding, wordt in Hoofdstuk 2 ingegaan op de gebruikte (MNS) hardware en software. Wij konden aantonen dat MNS fluoroscopie tijden, de tijd die nodig is om een lesie te passeren en het gebruik van voerdraden drastisch te reduceren in fantoom modellen. Interventie cardiologen die ervaring met MNS hadden, bleken een voordeel over onervaren cardiologen te hebben, hetgeen duidelijk aangeeft dat er sprake is van een leercurve. Bij de evaluatie van de software vonden wij dat één van de 3D software systemen, het CAAS 5 3D QCA systeem een grotere graad van nauwkeurigheid en precisie heeft dan het 3D QCA systeem van Navigant® CardiOp-B met betrekking tot het lumen/ area van het. Wij identificeerden beperkingen in het systeem met betrekking tot de kalibratie methode.

De concentrische fantomen die voor de validatie worden gebruikt zijn tot op heden niet representatief voor de excentriciteit van de plaque of de natuurlijke complexiteit in een dynamisch kloppend hart. In Hoofdstuk 3 identificeerden wij patiënten die mogelijk het meest van het magnetische navigatiesysteem zullen profiteren. Multivariable logistische regressie en de lineaire shrinkage met bootstrapping werden gebruikt om te voorspellen welke lesies eenvoudig of moeilijk te passeren zijn. Een correlatie werd aangetoond tussen de kenmerken van de lesie en het vat (zogenaamde Naviscore) en vertraging bij het passeren van de stenose ten opzicht van conventionele voerdraden. Routinematig gebruik bij niet geselecteerde patiënten toonde een langere passagetijd en fluoroscopie tijd aan bij het gebruik van conventionele draden (72.9 ± 50.3sec versus 58.1 ± 47.2sec, $p< 0.001$ en 66.2 ± 44.1sec versus 55.2 ± 44.4sec respectievelijk $p=0.03$). Er bleek echter wel een trend in het voordeel van complexe procedures (geïdentificeerd door Naviscore). Opmerkelijk was de significante reductie in het gebruik van contrastvloeistof bij het gelijktijdig gebruik van een virtuele 3D reconstructie van de coronairarteriën.

In Hoofdstuk 4 ligt het accent op het evalueren van geselecteerde complexe lesies. Wij vonden dat in bifurcatielesies MNS een beter passerend vermogen had ondanks de tragere passagetijd.

MNS bleek efficiënter in de passage van overlappende (dubbel gelaagde) stent struts ter hoogte van het ostium van een zijtak dan een enkele laag stent struts door vermogen om de voerdraad terug te trekken en van richting te laten veranderen door gebruik te maken van de magneet. Als voorloper van de onderzoeken bij chronisch afgesloten coronairarteriën in Hoofdstuk 5 toonden wij aan dat het integreren van CTscan van de coronairarteriën (CTCA), waarmee het mogelijk is een 3D reconstructie van de volledig afgesloten coronairarterie (CTO) te maken. Dit leidde tot het concept waarbij de mogelijkheid om een pre-procedurele CTCA te gebruiken om een interventie uit te voeren zonder contrastvloeistof. Dit opende vervolgens de mogelijkheid om alternatieve beeldvormende technieken te gebruiken dan de standaard 2-D röntgen met bijbehorende technische beperkingen.

Bij de evaluatie van onze ervaringen bij het gebruik van magneet navigatie voerdraden om CTOs te passeren rapporteren wij in Hoofdstuk 6 het toegenomen succes van aanvankelijk 40% tot een maximum van 56% over een periode van 52 maanden. Een belangrijke observatie was echter het hoge percentage bailout PCI procedures met conventionele technieken, hetgeen het extra voordeel van MNS techniek ten opzichte van verfijnde conventionele CTO draden teniet deed. Belangrijk was ook dat het mede-integreren van CTCA het resultaat niet beïnvloedde, hoewel dit succespercentage hoger was in stenoses met weinig kalk, centrale stomp en zonder het overbruggen van collateralen. In Hoofdstuk 7, laten we zien dat het plaatsen van een linker ventrikel lead met behulp van MNS effectief is, wanneer gebruik gemaakt wordt van 3D reconstructie. In dit hoofdstuk wordt ook aandacht geschonken aan de methodologie en het materiaal dat voor een toegelaten magnetisch injectienaald wordt vereist en de nauwkeurige implantatie van de stamcellen binnen het myocardium te vergemakkelijken.

CONCLUSIES

Het magnetische navigatiesysteem kan veilig op niet-selectieve percutane coronaire en niet-coronaire interventies worden toegepast. Het is belangrijk hierbij op te merken dat dit systeem nog technische beperkingen heeft. De stijve 2-3mm lange magnetische tip van de voerdraden beperkt gewenste flexibiliteit in vergijking met verfijndere standaard conventionele voerdraden met een geleidelijke overgang tussen de schacht en tip van de voerdraad. Bovendien schijnt de `oog-handcoördinatie' van de ervaren interventie cardioloog bij conventionele PCI momenteel onverslaanbaar, daar veel tijd verloren gaat bij het bewegen van de grote externe magneten in de gewenste vectoren. Verder dient te worden opgemerkt dat er sprake van een dure technologie, waarbij sprake is van een leercurve. Deze nieuwe techniek om voerdraden gericht te sturen, alsook de mogelijkheid om effectief gebruik te maken van 3D beeldvormende technieken hebben de potentie om de huidige praktijk van percutane interventie technieken drastisch te veranderen.

ACKNOWLEDGEMENTS

My journey to the Thoraxcenter began following Professor Serruys's EuroPCR05 opening ceremony lecture. I was mystified by his charisma and the manner he captivated his audience with the broad spectrum of research he commanded. The Thoraxcenter sounded like a truly fascinating place, filled with high tech futuristic 'stuff' that could have been taken out of a Stephen Spielberg movie. I was smitten by what I saw at that meeting, so much so that I waited for an opportune moment to approach Prof just as he was about to climb up the elevator to chair yet another session with a request that would he consider having me as one of his fellows. It was a truly scary encounter as I was unsure as to how he would react but my fears were unfounded when his forehead furrowed to enquire further about my background and said that I should send him my CV. I could not believe I had just spoken to the Professor Serruys. Nervously I attended the interviews despite being reassured by Angela (Hoye) that all would be fine. At the interviews I met several people who later became great colleagues and earnest friends. Wiliem (Barthelemy) who I must thank for organising my BIG registration, accommodation and a very expensive Dutch language course. Anja, a truly amazing lady who magically can fit you into Professor's busy agenda. Anja has been a 'tour de force' in keeping us fellows abreast to Professor wishes and without her help many would be lost and so deserves overwhelming thanks. That morning I met Prof in his office where on his desk laid on top of several dozen of down loaded emails was my CV and several journals with pages folded back on articles and neatly stacked one above each other. Prof was meticulous as he went through my CV and explained what the Thoraxcenter demanded from her fellows. I so wanted to be there that I would have accepted anything that he asked of me no matter how tough the task could have been. This was probably very naïve since after I started and Prof went through the numerous projects I did not realise that I had to choose just one rather than everything he offered.

The many projects did however widen my knowledge and allow me to meet many fascinating people associated with the Thoraxcenter. There was always something to talk about, to have an opinion on or to discuss ideas with. None more so than with Jurgen a true master of IVUS who I was fortunate to sit next to in BD 412. Jurg always had time for the fellows and without his help I could never get through many of the presentation or publications. A genius in Photoshop only surpassed by the great Jan Tuin and his protégé Rakesh. Their great sense of humour and calming personalities could resolve any global catastrophe…. including oil crises and wars. I learnt an amazing amount of grey scale IVUS from Jurg and maybe also some VH (when there is no calcium around) 'I like my coffee black like my soul' will always be recognised as his anthem. Apart from Jurg, I was fortunate to share a room with many Dutch Arts and Clinical Fellows. I inherited my desk from Sophia, now an interventional cardiologist in Athens – a very caring person, ripe full of energy, fond of mobile phones and I must thank her for my first article. Amongst the other clinical fellows Neville from London and Anne Louise from Denmark shared the on calls

and I thank them for cross covering patients on the cardiology wards. Thanks Anne Louise for the many free classical concerts at de Doelen. I owe a lot to the Dutch Arts, Ramon, Marco, Celia, Arend, Annemien and Bodewijn, for helping me with my consenting of patients. Special thanks to Carl with whom I shared projects on CT and magnetic navigation. His enthusiasm for the projects was much appreciated and together with Bob, Annick and Francesca, the guys from radiology a great part of this Thesis would not have realised. I cannot leave radiology without mentioning Sharon, who with her persuasive yet charming personality can get any fellow to do her CFR and FFR measurements. I learnt a lot from her and hopefully we can work together in the future. It's been my pleasure also to know Carlos van Mieghem, an amazing scientist and great colleague who I cannot thank enough for his kindest, guidance and cherished friendship. Koen Nieman, Peter Barliss and Joanna although the time we crossed paths was rather short it was fun to know you all and I hope that we will keep in touch. Of the research guys I must thank Joost for all the help with statistics and sorting out my numerous computer problems. Hector and Nieves for their help with SECRITT, Yoshi and Shuzhuo for helping me with Prof's powerpoint presentations and Emanule for being just there to chat about nice cars, Italian life and many wise things in general.

I am indebt to all the catheter lab staff for their training and for acquiring the data used to make Thesis possible. Firstly, Marjo, Caroline and Elza for organising cases so that there was enough time to get data. It was a pleasure to work with them and I am truly grateful for letting me do a fair share of spoedje. Kim, Evelyn, Marianne, Nico and Dick, what can I say apart from kleine 'xxxx' mevrouw. I wish you all could have let me know what I was saying much sooner. I could have been arrested but then again I was in Holland after all. It's been a great experience to know you all and I must thank you for making me feel at home with all the YouTube videos and toasties. Enormous thanks goes to the many technicians who went beyond the call of duty to help with QCA, data acquisition and 3D reconstructions. Sanders, the last Dutch convict to escape from Australia, many thanks for the electronic database. I hope that you will invite me to your next leaving party… or welcome back party … whatever comes first??. Gio you've been wonderful in sorting out the magnetic system and I am sure that you will agree that Toto would never be same after Robert made his mark on the dance floor. To Anne Marie, John and Elco thanks for being so helpful and for never saying no when it came to data acquisition for the magnetic system. Paul, Peter and the big guy Rob thank you for correcting my Dutch letters ….you all are such good liars – as I know that they did not really improved with time. As for the clinical research team- Arno, Mattie, Cecile, and Stein without your earnest input (METC approval) many of the technology described in this Thesis could not be used, and also thanks for all the chocolates you fed me between cases. To Titia, Mieke and the guys on CCU and Ward 1200, I greatly appreciate the efforts made to speak in English.

I am truly grateful for the skills and training that I received from the senior cardiologist. It was a real pleasure to be taught by Martin and George on how to tackle an occlusion. I thank them both and knew that I must have learnt something when Martin would leave me to get on with the cases whilst he was in CCU. George your skills are incredible, thanks for sharing the knowledge on how to manipulate a guide catheter and the technique of 'doucement'. Wim and Pim what can I say, pure geniuses in the lab so cool, so calm and so gifted. Wim I must thank you and Helene for showing me how to deliver stents in pigs. I thoroughly enjoyed your love for the good music of the yesteryear. I remain baffled by Pim de Feyter ability to cross a lesion that seem to require Magnetic Navigation with his bare hands and be so modest about it…. his mantra of 'Oops it just slipped in …I am telling you Steve'. To Evelyn and Eric thanks very much for many cases and looking after the welfare of the fellows. It is a hard job and both of you do it very well and we really appreciate it. Peter you're just a truly great guy, a passionate person whose attention to detail I admire tremendously and hope to emulate. To the guys from outside, Arie and Attila, - a heartily thanks for the all the cases you gave me whilst on call. I must not forget the EP guys for all their help especially Prof Luc, Maximo, the two Emile(s), Rob and …. together with the people I worked with at Cardialysis. Especially to Marie -Angele, Micheal, Monique and Gerrit for all their help.

There are several people who were directly connected with the papers in this Thesis that I must thank. Mark (Patterson) for laying the foundation for things to develop. Fredinand (Kiemeneij) for his enthusiasm on the subject of extending MNS to PCI. Eric (Boersma), Ron (van Domburg), Saskia (Wemelsfelder) and together with numerous people from Stereotaxis and Siemens. But special mention to Heather (Dury), Michael (Diaz), Emmanuel (de Pins), John (Lovell), Diran (Guiliguian) David (Curd) and Paul (Preziotti) from Stereotaxis and Cheng Yang (Xu), Erik (Bush), Thomas (Flohr) and Dr Klaus (Klingenbeck) from Siemens. Importantly, I also wish to thank my examiners and Erasmus for the opportunity to defend this Thesis.

Finally… to Prof and Robert jan

Robert Jan, it was a shear pleasure to work with you. Without your help I could have never done a Thesis on an entirely new subject whilst being fully in the lab and that is a testament to your input to the numerous different projects. Our working relationship was special and I had great admiration in the fact that you are willing to try something new and wacky in the lab whenever it was possible. Our strong friendship meant that we shared great times out of the lab… sometimes a little crazy with me piggy-backing on your bike all over Rotterdam… such good memories. I hope that we will continue to work together in the future.

Dear Professor, the Thoraxcenter has been everything you said it would be when you spoke in EuroPCR05. I was privileged to be a part of the experience and sincerely thank you for giving me

the opportunity to come to Rotterdam. I thoroughly enjoyed the Science, the People and the City. I am truly grateful for you taking me under your wings in the lab, working late in the attic to read each sentence of my paper, restructuring and correcting the English. Moreover teaching me how to think as an interventionist, how to challenge the norm and to push the envelope in order to improve our current practices – 'Steve - PCI is not in the hands but in your head'. Although Prof, I also believe that it is also in YOUR hands and guess most people in this passionate field of interventional cardiology knows and respect this. Certainly, I have never come across anyone who works as hard as you, keep so many ideas afloat and take a personal interest in the welfare of so many people. It is therefore with the utmost salutation and admiration that I sincerely thank you for this Thesis.

A little bit more…

I would like to thank Veronique, my mum and dad together with my two sisters Anna and Mary for everything else and seeing me through - 'From Trinidad to the Thoraxcenter an unexpected journey'.

CURRICULUM VITAE

Steve Ramcharitar was born in Trinidad. He graduated with a first class degree in Chemistry and Biochemistry from London. After obtaining a PhD on the synthesis of antibiotics under Sir Jack Baldwin FRS in Oxford he researched on Encoded Combinatorial Libraries with Sir Sydney Brenner FRS Nobel Laureate-Medicine 2002 at Scripps Research Institute, La Jolla USA. As a Royal Society and the Japan Society for the Promotion of Science (JSPS) Fellowship awardee he researched on BINAP mediated Asymmetric Hydrogenation with Professor Ryoji Noyori Nobel Laureate-Chemistry 2001 in Nagoya, Japan. During his medical schooling as the University's Pre-Clinical Advisor's Medical Scholar he worked with Sir Edwin Southern FRS on DNA sequencing by hybridisation and was elected a Foulkes Foundation Fellow. He did his basic medical training at the John Radcliffe Hospital, Oxford, UK and is currently a Cardiology Specialist Registrar at Glenfield Hospital, Leicester UK with Professor Tony Gershlick. He obtained a Diploma in Interventional Cardiology from Professor Patrick Serruys at Thoraxcenter.

Publications

1. 'Synthesis and Stereoselective Chemistry of a Novel Cyclopentadienyl Sulphone' G.M.P Gliblin, S.H. Ramcharitar and N.S. Simpkins, *Tetrahedron Lett*., 1988, **29**, 4197
2. 'Intramolecular Palladium-catalysed Cross Coupling: a Route to α-Oxo-βγ-unsaturated Macrolides', J.E. Baldwin, R.M. Adlington and S.H. Ramcharitar, *J. Chem.Soc., Chem. Commun*., 1991, 940
3. 'Intramolecular Palladium-catalysed Cross Coupling: a Route to α-Oxo-βγ-unsaturated Macrolides', J.E. Baldwin, R.M. Adlington and S.H. Ramcharitar, *Tetrahedron*, 1992, **48**, 2957,
4. 'Free Radical Macrocyclisation via Propiolate Ester', J.E. Baldwin, R.M. Adlington and S.H. Ramcharitar, *Tetrahedron*., 1992, **48**, 3413,
5. 'A Short Asymmetric Synthesis of (R,R)-(-)-Pyrenophorin', J.E. Baldwin, R.M. Adlington and S.H. Ramcharitar, *Synlett*., 1992, 875
6. Ramcharitar S, Patterson MS, van Geuns RJ, PW.Serruys, Magnetic navigation system used successfully to cross a crushed stent in a bifurcation that failed with conventional wires *Catheter Cardiovasc Interv* 2007 May 1; 69(6):852-5
7. Ramcharitar S, Patterson M, van Geuns RJ, van der Ent M, Welten G, van Domburg RT, Serruys PW, A Randomised controlled study comparing Conventional and Magnetic guidewires in a 2-Dimensional Branching Tortuous Phantom simulating angulated coronary vessels *Catheter Cardiovasc Interv* 2007 Nov 1;70 (5):662-8.
8. Ramcharitar S, Vaina S, PW.Serruys, The Next Generation of Drug-Eluting Stents: What's on the Horizon for this Technology; *Am J Cardiovasc Drugs*. 2007, 7(2):81-93
9. Ramcharitar S, Vaina S, Serruys PW, Sianos G, Treatment of a distal Left Main Trifurcation supported by the TandemHeartTM device *Hellenic J Cardiol* 2007 Mar-Apr; 48(2): 110-4
10. Ramcharitar S, Serruys PW, Newer Stents: looking at the horizon, *Indian Heart J* 2007, Suppl. B, B59-B71
11. Ramcharitar S, Ligthart J,van der Giessen W Stent under-sizing can result in procedural related Late Stent Thrombosis, *Journal of Invasive Cardiology*, 2007; 19, E276-E277
12. Ramcharitar S, Gaster AL, Daemen J, Serruys PW, Drug eluting stents, Restenosis and Revascularization, *Herz* 2007 Jun; 32(4): 287-295
13. Ramcharitar S, Garcia-Garcia HM, Nakazawa G, Kukreja N, Ligthart J, Virmani R, Serruys PW, Ultrasonic and Pathological Evidence of a Neo-intimal Plaque Rupture in Patients with Bare Metal Stents, *Eurointervention* 2007, 3, 289-290
14. Laborde JC, Borenstein N, Behr L, Ramcharitar S, Stentys Coronary Bifurcated Stent, *Eurointervention* 2007, 3, 162-165
15. Kaplan AV, Ramcharitar S, Louvard Y, Müller R, Richard Davis H, Morice, M.C, Serruys PW, Grube E, Tryton I (First-In-Man) Study: Acute and 30 Day Outcome, *Eurointervention* 2007 3, 54-59
16. Meliga E, Garcia-Garcia H, M, Kukreja N, Daemen J, Tanimoto S, Ramcharitar S, van Mieghem C, Sianos G, van der Ent M, van der Giessen WJ, de Feyter P, van Domburg R, Serruys PW Chronic Total Occlusion Treatment In Post-CABG Patients: Saphenous Vein Graft Versus Native Vessel Recanalization. Long-Term Follow-Up In The Drug Eluting Stent Era *Catheter Cardiovasc Interv* 2007 Jul 1;70(1):21-5.
17. Gaster AL, Tanimoto S, Skjoldborg U, Ramcharitar S, Serruys PW, Economic issues in the clinical use of percutaneous coronary interventions, *Journal of Medical Economics* 2007, 10, 179-198
18. Ramcharitar S, Gaster AL, Hochadel M, Yoshinobu O, Gitt A, Serruys PW An Insight into the current use of Drug Eluting stents in Acute and Elective Percutaneous Coronary Interventions in Europe. *A report on the EuroPCI Survey Eurointervention* 2007, 2, 429-441
19. Patterson M, Ramcharitar S, Serruys PW Magnetically Supported PCI: Success after failed surgery and conventional PCI *Cath Lab Digest* 2007 (15) 03,1-14
20. Ramcharitar S, Serruys PW, Drug eluting stents: indications, limits and future developments *Cardiology International* Summer 2007, 49-55

21. Ramcharitar S, Daeman J, Patterson M, van Geuns RJ, Boersma E, Serruys PW and van der Giessen WJ The first direct in vivo comparison of two commercially available 3-Dimensional Quantitative Coronary Angiography systems *Catheter Cardiovasc Interv* 2008 Jan 1;71 (1):44-50.
22. Ramcharitar S and Serruys PW, Biodegradable Coronary Stents *Am J Cardiovasc Drugs*. 2008 (in press)
23. Patterson MS, Duckers E, Ramcharitar S, Meliga E, van Weenen S, Maugenest AM, Perin E, Serruys PW, Magnetically supported procedures and Cardiac Regeneration *EuroIntervention Supplement B 2007; 2, B42-B46*
24. Van Mieghem CAG, Ramcharitar S, Weustink AC, de Feyter, PJ, Noninvasive cardiac computed tomography: an interventional cardiologist's perspective, *Chest* 2008 (submitted)
25. Ramcharitar S, Onumo Y, Aben J-P., Consten C., Weijers B., Morel M.-A., Serruys PW, Novel Bifurcation Analysis Methodology, *Eurointervention* 2008, 3, 553-557
26. Yoshinobu O, Müller R, Ramcharitar S, van Geuns RJM, Louvard RJ; Morel M-A, Morice M-C, Davis, R; Kaplan AV; Lefèvre, T; Grube, E; Serruys, P, First-in-man (FIM) study: Clinical and angiographic outcome, Analysis with new quantitative coronary angiography dedicated for bifurcation, *Eurointervention* 2008, 3, 546-552
27. Ramcharitar S, Serruys PW, The Magnetic Navigation wires, 'Chronic Total Occlusions: A Guide to Recanalization' edited by Ron Waksman, Ed Wiley-Blackwell 2008
28. Ramcharitar S, Sianos G,van der Giessen W Use of Thrombus extraction catheter in (Thrombuster IIR) in an Acute Myocardial Infarction, *Eurointervention 2007* 3, 529-531
29. Ramcharitar S, Pugliese F, Patterson M, van Geuns RJ; de Feyter P, Guiliguian D, Serruys PW, Navigant® software facilitates Magnetically Assisted Percutaneous Interventions by directly co-integrating the Multi-Slice Computer Tomography Scan, *Eurointervention 2008* (in press)
30. Rivero-Ayerza, Jessurun, E, Ramcharitar S, van Belle Y, Serruys PW, Jordaens LJ; Magnetically guided left ventricular lead implantation base on virtual 3D reconstructed image of the coronary sinus (in press EuroPACE)
31. Patterson MS, Hoeks SE, Ramcharitar S, Rijkenberg S, van Geuns RJ, Tanimoto S, van Domburg RT, Serruys PW; Integration of 3D reconstruction in the SELection Criteria for Excessive Crossing Times for Magnetically Supported Percutaneous coronary intervention SELECT-MP; *Eurointervention 2008* (in press)
32. Riezebos RK, Patterson MS, Braat JH, Ramcharitar S, Serruys PW, Kiemeneij F, Primary Percutaneous Coronary Intervention using Magnetic Navigation, *Eurointervention 2007*, 12,
33. Barlis P, Ramcharitar S, Redwood S, Tan H-C, Dimopoulos K, Kaplan S, O'Kane P, Sianos G, Ferrante G, Regar E, Serruys PW, Di Mario C, Long-term outcomes of bifurcation stenting using the culotte technique with drug-eluting stents (*Eurointervention* submitted for publication)
34. Brennan JF, Nazemi J, Motz J, Ramcharitar S, Intravascular Raman spectroscopy: a view on plaque composition *Eurointervention 2008*, 3, 635-638.
35. Ramcharitar S and Serruys PW, Biodegradable stents, *Minerva Cardioangiol*. 2008 Apr; 56 (2): 205-13.
36. Ramcharitar S, Patterson MS, van Geuns RJ, van Meighem C, Serruys PW, Technology Insight: magnetic navigation in coronary interventions, *Nat Clin Pract Cardiovasc Med*. 2008 Mar; 5 (3): 148-56. Epub 2008 Feb 5
37. Ramcharitar S and Serruys PW, Cardiovascular Interventions in Clinical Practice, edited by Jürgen Haase, Hans-Joachim Schäfers, Horst Sievert and Ron Waksman. Chapter 42, Magnetic catheter navigation for PCI
38. Ramcharitar S, Meliga E, Kirschbaum SW, ten Cate FJ, van Geuns RJ and Serruys PW, Acute haemodynamic changes in percutaneous transluminal septal coil embolisation for obstructive hypertrophic cardiomyopathy, *Nat Clin Pract Cardiovasc Med*. 2008, (in press).
39. van Mieghem C., Ramcharitar S., Barlis P., Oosterhuis W., Kik C., de Feyter P., Serruys P.W. Myocardial infarction in a patient with sickle cell trait. Treatment dilemmas and imaging findings at follow-up *Eurointervention 2008*, 3, 627-634.

40. Ramcharitar S, van Geuns RJ, Patterson MS, van der Ent M, van der Giessen WJ, van Domburg RT, Serruys PW, A Randomised Comparison of the Magnetic Navigation System versus Conventional Percutaneous Coronary Intervention, *Catheter Cardiovasc Interv* (in press)
41. Onuma, Y, Kukreja N, Ramcharitar S, Hochadel M, Gitt A, Serruys PW, Interventional treatment in diabetics in the era of drug-eluting stents and compliance to the ESC guidelines, *Eurointervention 2008* (in press)
42. Ramcharitar S, van Geuns RJ, van der Giessen WJ, van der Ent M, de Feyter PJ, Serruys PW A Randomised Comparison of the Magnetic Navigation System versus Standardwires in the treatment of Bifurcations *(submitted)*
43. Ramcharitar S, van Geuns RJ, van der Giessen WJ, van der Ent M, de Feyter PJ, Serruys PW Single Center Experience of Magnetic Navigation in the Management of Chronically Occluded Vessels, *(submitted)*
44. Ramcharitar S, Pugliese F, Schultz C, Ligthart J, de Feyter P. J., Li, H., Mollet N., vd Ent M, Serruys P.W.J.C., van Geuns. R.J.M.Integration of Multislice Computer Tomography with Magnetic Navigation facilitates Percutaneous Coronary Interventions without contrast agents – A proof of concept paper *(submitted)*
45. Ramcharitar S, Gonzalo N, van Geuns RJ, Garcia-Garcia H, Ligthar JMR, Regar E, Serruys PW, Stenting of the vulnerable plaque, the dawn of a new era - The first case; *Nat Clin Pract Cardiovasc Med*. 2008, *(submitted)*

Financial contribution for the production of this thesis is gratefully acknowledged from the following companies

Stereotaxis
Siemens
Tryton
Stentys
Minvasys
Pie Medical
Precient
Cardialysis

CHAPTER 1

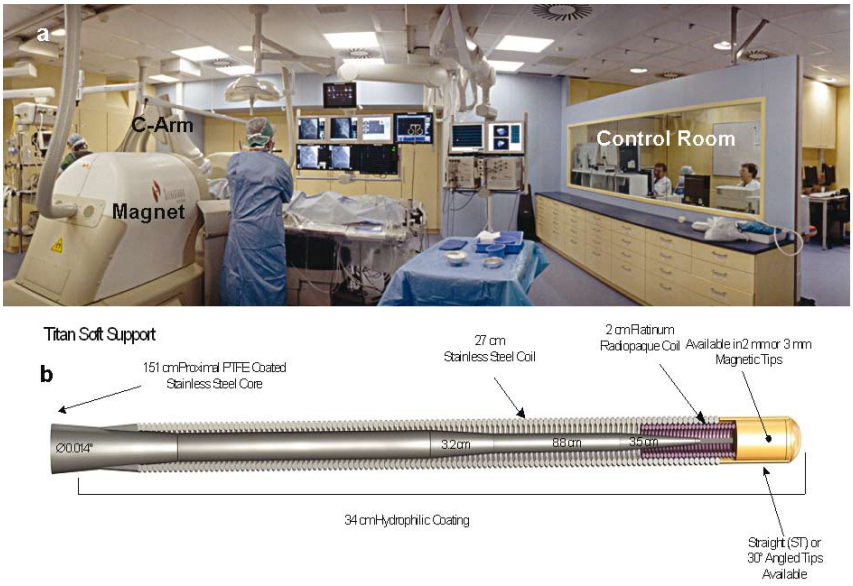

Figure 1 *The Niobe® Magnetic Navigation System.*
*(**a**) A typical magnetic navigation system set-up showing the magnets, C-arm and the control room.*
*(**b**) The Titan® magnetic navigation wire showing the 2 or 3 mm magnet located at its tip.*

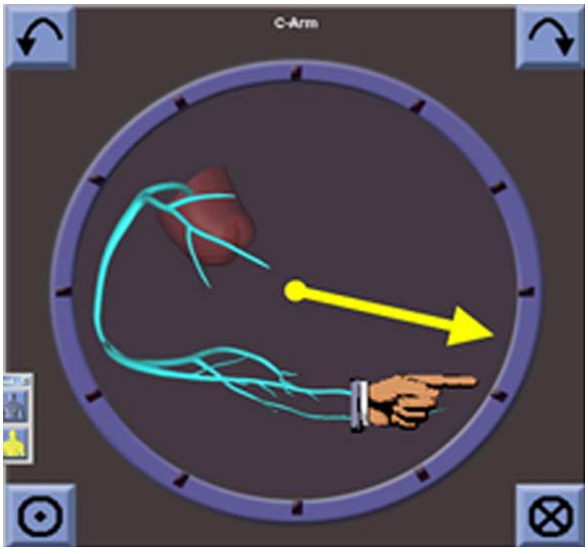

Figure 2 *The clockface navigational mode*
By touching the perimeter the vector moves in that direction; controls for anterior and posterior movements are at the edges.

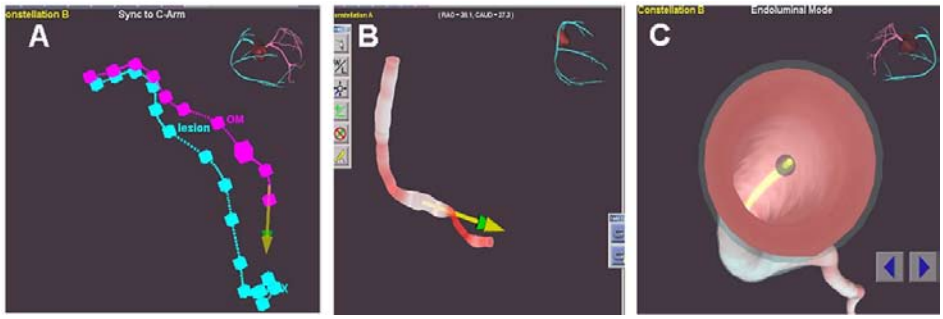

Figure 3 *True-vessel navigation using an accurate three-dimensional representation of the coronary artery* (**A**) A constellation road map created from two-dimensional X-ray images; chosen points are depicted by squares along the navigational path. (**B**) Navigation using a three-dimensional reconstruction created with the CardiOp®-B software. (**C**) Navigation by means of the endoluminal view. Abbreviation: OM, obtuse marginal branch.

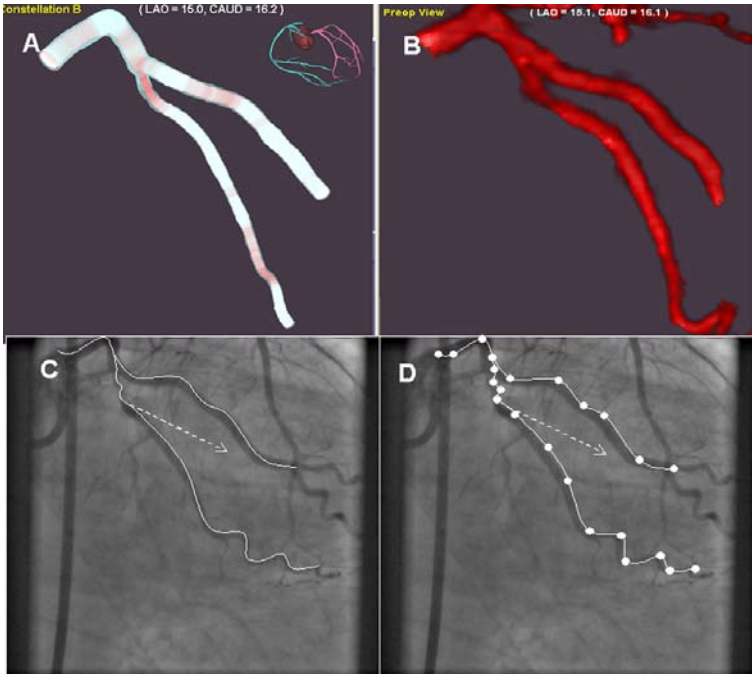

Figure 4 *Three-dimensional representation of the coronary artery.*
*(**A**) A three-dimensional reconstruction of the artery using the CardiOp®-B software. (**B**) The same arteries extracted from a multislice CT data set (**C** and **D**), displayed as navigational centerlines with a directional vector on the live fluoroscopic images.*

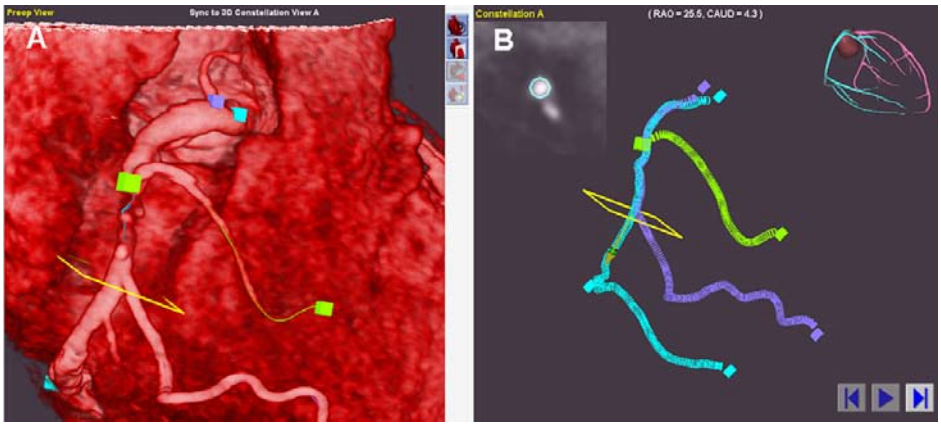

Figure 5 *Using the Navigant® system the multislice CT data set can be used to create: (A) a road map of a chronic total occlusion not seen angiographically and (B) cross-sections along the map.*

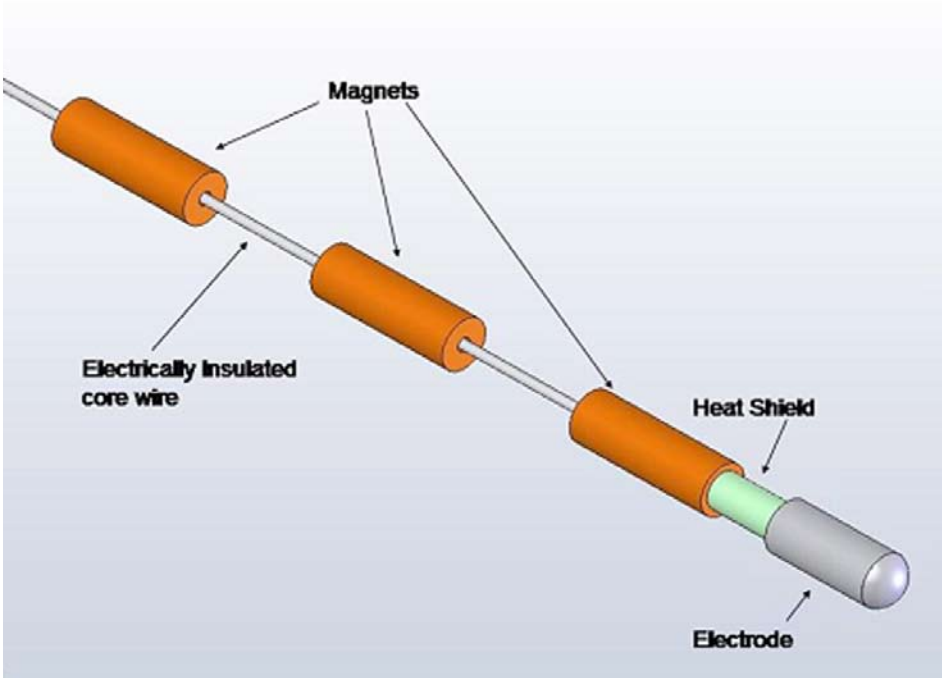

Figure 6 *A diagrammatic representation of the magnetically enabled radiofrequency ablating wire for chronic total occlusions.*

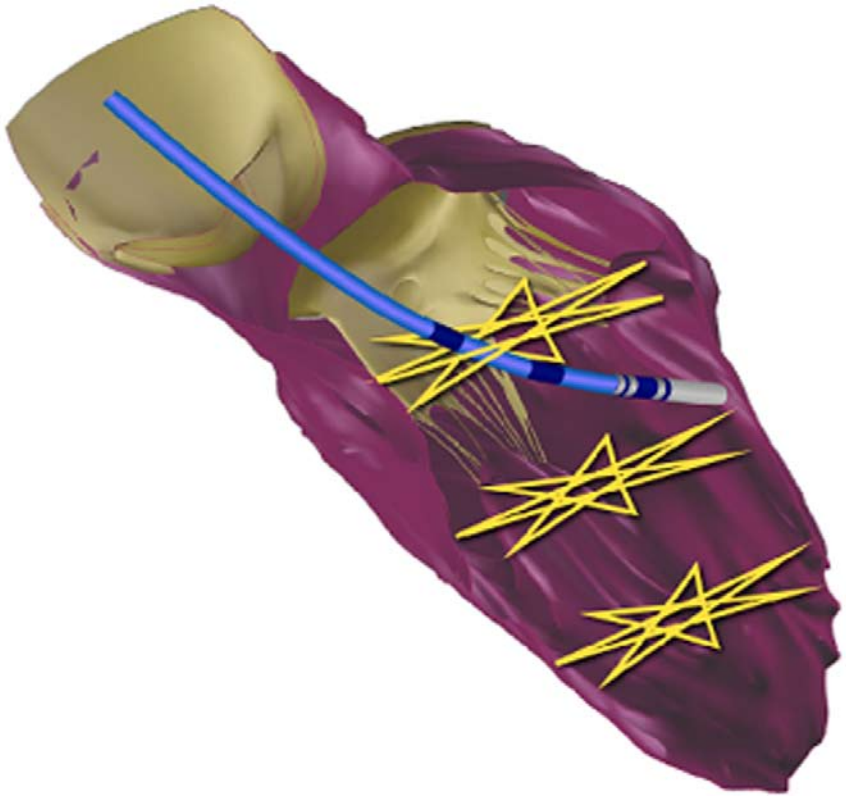

Figure 7 *A diagrammatic representation of magnetically enabled cell injection catheter following an automatic map in the myocardium.*

CHAPTER 2

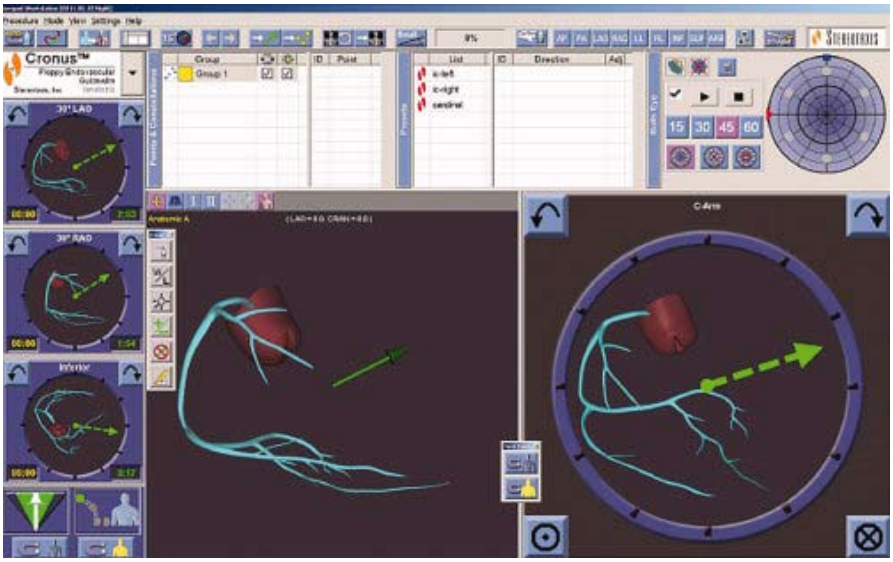

Figure 1 *The "clockface" navigation system*

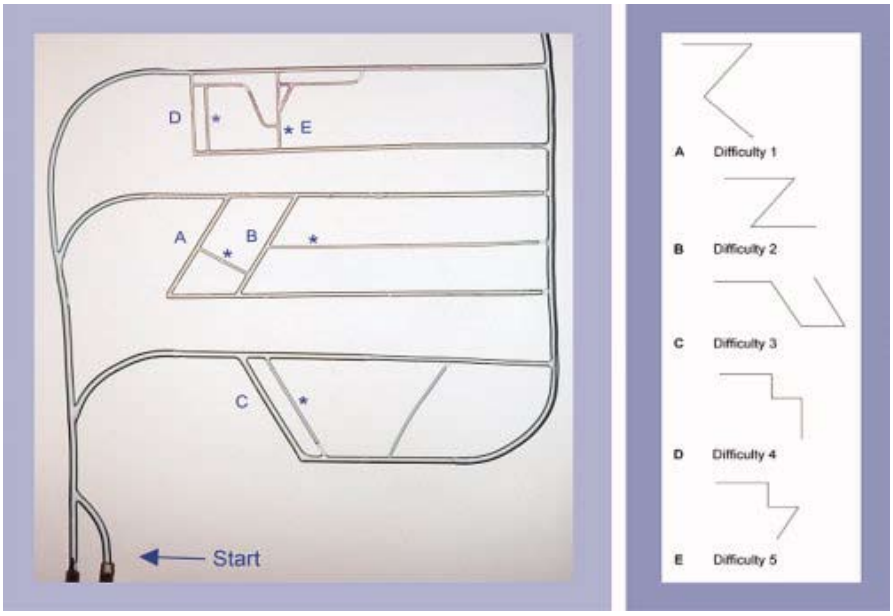

Figure 2 *The phantom A-E with diagramatic representation of the level of difficulty. The angles and "vessel" caliber are as follows: (A) 3 mm, 120° turn into a 3 mm, 90° turn; (B) 3 mm, 120° turn into a 3 mm, 90° turn; (C) 3 mm, 60° turn into a 3 mm, 120 turn and then into a 60° turn to a 2 mm vessel; (D) 3 mm, 90° into a 2 mm followed by a 90° turn; (E) 3 mm, 90° into a 2 mm followed by a 120° turn. The "arrow" indicates the starting point and the asterisk (*) show the end of each phantom run.*

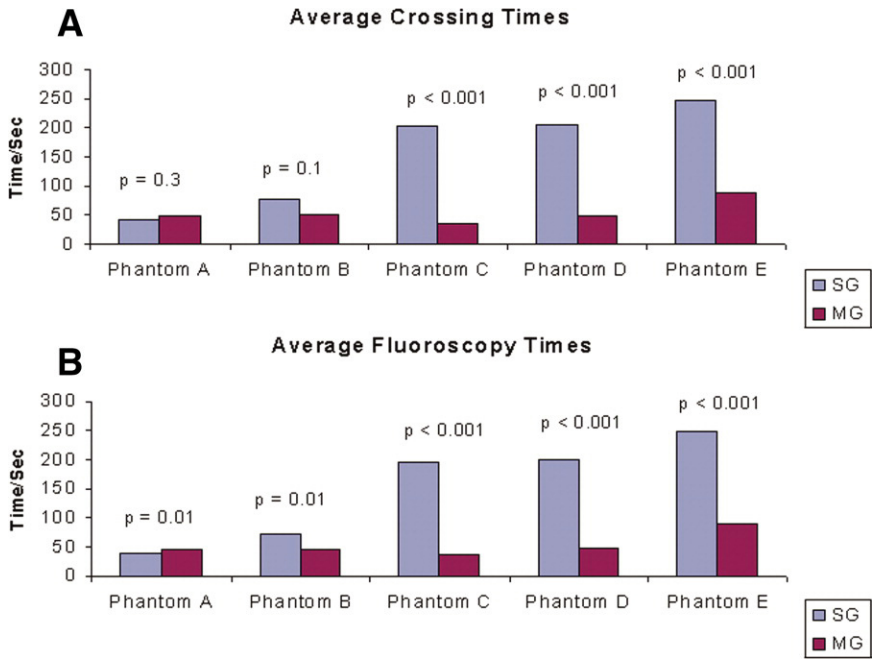

Figure 3 *(A) The average crossing times/sec obtained using SG and MG for all operators with phantoms A-E. (SG, standard guidewire; MG, magnetic guidewire). (B) The average fluoroscopy times/sec obtained using SG and MG for all operators with phantoms A-E. (SG, standard guidewire; MG, magnetic guidewire).*

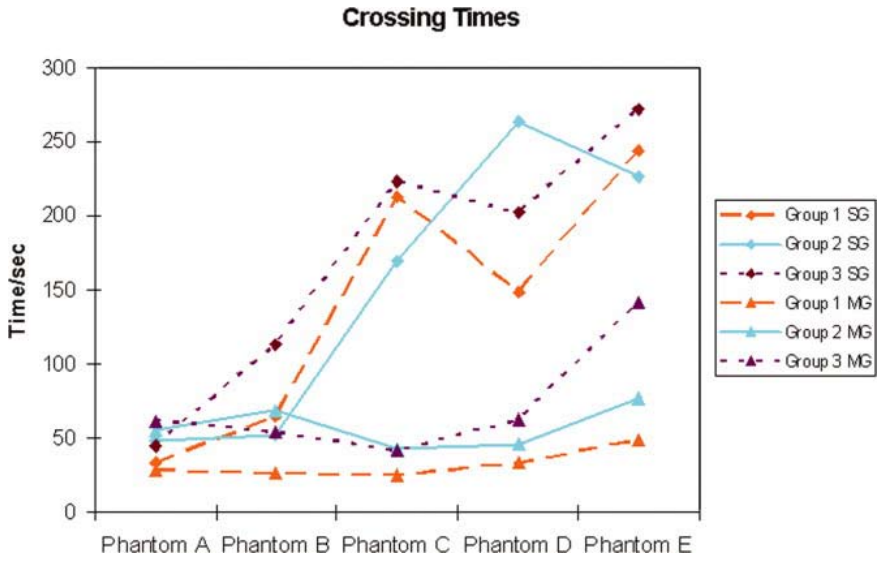

Figure 4 *The average crossing times/sec obtained using SG and MG for groups 1-3, operators with phantoms A-E. (SG. standard guidewire; MG, magnetic guidewire).*

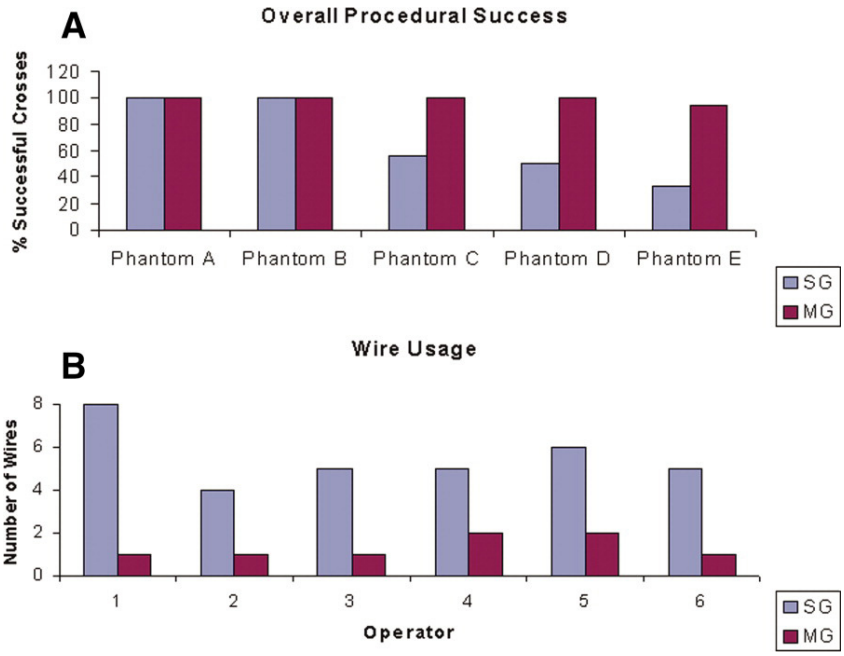

Figure 5 *(A) The overall procedural success using SG and MG for phantoms A-E. (SG, standard guidewire; MG, magnetic guidewire). (B) The SG and MG usage in operators 1-6 for phantoms A-E. (SG, standard guidewire; MG, magnetic guidewire).*

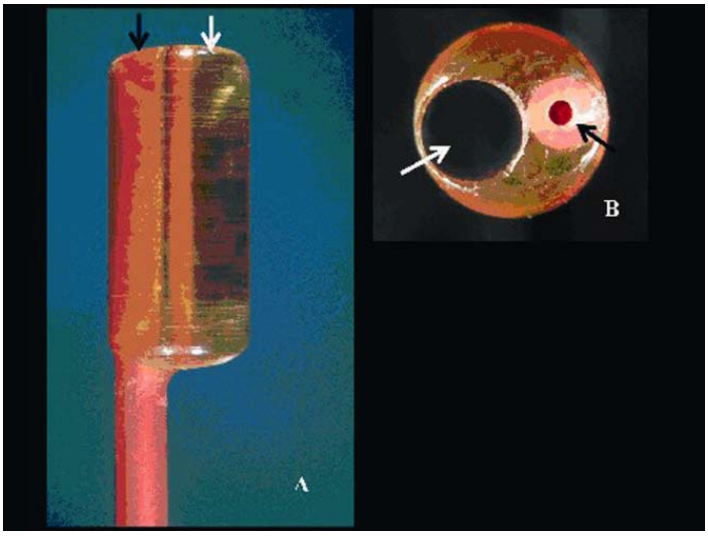

Figure 1 *The magnified tip of one of the Fogarty catheters view along its long (A) and short axis (B) with a transparent radiolucent cylinder (phantom) having a channel of 1.9 mm diameter (white arrow) and the catheter lumen used for insertion of removable metallic stylet (black arrow) to aid positioning.*

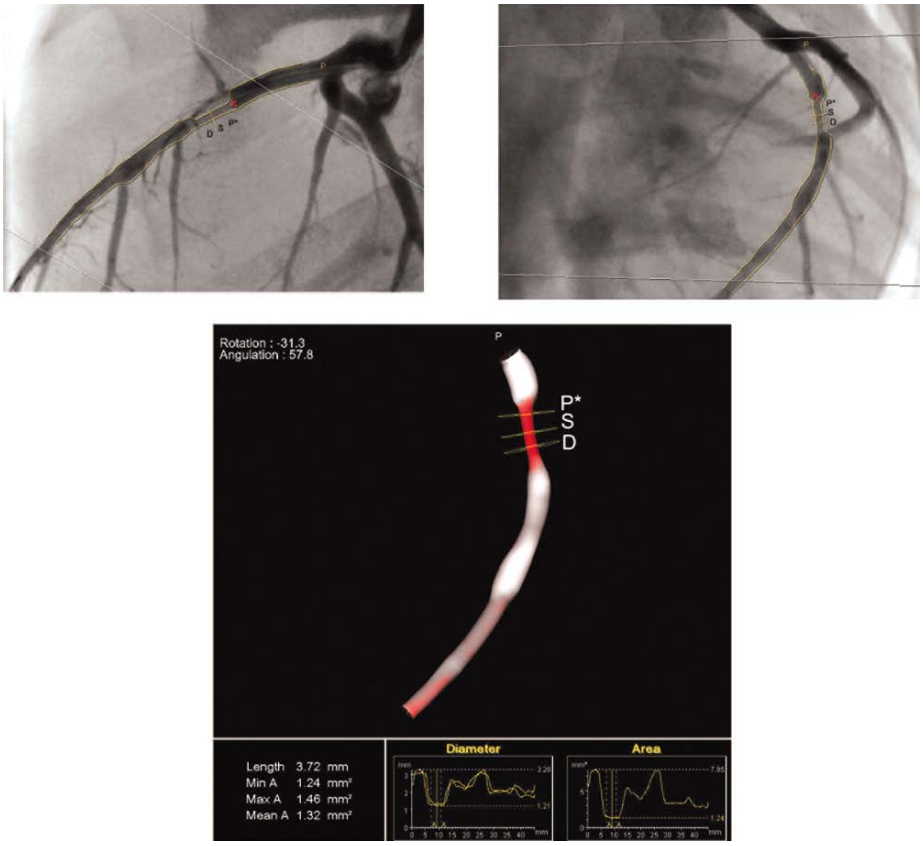

Figure 2 *The 3D reconstruction of a phantom derived from two orthogonal views (frontal and lateral) using the CASS 5 system. The 3D color varies according to the severity of stenosis ranging from white (healthy vessel) to dark red (99% cross-sectional area stenosis). The yellow squares denote proximal reference point (P*), most stenotic point (S), and distal reference point (D) of the target lesion, respectively. The region of interest (ROI) for calculation of mean luminal diameter can be manually defined by moving the proximal (P*) and distal (D) points (Definition of ROI for mean LD; Graph view).*

CHAPTER 3

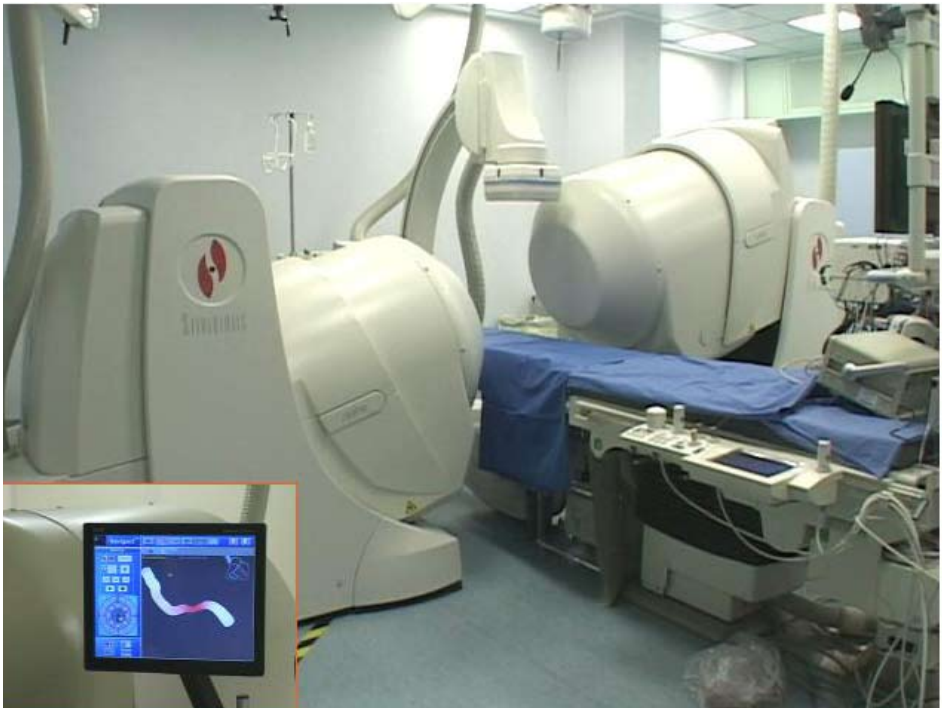

Figure 1 *Magnetic navigation system is shown with the magnets in the tilt position on either side of the patient. Inserted at the bottom left hand panel is the touch screen monitor used to direct the navigation along the chosen vessel*

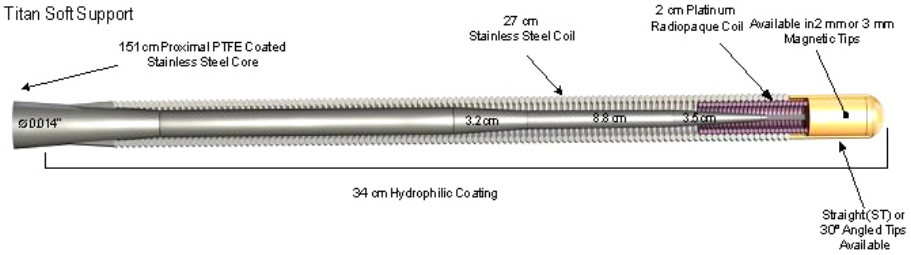

Figure 2. *The Magnetic Guidewire with the 2-3mm embedded gold encapsulate neodynium iron boron magnet at the distal tip*

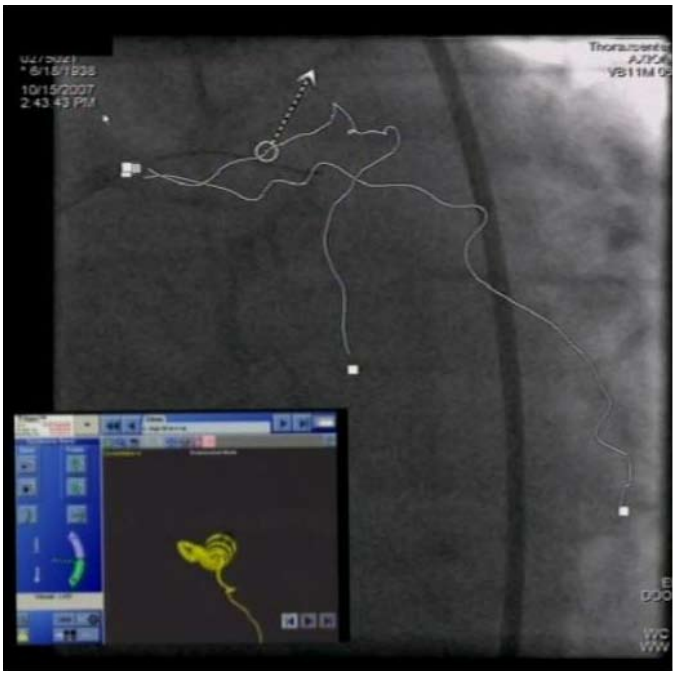

Figure 3 *The chosen vector is displayed as a dotted arrow on navigational path-line on the live fluoroscopy image. The bottom left panel shows what the operator sees on the touch screen monitor.*

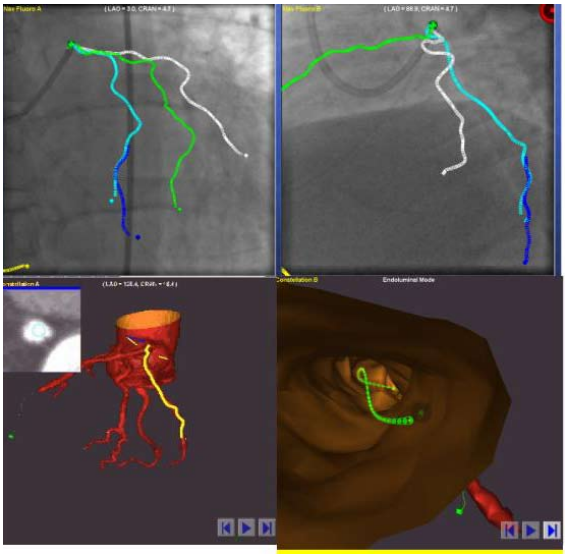

Figure 4 *Top panels showing the tip of the catheters in fluoroscopy image co-registered with the extracted coronaries derived from the MSCT dataset. These give the specific 3-D coordinates that allow integration of the 2 modalities. Bottom panels showing the extracted coronaries with the centerline together with multiplaner reconstructed cross-section displayed in the Navigant® and the endoluminal views for MSCT based navigation.*

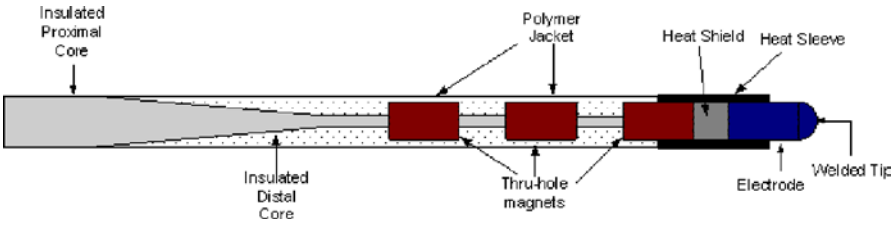

Figure 5 *The magnetically enabled RF wire*

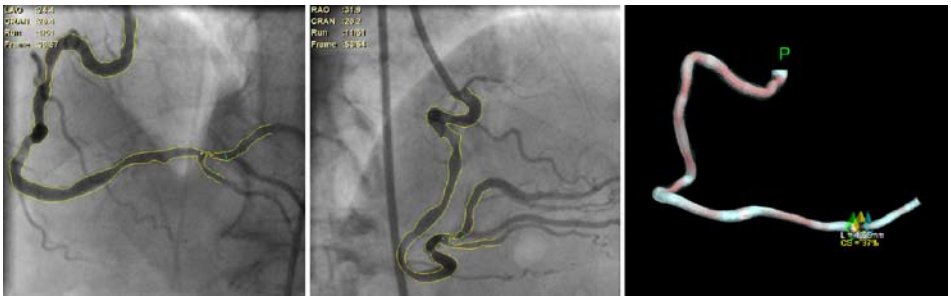

Figure 2 *The left 2 panels show separate angiographic angulations with edges detected and the right panel shows a 2D image of the 3D reconstruction.*

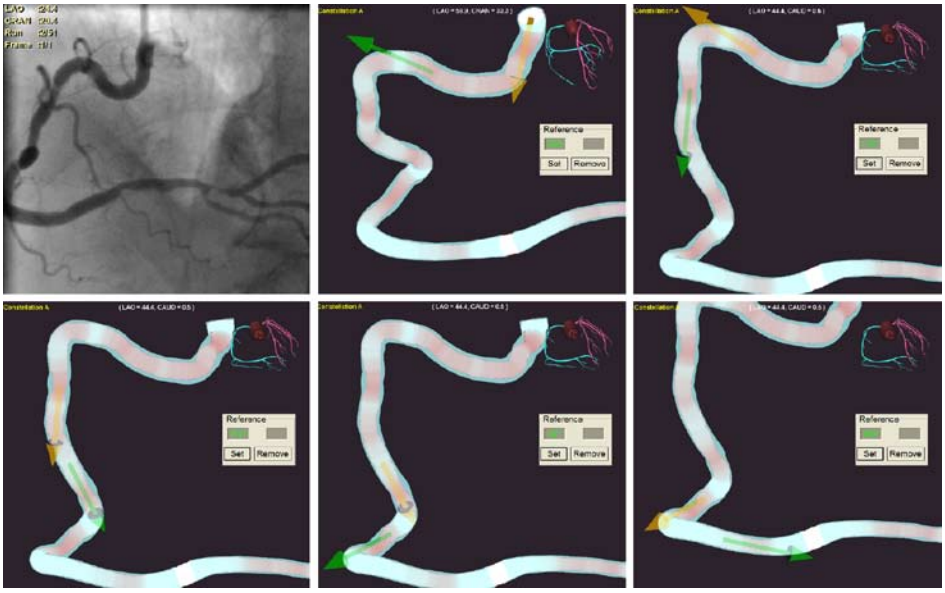

Figure 3 *Identification of the bends in a vessel and measurement of each angle (possible in the Navigant program) The total angulation of the 5 worst bends, (Vta), (Figure 3)*

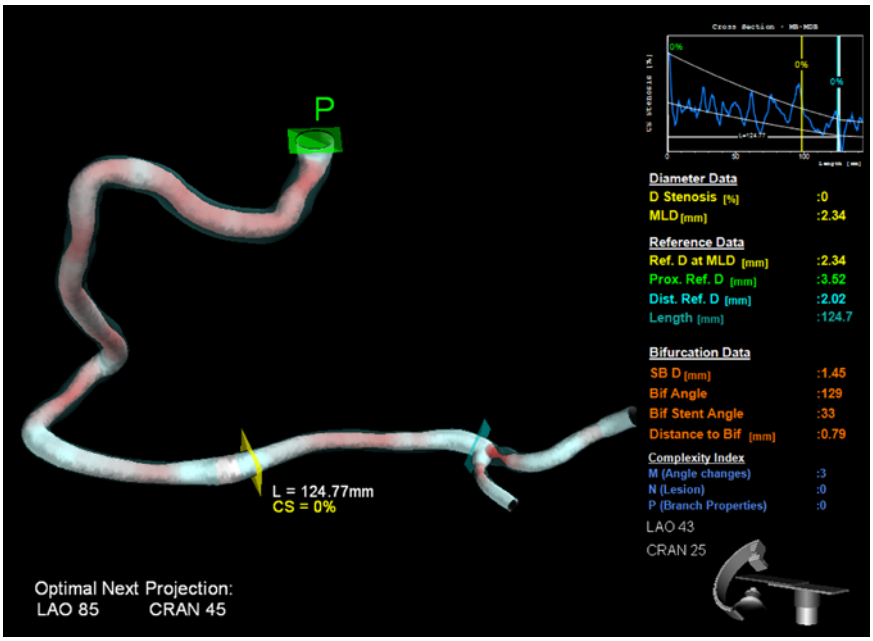

Figure 4 *The measurement of the length from the vessel ostium to the lesion in CardiOp-B (green square indicates proximal marking point and blue square indicates distal marking point)*

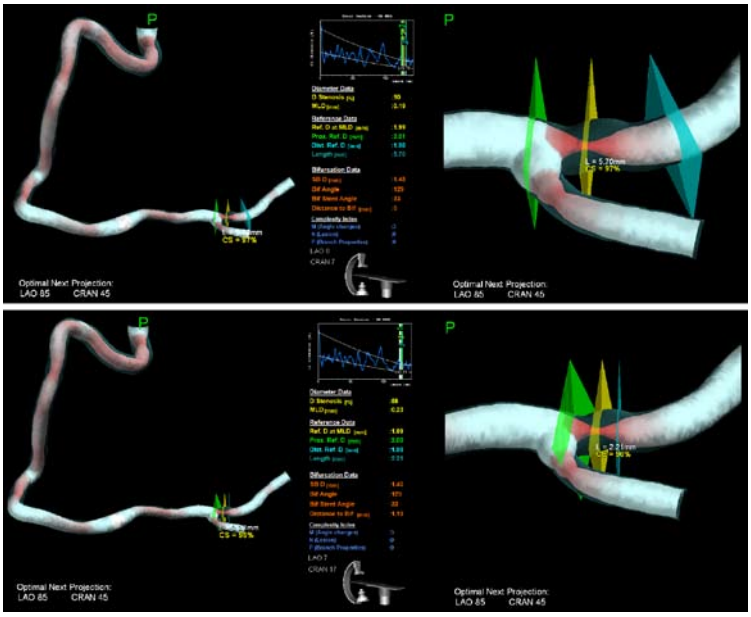

Figure 6 *The top panels show the measurement of the lesion length (green square indicates proximal marking point and blue square indicates distal marking point). The lower panel shows the segment greater than 80% measured in CardiOp-B (green square indicates proximal marking point and blue square indicates distal marking point).*

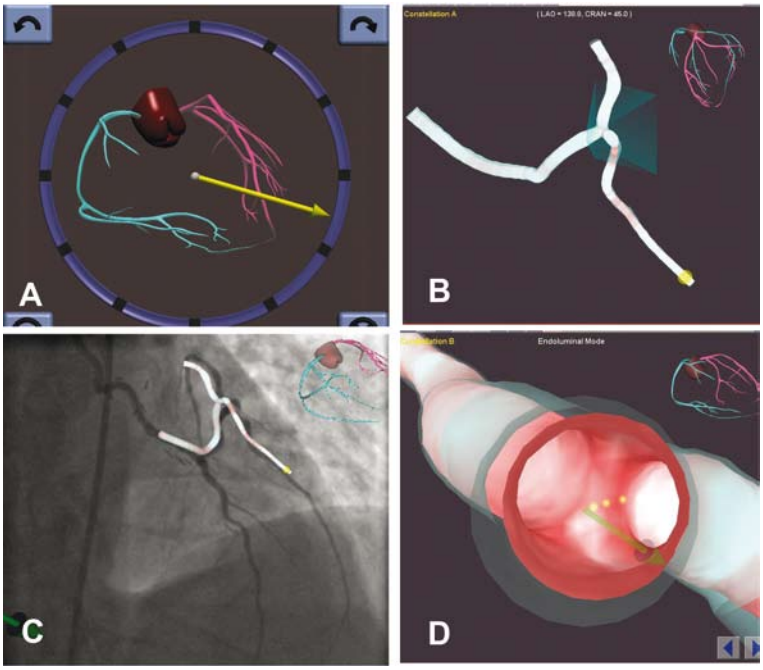

Figure 1 *The clockface navigational mode showing a vector depicted by an arrow that can be repositioned by selecting points around the perimeter of the clock; B) a 3-dimensional reconstruction of a coronary bypass graft to the native left anterior decending artery and C) the registration with the fluoroscopic image; D) navigating at the bifurcation of the virtual reconstructed graft showing a navigational pathway through the lumen*

CHAPTER 4

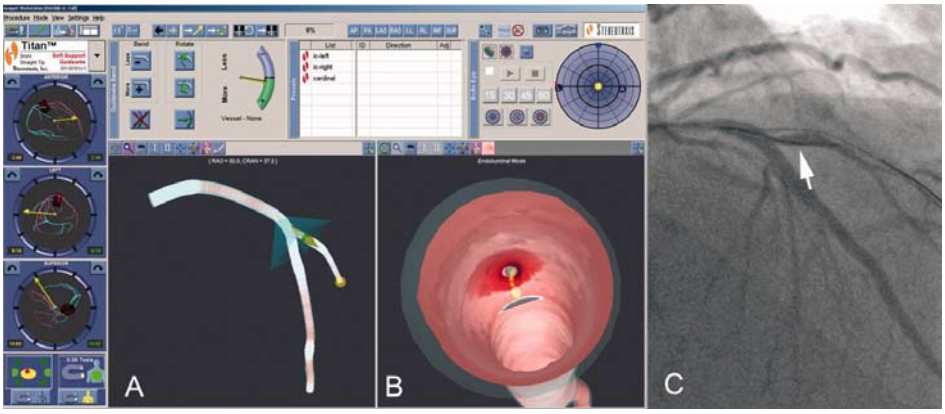

Figure 2 *The 3D reconstruction (A) and the endoluminal view of the LAD/diagonal bifurcation (B). The magnetically guided TitanTM Soft Support wire (arrowed) successfully crosses the stent strut into the true lumen and the Graphix Intermediate wire preferentially chose the false lumen of the dissection (C).*

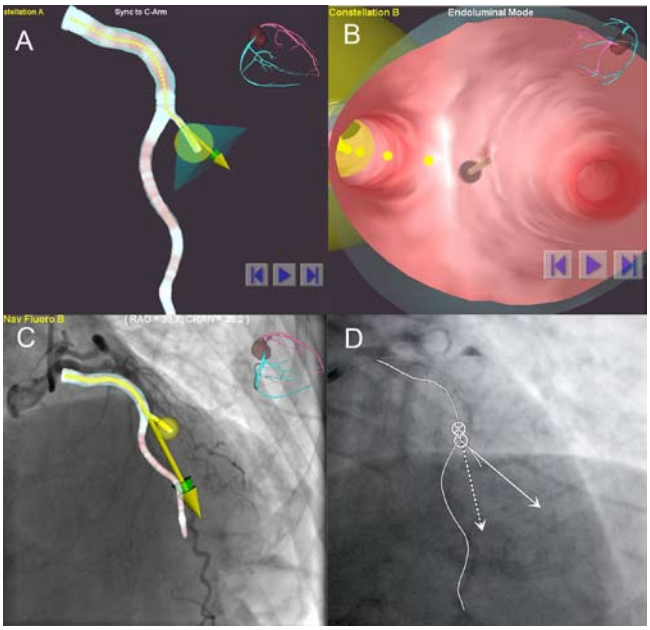

Figure 1 *A) A virtually reconstructed bifurcation using the Paeion software displaying a directional vector created in the Navigant; B) The endoluminal view of the virtual carina at the bifurcation showing the navigational path in one of the branches; C) Co-registration of the virtual vessel to the angiographic image; D) The navigational vectors and centrelines displayed on the live fluoroscopic image.*

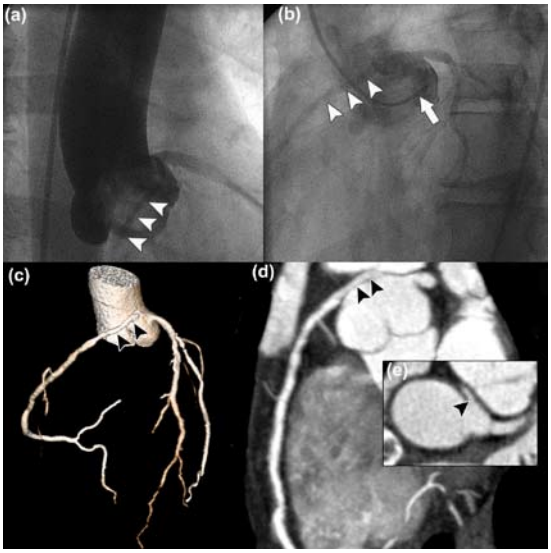

Figure 4 *Anomalous origin of the right coronary artery (RCA). (a) An aortogram was performed to localize the origin of the RCA, whose contours are faintly visible (arrowheads). (b) Non-selective injection confirms its origin (arrowheads) out of the left coronary cusp. (c, d, e) CT coronary angiogram clearly showing the anomalous origin (arrowheads) and course of the RCA*

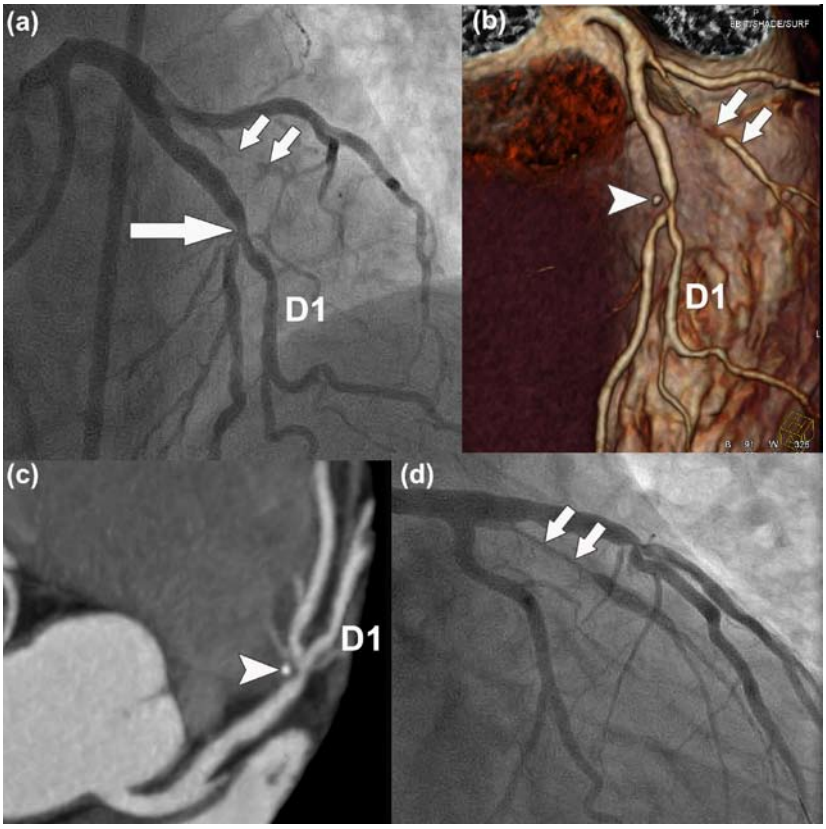

Figure 7 *(a) Invasive coronary angiogram showing a significant bifurcation lesion (large arrow) of the left anterior descending coronary artery with the first diagonal branch (D1). Also note the limited contrast enhancement (small arrows) in what looks like a small side branch. (b) Three-dimensional reconstruction of the heart with CT showing the bifurcation lesion. The dense spot within the lesion (arrowhead) corresponds to calcification. The branch that was faintly visible angiographically, can now be clearly recognized without interference of overlapping vessels as the intermediate branch (arrows). (c) 3-mm thick maximum intensity projection clearly showing the calcified (arrowhead) and non-calcified plaque components causing the lumen narrowing. (d) After wiring the intermediate branch its true dimension can be well appreciated (arrows).*

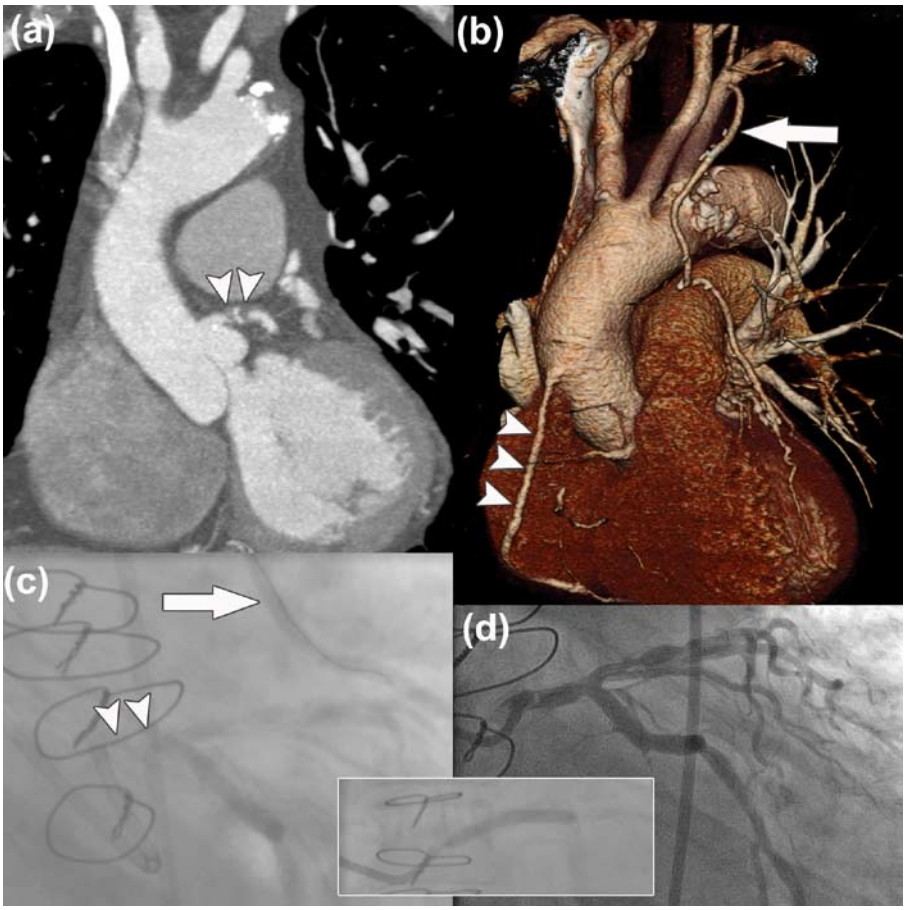

Figure 9 *Patient with recurrent angina after previous coronary bypass graft surgery, including a venous graft to the right coronary artery (RCA) and left internal mammary artery (LIMA) to the left anterior descending coronary artery. At initial invasive catheterization the origin of the left coronary artery appeared occluded. (a) Cardiac CT scan, coronal view, indeed showing a short occlusion (arrowheads) of the left main stem. (b) Three-dimensional reconstruction of the heart showing the patent LIMA (arrow) and venous graft to the RCA (arrowheads). (c) Contrast injection after wiring of the LIMA (arrow) results in opacification of the native coronary artery up to the distal part of the left main stem. (d) Six-month angiographic result after successful PCI (inset) of the left main stem.*

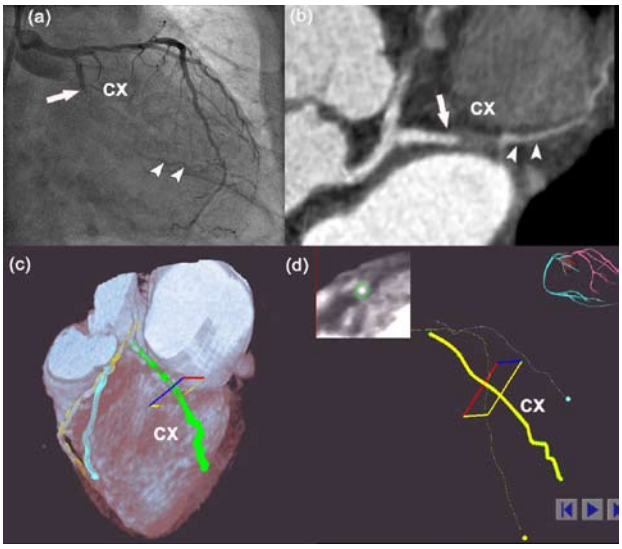

Figure 11 *(a) Invasive coronary angiogram, showing a chronic total occlusion (arrow) of the circumflex artery (CX). Only the very distal part of the vessel is visible through collaterals (arrowheads) (b) Corresponding CT image (curved multiplanar reconstruction): compared to the angiographic information the occlusion appears much shorter and consists of non calcified tissue. (c) The CT dataset has been uploaded in the navigation software; the course of the CX, including the path of the occlusion, is marked by a green line overlay. (d) The course of the CX has been marked as a yellow line. The rectangular which is present in panel c and d marks the location of the wire tip in the vessel. The inset in panel d represents the perpendicular cross-sectional view of the vessel to allow the steering of the guidewire in the desired direction.*

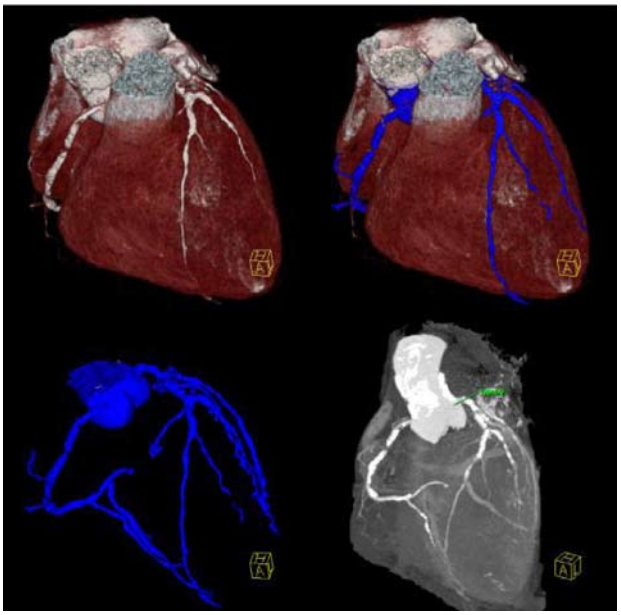

Figure 1 *Volume-rendered MSCT image with coronary segmentation is displayed in blue with vessel calcification shown in bottom right image*

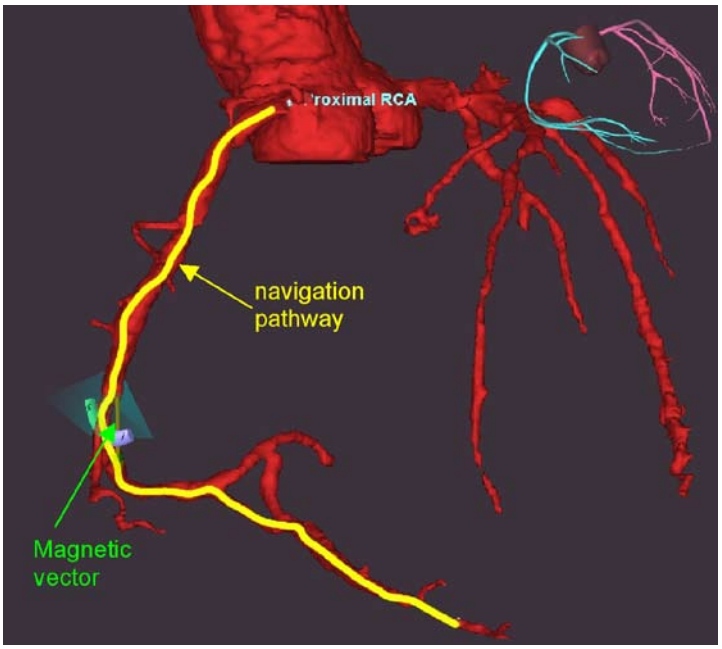

Figure 2 *Coronary tree with the automatically computed pathway and the tangent magnetic vector*

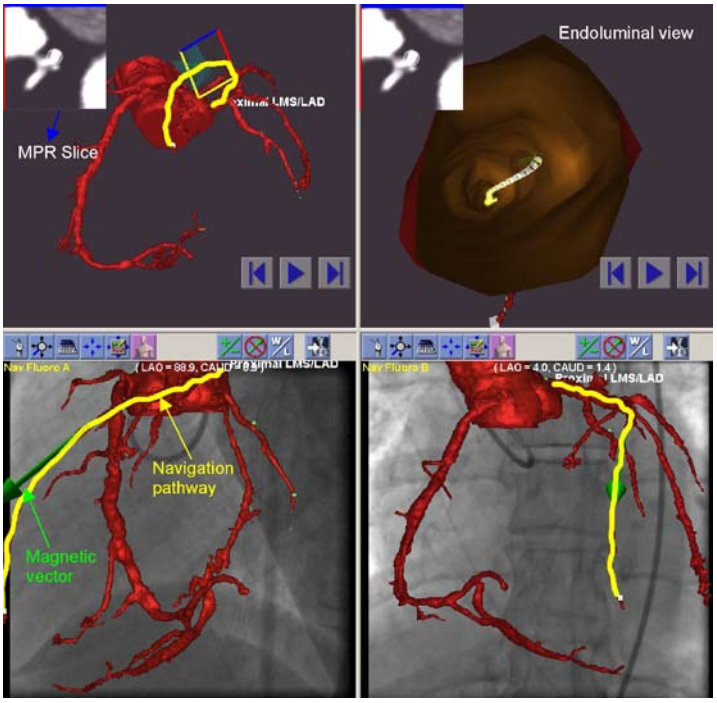

Figure 3 *Navigation and tools for the operator*

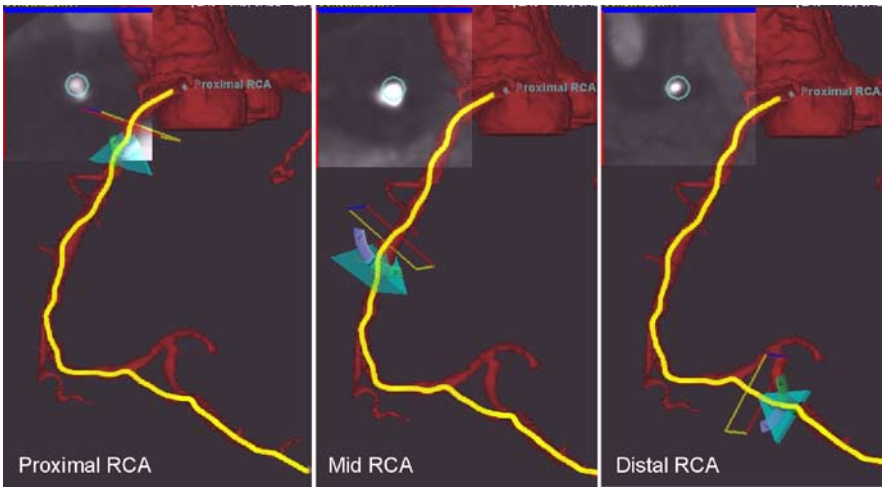

Figure 4 *Automated vessel sequencing MPR slices upper left quadrant*

CHAPTER 5

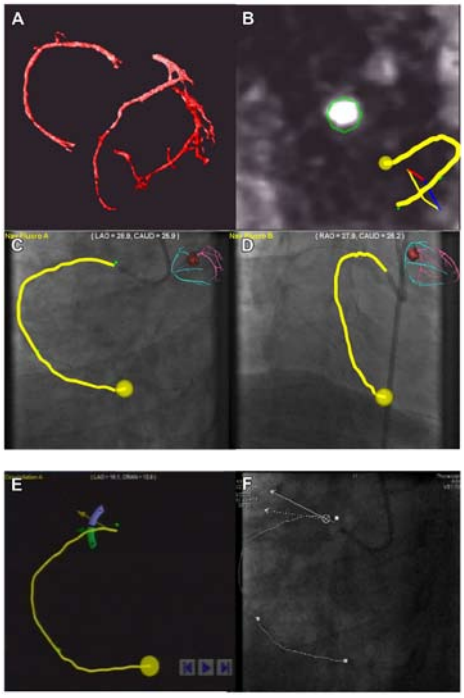

Figure 2 *A) Extracted coronaries arteries from the CTCA dataset to be introduced directly into the MNS; B) slice through a navigational pathway (depicted by yellow line) simultaneously showing the corresponding MPR cross-section at that position; C and D) Co-registration of the navigational pathway to the guiding catheter in two orthogonal planes; E) the navigational pathway with a directional vector and F) it being displayed on the live fluoroscopic image*

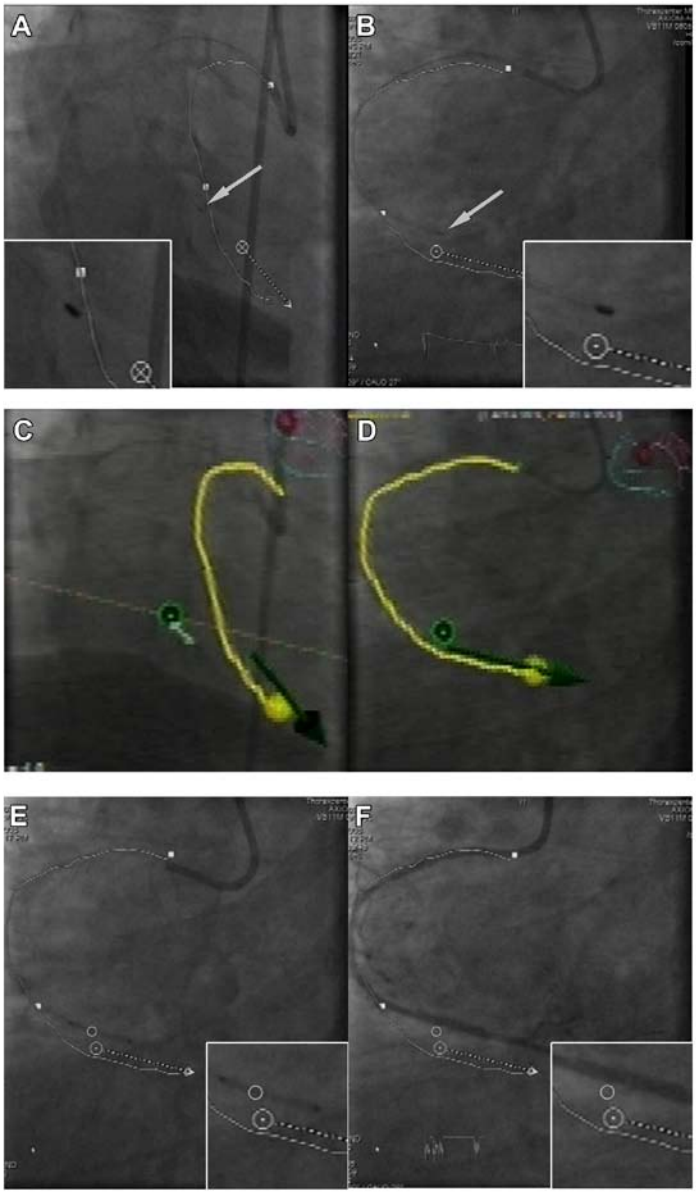

Figure 3 *A and B) Radiographic recordings of two orthogonal images IVUS probe positioned in the middle of the lesion and C and D) these two points co-registered as a new reference point (green circle) in the 3D space of Navigant®; E) the overlay of the location of this point (open white circle) on the live fluoroscopic was used to position the stent on the middle of the lesion; F) The stent being deployed following a single "safety check" angiogram.*

CHAPTER 6

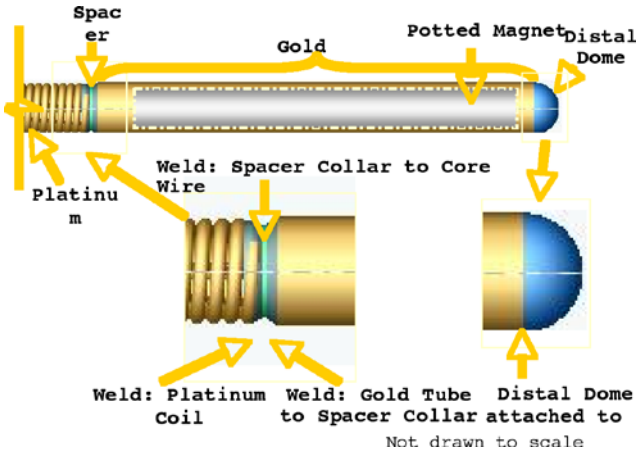

Figure 1 *The basic design at the tip of a magnetically enabled wire*

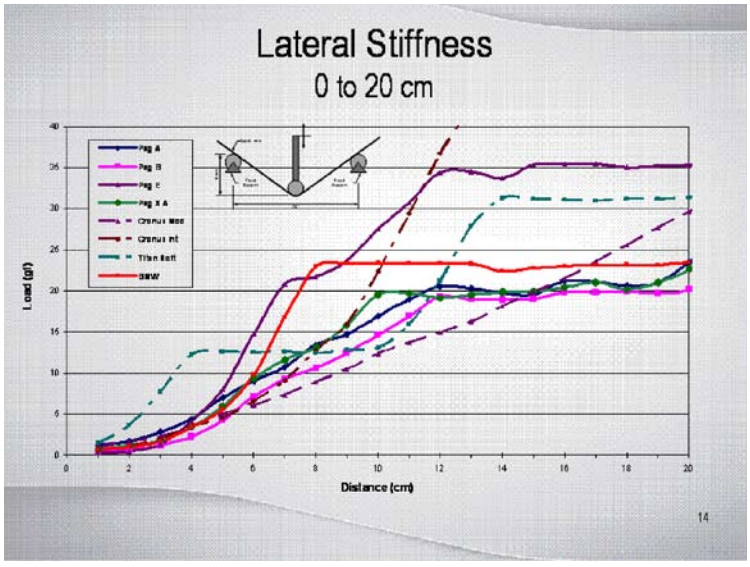

Figure 2 *The lateral stiffness of magnetically enabled wire as determined by three point testing*

Tip Load @ 1cm Extension	
Guidewire	Tip Load (gf)
Cronus Soft	1.0
Cronus Moderate	1.8
Cronus Assert	3.5
Titan Soft	1.3
Titan Super Support	1.8
Titan Assert	3.5
BMW	0.6
Asahi Miracle 3	3.3

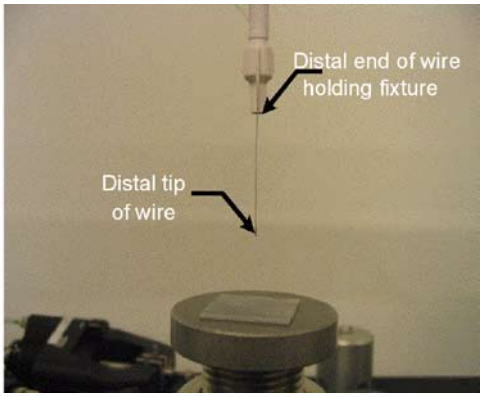

Figure 3 *The tip load comparison of magnetically enabled and conventional wires*

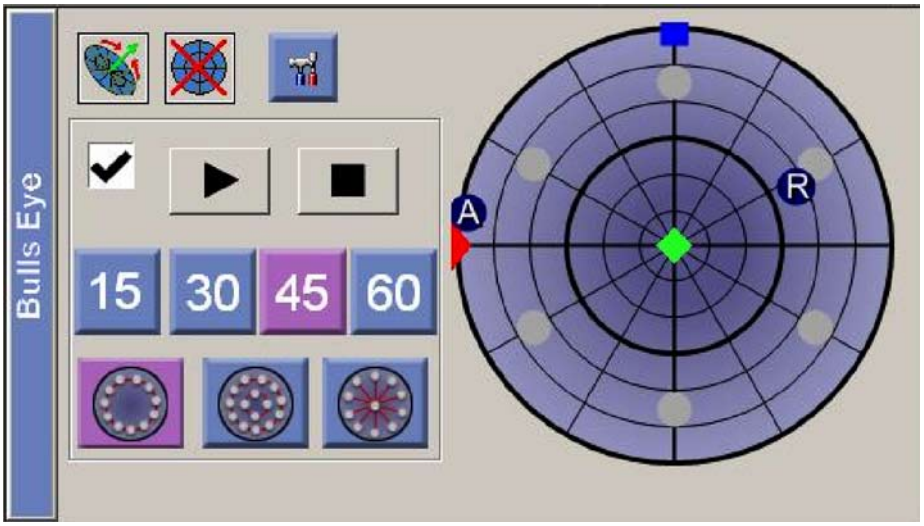

Figure 4 *The Bulls Eye Navigational mode depicting the various interrogation patterns and tip angulations that can be utilized in searching for a micro channel in a CTO*

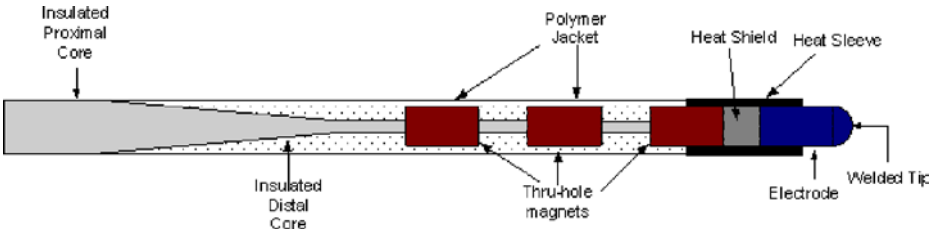

Figure 5 *The magnetically enabled RF wire*

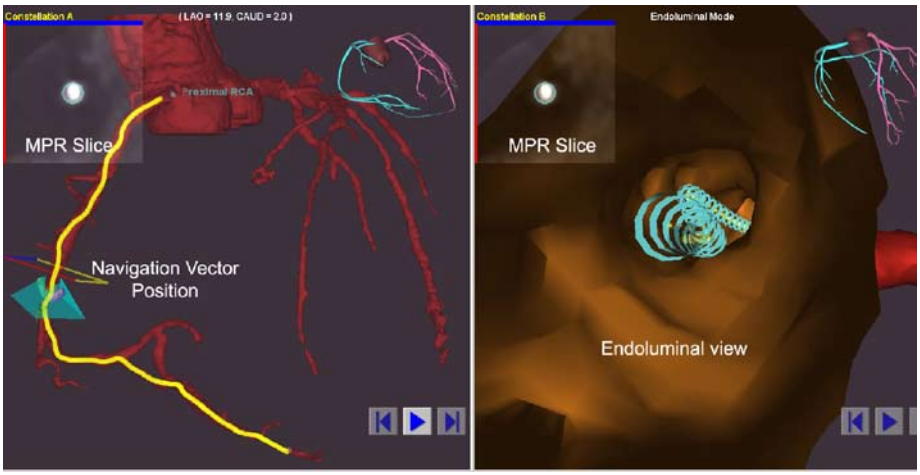

Figure 6 *Navigation through MSCT co-integration demonstrating the MPR cross-section slice (left upper quadrant at the site of the navigational vector and the corresponding endoluminal view in the right panel.*

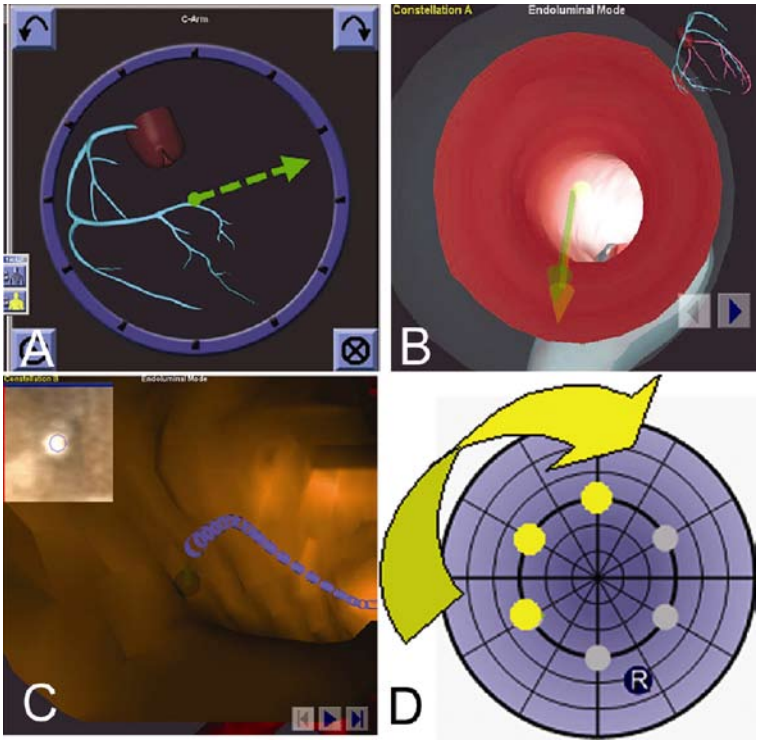

Figure 1 *A) Clockface navigation mode vectors are orientated by through a touch sensitive monitor; B) CardiOpB® virtual 3DRC vessel showing fly-through endoluminal view for navigation; C) extracted CTCA virtual fly-through endoluminal view with MPR slice in the top left corner; the Bull's eye navigational mode demonstrating the ability to reorient wire tip in a systematic manner.*

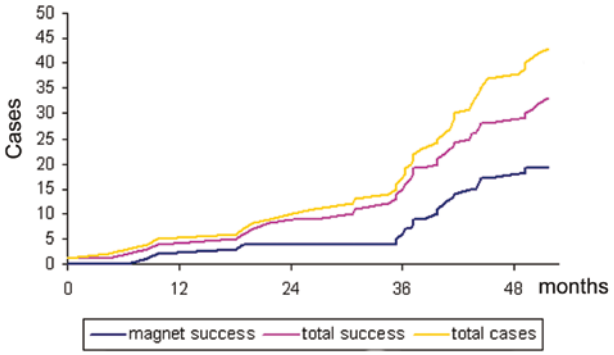

Figure 2 Cumulative curve of CTO success with the MNS with respect to the total success and cases.

CHAPTER 7

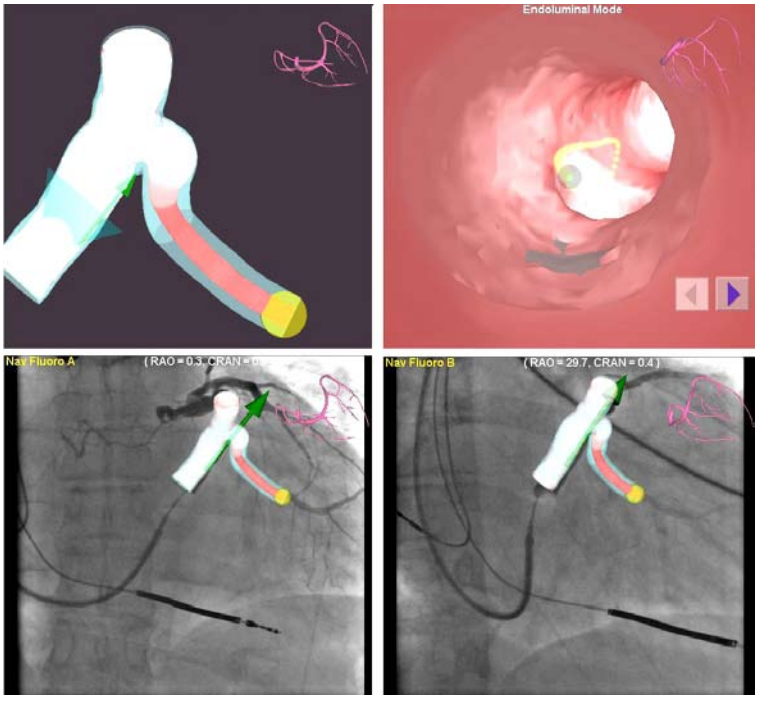

Figure 1. *Top: at the left, 3D reconstruction of the coronary sinus with one side branch in an antero-posterior view. Note the marked angulation of the lateral side-branch. At the right, a flythrough image of the reconstruction. Bottom: Reconstructed model aligned to the fluoroscopic view in LAO projection (left panel) and AP projection (right panel). In green, the automatically selected vector.*

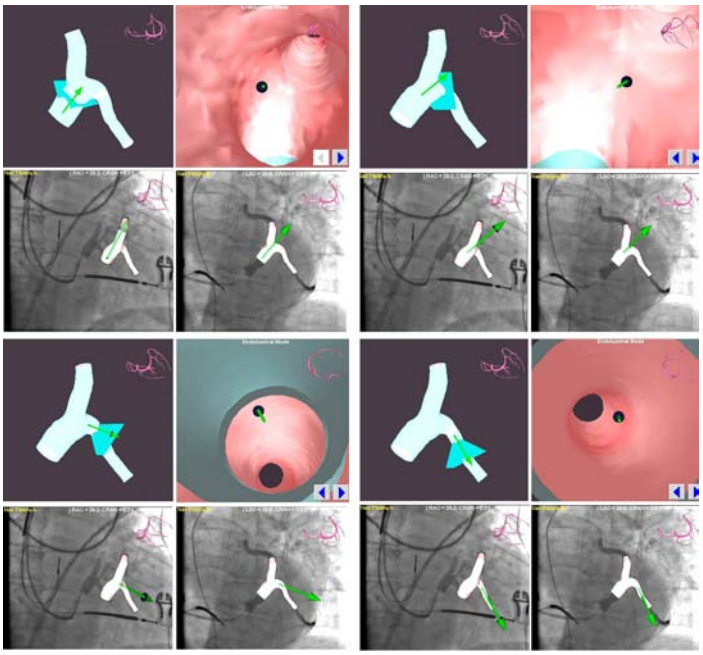

Figure 2. *Four panels, as seen in real time, showing the different automatically selected vectors (green arrows) chosen to navigate within the reconstructed coronary sinus (CS) model. In each panel, at the top left: 3D reconstruction of the CS; top right: endovascular view; bottom left: RAO projection and not aligned 3D model to facilitate visualization of the side branch; bottom right: LAO projection with aligned 3D model. Note how the vector changes according to the portion of the vessel it is aiming at.*

Figure 1. *Magnetic navigation system is shown with the magnets in position on either side of the patient.*

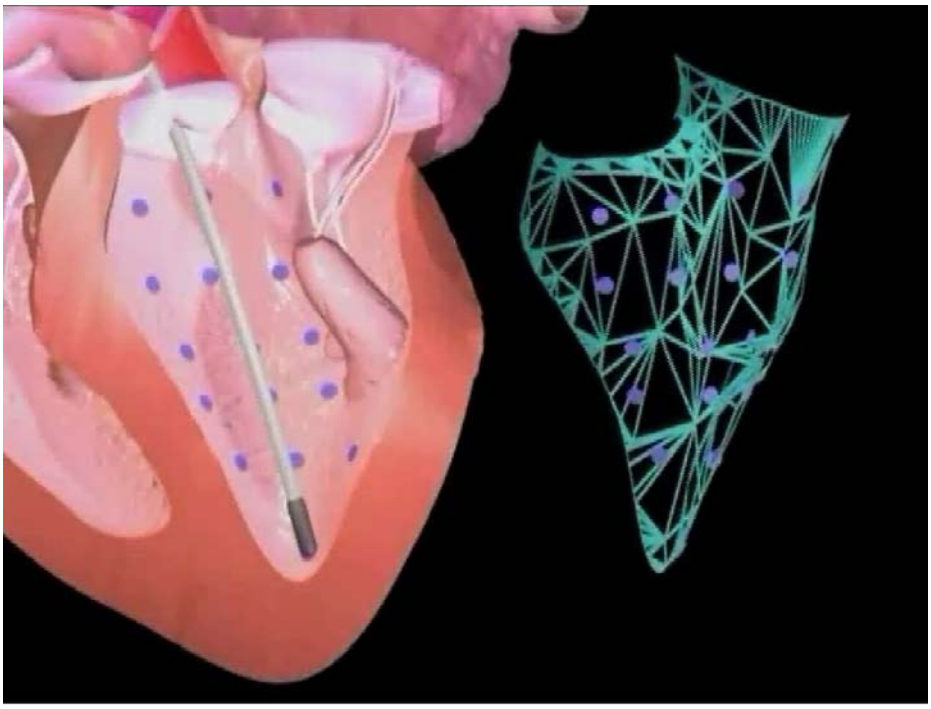

Figure 2 *Graphic showing reconstruction of LV mapping*

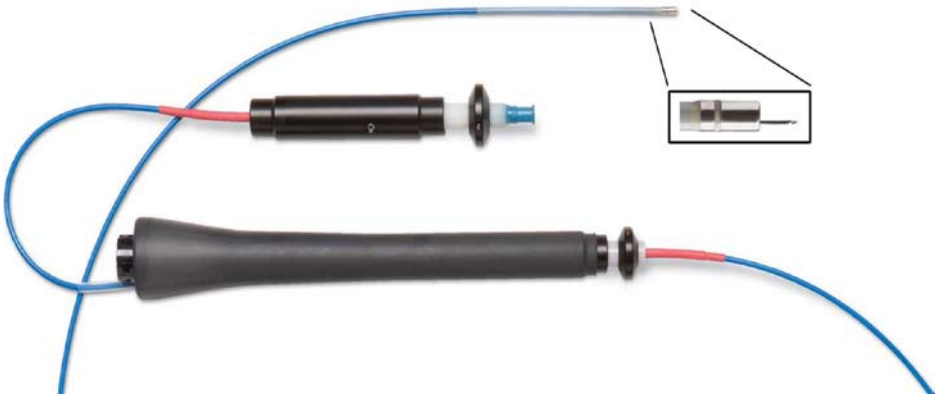

Figure 3 *MYOSTAR™ Injection Catheter to have electromechanical guidance provided by the NOGA® XP.*

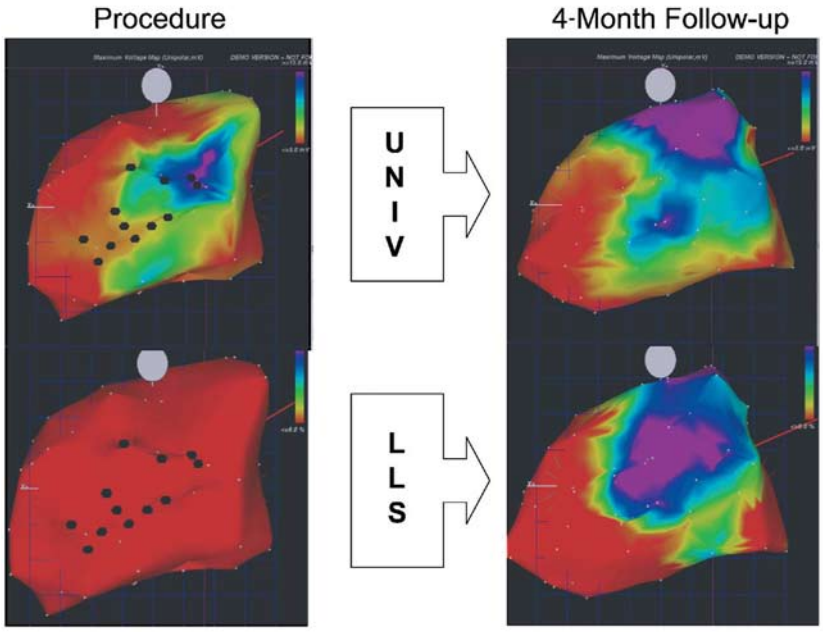

Figure 4 *NOGA™ electrical (UNIV, at top) and mechanical (LLS, at bottom) maps from a human patient in the stem cell treatment group. The maps on the left are those performed at the time of injection and maps at right are those at 4-month follow-up. An area of viability, showing normal electrical activity, can be noted on the upper-right map. The maps on the right show improvement in both electrical and mechanical function. LLS = linear local shortening; UNIV = unipolar voltage.*

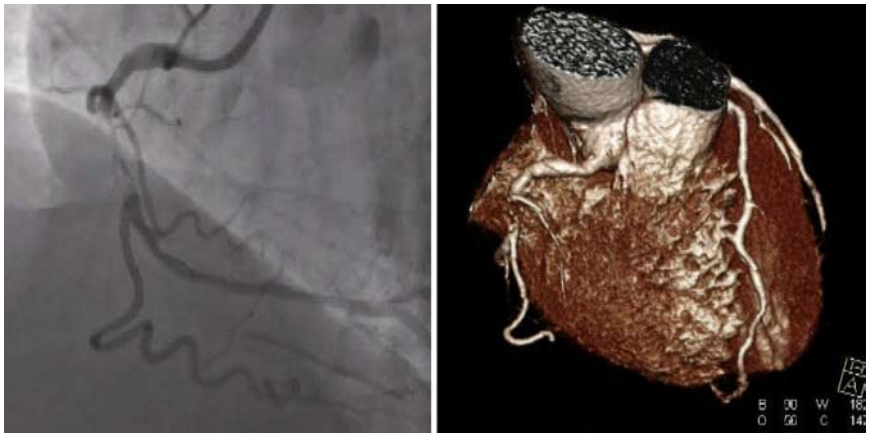

Figure 5 *The panel on the left shows the raw data from angiography and the panel on the right shows the reconstructed MSCT.*

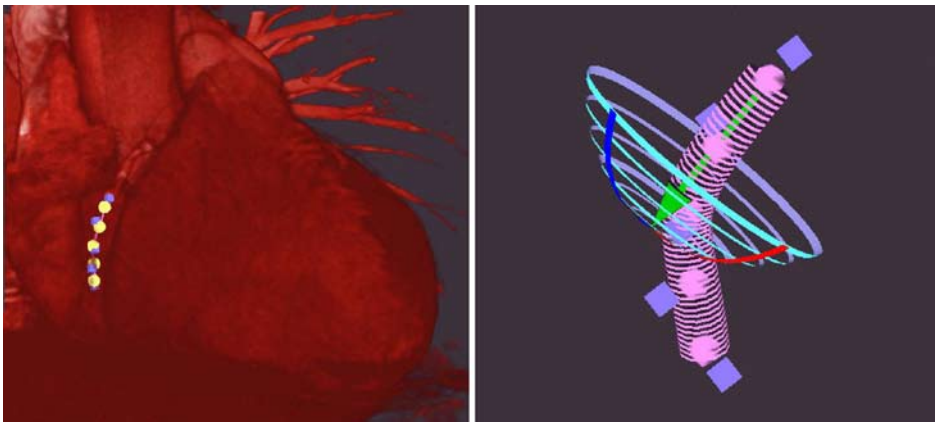

Figure 6 *The panel on the left shows the co-registered points applied to the MSCT image that was imported into Navigant and the panel on the right shows the computer reconstructed pathway that is derived from CT and projected onto the reconstruction in Navigant.*

CHAPTER 8

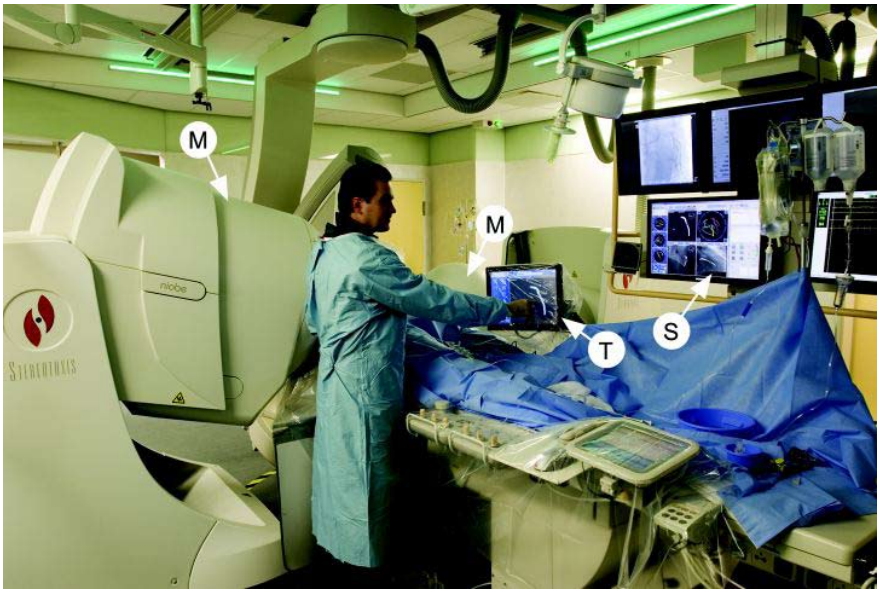

Figure 1 *System in position for PCI. M indicates magnets in tilt position for better lateral movement of the image intensifier. T indicates touch screen interface to give real-time instruction to the MNS. S indicates in-lab main screen monitor.*

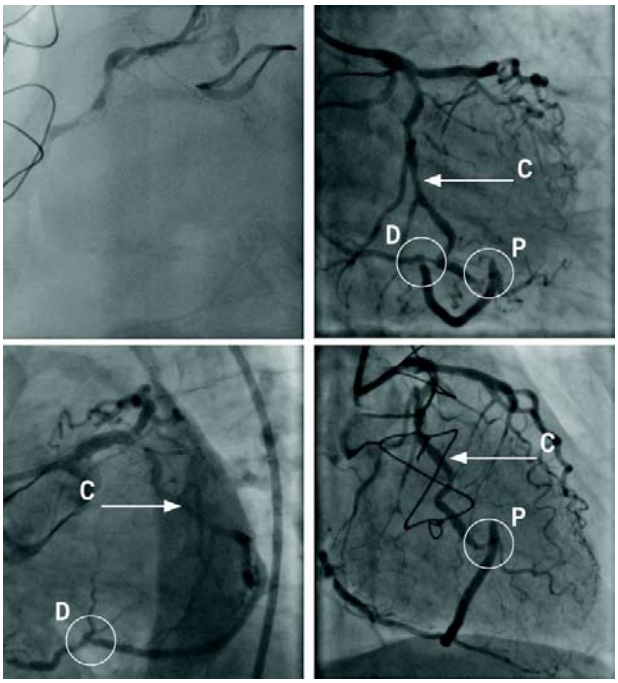

Figure 2 *The top left panel shows the occluded RCA that could not be opened anterogradely. The other three panels are different views showing Cx tortuousity and severe lesions at proximal and distal anastomoses of the SVG. C indicates the Cx. P indicates the proximal anastomosis. D indicates the distal anastomosis*

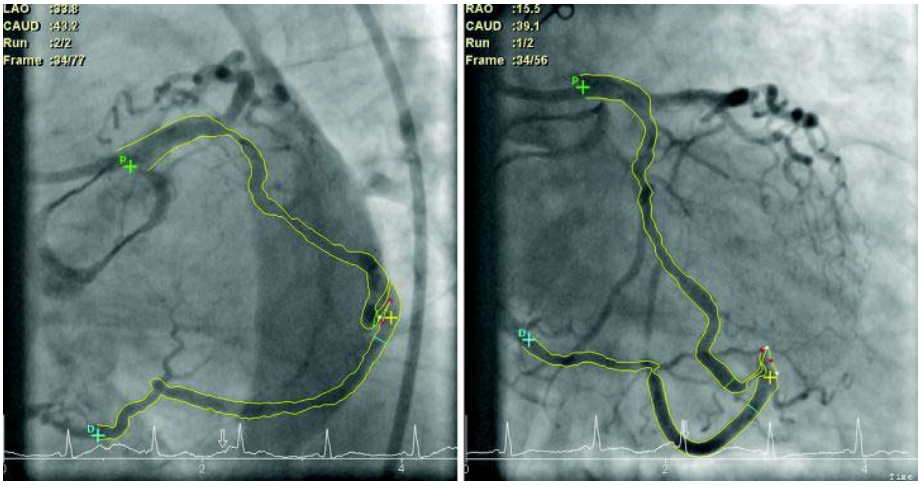

Figure 3 *Panels showing different fluoroscopy views with vessel edges marked by edge detection software (CardiOp-B, Paieon Medical Inc., Rosh Ha'ayin, Israel) before reconstruction. P indicates proximal point. D indicates distal point*

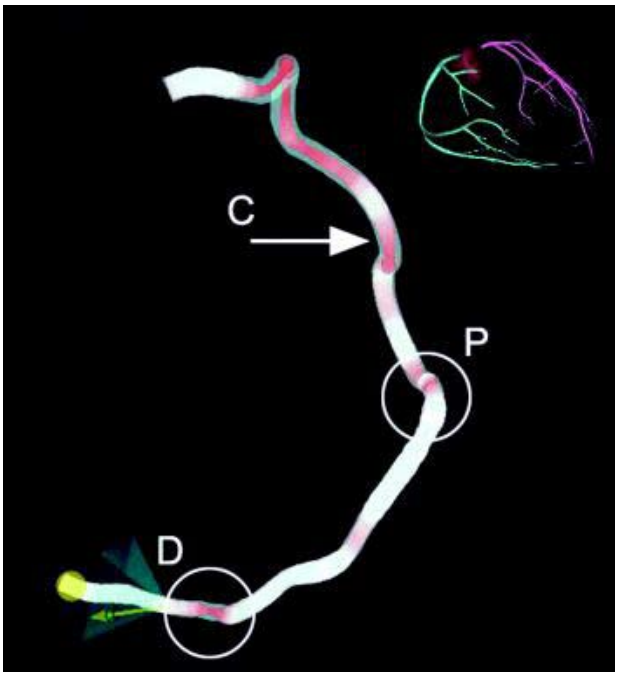

Figure 4 *Three-dimensional reconstruction of target pathway. C indicates the tortuous Cx. P indicates the proximal anastomosis. D indicates the distal anastomosis*

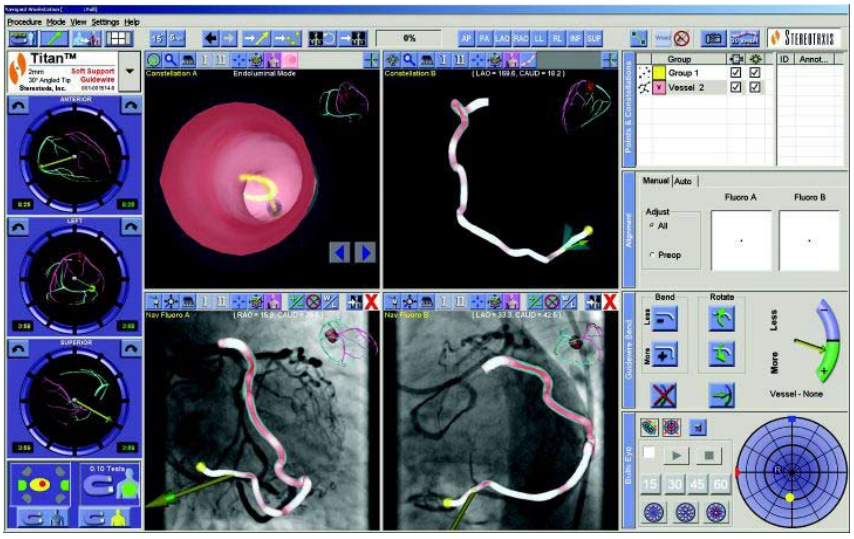

Figure 5 *Screen of Stereotaxis Navigant program during procedure, showing top left panel with endoluminal view. The top right panel shows the reconstruction. The bottom 2 panels are static-captured fluoroscopy images with the reconstruction for that angle superimposed.*

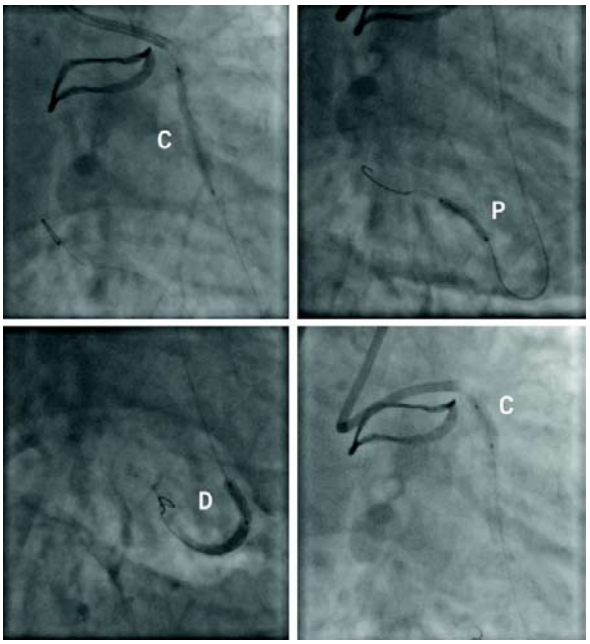

Figure 6 *Interventions. The top left panel shows predilation of Cx. The top right panel shows stent placement in distal anastomosis. The bottom left panel shows stent deployment at the proximal anastomosis. The bottom right panel shows one of the stents being deployed in the Cx. C indicates the Cx. P indicates the proximal anastomosis. D indicates the distal anastomosis.*

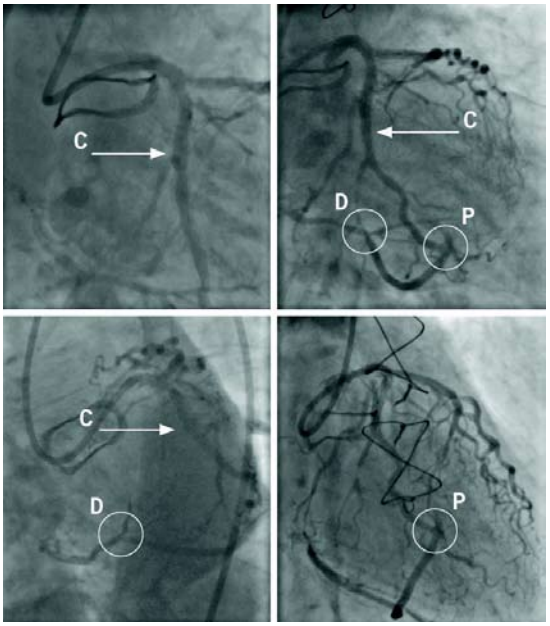

Figure 7 *Results of stenting form different views. C indicates the Cx. P indicates the proximal anastomosis. D indicates the distal anastomosis.*

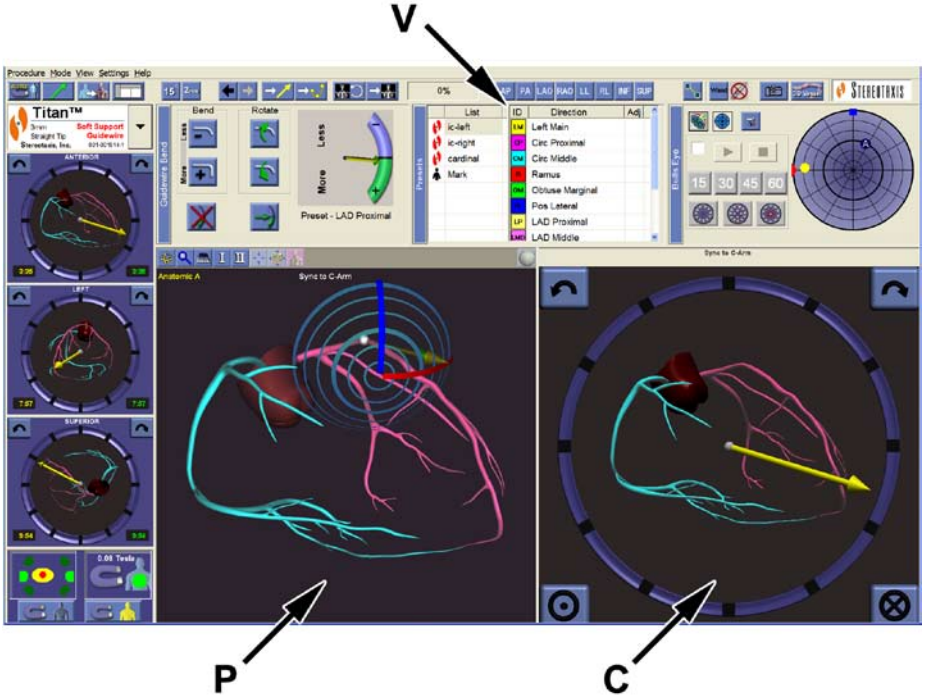

Figure 1 *The screen of the Navigant workstation, the panel (P) shows virtual coronary tree of the preset navigation with the list of preset vectors (V) seen above. The panel (C) shows the 2D clockface.*

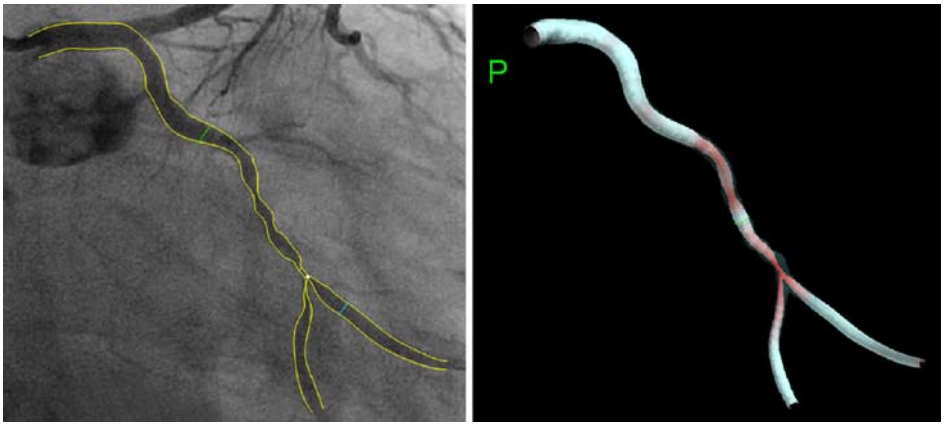

Figure 5 *The left panel shows the edges detected on the fluoroscopy image (2 views required), the right panel shows the 3 dimensional reconstruction of the infarct related coronary artery.*